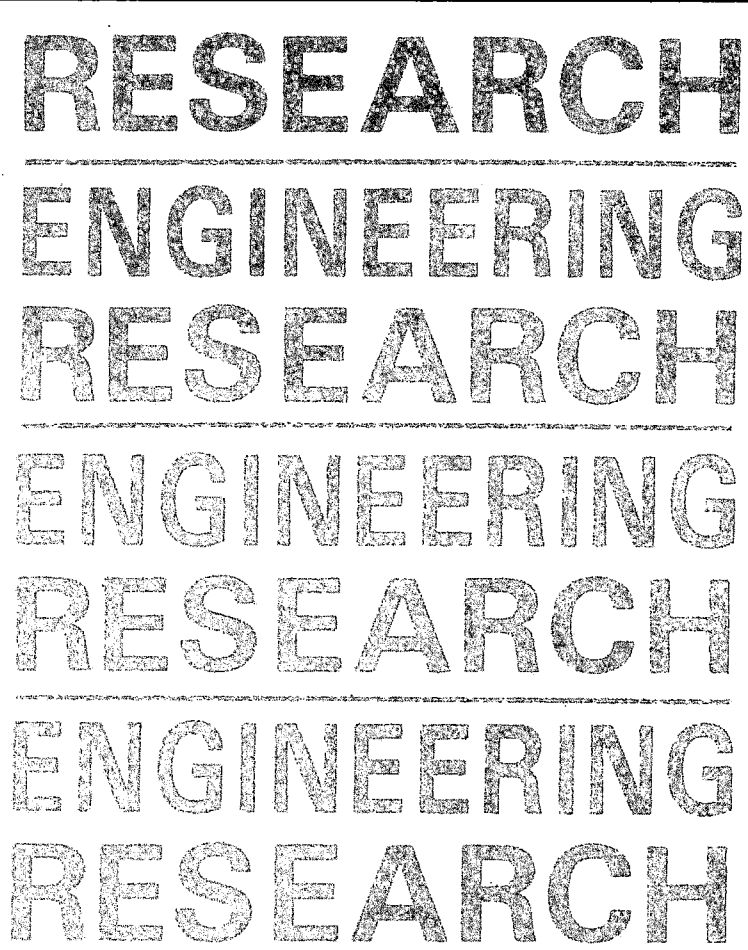

ENGINEERING
RESEARCH
INSTITUTE

IOWA STATE
UNIVERSITY
AMES, IOWA

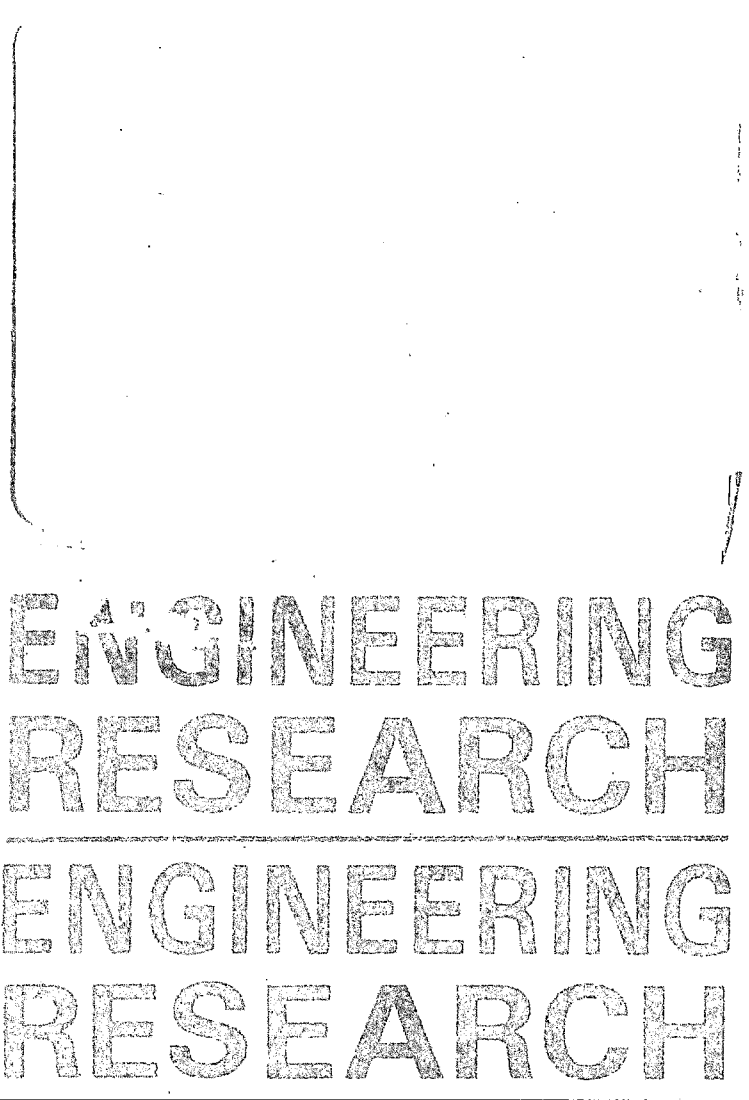

12-2

ENGINEERING RESEARCH

ENGINEERING RESEARCH
ENGINEERING RESEARCH
ENGINEERING RESEARCH
ENGINEERING RESEARCH

FINAL REPORT

DISTRIBUTION OF WHEEL LOADS ON HIGHWAY BRIDGES

W.W. Sanders, Jr. — H.A. Elleby
Department of Civil Engineering

December 1968

HIGHWAY RESEARCH BOARD
NATIONAL COOPERATIVE HIGHWAY RESEARCH PROGRAM
NATIONAL ACADEMY OF SCIENCES

ERI-361
Project 599-S

ENGINEERING RESEARCH INSTITUTE
IOWA STATE UNIVERSITY AMES

DISTRIBUTION OF WHEEL LOADS ON HIGHWAY BRIDGES

ABSTRACT

The purpose of the research was to develop a more realistic design criteria for distribution of wheel loads on highway bridges. A comprehensive study was made of the static load distribution in a broad range of short and medium span bridge types used by today's designers.

The bridge types studied were classified into three general categories: beam and slab; multi-beam; and cast-in-place concrete box girder. The behavior of these bridges was characterized by the following major variables: aspect ratio (bridge width/bridge span), relative stiffness of beams and floor, and relative diaphragm stiffness. The effect of these variables, as well as others, on the load distribution was investigated with respect to the number and position of wheel loads. The theories used for the major studies were: for beam and slab bridges, orthotropic plate theory; for multi-beam bridges, articulated plate theory; and for concrete box girder bridges, folded plate theory.

The validity of the theories to predict the behavior of an actual bridge under load was determined by correlation of the moments or stresses obtained from actual field tests with those computed by the applicable theory using the actual bridge geometry and loading.

Extensive numerical studies relating beam moments to the number and the lateral position of standard truck loadings for various combination of the variables listed were conducted. However, the complexity of the interrelation of the variables makes the use of the numerical data in a design office virtually impossible. Thus, an empirical equation was formulated and is presented in a proposed revision to the current AASHO

"Standard Specifications for Highway Bridges." Although numerous revisions are proposed in Section 3 on "Distribution of Loads," the major change is recommended for Article 1.3.1(B) in distribution of bending moment in stringers and longitudinal beams.

CONTENTS

FIGURES

TABLES

ACKNOWLEDGMENTS

The research was conducted by the Structural Engineering Research Laboratory staff, Engineering Research Institute, Iowa State University, Ames. It was sponsored by the American Association of State Highway Officials in cooperation with the Bureau of Public Roads through the National Cooperative Highway Research Program, which is administered by the Highway Research Board of the National Academy of Sciences — National Research Council.

The investigation was directed by Wallace W. Sanders, Jr., Associate Professor of Civil Engineering, serving as Principal Investigator, and Hotten A. Elleby, Assistant Professor of Civil Engineering, serving as Co-investigator. Graduate research assistants working on the study were James G. Arendts, Orhan Gurbuz, and Eiichi Watanabe.

The assistance and cooperation of many persons and agencies in furnishing information and making suggestions on specific details of the conduct of this study are acknowledged. Special thanks are given to the many researchers whose studies were used as the basis or stimulation for much of the work reported herein. The authors' special appreciation also goes to Mr. Arendts and Mr. Watanabe for their enthusiastic efforts during the entire investigation.

DISCLAIMER

This copy is the Final Report as submitted by the research agency. A decision concerning acceptance by the Highway Research Board and publication in the regular NCHRP series will not be made until a complete technical review has been made and discussed with the researchers. The opinions and conclusions expressed or implied in the report are those of the research agency. They are not necessarily those of the Highway Research Board, the National Academy of Sciences, the Bureau of Public Roads, the American Association of State Highway Officials, or of the individual states participating in the National Cooperative Highway Research Program.

DISTRIBUTION OF WHEEL LOADS ON HIGHWAY BRIDGES

SUMMARY

The research reported herein was undertaken for the purpose of developing more realistic design criteria for distribution of wheel loads on highway bridges.

For over 30 yr the "Standard Specifications for Highway Bridges" of the American Association of State Highway Officials (AASHO) has included a procedure for determining this load distribution. Although several detailed studies were conducted on specific bridge types, many of the criteria have been based on extensions developed from separated limited studies. It is the purpose of this investigation to study at one time the static distribution of movable wheel loads in a broad range of bridge types used by today's designers. This approach gives a uniform approach to the development of specification criteria.

The current AASHO specifications for load distribution were essentially developed in their present format about 25 yr ago. Although some minor changes in procedures have been made and several new bridge types included, the basic approach has remained unchanged since that time. Presently, the only major variables considered are beam spacing and general bridge floor system makeup. However, many other variables affect the behavior (some quite significantly), and with the many analytical tools available, more realistic distribution criteria can be developed. It is for this purpose that this study was undertaken.

However, the study was limited to short and medium span bridges, that is bridges with spans up to about 120 ft. In this span range, the bridge types can be classified into three general categories: beam

and slab; multi-beam; and cast-in-place concrete box girder. The behavior of these bridges can be characterized by the following major variables: aspect ratio (bridge width/bridge span), relative stiffness of beams and floor, relative diaphragm stiffness and extent of bridge continuity. The effect of these variables on the load distribution was investigated with respect to the number and position of wheel loads.

During the past 50 yr many theories have been proposed and developed which are applicable to the determination of the behavior of the floor system under load. These include: orthotropic plate theory, articulated plate theory, flexibility or stiffness methods, grillage method, finite element method, harmonic analysis, folded plate theory and moment distribution procedures. Each of these theories has particular inherent assumptions which make it more applicable to a particular bridge geometry. However, since a wide variety of bridge types is considered herein, several generally applicable modifications of the plate theory have been employed in the overall analysis. To limit complexity, the general plate theory was used and adapted to the specific bridge types listed above. Thus, a similar set of geometric parameters is applicable to the bridge types studied. For the beam and slab bridges, the orthotropic plate theory was used; for the multi-beam bridges, the articulated plate theory; and for concrete box girder bridges, the folded plate theory.

To verify the validity of the theories and their assumptions in predicting the behavior of an actual bridge under load, correlations were made between moments or stresses obtained from actual field tests and those computed by applicable theories using the actual bridge geometry and loading. These correlations indicate that the theories selected do adequately predict the load distribution in the particular bridge types.

Extensive numerical studies relating beam moments to the number and the lateral position of standard truck loadings for various combinations of the variables previously listed were then conducted. These results were used to determine a number of influence lines for beam moment. However, the complexity of the interrelation of the variables makes using these charts in a design office virtually impossible. Thus, an empirical equation developed from these charts was formulated and is presented in a proposed revision to the current AASHO Specifications (279) for load distribution.

Although numerous revisions have been proposed in Section 3 on "Distribution of Loads," the major change has been recommended for Article 1.3.1(B) in distribution on bending moment in stringers and longitudinal beams. Even though these changes, in many cases, do not significantly affect current designs, they do make them more realistic and do consider the benefits derived from improving bridge properties. It is recommended that this entire article be replaced as follows. Shown below is the new Article 1.3.1(B) recommended for inclusion in the AASHO Specifications (279):

1.3.1 — DISTRIBUTION OF LOADS TO STRINGERS, LONGITUDINAL BEAMS AND FLOOR BEAMS.

(A) Position of Wheel Loads for Shear — unchanged.

(B) Live Load Bending Moment in Stringers and Longitudinal Beams for Bridges Having Concrete Decks*.

In calculating bending moments in longitudinal beams or stringers, no longitudinal distribution of the wheel load shall be assumed. The lateral distribution shall be determined as follows:

(1) Load Fraction (all beams).

The live load bending moment for each beam shall be determined by applying to the beam the fraction of a wheel load (both front and rear) determined by the following relations:

$$\text{Load Fraction} = \frac{S}{D}$$

where S is

S_a for beam and slab bridges**

---

*In view of the complexity of the theoretical analysis involved in the distribution of wheel loads to stringers, the empirical method herein described is authorized for the design of normal highway bridges. This section is applicable to beam and slab, concrete slab, multi-beam, and concrete box girder bridges. For composite steel box girder bridges, the criteria specified in Article 1.7.104 should be used.

**For slab bridges, S = 1 and the load fraction obtained is for a one foot width of slab.

$\frac{12N_L + 9}{N_g}$ for multi-beam bridges*, and the maximum of the two values for concrete box girder bridges

and the value of D determined by the following relationship:

$$D = 5 + \frac{N_L}{10} + (3 - \frac{2N_L}{7})(1 - \frac{C}{3})^2 , \qquad C \leq 3$$

$$= 5 + \frac{N_L}{10} , \qquad C > 3$$

where: S_a = average beam spacing, feet,

N_L = total number of design traffic lanes from Article 1.2.6,

N_g = number of longitudinal beams,

C = a stiffness parameter which depends upon the type of bridge, bridge and beam geometry and material properties.

The value of C is to be calculated using the relationships shown below. However, for preliminary designs, C can be approximated using the values given in Table 1.3.1. For beam and slab** and multi-beam bridges:

$$C = \frac{W}{L}\left[\frac{E}{2G} \cdot \frac{I_1}{(J_1 + J_t)}\right]^{1/2} .$$

For concrete box girder bridges:

$$C = \frac{1}{2}\frac{W}{L}(1 + N_g\sqrt{\frac{d}{W}}) \cdot \left[\frac{E}{2G(1 + N_d)}\right]^{1/2}$$

---

*A multi-beam bridge is constructed with precast reinforced or prestressed concrete beams which are placed side by side on the supports. The interaction between the beams is developed by continuous longitudinal shear keys and lateral bolts which may or may not be prestressed.

**For noncomposite construction, the design moments may be distributed in proportion to the relative flexural stiffnesses of the beam and slab section.

where: W = the overall width of the bridge, feet,

L = span length, feet (distance between live load points of inflection for continuous spans),

E = modulus of elasticity of the transformed beam section,

G = modulus of rigidity of the transformed beam section,

I_1 = flexural moment of inertia of the transformed beam section per unit width*,

J_1 = torsional moment of inertia of the transformed beam section per unit width* ($J_1 = J_{beam} + \frac{1}{2} J_{slab}$),

J_t = 1/2 of the torsional moment of inertia of a unit width of bridge deck slab*

and for concrete box girder bridges:

d = depth of the bridge from center of top slab to center of bottom slab,

N_g = number of girder stems, and

N_d = number of interior diaphragms.

For concrete for girder bridges, the cantilever dimension of any slab extending beyond the exterior girder shall preferably not exceed S/2.

When the outside roadway beam or stringer supports the sidewalk live load and impact, the allowable stress in the beam or stringer may be increased 25 percent for the combination of dead load, sidewalk live load, traffic live load, and impact.

---

*For the deck slab and beams consisting of reinforced or prestressed concrete, the uncracked gross concrete section shall be used for rigidity calculations.

TABLE 1.3.1 VALUES OF K TO BE USED IN THE RELATION: $C = K \frac{W}{L}$

BRIDGE TYPE	BEAM TYPE AND DECK MATERIAL	K
Beam and slab (includes concrete slab bridge)	Concrete deck:	
	Noncomposite steel I-beams	3.0
	Composite steel I-beams	4.8
	Nonvoided concrete beams (prestressed or reinforced)	3.5
	Separated concrete box-beams	1.8
	Concrete slab bridge	0.6
Multi-beam	Nonvoided rectangular beams	0.7
	Rectangular beams with circular voids	0.8
	Box section beams	1.0
	Channel beams	2.2
Concrete box girder	Without interior diaphragms	1.8
	With interior diaphragms	1.3

(2) Total Capacity of Stringers.

The combined design load capacity of all the beams in a span shall not be less than required to support the total live and dead load in the span.

(3) Edge Beams (Longitudinal).

Edge beams shall be provided for all concrete slab bridges having main reinforcement parallel to traffic. The beam may consist of a slab

section additionally reinforced, a beam integral with and deeper than the slab, or an integral reinforced section of slab and curb.

It shall be designed to resist a live load moment of 0.10 PS, where

P = wheel load, in pounds (P_{15} or P_{20})

S = span length, in feet.

This formula gives the simple span moment. Values for continuous spans may be reduced 20 percent unless a greater reduction results from a more exact analysis.

CHAPTER 1: INTRODUCTION

STATEMENT OF PROBLEM

This study was undertaken to develop a more realistic analysis of and to develop better design specifications for the distribution of live load in the floor systems of highway bridges. Numerous analytical and experimental studies have been made to help improve the methods used for highway bridge design; however, in some areas the studies have not resulted in realistic, yet simple, procedures for design. One of these areas is in highway bridge floor systems.

It has been suggested that the present specifications (279), although giving satisfactory designs for service, are too conservative and limited in consideration of variables affecting behavior. They provide no satisfactory consideration of such important variables as the flexural and torsional stiffnesses of the floor slab and beams, the bridge span and the bridge width in the determination of the distribution of beam live loads. In addition, they do not provide consistent design criteria for all types of highway bridges. Thus, changes, where warranted, are recommended in the current specifications for distribution of wheel loads for use in design of floor systems for highway bridges.

The study outlined herein relies significantly on the theoretical methods and field test results of other investigators. These studies were used as the basis for the investigation. Modifications and extensions of the applicable theories were made so that the theories would be applicable to all bridge types considered. After correlation with the field test results, extensive analytical results were obtained relating all significant variables. From these results, proposals for appropriate specification changes have been developed and are presented.

STATE-OF-THE-ART

For over 25 yr, numerous researchers have studied the behavior of bridge floor systems. Although most of these studies were limited to theoretical behavior, a significant number of field tests have been reported in the literature. An extensive bibliography of available references in both areas is given in Appendix C. An extensive report of the state-of-the-art of the analysis of most common bridge types has been presented by Reese (182). The succeeding paragraphs in this section briefly outline available theoretical and experimental studies.

The designs of the floor systems of highway bridges are quite varied and depend upon many factors. These varied designs, however, may be classified, based on their assumed behavior, into a few major categories. There are several types of structures that may be analyzed by the same theoretical methods, although their physical nature may be somewhat different. Slabs, plates, open grid frameworks, interconnected bridge girders, bridge decks and cellular plate structures, for example, may all be classified as grids. Nearly all of the floor systems of the many types of highway bridges fall, in one form or another, into one of the classifications. For this study, the various types of bridges have been classified as shown in Figure 1, into three major categories: beam and slab type, multi-beam and concrete box girder bridges.

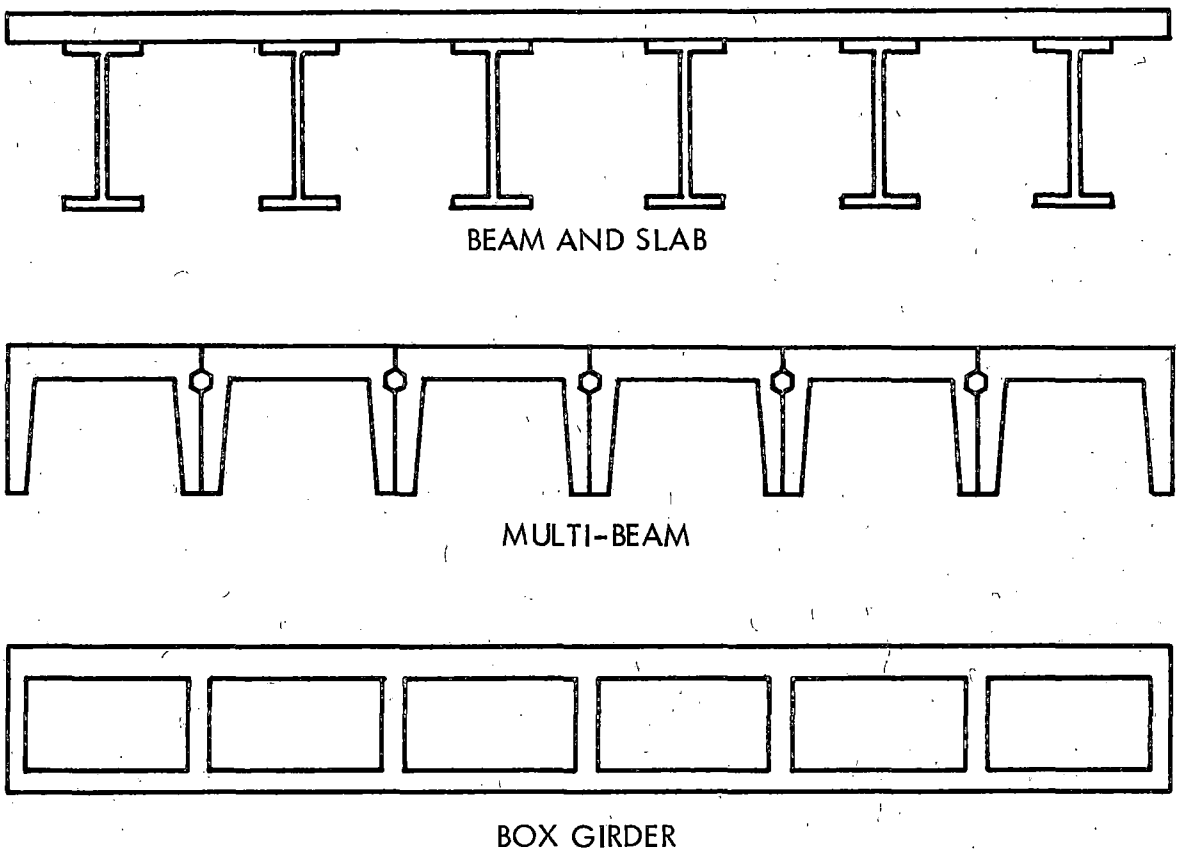

Figure 1. Intermediate length highway bridge types.

Theoretical Analyses

Beam and Slab Bridges

Theoretical investigations of beam and slab bridges vary in their approach as well as in their accuracy and assumptions. The majority of the analytical approaches can be placed into the following four classifications:

1. unit or plate analysis,
2. redundant or grid analysis,
3. combination of plate and grid analyses, and
4. specialized methods.

The unit method, commonly known as orthotropic plate analysis, replaces the actual structure with an equivalent orthogonally anisotropic plate. This method is characterized by a relatively complex closed form solution. The equivalent plate has the same transverse and longitudinal torsional and flexural rigidities as the actual structure. Initial development of the orthotropic plate analysis as applied to bridge decks is due to the work of Guyon (67, 68) who found solutions for the limiting cases of torsional rigidity in the equivalent plate. His results are valid for the no-torsion condition and the full-torsion or isotropic condition. Massonnet (129 – 133) extended the analysis to include intermediate values of torsional rigidity through the use of an interpolation formula. Both of these investigators assumed Poisson's ratio of the equivalent bridge materials to be zero. Rowe (195 – 199, 201) extended the analysis by providing for the inclusion of any value of Poisson's ratio. Another solution of the orthotropic plate equation was found by Sanders and Munse (210) and Roesli (191) who considered the applied load to be uniformly distributed over a small rectangular area. A third solution of the orthotropic plate equation has been proposed by Stein (236). In this case, singularity functions are used to represent Huber's orthotropic plate equation and the solutions found after transformations between the singularity and cartesian systems. Numerical solution of the plate equation has also been employed by various investigators. Notable are Heins and Looney (74, 75) who applied finite difference techniques to the plate equation for comparison with experimental results from tests on several different bridge types. Detailed reviews and analyses of the development of the orthotropic plate solution can be found in the references cited or in Appendix A of this report.

In the second general method of analysis, the actual bridge structure is replaced with an equivalent grid system. A direct solution of gridworks through the use of slope-deflection and compatibility equations has been developed by Homberg (84, 85). Lazarides (108, 122) has solved the gridwork problem by determining the deflection compatibility equations at each beam intersection and solving the resultant simultaneous equations. Numerical solutions have also been used for gridwork analysis by Leonhardt (109, 110) through the use of moment or torque distribution, while Scordelis (223) used shear distribution and Fader (50) used a reaction distribution method. The gridwork or redundant analysis usually involves a large number of simultaneous equations if solved exactly, or numerous arithmetic calculations if one of the numerical techniques is employed.

The third general analytical approach to the load distribution problem, a combination of the plate and redundant procedures, is represented by two theories: harmonic analysis and numerical moment distribution.

The development of harmonic analysis as a technique for the determination of load distribution in highway bridges results from the work of Hendry and Jaeger (76 – 79). This procedure considers the same flexural and torsional rigidities as the orthotropic plate analysis with the exception that torsional rigidity in the transverse direction is neglected. The harmonic analysis, however, requires the calculation of a number of constants, which are utilized in an infinite series summation. Preliminary calculations for the determination of these constants are somewhat lengthy. This procedure is also characterized by a relatively slow convergence of the series for the most highly stressed beam.

The second method of analysis that combines the plate and redundant member technique is the numerical moment distribution procedure developed by Newmark (152, 154 – 157) and Jensen (94). In this procedure the slab is first considered independent of the beams and is assumed to be isotropic. From boundary conditions and the Levy series expression for loading, a solution of the isotropic plate equation is found. A slab strip is now considered to be a beam continuous over flexible supports (the actual beams), and a Hardy Cross moment distribution procedure is carried out to determine moments in the actual beams.

The fourth general category of distribution procedures, specialized methods, contains widely differing approaches. An approximate gridwork solution was developed by Pippard and deWaele (171). This procedure requires the replacement of all transverse grid members by a single member at midspan with equivalent stiffness. This approximation results in fewer calculations than those required in the general gridwork solution. The beam on elastic foundation analogy has been proposed by Massonnet (131). Because of similarity between the plate equation when the torsional term is ignored and the beam on elastic foundation equation, the elastic foundation analogy can be used for bridges with little torsional rigidity with only a small error if the equivalent plate is assumed to have zero torsional rigidity. If a bridge system has few longitudinal beams and if transverse beams or diaphragms are ignored, another approach can be used by considering the bridge to be a complex beam. This analysis is relatively simple but has limited applicability. In fact, all of the approximate methods can be applied with reasonable accuracy to very specific beam and slab types, but chance of potential error is greatly magnified when these methods are applied to the general beam and slab bridge.

Multi-Beam Bridges

The number of methods available for the analysis of multi-beam bridges is somewhat more limited. About 10 yr ago, Duberg, Khachaturian and Fradinger (45) analyzed a multi-beam bridge by assuming that it consisted of beam elements placed side by side and connected to each other along the span by hinges at the corners of the cross section at the level of the top fiber. Other investigators (80, 171) have made similar assumptions, such as:

1. no rotation of individual members at their intersections with other members,
2. floor system prevents twist of main girders, and
3. cross girders are replaced by a continuous connecting system.

The behavior of multi-beam bridges is in many respects similar to that of the beam and slab bridges. The major difference is the elimination of the moment restraint between the individual beam units which leads to some modifications in the applicable theories. The methods of analyses can be divided into two major categories. The first category is normally called the method of compatible deformation based on the flexibility method. The second category can be classified as a plate theory.

The first step involved in the first category is to consider the equilibrium of the mechanical system and express various mechanical quantities such as deflection and bending moments in terms of certain unknown forces acting on the system. The solutions are obtained by considering the compatibility conditions of the system; subsequently, the last step is to solve simultaneous linear equations for these unknown forces. Arya (6) and Pool (100, 172, 173) used this method of compatible deformation to analyze multi-beam bridges.

The second category assumes that the number of beam elements is large enough for the real structure to be replaced by an idealized plate with continuous properties so that differential calculus can be applied. The plate theory can be divided into several methods. One method assumes no flexural rigidity in the transverse direction of the bridge because of the discontinuities at the shear keys. On the other hand, another method would allow some flexural rigidity in the transverse direction taking into account the effect of transverse prestress force and some continuity even at the location of shear keys. The first method is usually known as articulated plate theory, while the latter is termed orthotropic plate theory which was first studied by Guyon and Massonet and has been extensively used in the analysis of beam and slab bridges, as previously mentioned. Roesli (189), Nasser (151) and Pama (38, 165, 166) used these theories to analyze multi-beam bridges.

Concrete Box Girder Bridges

Numerous analyses of concrete box girder bridges have been carried out by Scordelis (221, 222, 224). The method of analysis used was based upon a direct stiffness solution of a folded plate harmonic analysis based on an elasticity method (41). Scordelis used elastic plate theory for loads normal to the plane of the plates and two-dimensional plane stress theory for loads in the plane of the plates. This is the only method of analysis used extensively for this bridge type.

Field Test Investigations

There are a number of field tests of the types of bridges considered in this study. However, most of these tests were conducted on beam and slab bridges. The most extensive single effort of field testing was conducted at the AASHO Test Road at Ottawa, Ill. (278). Eighteen bridges of the four general beam and slab bridges types were tested. These types were:

1. noncomposite steel wide-flange beam bridges,
2. composite steel wide flange beam bridges,
3. reinforced concrete beam bridges, and
4. prestressed concrete beam bridges.

In addition, numerous field tests of this bridge type have been reported in the literature. A summary of these tests performed up to 1965 has been prepared by Varney and Galambos (252). Numerous tests have been conducted since that time on beam and slab bridges. These include a series of tests of box beam bridges by Van Horn et al. (44, 62, 63, 113) and three tests in Maryland by Reilly and Looney (183). A summary of a number of these tests of beam and slab bridges has been prepared by Arendts (5).

As indicated previously, the number of tests of multi-beam and concrete box girder bridges is limited. Only three full-scale tests of the type of multi-beam bridges studied herein are reported (23, 202, 204). The first test (23) was conducted on a bridge consisting of channel sections; the second (204) on a bridge with solid sections with holes; and the third (202, 204) on a bridge composed of solid sections. The latter two tests were conducted in England. All of the tests of

concrete box girder bridges have been conducted on bridges constructed by the California Department of Highways. The only field test reported to date was conducted by Davis, Kozak and Scheffey (39, 222) on the Harrison Street Undercrossing in Oakland, Calif.

Although limited in some cases, the number of tests and the types of bridges studied in the field tests are sufficient to verify the applicability of the theories used to predict the behavior of the particular bridge types included in this investigation.

SCOPE OF INVESTIGATION

The determination of beam bending moments in highway bridges requires a design procedure to predict with reasonable accuracy the maximum beam moment produced by a standard loading. This design procedure should be governed by bridge behavior characteristics or parameters which reflect the bridge behavior. The development of this procedure and of the recommendations for changes in the current AASHO Specifications (279) were based on:

1. A thorough bibliographic search for all available studies into the theoretical and experimental behavior of highway bridges. This bibliography is given in Appendix C.
2. The study of these references to determine the theoretical procedures which were most applicable to the bridges included in the study scope. These theoretical procedures were then used to predict the behavior of field tested bridges. A comparison of these results with those actually obtained in the field tests was used to verify the applicability of the

procedures. The comparisons are discussed in detail in Chapter 2.

3. An extensive study of the effect of the variation in the parameters affecting the wheel load distribution. The procedures selected were used to determine the maximum beam bending moments due to numerous possible loading conditions. The results of this analytical study are given in Chapter 3.
4. The simplification of these results into a form that would still be readily usable in the design office, yet give sufficient accuracy in the prediction of load distribution. Where the difference in accuracy between these procedures and the current specification was felt to warrant changes, recommendations for new criteria were then made. The details of this simplification and the resulting recommendations are given in Chapters 4 and 5.

After a thorough study of the theoretical procedures found in the bibliographic search, procedures were selected for use in the analytical studies which were felt to best predict the behavior of those bridges included in this investigation. For beam and slab bridges, the orthotropic plate theory and harmonic analysis were selected; for multi-beam bridges, the articulated plate theory; and for concrete box girder bridges, the theory of prismatic folded plate structures. Numerous other procedures were considered and although applicable to specific bridge geometries, it was felt that those selected were more generally applicable.

Because of the existence of a wide variety of highway bridge geometries, some bridge geometrical restrictions were specified to

limit the scope of the study. The bridges studied conform to the following geometrical conditions.

1. The longitudinal axis of the bridge is at right angles to the piers or abutments.
2. The bridge spans between adjacent piers or abutments are simple or noncontinuous, although the effects of bridge continuity are considered based on other investigations.
3. The spans are of short or intermediate length (20 to 130 ft).

In addition to the above constructional and geometric conditions, the study of the bridges was restricted to statically applied live loads only. This loading condition requires that the test load vehicles in the field tests be either stopped on the bridge or moving at creep speeds (less than about 5 mph) while measurements were in progress. Furthermore, the consideration of beam and slab type bridges with composite wood-concrete members or timber stringers and orthotropic plate deck type bridges were not within the scope of the study. Even though the above constructional and geometric conditions may seem quite restrictive, these conditions will be satisfied for the construction and design of the majority of actual highway bridges.

Major variables or geometrical parameters which were considered in the study included: torsional and flexural stiffness of the beams, deck and diaphragms; the width of bridge; the roadway width; the span of the bridge; and the number and position of design traffic lanes. In addition, although the stiffness of the floor such as the concrete slab or steel grid was considered in the distribution of wheel loads in beam and slab bridges, the actual design of the floor was not considered.

The details of these parameters and the theories are presented in Chapter 3.

Beam and slab, multi-beam, and box girder highway bridges are classified as different type bridges due to their differences in construction and structural behavior under load. Figure 1 illustrates the differences in construction.

Beam and slab bridge construction is characterized by separated longitudinal beams which support a deck slab. The beams, as shown in Figure 2, can vary in material as well as construction. Steel beams may be rolled shapes or plate girders and may have either a composite or noncomposite deck slab. If the beams are prestressed concrete, then composite action is generally provided for through shear connectors. Prestressed concrete beams are usually precast as "I" shapes, but other beam shapes are possible such as "T" shapes where the beams are cast monolithically with a portion of the deck slab. Also, in reinforced concrete beam bridges, the beam shape is considered as the "T" formed of the beam stem and a portion of the slab. In fact, when any beam and slab bridge is compositely constructed, a portion of the slab is always considered to be a part of the beam.

Multi-beam bridges consist of several longitudinal beams placed side by side. The beams are usually precast prestressed concrete and are connected by longitudinal shear keys. In addition, the beams are usually tied together by post-stressed transverse steel cables. Although transverse prestressing may be present, it may not be of sufficient magnitude to provide transverse continuity through the loading spectrum. Beam shapes vary, but a common configuration is the concrete channel beams

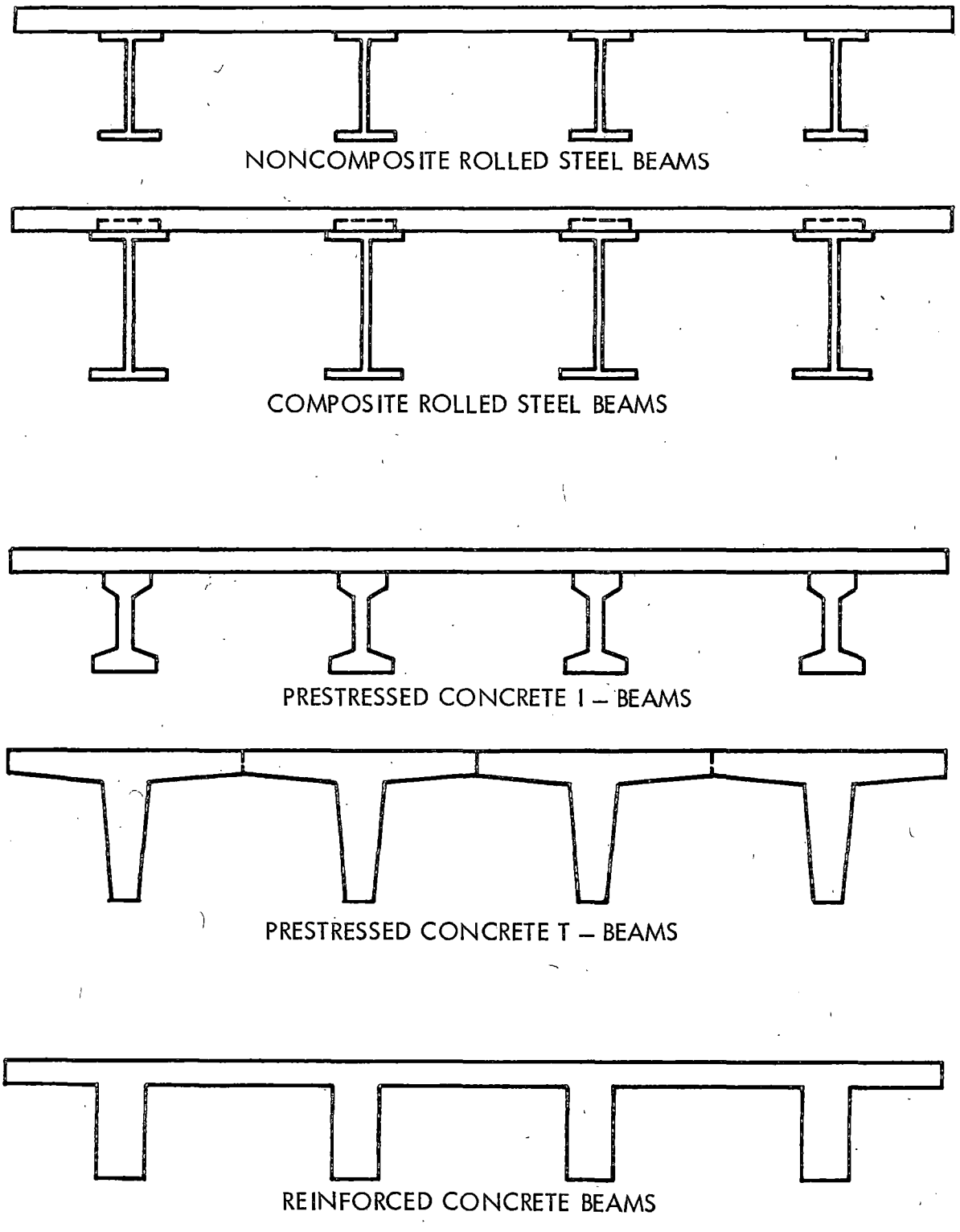

Figure 2. Beam and slab highway bridge types.

shown in Figures 1 and 3. Nonvoided rectangular, tee, and voided or hollow rectangular beam shapes, as shown in Figure 3, are also common.

Box girder bridges are usually made of monolithically cast reinforced concrete, but a recent method of construction combines light gage steel box sections with a composite concrete deck. The reinforced concrete box girder bridge shown in Figure 1 is constructed of two continuous flanges with monolithic vertical webs. Separated box-beam and slab bridges should not be confused with concrete box girder bridges. The composite steel concrete box girder bridges are characterized by a separation of the steel boxes and are, thus, in reality, beam and slab type bridges.

Structural behavior is important to the classification of beam and slab, multi-beam, and concrete box girder bridges. Both beam and slab and multi-beam bridges can be represented by an equivalent plate, but the structural models representing these plates differ. The principal difference is the ability of the bridge or equivalent plate to transmit bending moment in the transverse direction. Beam and slab bridges are flexurally continuous in the transverse direction due to the deck slab's and transverse beam's or diaphragm's ability to transmit bending moment. On the other hand, the shear keys connecting the individual beams of a multi-beam bridge act as hinges. Therefore, transverse flexural continuity is not present in multi-beam bridges and the equivalent plate must be treated differently from the equivalent orthotropic plate that represents the beam and slab bridge. Concrete box girder bridges differ from the previous two bridge types in that procedures are not currently available for theoretically representing the

SOLID CROSS SECTION

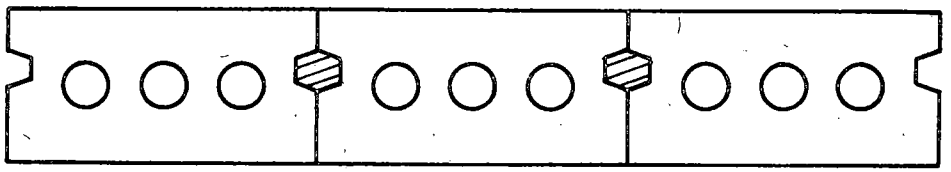

SOLID CROSS SECTION WITH CIRCULAR HOLES

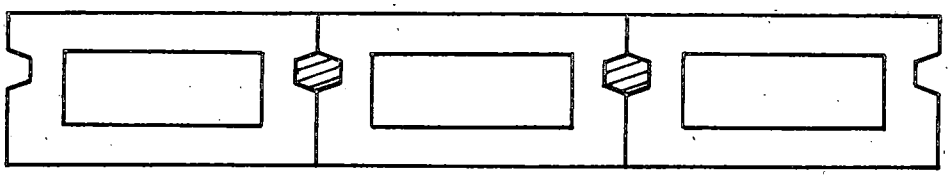

BOX CROSS SECTION

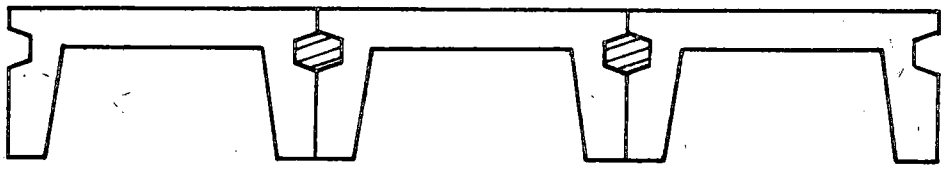

CHANNEL CROSS SECTION

Figure 3. Multi-beam highway bridge types.

entire structural system as a single equivalent plate. Each plate element in the concrete box girder bridge can be treated individually by using folded plate analysis or a similar procedure. This does not, however, mean that approximate design methods could not be developed for this type of bridge.

CHAPTER 2: COMPARISON OF FIELD TEST RESULTS WITH THEORETICAL STUDIES

GENERAL

The validity of the use of any theoretical procedure for predicting load distribution characteristics can be determined by comparing the results obtained from field tests of bridges to similar results as predicted by the theory. The research outlined herein was conducted for that purpose. The results show the validity of the theories selected. In this investigation the procedures used for determining the distribution in beam and slab bridges (5) and in multi-beam bridges (261) were studied. However, the method of analysis used for studying concrete box girder bridges was not used to investigate actual bridges because of the verification provided by Scordelis in the procedure development (222, 224).

A literature search has indicated that existing work dealing with load distribution in beam and slab and multi-beam highway bridges can be separated into two categories: reports of experimental investigations on prototype and model bridge structures, and theoretical investigations on idealized structures. Although load distribution tests have been conducted on both model and actual highway bridges, only experimental research dealing with prototype bridge structures was considered for verifying the procedures for actual conditions. Much of the experimental work stems from dynamic studies of highway bridges. Only the results obtained for calibration of these bridges were considered since results usable for predicting static load distribution are obtained only at static or creep speeds (0 – 5 mph). Another important but limited source of field test data is reports dealing solely with static or creep loading.

It can be seen in the bibliography that there have been numerous field tests of beam and slab bridges reported in literature. These studies of highway bridges can be categorized according to the type of supporting beams. The most numerous experimental reports deal with bridges with reinforced concrete deck slabs supported by steel beams. The beam and slab system is constructed as either composite (connected by shear transfer devices) or noncomposite. Prestressed concrete beams composite with a reinforced concrete slab form the second type of bridge studied. Reinforced concrete beams monolithic with a concrete deck is the third type of bridge studied experimentally. In all beam and slab bridge types, transverse beams, bulkheads, cross-bracing or diaphragms are usually present. A detailed study was conducted of eleven bridges covering all types of the beam and slab bridges listed. However, in this summary report, only results of three typical bridges are discussed in detail. The studies of the remaining bridges are discussed in Reference (5).

The number of reported tests on multi-beam bridges is very limited. In addition, some of the reported results are for bridges with substantial skew and, thus, are not of significant value. In verifying the validity of the theoretical procedure used, the results of four test bridges were analyzed (261). The study of three of these is presented herein to indicate the general trend of the results.

In each case, the theories proposed for the type of bridge being studied were used to determine the moments in each beam element for the particular loading on the bridge. The results of these analyses were then compared with the results of the field test to determine the validity

of the procedure in predicting actual behavior. The comparisons are shown using moment or deflection distribution coefficients, i.e. the individual beam moment or deflection divided by the average moment or deflection. These coefficients were used to normalize the plots for ease in comparison.

BEAM AND SLAB BRIDGES

The studies of the three bridges discussed in detail cover the cross section of bridge types generally constructed. The bridge types included are:

1. a prestressed concrete "T" beam bridge with the top flanges forming the roadway,
2. a two lane composite concrete deck and rolled steel I-beam bridge, and
3. a simple span structure consisting of a reinforced concrete slab composite with box-section prestressed concrete longitudinal girders.

The overall investigation (5) also included four of the beam and slab bridges constructed and tested as part of the AASHO Test Road at Ottawa, Ill. (278). One bridge of each of the four generally designed types was studied: 9-A, a noncomposite steel wide-flange beam bridge; 2-B, a composite steel wide-flange beam bridge; 7-A, a reinforced concrete beam bridge; and 5-A, a prestressed concrete beam bridge. In addition, four other steel beam bridges (15, 82, 101, 103) were considered. These included:

1. a 41 ft composite slab and beam, simple span bridge,

2. two separate, but identical, 67.5 ft bridge spans from multi-simple span structures; each consisting of 4 longitudinal girders composite with a concrete slab, and
3. a 45 ft simple span portion of a four-span system composed of four rolled beams supporting a noncomposite concrete slab.

The distribution of moments in each of these bridges was analyzed using both orthotropic plate theory and harmonic analysis. These two theories were selected because of their application to the broad range of beam and slab bridges and the availability of generalized functions to predict behavior. The application of these theories to actual test bridges assumed the properties of the cross sections conformed to the following assumptions of the theories.

1. The bridge is rectangular in plan.
2. All beams and diaphragms are evenly spaced.
3. All beams are of equal stiffness.
4. All diaphragms are of equal stiffness.
5. All beams and diaphragms are prismatic.
6. The deck slab does not contain joints or hinges.
7. The bridge behaves elastically.

In addition, for the particular solutions of the governing equations, the following support conditions were also assumed: two opposite edges are simply supported and the other two edges are free. The development of the two theories is presented in the next chapter and in Appendix A. However, the relationship between the theoretical and experimental results is presented in this chapter to show the validity of the theories in predicting load distribution. The procedures used

for calculating the geometrical parameters used in the theories are given in Appendix B.

The general trend of the results can be seen by examining in some detail the comparisons of theoretical and experimental behavior for three of the bridges studied. The results are typical of all bridges studied.

Shawan Road Bridge (183)

This bridge, as shown in Figure 4, was built of nine prestressed concrete "T" beams placed side by side so that the top flanges form the roadway. This structure is not a multi-beam bridge due to the presence of full transverse prestressing cables in the top flanges of the beams and through the diaphragms. The bridge is 36.5 ft wide and spans 100 ft. Interior diaphragms are located at the quarter-span points. The diaphragms are monolithic portions of the longitudinal girders and are post-stressed together.

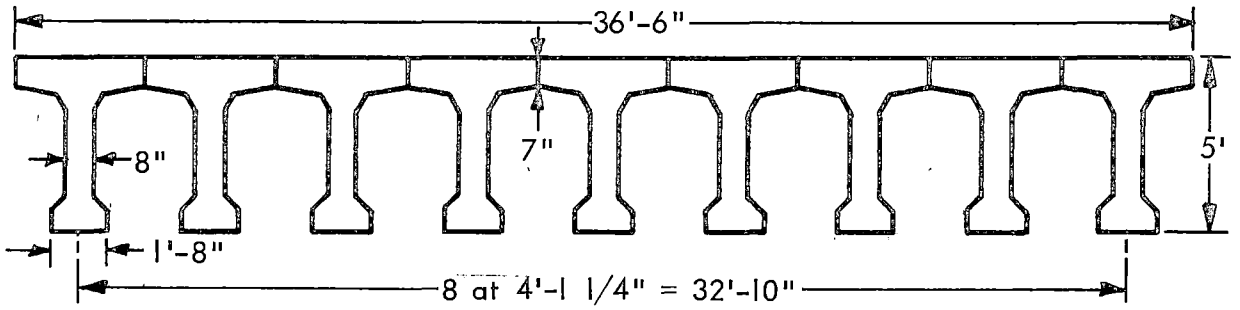

NOTE: EXTENSIVE TRANSVERSE PRESTRESSING IN EFFECT MAKES TOP FLANGES ACT AS CONTINUOUS TRANSVERSE SLAB

Figure 4. Cross section of Shawan Road prestressed concrete beam bridge.

The results of the analysis, shown in Figure 5, indicate good agreement between both theoretical procedures and the moments obtained

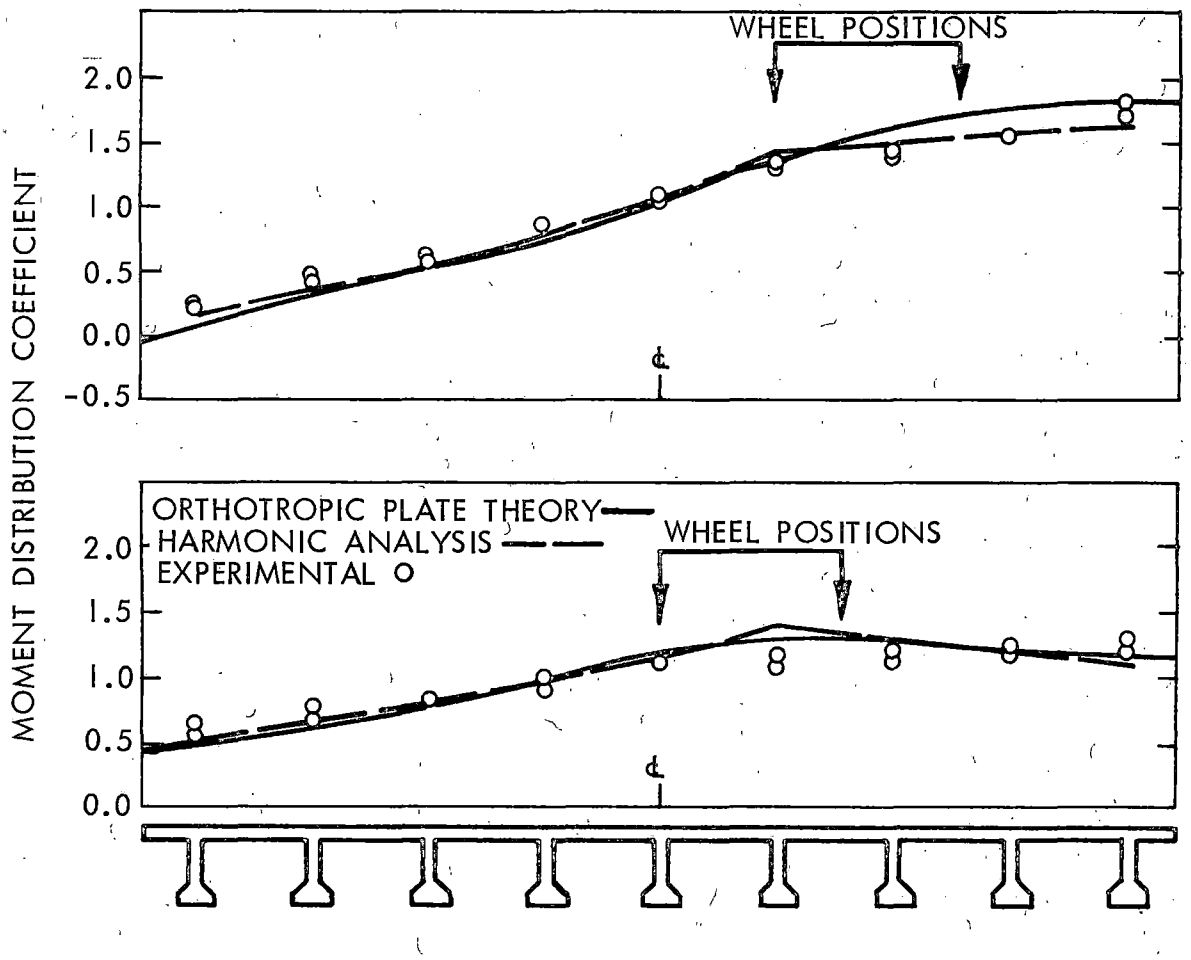

Figure 5. Transverse moment distribution in Shawan Road Bridge.

from strain readings on the actual bridge. In the vicinity of the load the harmonic analysis does, however, predict moments about 20 percent higher than the experimental moment for the central loading, but about 10 percent lower for the eccentric loading.

In addition to the wheel positions shown in the figure, two other tests with eccentric loadings were conducted. Combining the results of one of these with those presented in Figure 5, a loading pattern similar to that expected from the current AASHO loading criteria can be obtained. In this case, the maximum moment coefficient (i.e. the ratio of the

individual beam moment to the average beam moment) was 1.232 and occurred in the outside girder. The orthotropic plate theory predicted a coefficient of 1.282 (a + 4.5 percent error) and the harmonic analysis one of 1.178 (a - 4.4 percent error). The current AASHO distribution formula would have predicted a coefficient of 1.680 or 35 percent higher than that actually obtained from a loading similar to that expected from the specifications.

Holcomb Test Bridge (82)

This bridge, located in Ames, Iowa, is a two-lane 71 ft bridge composed of four rolled beams supporting compositely an 8 in. concrete slab. The details of the bridge cross section are shown in Figure 6. The 16WF36 transverse interior diaphragms are located at the third span points.

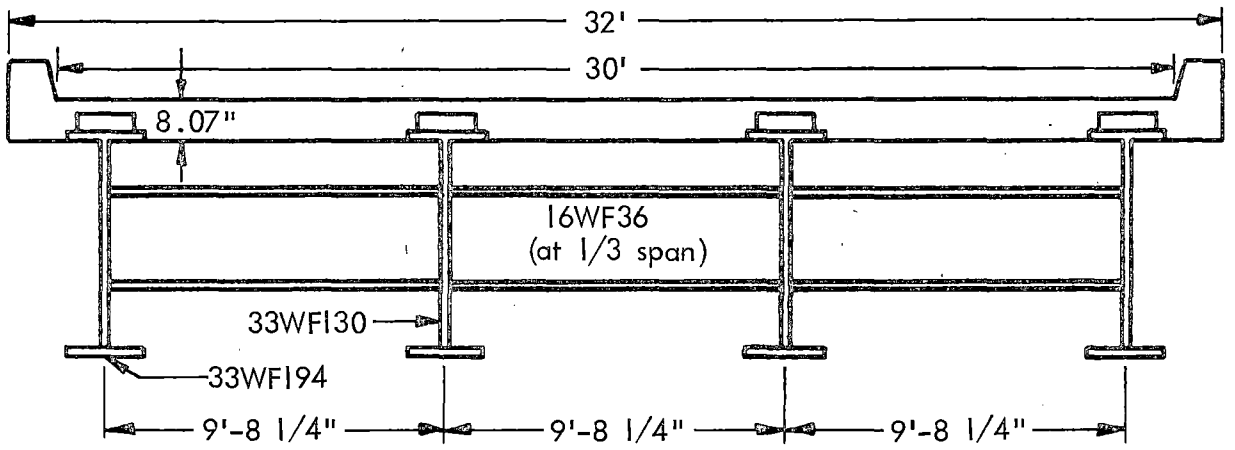

Figure 6. Cross section of Holcomb field test bridge.

The results of the comparative analyses are shown in Figure 7. It can be seen that for the central loading that the two theories compare favorably with the experimental results. However, for the wheel loads in

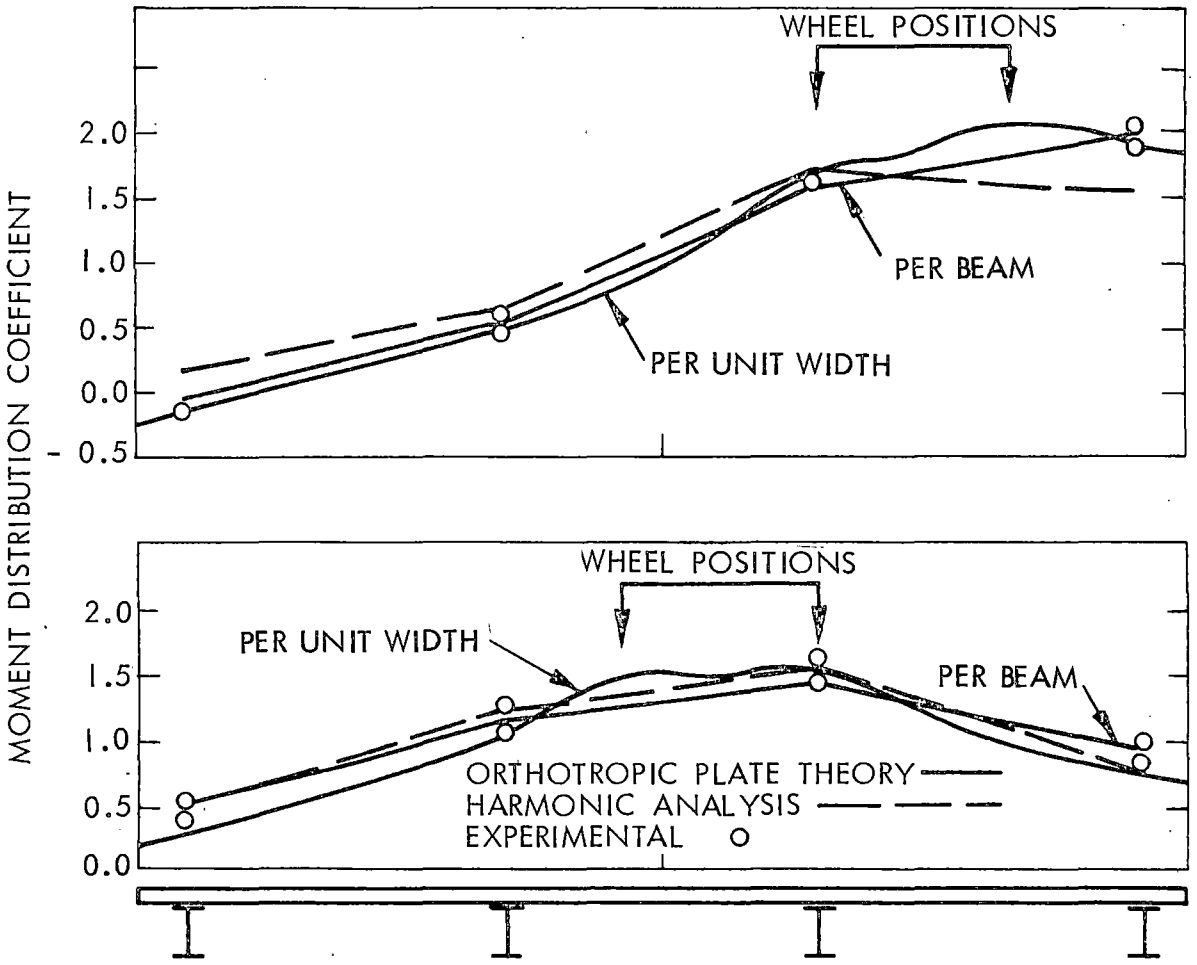

Figure 7. Transverse moment distribution in Holcomb test bridge.

an eccentric position, the orthotropic plate theory predicts the behavior, whereas the harmonic analysis underpredicts the maximum beam moment by 21 percent (moment distribution coefficient of 1.920 vs 1.518). The results from the orthotropic plate theory are shown on both a per foot basis and a per beam basis. The per beam coefficient is simply obtained by integrating the area under the distribution coefficient per foot curve over a width of half the distance to each adjacent beam and normalizing the answer.

Four additional tests were conducted: one with a single truck and the other three with two trucks for the loading.

The results for these tests were similar with both theories predicting behavior favorably for the central loadings, whereas for eccentric loadings the harmonic analysis significantly underpredicts the maximum beam moment.

For the loading which corresponds most closely to the AASHO loading, the maximum moment distribution coefficient obtained from the field test was 1.490 for an exterior beam. Using the current AASHO procedure, the coefficient would be 1.761; whereas from the orthotropic plate theory the maximum coefficient was 1.554; and from the harmonic analysis it was 1.278. It can be seen that the results of the AASHO procedures are 18 percent higher than the field test result and the harmonic analysis is 14 percent lower, while the orthotropic plate accurately predicts the maximum moment.

Drehersville Bridge (44)

This is a simple span structure consisting of a 6.7 in. reinforced concrete slab composite with five identical box-section prestressed concrete longitudinal girders. The overall width of this structure, as shown in Figure 8, is 35.5 ft and the span is 61.5 ft. Each beam is 33 in. deep by 48 in. wide and consists of 5-in. vertical and bottom walls with a 3-in. top wall. A 10-in. thick cast-in-place transverse diaphragm is located at midspan.

The results of the comparisons are shown in Figure 9. For both the central loading and the eccentric loading, the coefficients predicted by both theories are in good agreement with the field test results. However, for the combination of truck loads which most nearly conform to the AASHO loading, the maximum moment distribution coefficient from the

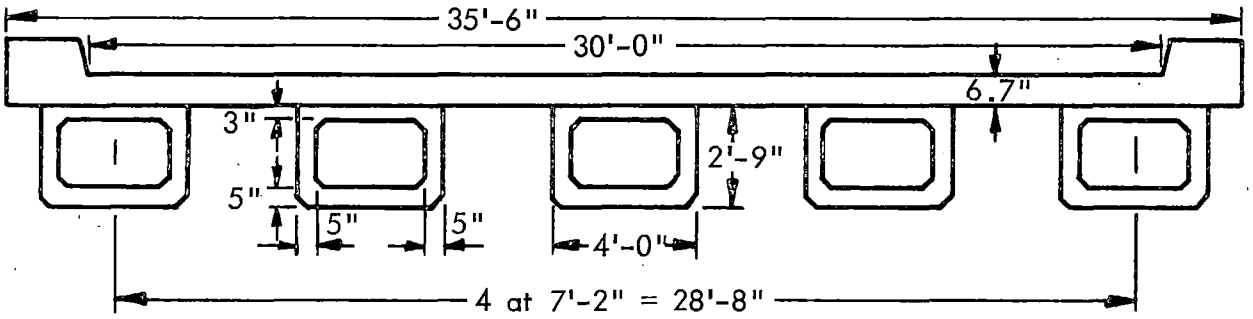

Figure 8. Cross section of the Drehersville Bridge.

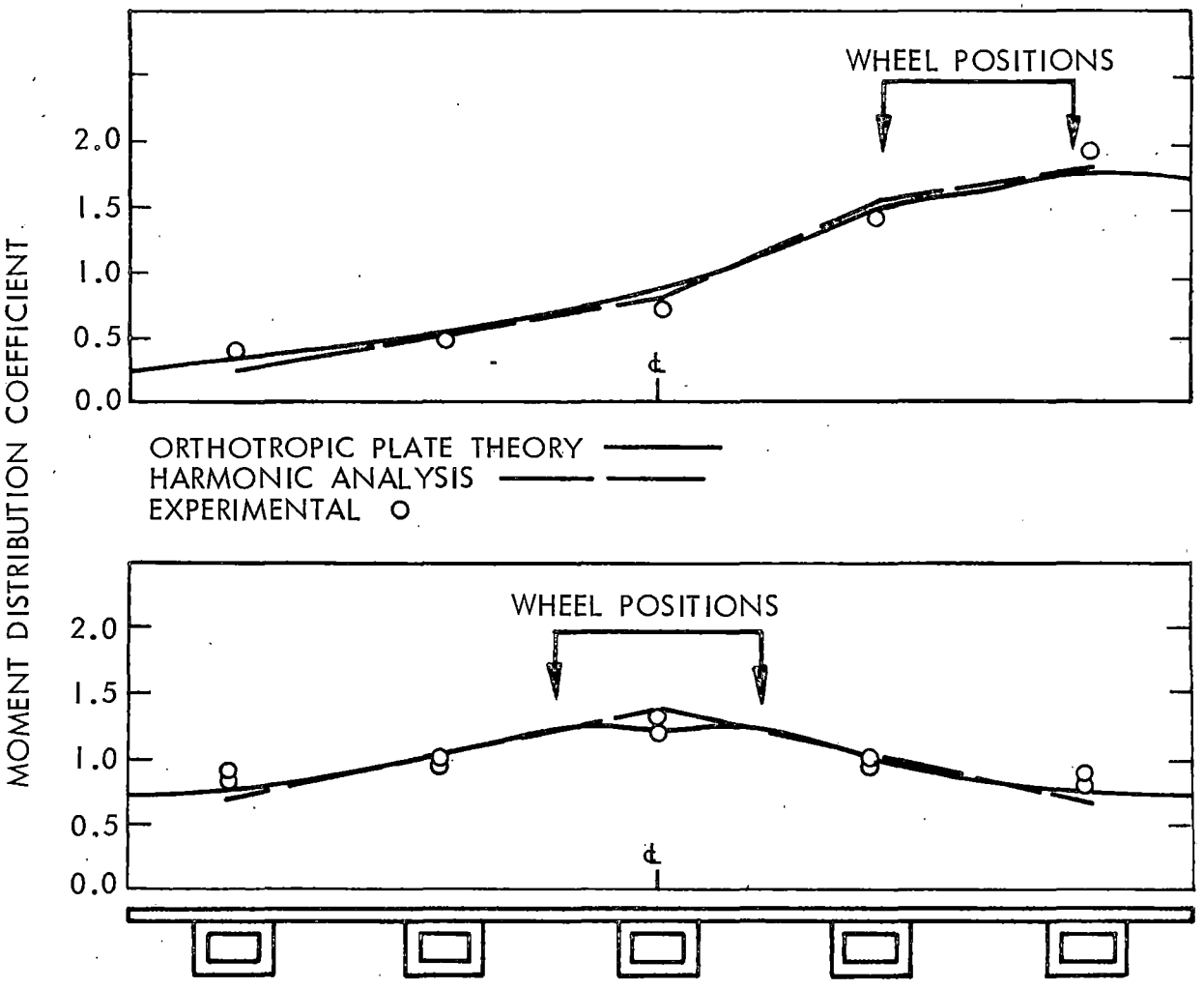

Figure 9. Transverse moment distribution in the Drehersville Bridge.

field tests was 14 percent less than that predicted by the current specifications, but 10 percent above those from the two theories.

In the studies presented herein, three major beam and slab bridge types are represented by comparisons of experimental results with analytical predictions of beam moments. In addition, similar results were obtained from comparison for eight other bridges consisting of either steel beam and concrete deck bridges or nonvoided prestressed and reinforced concrete beam and concrete deck bridges. When all loading conditions for all test bridges are examined, the following conclusions are found:

1. Of the total of 18 maximum beam moment cases considered, orthotropic plate theory predicted 11 moments conservatively (positive error) while harmonic analysis predicted five moments conservatively. The conservative harmonic analysis predictions were all within 10 percent of the field test results, while all orthotropic plate predictions were in error by less than 10 percent except two which were 12 and 28 percent in error.

2. Harmonic analysis predicted thirteen unconservative moments (negative errors) of which seven errors were between 10 and 20 percent, with the remaining errors less than 10 percent. Orthotropic plate theory predicted seven unconservative moments when compared to the field test results with all less than about 10 percent in error.

It can be seen from the above summary that harmonic analysis predicted unconservative maximum moments more frequently with errors of greater magnitude. The converse is true of the conservative results. Table 1 presents the maximum moment error for all bridges.

TABLE 1

MAXIMUM BEAM MOMENTS, AVERAGE ERRORS[a]

	ORTHOTROPIC PLATE THEORY		HARMONIC ANALYSIS		AASHO	
	POS. ERROR	NEG. ERROR	POS. ERROR	NEG. ERROR	POS. ERROR	NEG. ERROR
	Single truck loads					
Avg error	10.6	4.7	8.6	8.4	—	15.4
Tests run	6	5	4	7	0	4
	2 truck loads superimposed					
Avg error	6.5	5.7	2.6	10.3	23.2	—
Tests run	3	2	1	4	5	0
	2 truck loads as measured					
Avg error	3.2	—	—	18.6	7.3	—
Tests run	2	0	0	2	2	0

[a]For all beam and slab bridges analyzed.

From the comparisons presented herein and those also presented by Arendts (5), it can be seen that the shape of the predicted moment coefficient curves from orthotropic plate theory is in close agreement with the experimental distributions. However, not only are some of the harmonic analysis distribution curves not consistent with the experimental distributions, but all the maximum moments occurred at interior girders, although test results place the maximum moment at the exterior girder. In fact, most of the harmonic analysis comparisons tended to underpredict the exterior beam moments, especially for loads with large eccentricities.

From these results, it is felt that the orthotropic plate theory is the more accurate of the two theories considered. This conslusion is

based on the accuracy of the prediction of the maximum bean moment, the beam location of the maximum moment, and the general distribution curve. Furthermore, the procedures used for determining the stiffness parameters, as presented in Appendix B, are felt to accurately represent the behavior of the types of beam and slab bridges studied. It is obvious that both an accurate analytical procedure and an accurate method of computing stiffness parameters are necessary for satisfactory comparisons. The comparisons of experimental results and theoretical predictions support this conclusion. However, it is felt that the harmonic analysis is still a valuable tool to use as a check for the validity of the orthotropic plate theory in ranges of variables beyond those considered in the field test comparisons.

The results of comparison of the current AASHO distribution procedure with the individual test results and the summary in Table 1 showed that the current procedures are inconsistent with experimental results. The comparison showed that the average errors were + 15 percent for single truck loads and + 23 percent for two truck loads superimposed. However, for individual bridges, the AASHO predictions ranged from very conservative (+ 35 percent error) for two-lane bridges to unsafe (- 23.8 percent error) for the one-lane AASHO Road Test Bridges. Also, only two AASHO predictions were relatively accurate (less than 10 percent error) and one of these was unconservative. These results show that a new design procedure is vitally needed to accurately predict load distribution by considering more fully the overall behavior.

MULTI-BEAM BRIDGES

The number of field tests and large-scale laboratory tests of multi-beam bridges is limited. After an extensive literature search, reports of only four such tests that were applicable to this study were located. These are summarized in Table 2. It can be seen that, although the number of tests is small, the types of cross sections investigated do include the three most commonly used multi-beam systems. The results of the tests of the three actual bridges will be discussed in some detail to show the accuracy of the theoretical procedure in predicting behavior. A complete analysis of all four tests is presented in Reference (261).

The behavior of each of these bridges was predicted using the articulated plate theory. This theory has also been used by other investigators to analyze similar bridges (6 – 8). It was selected initially because of the good relationship of the assumptions in the analysis with the structural geometry and, also, because of the similarity of parameters with the plate theory and harmonic analysis considered for beam and slab bridges. A detailed outline of the theory is given in Chapter 3 and Appendix A. The procedures used in computing the geometrical parameters are presented in Appendix B.

The validity of the proposed procedures can be seen by examining the results of the comparison of the moment distribution coefficients obtained from the theory and parameter calculations and from the field test results for each of the three bridges.

TABLE 2

DIMENSIONS AND CHARACTERISTICS OF THE MULTI-BEAM BRIDGES TESTED

NAME	SPAN LENGTH	NO. OF BEAMS	BRIDGE WIDTH	CROSS SECTION	SHEAR KEY	TRANSVERSE PRESTRESS	SCALE	LOADING SYSTEM	MEASUREMENT
North Carolina	30'-0"	10	25'-6"	Channel curb: 9" PC beams	Mortar	At 7 locations, up to 18,900 psi each	Full	22FG Corbett truck 18.72 t/truck	120 strain gauges (SR-4), deflection dials of 0.001" least reading
Centerport	32'-0"	9	27'-0"	Solid with 2 circular holes curb: 8" RC beams	Dry-packed mortar	No prestressing in transverse direction, a 2 in. ϕ tie rod at E	Full	Scale truck and tractor trailer truck and hydraulic jacks	Control gauges, level bar readings
Langstone	31'-0"	16	34'-0"	Solid PC beams curb + footpath: 5'-5"	Dry-packed mortar	0.2" ϕ Freyssinet cables at 12 points	Full	Two bogie vehicle total load: central loading 20.8 — 90t eccentric loading 60.7 — 90t	39 Ames dial gauges of 0.001 to 0.001 least reading, level bars, strain gauges
Lab. test by Best	17'-10"	12	11'-10"	Solid PC beams	Mild-steel shear loops	None	1/4	Hydraulic jack: pads; 3-3/4" X 1-1/2", up to 18 tons	6 dial gauges, 8' Demec gauges (strain gauges)

North Carolina Bridge (23)

This test bridge is composed of 10 precast, prestressed concrete, channel beam elements. The cross section of the bridge is shown in Figure 10. The shear connection consists of a tongue and groove type of key, triangular in shape, which was packed from the top with a jute fiber and grouted to prevent the asphalt seal from entering the joints. The interior members are channel sections and prestressed longitudinally with five cables of 7/16 in. diam in each stem; the exterior members were constructed by casting a curb to an interior beam element.

The comparison of the distribution coefficients from the theory with those from the field test results is shown in Figure 11. It should be noted that because of damage to the strain gauges during loading, the distribution coefficients from the field test are based on the deflection gauge readings. The theoretical distribution is, however, based on the beam moments. The field test experiment showed that the change of prestress force significantly affects the distribution of wheel loads as can be seen from the widely scattered experimental values. In addition, the prestress force reduces the coefficient near the loading points. When the average experimental values are considered, the results have reasonably good correlation with the theory.

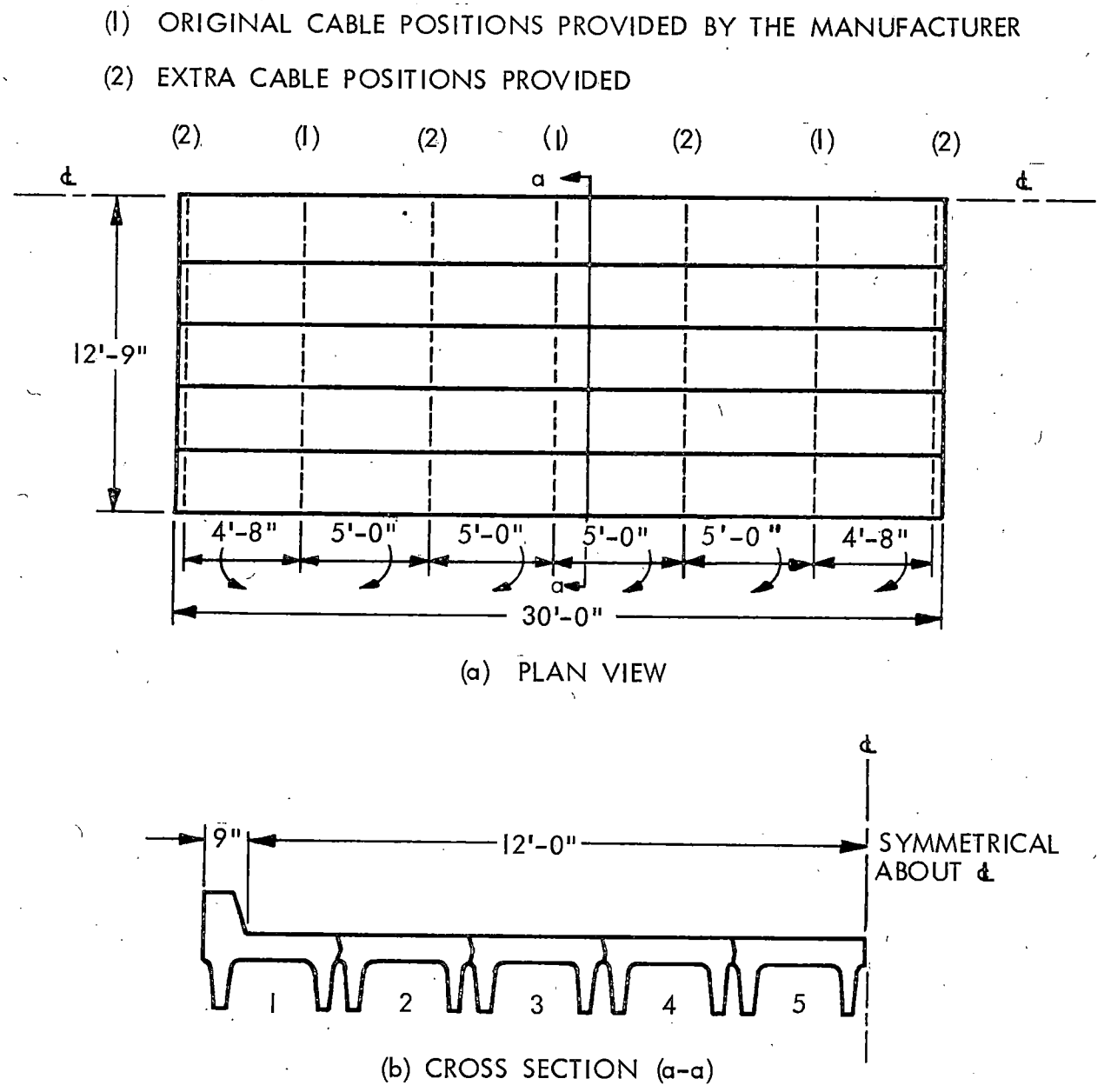

Figure 10. Details of North Carolina Bridge.

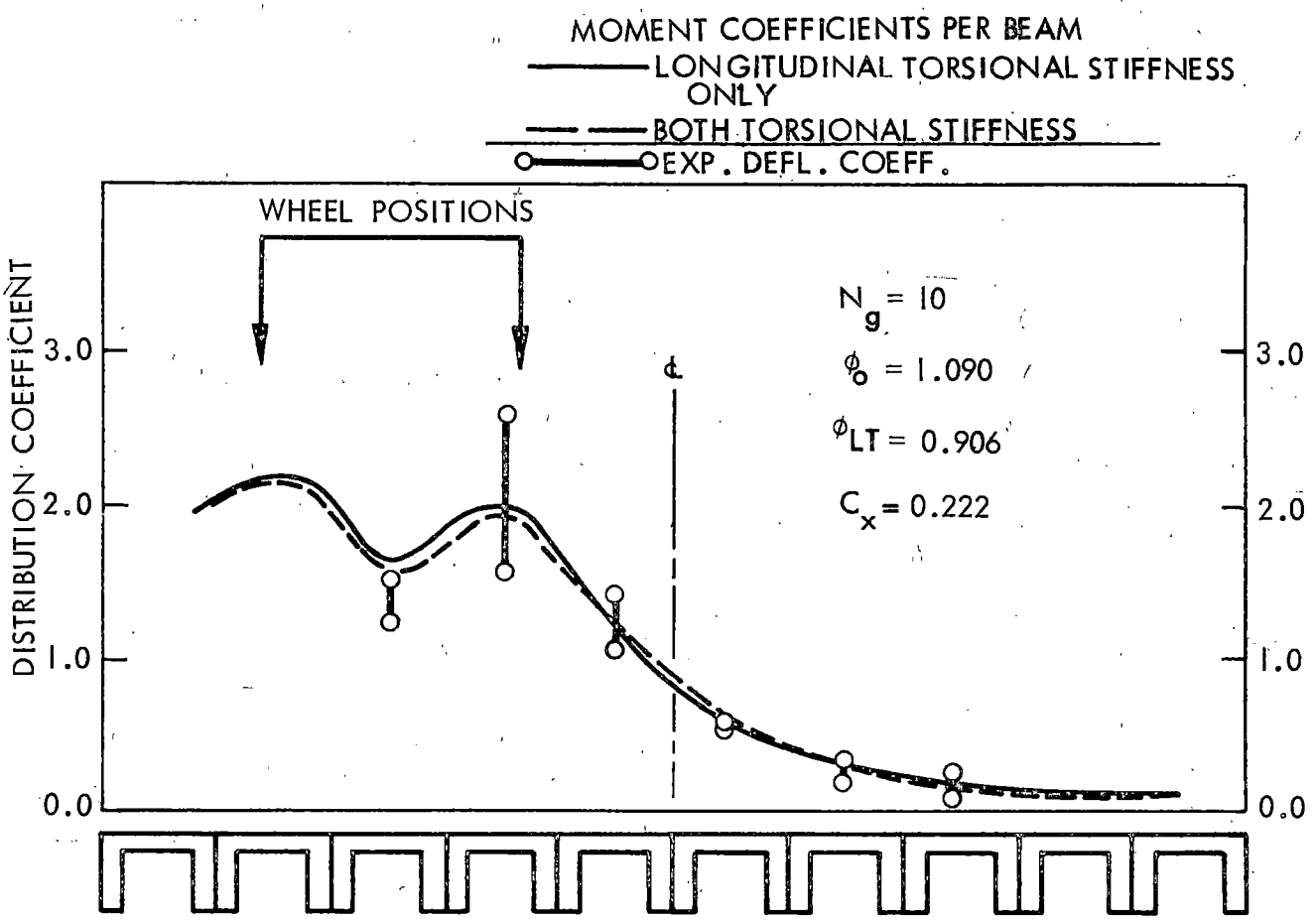

Figure 11a. Distribution coefficients for a single truck load, North Carolina Bridge.

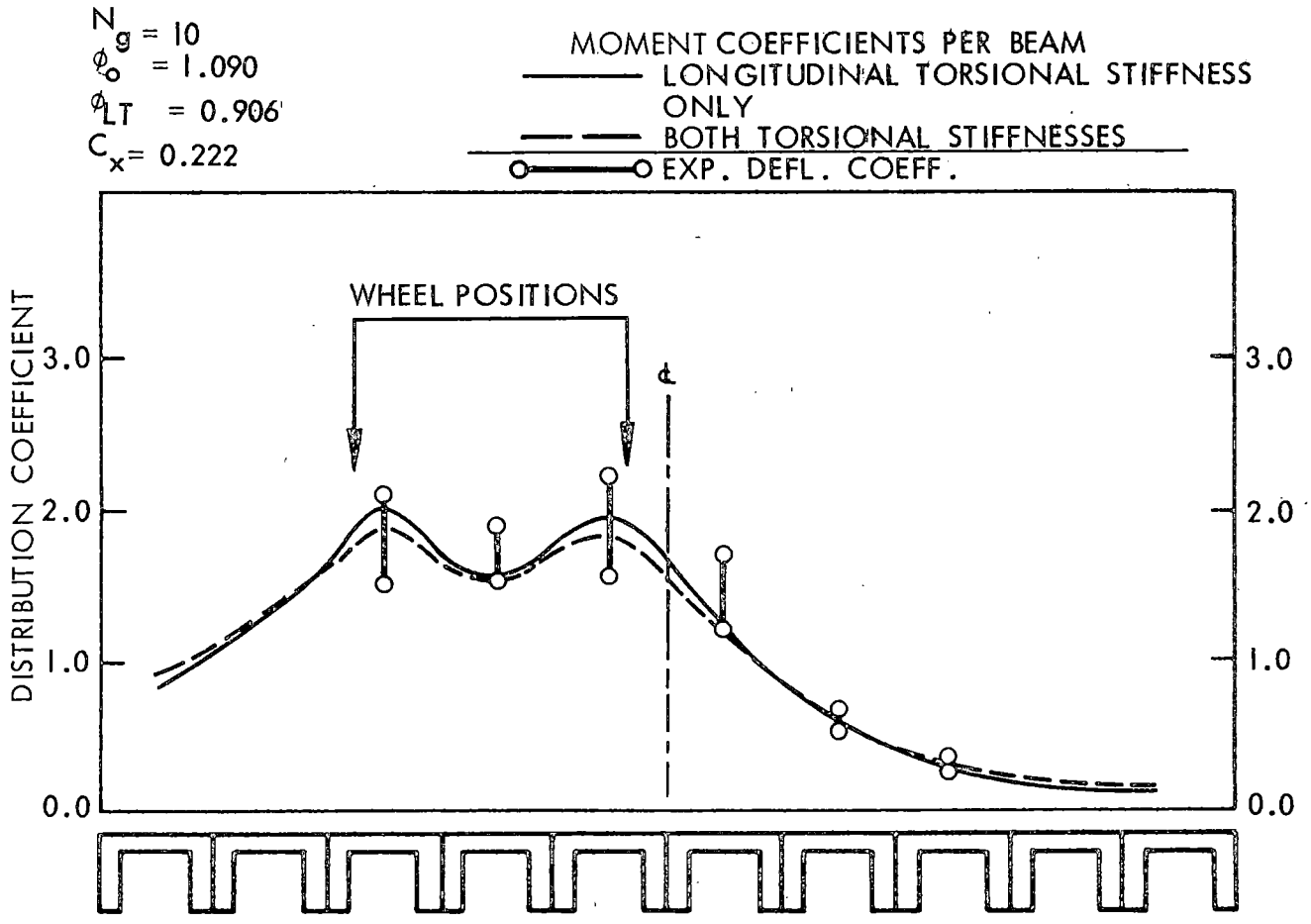

Figure 11b. Distribution coefficients for a single truck load, North Carolina Bridge.

Centerport Bridge (204)

This test bridge is composed of nine precast, prefabricated beam elements. It has a clear span of 32 ft and a width of 27 ft. These beam elements were placed side by side, as shown in Figure 12, and connected by dry-packed mortar and a steel bolt at the midspan. Each beam element had a cross section of 36 in. X 21 in. and an overall length of 35 ft-6 in. The rectangular cross section had two hollow circular cores of 12-1/2 in. diam.

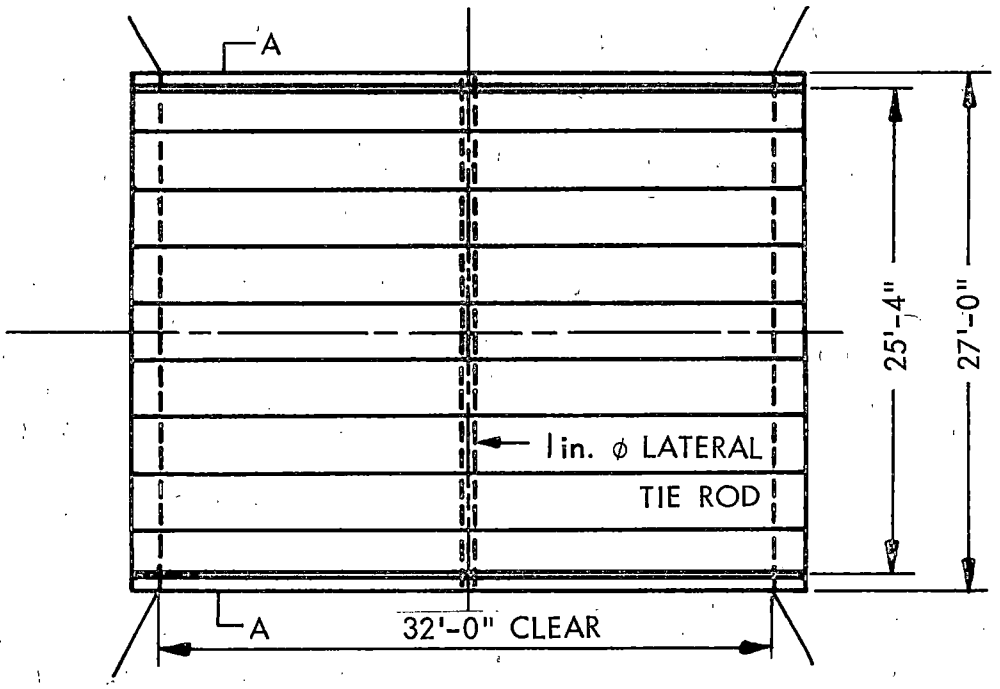

(a) PLAN VIEW

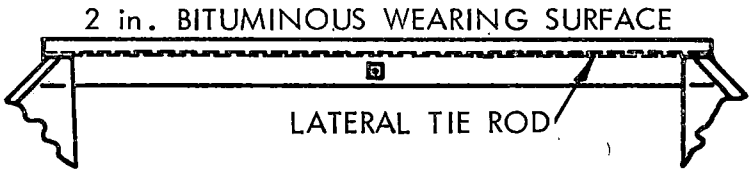

(b) ELEVATION VIEW

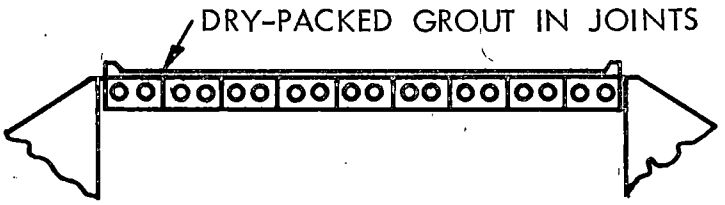

(c) CROSS SECTION A-A

Figure 12. Details of Centerport Bridge.

The results of the comparison of theoretical and experimental moment distribution coefficients are shown in Figure 13a and b. The maximum deflection coefficients by experiment turned out to be roughly 10 to 20 percent higher in average than the theoretical deflection values. Also, the range of the experimental coefficients at or near the loading positions was roughly 20 percent of their average ordinates. However, the experimental coefficients were in good correlation with the theoretical moment coefficients per beam. It should be noted that the effect of the transverse torsional stiffness was so small compared with the stiffness in the longitudinal direction that the difference between the theoretical distribution coefficients corresponding to both torsions and to longitudinal torsion only was hardly recognizable.

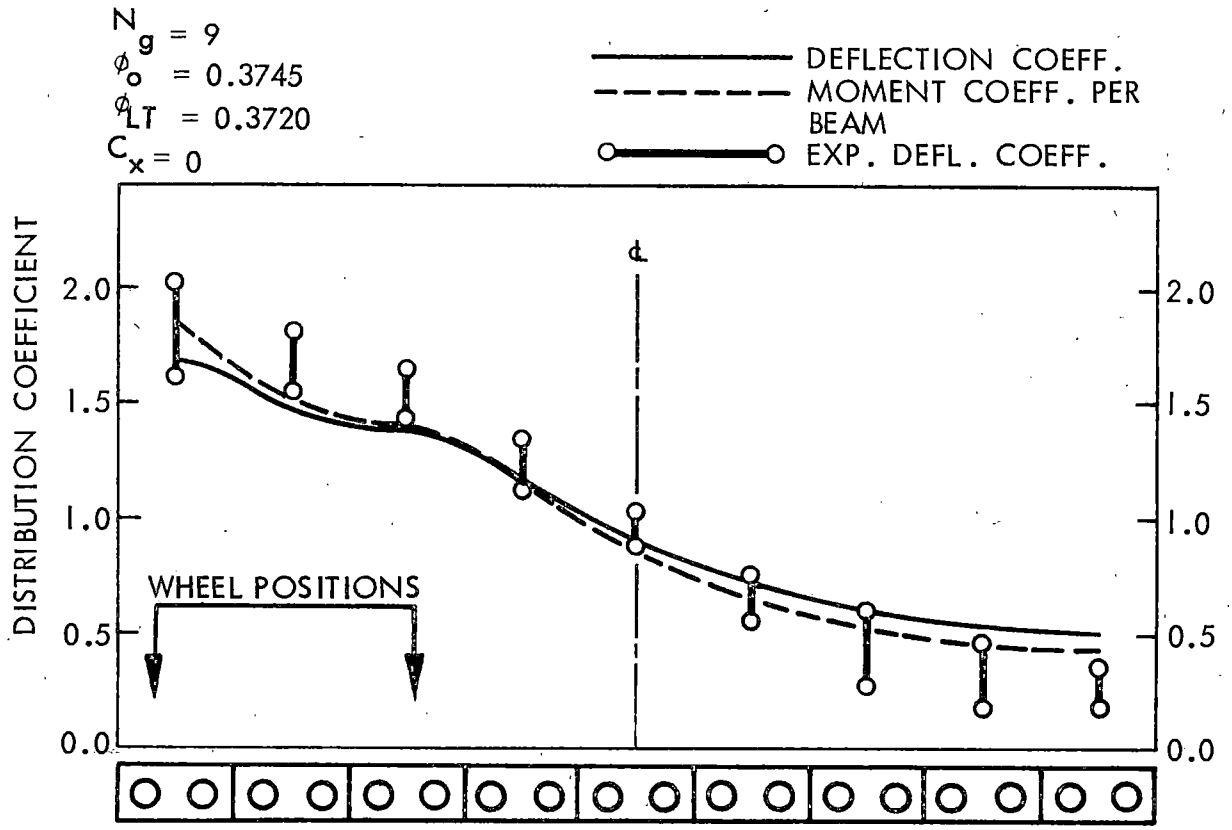

Figure 13a. Distribution coefficients for a single truck load, Centerport Bridge.

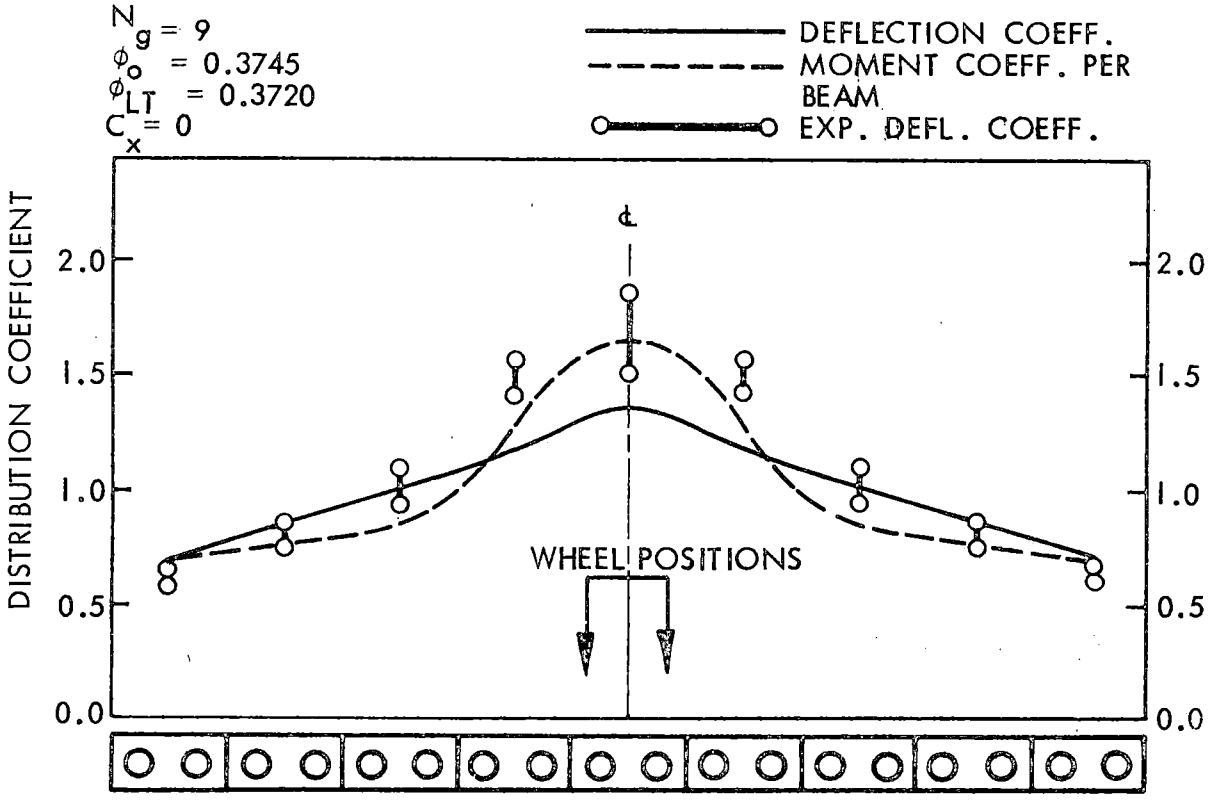

Figure 13b. Distribution coefficients for two jack loads, Centerport Bridge.

Langstone Bridge (202, 204)

This bridge comprises twenty-nine simply supported beams, each of 31 ft effective span. Each beam element, as shown in Figure 14, was 18 in. in depth and 18 in. in width. Sixteen elements were placed side by side jointed with a dry-packed mortar and transversely stressed with twelve cables. This bridge has two prestressed concrete "fascia" beams at the edges. The bridge was loaded with two bogie loads consisting of eight solid wheels on two axles. Two loading patterns were considered: one pattern yielded a symmetric loading with respect to the middle line of the bridge, while the other was such that the external wheels were one ft from the curb.

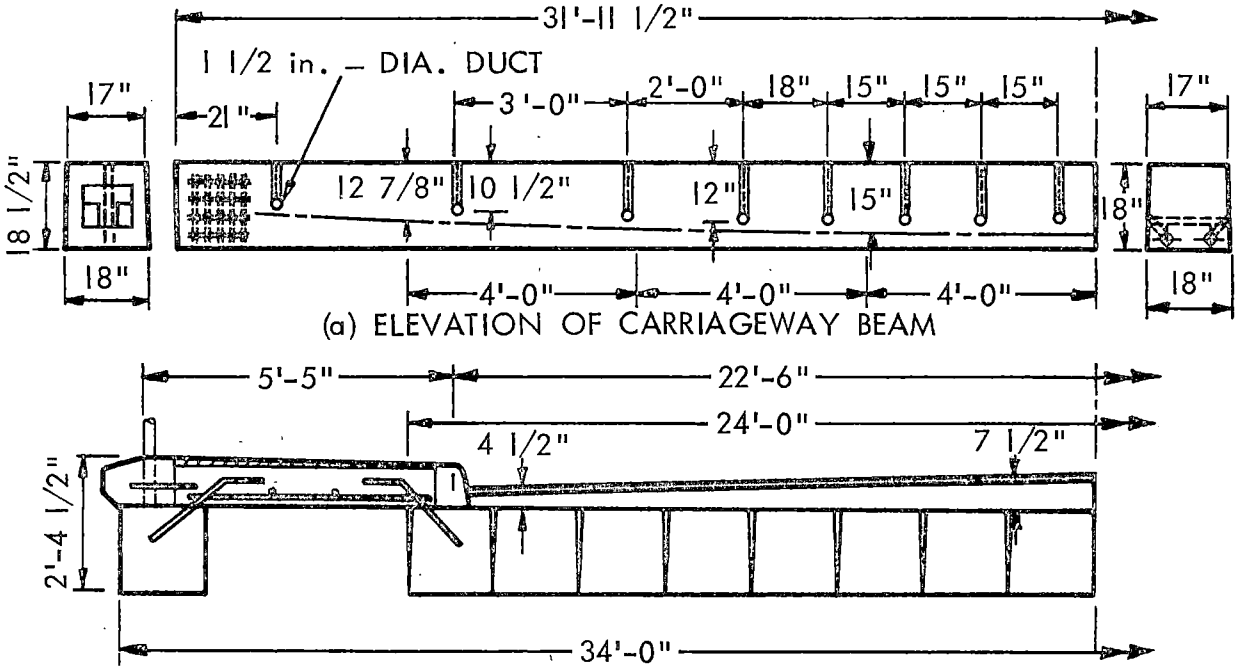

Figure 14. Details of Langstone Bridge.

The comparisons of the distribution coefficients as predicted by applying the articulated plate theory to the properties of the actual loaded bridge with those obtained in the field test are shown in Figure 15. The theory was applied only to the sixteen beam elements carrying the roadway without regard to the edge beams. The results are in good agreement with the theory. Furthermore, when the theory is based on the single torsional rigidity in the longitudinal direction, the maximum error was less than 5 percent for the central loading, while 15 percent for the eccentric loading. If both the transverse and the longitudinal torsional rigidities are taken into account, the maximum error was found to be around 10 percent for the central loading and almost none for the eccentric loading.

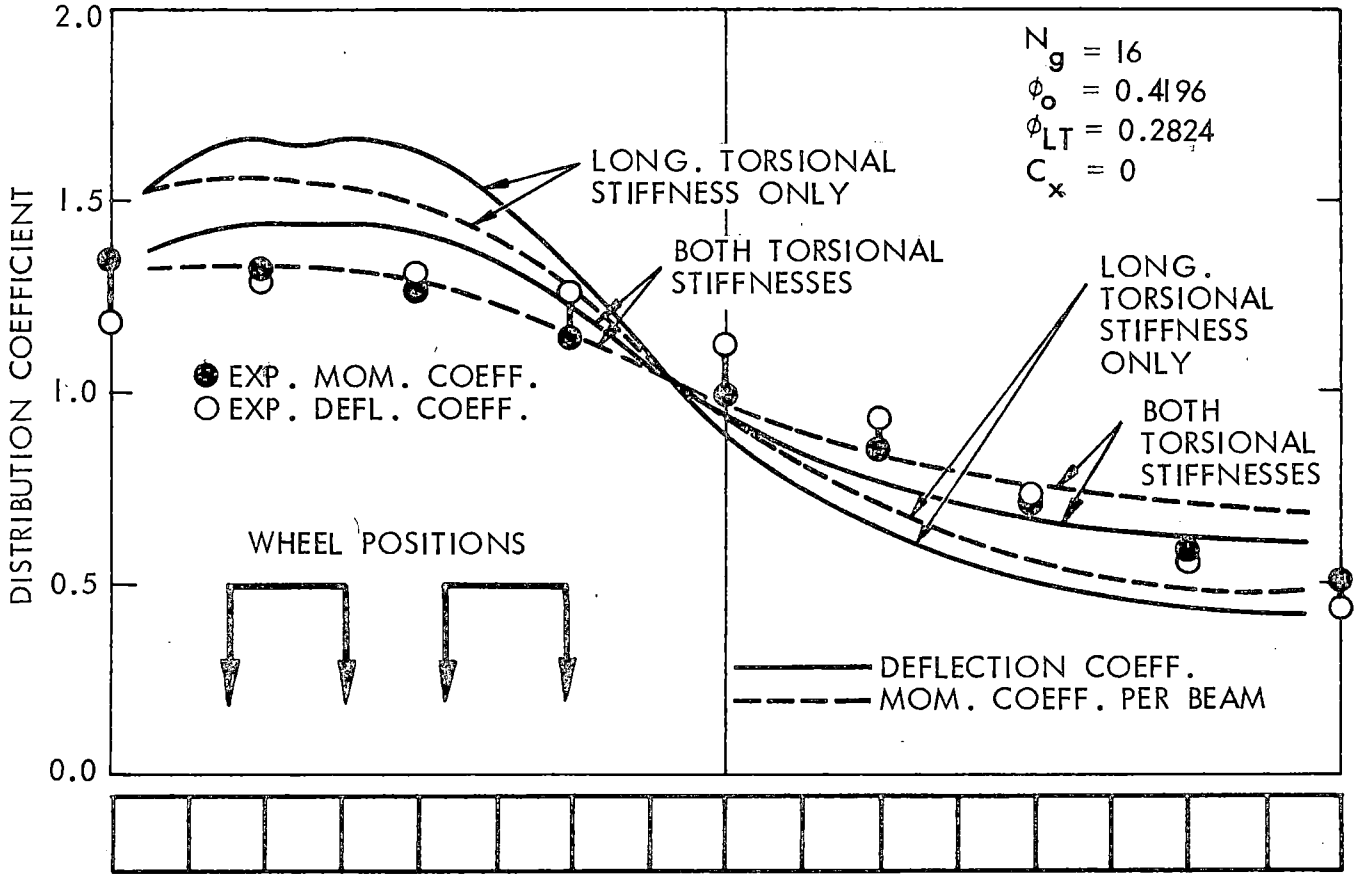

Figure 15a. Distribution coefficients for two truck loads, Langstone Bridge.

In summary, the comparison of test results with theory for all three bridges shows relatively good correlation of the theory with the tests. The theory tends to underpredict the maximum bending moment in most cases by less than 10 percent. In some cases, though, the error was up to 20 percent. However, it is felt that the articulated plate theory as developed herein has sufficiently predicted the behavior. The only other major theory considered, that proposed by Arya and others (6 – 8), predicted even lower moments than those obtained from the theory used in this investigation. Thus, the articulated plate theory as outlined in Chapter 3 was used for the study of multi-beam bridges.

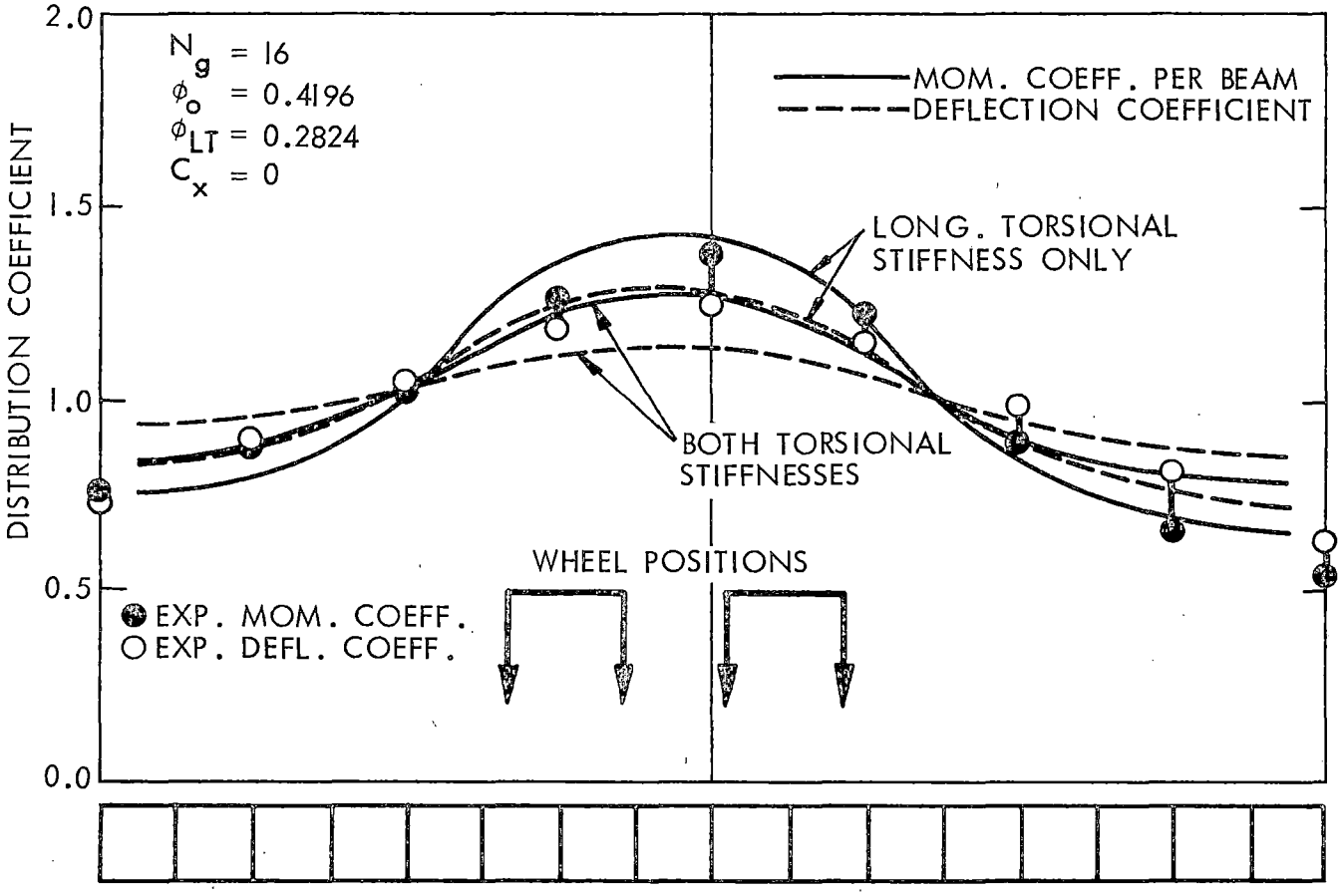

Figure 15b. Distribution coefficients for two truck loads, Langstone Bridge.

CONCRETE BOX GIRDER BRIDGES

As mentioned earlier, the theory considered for the study of concrete box girder bridges is based on the theory of prismatic folded plates developed by Goldberg and Leve (57). The solution procedure was developed by Scordelis of the University of California at Berkeley (222). To indicate the validity of this theory for predicting the bridge behavior, an analysis was made by Scordelis of the results obtained from the test of the Harrison Street undercrossing (39). In addition, studies were

also made of the following California bridges: the La Barranca Way Undercrossing, the College Avenue Undercrossing, and the Sacramento River Bridge and Overhead. The details of these studies are presented by Scordelis (222).

The validity of the theory to predict the behavior of concrete box girder bridges has been shown in the development of the theory.

SUMMARY

The validity of the theories proposed for the study of the behavior for each type of bridge considered in this investigation has been demonstrated in this chapter and in supporting work (5, 222, 261). Thus, for the studies of the effect of variations in loading pattern and bridge geometry on load distribution, the theories as outlined have been used.

1. Beam and slab bridges: Orthotropic plate theory. However, harmonic analysis has been used to verify results when studies are made in ranges extended beyond those studied in field tests.
2. Multi-beam bridges: Articulated plate theory.
3. Concrete box girder bridges: Theory of prismatic folded plate structures.

CHAPTER 3. ANALYTICAL STUDIES ON THE EFFECTS OF VARIABLES

GENERAL

Extensive analytical studies were conducted to determine the theoretical load distribution characteristics of each type of bridge considered in the program. The studies of these bridges encompassed the range of each of the variables that probably will occur in practice in each bridge type. The initial analytical results provided the transverse variation of the longitudinal beam moment for numerous transverse positions of a single wheel, i.e. influence lines were generated. Thus, any combination of specific wheel positions could be considered for the determination of maximum beam moments. The use of these influence lines in combination with all of the loading conditions possible under the loading criteria yielded the maximum design moments.

The direct use of moments as a specification criteria would require significant changes in the design procedures. However, there is a direct relationship between the beam moment and the width over which a wheel load is distributed. This width is, in fact, used in the current specification in the distribution load factor equation, S/D. Thus, results of the load distribution studies were expressed in terms of D, the width of bridge over which one longitudinal line of wheels is distributed. If a satisfactory relationship between all of the variables and this width can be obtained, a more accurate and realistic distribution could be obtained without significantly altering the general distribution procedure.

In this chapter, a brief outline of the analytical procedures used to develop the extensive results is provided. In addition, summaries of

the results obtained are given. Since there is significant variation in the analysis and behavior of each bridge type considered, the discussion of each bridge type is treated separately.

BEAM AND SLAB BRIDGES

Development of Theories

There are numerous theoretical methods for analyzing this bridge type, as outlined in Chapter 1. Each method has special features which make it more suitable for a particular cross section or loading. However, after reviewing the available methods for the analysis of beam and slab bridges under live loads, two methods were considered primary for determining the general behavior of this bridge type. These methods, as mentioned previously, are orthotropic plate theory and harmonic analysis. The reasons for this selection were:

1. These two theories seem to predict the load distribution more accurately than other methods for the entire range of geometries, configurations and materials used (82, 191).
2. They can be used to express the load distribution properties of a bridge as a function of only a few generalized dimensionless variables so that investigation of a large variety of bridge properties becomes feasible. Both theories assume the beams and slab to be replaced by a continuous medium, which eliminates the requirement for knowing the specific bridge beam geometry in the theory formulation. Most other theories require advance knowledge of beam geometry, bridge dimensions, etc.

3. Parameters used in one method can be expressed in terms of the parameters in the other. Thus, one method can readily be compared with the other as well as with field test results.

Extensive comparisons of theoretical results and field test results, as outlined in Chapter 2, have already shown that the plate theory can more accurately predict the behavior of the specific bridges considered. However, initially, analytical results from both of the theories were obtained to determine if any significant difference in the behavior of bridges as predicted by the theories could be seen. These comparisons were used particularly in the variable ranges where field test data were not available to verify the theories.

Orthotropic plate theory and harmonic analysis have been used extensively and detailed development of the theories is given in numerous references (28, 29, 76 – 78, 88, 199, 245). Thus, only the basic equations are presented herein. However, a more extensive review of the development of the theories is presented in the above references and in Appendix A for the orthotropic plate theory.

Orthotropic Plate

Orthotropic plate is the common name for an orthogonally-anisotropic plate. This is a plate that has elastic properties that are uniform but different in two orthogonal directions. In bridges, this is primarily due to the different moduli of elasticity and different flexural and torsional moments of inertia along the major axes of the bridges.

The governing differential equation for orthotropic plates has been known and extensively used for many years. Many methods have been devised for the solution of this basic equation. For this investigation, the

approach as originated by Guyon (67, 68) and expanded by Massonnet (130 – 132) was used.

In this method of analysis the following assumptions, in addition to those of the thin plate theory and small deflections, have been made:

1. Representation of the structural system with an "equivalent" orthotropic plate with uniform thickness in two orthogonal directions is sufficiently accurate. This is equivalent to stating that the effect of longitudinal edge stiffening is negligible in the overall behavior of the bridge.
2. Poisson's ratio is equal to zero.
3. All connections can transfer the full effects of moment, torque and shear.
4. In a beam and slab bridge, spacing of the beams as well as the diaphragms is uniform.

The first of these assumptions has been verified by experimental work and field test results. In effect, this permits the change of the beams to an equivalent continuous medium which is then considered as part of the slab. Details of behavior comparisons between predictions by theory and field test results were presented in Chapter 2.

The second assumption is theoretically not correct. Poisson's ratio, if considered, tends to increase the value of the maximum moment coefficient. However, this increase is usually small and can be neglected. For beam and slab bridges, this effect was found to be within 2 to 3 percent if Poisson's ratio is assumed to be 0.15 for concrete (199).

The third assumption holds true if the connections between the various elements of the bridge are rigid. For semirigid or flexible

connections, as are most bolted or riveted joints, a reduction of the corresponding rigidities is necessary. Sanders and Munse (210), for example, suggested that the effective rigidity of diaphragms of railroad bridges be taken as 25 percent of the computed value because of flexibility of the connections at the beams. Similar reductions would be applicable in highway bridges with steel diaphragms.

The fourth assumption is generally true with respect to current practice. This assumption relates to the first in that generally a nonuniform beam spacing is similar in effect to edge stiffening. If the spacing is nonuniform the total stiffness can be spread uniformly across the cross section with sufficient accuracy.

Considering these assumptions, the behavior of the plate satisfies the following fourth order linear differential equation (245). The equivalent plate used has the same average flexural and torsional stiffnesses in the two orthogonal directions as the actual bridge structure being studied. So,

$$D_x \frac{\partial^4 w}{\partial x^4} + 2H \frac{\partial^4 w}{\partial x^2 \partial y^2} + D_y \frac{\partial^4 w}{\partial y^4} = p(x, y) \qquad (1)$$

where x and y are the axes of the coordinate system used as in Figure 16, and

$D_x = EI_x$, flexural rigidity per unit width in x direction,

$D_y = EI_y$, flexural rigidity per unit width in y direction,

$H = D_{xy} + D_{yx}$, sum of orthogonal torsional rigidities,

I_x = moment of inertia per unit width in x direction,

I_y = moment of inertia per unit width in y direction,

E_x = modulus of elasticity in x direction,

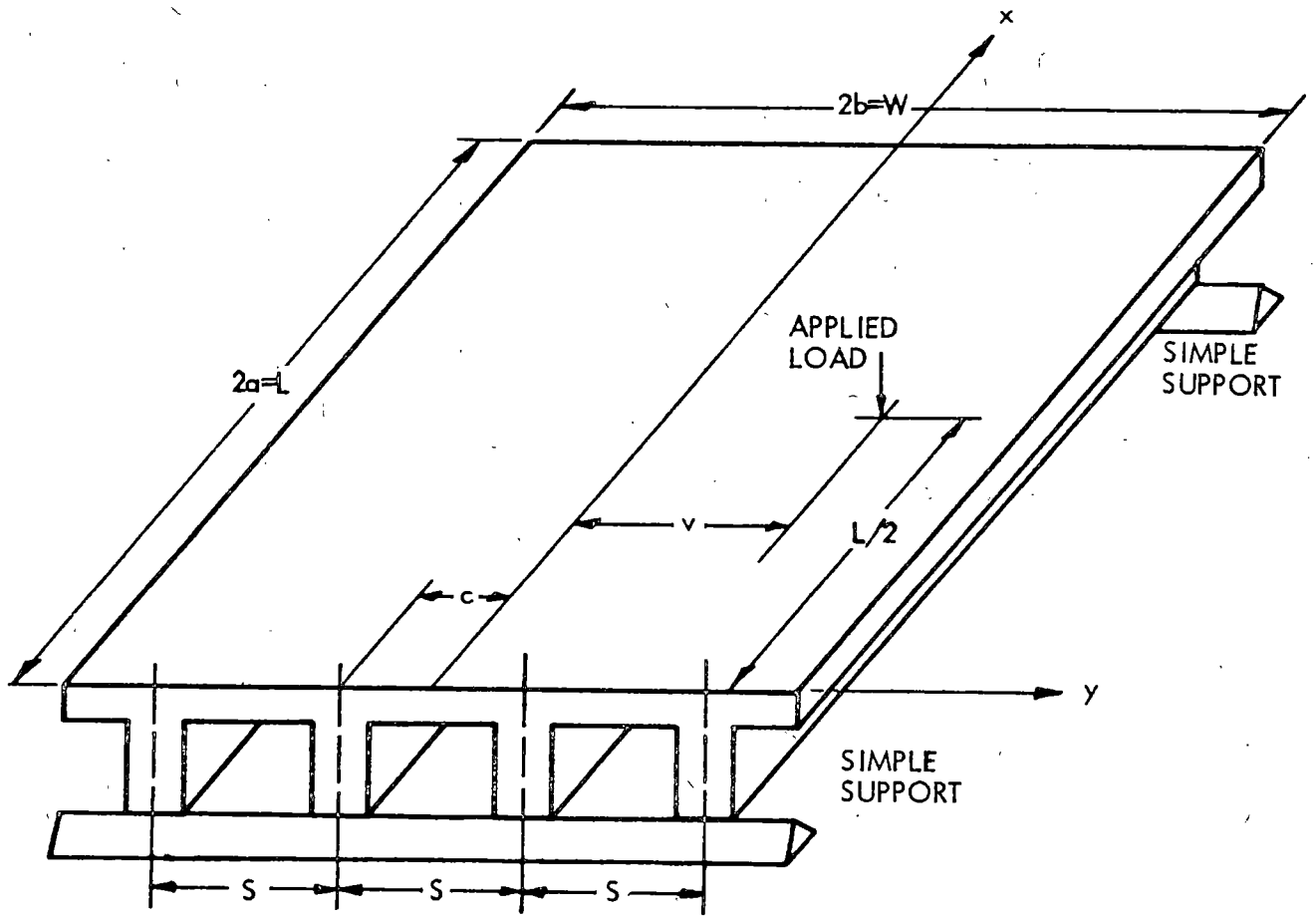

Figure 16. Bridge deck nomenclature for orthotropic plate theory.

E_y = modulus of elasticity in y direction,

D_{xy} = torsional rigidity per unit width in x direction,

D_{yx} = torsional rigidity per unit width in y direction, and

$p_{(x)}$ = function depending upon live load on bridge.

If the Levy series is used to determine the solution of the differential equation for the bridge with a concentrated load acting at midspan at a distance v from the centerline of the bridge, the deflection of the bridge is expressed in the following form:

$$w = \sum_{m=1}^{\infty} \frac{H_m}{16\, D_y \sqrt{2(1+\alpha)}} \left(\frac{w}{m\theta\pi}\right)^3 F(y, v, m, \theta, \alpha) \sin \frac{m\pi x}{L} \qquad (2)$$

where

$\alpha = \dfrac{D_{xy} + D_{yx}}{2\sqrt{D_x D_y}}$, a relative torsional stiffness parameter,

$\theta = \dfrac{W}{2L} \sqrt[4]{\dfrac{D_x}{D_y}}$, a relative flexural stiffness parameter,

$F(y, v, m, \theta, \alpha)$ = a function dependent on bridge parameters, location of deflection determination, location of concentrated load, and the boundary conditions of the bridge, and

H_m = Fourier constant for the concentrated load.

In the above equations defining θ and α, it can be seen that θ, the relative flexural stiffness parameter, primarily depends on the aspect ratio of the bridge (W/L) for its sensitivity rather than the ratio of the flexural stiffnesses. For example, if the cross-sectional geometries remain the same and the width doubles, the parameter θ doubles. On the other hand, doubling the longitudinal stiffness (D_x), the parameter θ is only increased by 19 percent, which is one-fifth as much. It can also be seen that the aspect ratio of the bridge has no effect on the relative torsional stiffness parameter, α. Thus, if the cross-sectional geometries of the bridge remain the same, the parameter α is unchanged and, hence, is only a measure of distribution due to local torsional conditions in the bridge.

If the load on the bridge was a concentrated line load acting transversely on the bridge at midspan instead of the concentrated load as represented in the equation above, the deflection of the bridge can be expressed in the following form:

$$w = \sum_{m=1}^{\infty} \frac{H_m}{WD_x} \left(\frac{L}{m\pi}\right)^4 \sin \frac{m\pi x}{L} . \qquad (3)$$

The longitudinal moments in the bridge are found by differentiating either deflection equation twice with respect to x and multiplying by the longitudinal stiffness. Thus,

$$M_x = - D_x \frac{\partial^2 w}{\partial x^2} . \qquad (4)$$

The second derivative of Equation (2) results in the series equation necessary to find the longitudinal moment at any point on the bridge. The second derivative of Equation (3) results in the series equation for the mean longitudinal moment at any transverse section of the bridge. The moment distribution coefficient for this concentrated load can be found by taking the ratio of these two series equations. Thus,

$$K_m = \frac{\theta\pi \sum_{m=1}^{\infty} \frac{H_m}{m} F(y, v, m, \theta, \alpha) \sin \frac{m\pi x}{L}}{\sqrt{2(1 + \alpha)} \sum_{m=1}^{\infty} \frac{H_m}{m^2} \sin \frac{m\pi x}{L}} \qquad (5)$$

where K_m is the moment coefficient for the concentrated load at midspan.

Harmonic Analysis

As mentioned previously, the second method of analysis considered was the harmonic analysis. In this method the bridge is assumed to consist of a continuous member supported by a set of elements in the longitudinal direction. In this respect, the method is quite similar to that developed by Newmark (152).

The Newmark method was developed for noncomposite beam and slab bridges and the torsional rigidity of the beams is neglected. Harmonic analysis on the other hand takes into account composite action of beams

with the slab. The torsional rigidity of the beams is also included in the formula developed. This comparison is made to indicate only the differences between the two methods.

The harmonic analysis method was developed by Hendry and Jaeger (77) and was found to correlate with experimental results by independent researchers (86). However, as mentioned in Chapter 2, the correlation between test results and the orthotropic plate solutions was found to be better. For this reason, only the briefest review of the harmonic analysis is given here. A detailed discussion of the theory is given in References (5), (65) and (77).

The assumptions in this method are basically the same as those used in the orthotropic plate method. The major difference in assumptions between the methods is that the effect of torsional rigidity in the transverse direction is neglected.

Harmonic analysis is used to compute bending moment coefficients by a distribution of the individual harmonics in the Fourier series expansion for concentrated loads acting on beam and slab bridge decks. The applied load is first distributed to the individual beams by assuming that the deck slab is a continuous beam over nondeflecting supports (the actual beams). Expressions for shear, moment, slope, and deflection for each beam are found by successive integrations of the load series. By using these expressions, transverse force equilibrium and the transverse slope-deflection equations, the load influence coefficients, P_{ijk}, can be found (77) which define bending moment according to the following expression (65).

$$M_i = \frac{2L}{\pi^2} \sum_{j=1}^{n} \left[\left(\sum_{k=1}^{\infty} \frac{1}{k^2} P_{ijk} \sin \frac{m\pi u}{L} \sin \frac{m\pi x}{L} \right) V_j \right] \qquad (6)$$

where i refers to the beam at which the moment is to be found,

j refers to the loaded beam,

k refers to the harmonic term,

V_j refers to the concentrated unit load reaction on the jth beam when the beams are nondeflecting,

N is the number of beams, and

L is the span length of the bridge.

Figure 17 illustrates the above terminology.

According to the definition of the moment coefficient, the expression for the coefficient at midspan due to a concentrated load acting at the midspan can be written as (65):

$$K_i = \frac{8N}{\pi^2} \sum_{j=1}^{N} \left[\left(\sum_{k=1,3\ldots}^{\infty} \frac{1}{k^2} P_{ijk} \right) V_j \right] \qquad (7)$$

where K_i is the bending moment coefficient for the ith beam.

In the above equation, P_{ijk} is a function of the number of beams, the transverse and longitudinal flexural stiffnesses and the longitudinal torsional stiffness. The parameters associated with the determination of the P_{ijk} values can be directly related to the stiffness parameters, θ and α, used in the orthotropic plate analysis. Thus it is possible to compare the two solutions for any bridge with the use of these two parameters.

Harmonic analysis predicted higher coefficients for bridges having few beams, but as the number of beams increased, harmonic analysis tended to predict lower coefficients. From the field test comparisons (Chapter 2) and the generally unconservative results found from the harmonic analysis

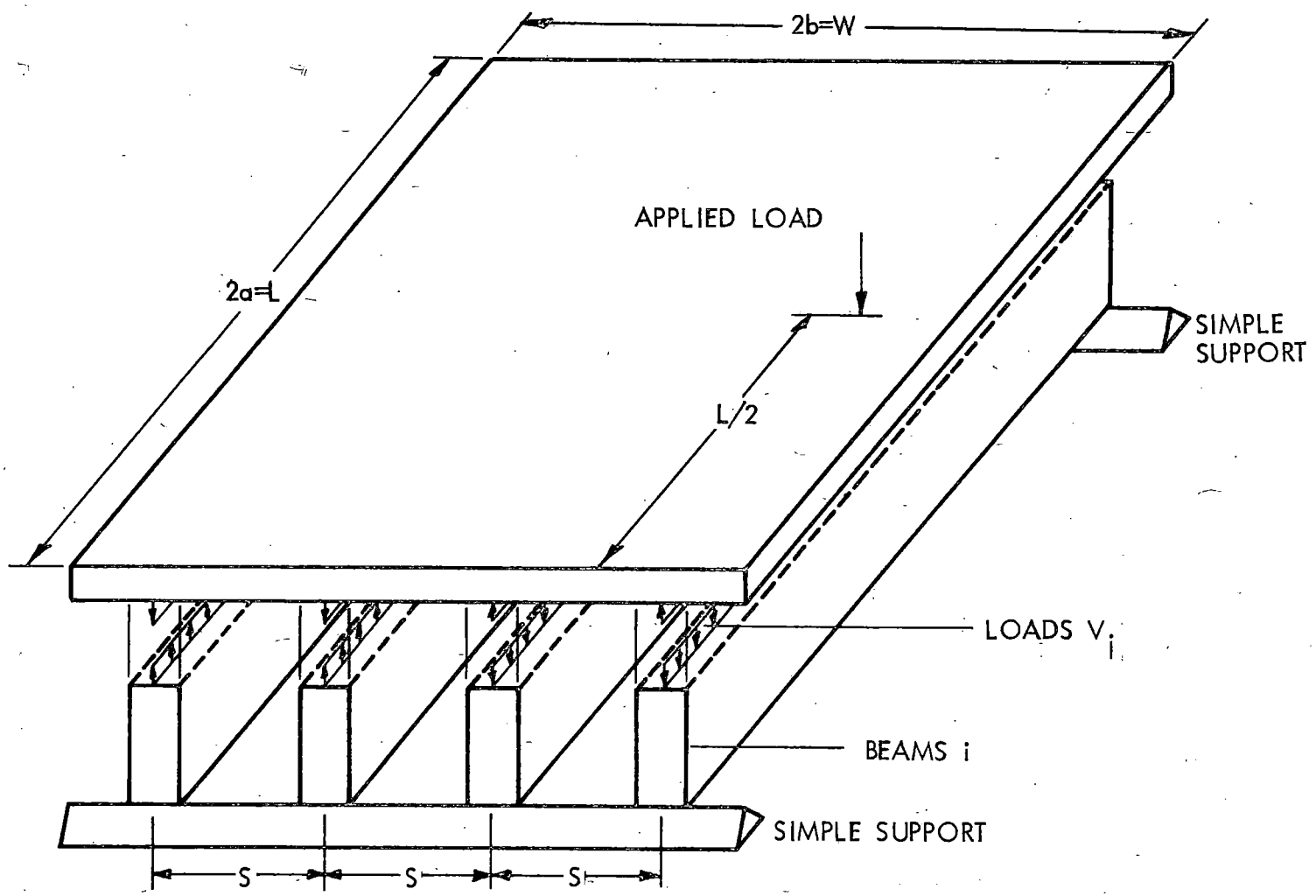

Figure 17. Bridge deck nomenclature for harmonic analysis.

in a rather extensive study of the variation of beam moment with variation in the bridge parameters, it was felt that in the final analysis, results of analytical studies used to generate design criteria should originate from the orthotropic plate analysis. The results, it was felt, would be more realistic over the entire range of parameters considered.

Range of Parameters

The maximum value of K_m at midspan for a concentrated load that is not placed at the midspan of the bridge is always less than the K_m value for a load at the midspan of the bridge. Thus, when multiaxle loads are considered, the K_m values for the midspan load are used, and the moment at any point on the transverse section at midspan is K_m multiplied by the mean static moment of all axles. This produces slightly conservative design moments, but this was preferable to introducing an additional parameter defining the longitudinal positions of the actual concentrated loads.

In the determination of a K_m value, it was estimated that using the first nine terms of the series yields at least 97 percent of the maximum moment coefficients for a single concentrated load. This percentage was based on studies of selected ranges of the variables with up to fifteen terms (65). However, other investigators have found that if only the first term of the moment series was used, the resulting value yielded only 85 to 90 percent of the maximum moment coefficient (67, 68, 144, 199, 210). Thus, the use of nine terms was felt to yield results of sufficient accuracy, since in nearly all other instances, conservative assumptions to maximize effects were used.

However, it should be noted that, because of rapid convergence, the deflection coefficients can be determined with sufficient accuracy using only the first term of the deflection series. This variation in rate of convergence between the moment and deflection coefficient series can lead to erroneous comparisons if only the first term of the respective series is used. The deflection coefficients would be quite accurate, but as mentioned previously, the moment coefficients would be 10 to 15 percent below the true value.

In the development of the K_m influence lines for concentrated loads acting at the midspan of the bridge, seventeen equally spaced points on the transverse section at midspan were considered. Making use of symmetry, nine moment coefficient curves were needed for each combination of the stiffness parameters, θ and α.

Rowe (199) stated that the range of the flexural stiffness parameter θ is about 0.3 to 1.13 for slab bridges, 0.5 to 1.2 for concrete T-beam bridges and 0.3 to 1.0 for box beam bridges. A study of standard bridges (281, 295) and of a number of typical bridge plans furnished by various state highway departments shows that the value of θ lies in a range from about 0.4 to 1.25 for all types of beam and slab bridges. Thus to encompass all of the values of the parameters currently found and to consider possible changes in sections, the range of θ used in computations was 0.25 to 1.25 with an interval of 0.25.

Rowe (199) also stated that the range of the torsional stiffness parameter α is from about 0.05 to 1.00 for the common bridges. The parameter for standard Bureau of Public Roads bridges (281, 295) was estimated to be from about 0.045 to 0.30. To include this range, the

load distribution was determined for values of the $\sqrt{\alpha}$ ranging from 0.0 to 1.0 at 0.2 intervals. These values of $\sqrt{\alpha}$ correspond to α values of 0.04, 0.16, 0.36, 0.64, and 1.00.

It can be seen that there will be 9 x 5 x 6 or 270 influence lines necessary to determine the K_m value for a load at any position at midspan for any of the 30 combinations of the stiffness parameters. In reality, however, not all of these combinations are possible because of design or physical limitations.

Loading System

Standard AASHO truck loading was used in the analysis for all bridge types. The criteria for its use are given in detail here for beam and slab bridges and are referred to in the discussions for other bridge types.

The current specifications (279) require in Section 1.2.6 that the standard truck "shall be assumed to occupy a width of 10 ft. These loads shall be placed in design traffic lines having a width of $W_L = W_c/N$ ..... The lane loadings or standard trucks shall be assumed to occupy any position within their individual design traffic lane (W_L), which will produce the maximum stress." In addition, the number of lanes is specified for various roadway widths, with the minimum width about 10 ft and the maximum at 15 ft. However, for all practical purposes, it is impossible to have normal lanes of less than 12 ft. Thus, for this study, several modifications have been made in these requirements to make the loading more consistent with the actual maximum loading conditions. Considerable discussion has occurred in the AASHO Bridge Committee over

a number of years concerning loadings and the loading criteria used in this study seem to be a conservative consensus of the proposed changes considered by the Committee. In addition, the criteria are similar to the loading system used in the development of the distribution procedure for composite box girders in the AASHO Specifications (279), Section 1.7.104, particularly conccerning the number of lanes in a roadway.

The criteria used for this study differ from the current requirements in that:

1. the number of design traffic lanes is the whole number of 12-ft lanes which can be placed within the roadway width, and
2. the 12-ft lanes are placed anywhere transversely across the roadway cross section to produce maximum stress, although they may not overlap.

Furthermore, the standard trucks are assumed to be centered in a 10-ft width which may be positioned for maximum effect anywhere within the 12-ft lanes. The maximum number of design traffic lanes is shown in Table 3.

TABLE 3

NUMBER OF DESIGN TRAFFIC LANES

BRIDGE WIDTH[a] W, FT	ROADWAY WIDTH W_c, FT	NO. OF LANES N_L
27 to 38.9	24 to 35.9	2
39 to 50.9	36 to 47.9	3
51 to 62.9	48 to 59.9	4
63 to 74.9	60 to 71.9	5

[a]Based on a 1.5 ft curb width.

Due to the different requirements used in placing the actual driving lanes within the curb to curb dimensions of a bridge, the 12-ft lanes were placed within this width without consideration of lane lines, but placed so as to produce maximum effects. Current practice, in some instances, requires safety or shoulder lanes which, under these criteria, produce more driving lanes than actually are used. However, considering the tremendous growth in traffic, the use of the full roadway width was considered a realistic conservative assumption. In any case, only as many 12-ft lanes were loaded as was necessary to produce maximum moment.

There were two conditions considered in the placement of the 12-ft lanes. The first consideration was the arrangement of the loads to produce maximum eccentricity with respect to the centerline of the bridge (or the eccentric loading case). This arrangement developed maximum moments in the exterior girders of the bridge. This was accomplished by arranging the 12-ft lanes side by side with the outside edge of the first lane 1.5 ft from the edge of the bridge (it was assumed that the curb width was 1.5 ft). The first 10-ft truck width was then positioned in each of the adjacent 12-ft lanes with an eccentricity of 2 ft. Therefore, the first wheel load was 3.5 ft from the edge of the bridge and, thus, 2 ft from the edge of the curb as specified by the AASHO Specifications (279). Arrangements of wheel loads for eccentric loadings are shown in Figure 18.

The second consideration was the arrangement of the loads to produce minimum eccentricity with respect to the centerline of the bridge (or the central loading case). This arrangement developed maximum moments in the center girders of the bridge. There are two possible arrangements

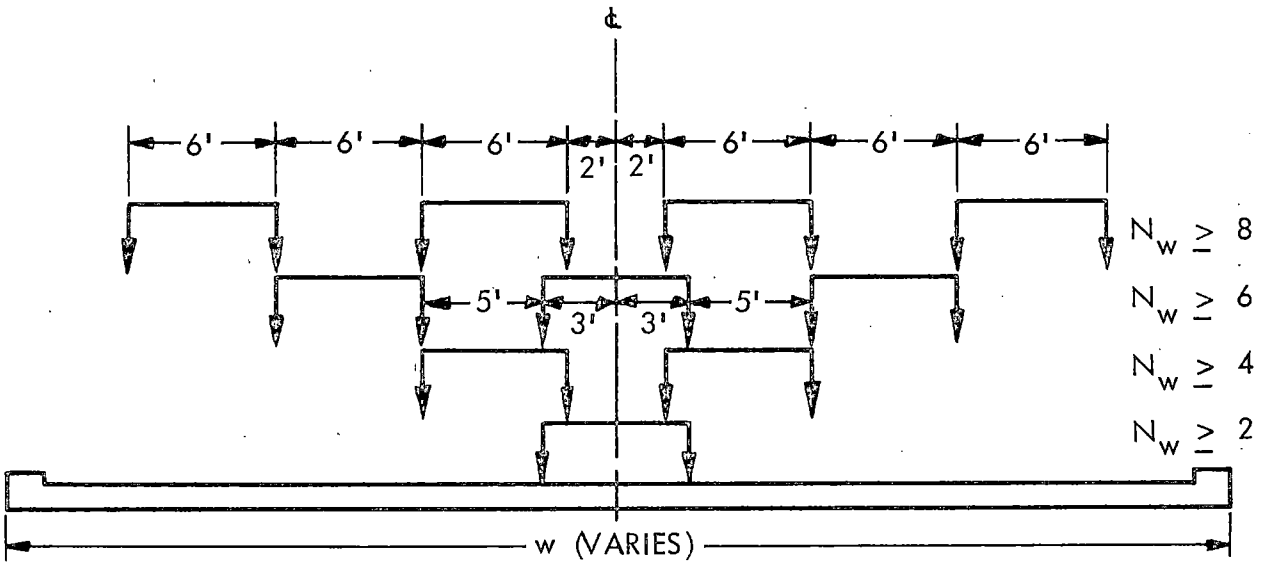

Figure 18. Loading cases considered for various bridge width-central loading cases.

that can be used to produce this effect. The first is with one 12-ft lane centered over the bridge centerline with the truck centered in this lane. The adjacent 12-ft lane would have the 10-ft truck widths positioned eccentrically 2 ft towards the centerline of the bridge. The second arrangement is with two 12-ft lanes placed side by side on the centerline of the bridge. The 10-ft truck widths would be positioned eccentrically in the 12-ft lanes, 2 ft towards the centerline of the bridge. Arrangements of wheel loads for central loadings are shown in Figure 19.

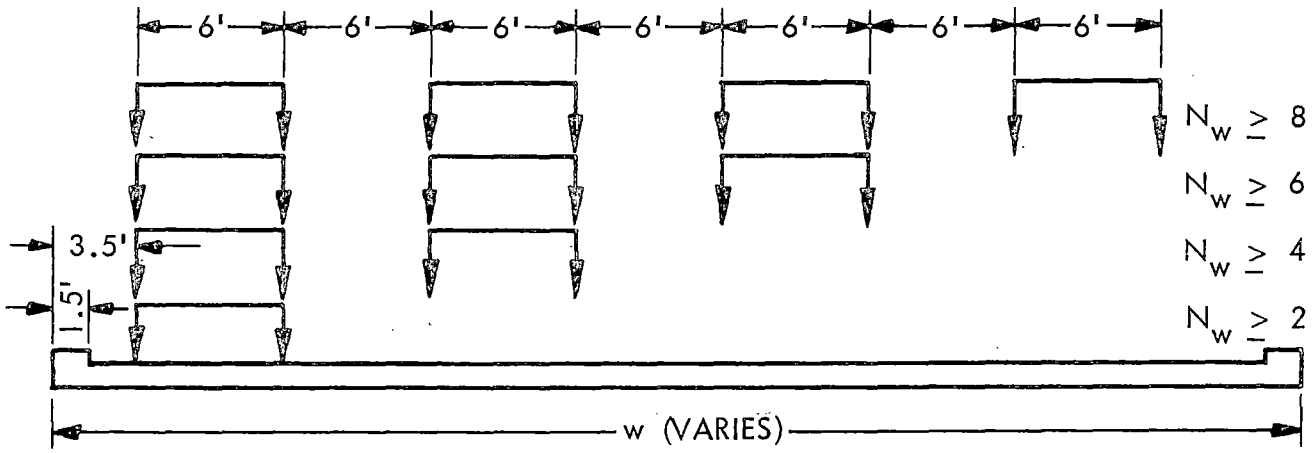

Figure 19. Loading cases considered for various bridge widths, eccentric loading cases.

Maximum Load Factors

To determine the maximum effect in each girder or beam, moment coefficient curves for seventeen positions across the width of the bridge were obtained using orthotropic plate theory for all combinations of stiffness parameters. When finding the moment curve for a particular concentrated load that does not fall at one of the seventeen positions, linear interpolation was used. The moment coefficient curve for a truck or combination of trucks is formed by summing the moment curves for each concentrated load position and dividing by the sum of the number of wheel loads. Thus, the average moment will remain unity. The moment coefficient curves are output for each combination of 12-ft lanes until the maximum number of lanes is reached for each possible combination. Table 4 shows the widths of bridges used for various numbers of lanes. Although the influence lines are nondimensional, the use of actual truck loading dictates the use of actual bridge widths for loading considerations.

TABLE 4

BRIDGES CONSIDERED FOR LOAD FACTORS

	NO. OF LANES			
	2	3	4	6
W (ft)	28	39	51	75
	33	41	53	
	37	45	57	
		49	61	

In conjunction with the determination of moment coefficient curves for each load combination, the value of D, the width of bridge over which one longitudinal line of wheels is distributed, was also obtained. These values were based on the assumption the bridge had eight girders or beams. Thus, the moment coefficient at any beam is:

$$K_{m8} = \frac{1}{6} (K_{m_{i-1}} + 4K_{m_i} + K_{m_{i+1}}) \qquad (8)$$

where the K_m terms are the values from the seventeen positions on the influence curves. The corresponding D value is found from the following equation.

$$D = \frac{W}{N_w K_{m8}} \qquad (9)$$

where W = width of bridge,

N_w = number of longitudinal lines of wheels,

D = equivalent width of bridge needed to support one line of wheel load as used by the current AASHO Specification in the Load Factor equation, L.F. = S/D, in which S is the spacing between girders.

In the calculation of K_m, the assumption of eight beams generally leads to a conservative value since bridges normally have fewer beams. Since the K_m value per beam is found by integrating under the K_m value per foot curve, the use of K_{m8} yields a higher value than that based on the actual number of beams because of the concentrated effect of the peak in the moment coefficient curve. If there are more than eight beams, the moment coefficient per foot and per beam curves are sufficiently close together to cause negligible difference.

The minimum D value from all possible load combinations for a particular bridge width and stiffness parameters, θ and α, is the theoretical value that was used to determine a design criteria. These theoretical D values for various bridge widths for different combinations of stiffness parameters, θ and α, are shown in Table 4A. The critical loading case is also indicated in this table.

The use of two loading criteria (one for maximum central loading and one for maximum eccentric loading) yields two critical values of D, one for each criterion. For the central loading case, the critical beam is at the center of the bridge, whereas for the eccentric loading case, it is near the edge of the bridge. In the latter case, the critical girder could be either the exterior girder or the first interior girder, depending upon the number (or spacing) of beams. It was felt, however, that the design should be based on the absolute critical case since the loading case which is critical varies with the bridge stiffness parameters. Thus, to determine different criteria for interior or exterior girders requires almost a complete analysis of a known bridge geometry. In addition, the difference between the two critical cases was not great enough to warrant the more complicated procedure.

TABLE 4A

THEORETICAL RESULTS FOR BEAM AND SLAB BRIDGES VALUE OF D IN EQUATION: LF = S/D

		W, WIDTH OF BRIDGE IN FT (N_w, NO. OF WHEEL LOADS)											
		28	33	37	39	41	45	49	51	53	57	61	75
θ	α	(4)	(4)	(4)	(6)	(6)	(6)	(6)	(8)	(8)	(8)	(8)	(10)
0.25	0.00	5.66	5.23	5.16	5.17	5.20	5.27	5.13	5.10	5.08	5.08	5.12	5.04
	0.04	5.97	5.78	5.82	5.87	5.88	5.72	5.68	5.68	5.70	5.76	5.65	5.63
	0.16	6.38	6.59	6.85	6.23	6.25	6.34	6.49	6.17	6.18	6.24	6.32	6.10
	0.36	6.60	7.12	7.55	6.33	6.46	6.73	7.01	6.24	6.34	6.54	6.75	6.16
	0.64	6.71	7.42	7.97	6.38	6.58	6.95	7.32	6.27[a]	6.43	6.71	6.99	6.18[a]
	1.00	6.78	7.61	8.25	6.40[a]	6.64	7.08	7.52	6.29[a]	6.48	6.81	7.14	6.19[a]
0.50	0.00	5.81	5.53	5.44	5.42	5.43	5.47	5.41	5.36	5.33	5.30	5.32	5.25
	0.04	5.89	5.70	5.63	5.63	5.64	5.67	5.57	5.53	5.51	5.50	5.53	5.45
	0.16	6.06[a]	6.07	6.10	6.09[a]	6.07	5.97	5.95	5.95	5.95	5.95	5.90	5.86
	0.36	6.17[a]	6.47	6.62	6.15[a]	6.24	6.29	6.36	6.03[a]	6.16	6.20	6.24	6.03[a]
	0.64	6.28[a]	6.79	7.08	6.20[a]	6.36	6.54	6.71	6.08[a]	6.26[a]	6.40	6.53	6.06[a]
	1.00	6.38[a]	7.05	7.45	6.25[a]	6.46	6.72	6.98	6.12[a]	6.31[a]	6.55	6.75	6.09[a]
0.75	0.00	5.13[a]	5.52[a]	5.86	5.58[a]	5.64[a]	5.73	5.74	5.49[a]	5.54[a]	5.66[a]	5.65	5.62
	0.04	5.21[a]	5.63[a]	5.92	5.63[a]	5.71[a]	5.83	5.86	5.54[a]	5.60[a]	5.73[a]	5.73	5.69[a]
	0.16	5.41[a]	5.89[a]	6.09	5.76[a]	5.86[a]	6.00	5.99	5.65[a]	5.73[a]	5.90[a]	5.96	5.77[a]
	0.36	5.62[a]	6.18[a]	6.33	5.88[a]	6.02[a]	6.15	6.17	5.76[a]	5.87[a]	6.09[a]	6.12	5.85[a]
	0.64	5.82[a]	6.43	6.61	5.99[a]	6.16[a]	6.30	6.39	5.86[a]	5.99[a]	6.23	6.29	5.92[a]
	1.00	5.98[a]	6.64	6.88	6.08[a]	6.27[a]	6.45	6.59	5.94[a]	6.09[a]	6.35	6.45	5.97[a]
1.00	0.00	4.64[a]	4.88[a]	5.15[a]	5.29[a]	5.29[a]	5.30[a]	5.37[a]	5.20[a]	5.20[a]	5.23[a]	5.29[a]	5.44[a]
	0.04	4.73[a]	4.98[a]	5.26[a]	5.35[a]	5.36[a]	5.40[a]	5.48[a]	5.25[a]	5.26[a]	5.31[a]	5.39[a]	5.48[a]
	0.16	4.93[a]	5.24[a]	5.56[a]	5.49[a]	5.54[a]	5.62[a]	5.74[a]	5.38[a]	5.42[a]	5.50[a]	5.61[a]	5.58[a]
	0.36	5.18[a]	5.56[a]	5.92[a]	5.66[a]	5.73[a]	5.88[a]	6.04[a]	5.52[a]	5.59[a]	5.73[a]	5.87[a]	5.68[a]
	0.64	5.41[a]	5.87[a]	6.27[a]	5.79[a]	5.91[a]	6.12[a]	6.21	5.65[a]	5.74[a]	5.93[a]	6.11[a]	5.77[a]
	1.00	5.61[a]	6.14[a]	6.54	5.91[a]	6.05[a]	6.29	6.36	5.76[a]	5.87[a]	6.10[a]	6.32[a]	5.85[a]
1.25	0.00	4.42[a]	4.58[a]	4.79[a]	4.91[a]	5.04[a]	5.15[a]	5.16[a]	5.06[a]	5.05[a]	5.06[a]	5.10[a]	5.28[a]
	0.04	4.49[a]	4.66[a]	4.88[a]	5.00[a]	5.13[a]	5.22[a]	5.24[a]	5.10[a]	5.10[a]	5.12[a]	5.17[a]	5.34[a]
	0.16	4.65[a]	4.86[a]	5.10[a]	5.24[a]	5.37[a]	5.40[a]	5.44[a]	5.21[a]	5.23[a]	5.28[a]	5.35[a]	5.45[a]
	0.36	4.86[a]	5.13[a]	5.41[a]	5.50[a]	5.54[a]	5.63[a]	5.70[a]	5.34[a]	5.39[a]	5.48[a]	5.57[a]	5.55[a]
	0.64	5.08[a]	5.42[a]	5.96[a]	5.64[a]	5.71[a]	5.85[a]	5.97[a]	5.47[a]	5.54[a]	5.67[a]	5.81[a]	5.64[a]
	1.00	5.29[a]	5.70[a]	6.06[a]	5.76[a]	5.86[a]	6.05[a]	6.20	5.59[a]	5.67[a]	5.85[a]	6.02[a]	5.73[a]

[a]Controlled by central loading; other values controlled by eccentric loading.

In nearly every case where central loading controlled, the minimum D value (or maximum K_m) was obtained in the central girder with all lanes loaded. However, for eccentric loading, although in the majority of the cases the critical value of D was obtained in the exterior girder with all lanes loaded, there were numerous cases where partial loadings

controlled. In these cases, the difference between the D value for the partial loading case and the fully loaded cases was very small. In a very few cases where eccentric loading controlled, the critical K_m (or D) value was found slightly inside the edge of the bridge which, if there were a number of girders, could lead to the first interior girder being critical. In each of these later cases, the critical conditions always occurred with all lanes loaded.

The reduction of the data in Table 4A to a useful design criteria will be treated in Chapter 4. However, there are many observations that should be made here as to the meaningfulness of this data. There are four principal variables:

1. α, the relative torsional stiffness parameter,
2. θ, the relative flexural stiffness parameter,
3. W, the actual width of the bridge, and
4. N_w, the number of longitudinal lines of wheel loads.

First, it can be seen that as α increases the value of D increases, an indication that load distribution characteristics improve. Second, as θ increases, the value D decreases, indicating a lessening of the load distribution characteristics. Third, as the bridge width increases for a specific number of wheel loads, the distribution characteristics improve. Fourth, as the number of longitudinal lines of wheel loads increase, the load distribution characteristics lessen.

The first observation can be explained in the following manner. Comparing a box section beam system to a steel WF type section system supporting similar slabs where the I_x and I_y values are the same, the α value for the box type section is larger due to the increase in the torsional

stiffness of the beams. Thus, with respect to load distribution, since the box type section is torsionally stronger, the lateral stiffness of the plate between the beams is greater. This improves the load distribution characteristics as is demonstrated by the data in Table 4A. The second observation can be explained by noting that as θ increases, I_y decreases if other variables remain the same. Thus, the lateral stiffness in the transverse direction is less, reducing the load distribution characteristics of the bridge. The third observation is rather obvious considering that the total width of the bridge is increased to support the same given total static moment. The fourth observation can be explained by considering the fact that as the number of wheels increases along with the width of the bridge, the concentrated wheel loads are relatively closer to the more critically loaded beam. As the spacing of the loads becomes relatively closer, it can be seen that the total moment on the beam increases since the influence line for the beam is curved in the vicinity of the beam. However as the bridge becomes increasingly wider, this effect gradually diminishes.

The value of D listed in Table 4A could actually be used in the design of highway bridges. However, to use this table, the user must employ a three-way interpolation between the three parameters involved, i.e.; the bridge width, the flexural stiffness parameter θ, and the torsional stiffness parameter α. Of course, this is highly impractical and the reduction of this table to a more usable form is outlined in Chapter 4.

MULTI-BEAM BRIDGES

Development of Theory

The analysis of multi-beam bridges used in this study was basically an extension of the work using articulated plate theory undertaken by Arya, Khachaturian, and Siess (6 – 8). In the method as presented by Arya, the solution is found by solving the simultaneous equations found through satisfying the compatibility equations of the structural system. The effect of transverse prestressing is not considered in this analysis.

The extension of this method of analysis by Watanabe (261) uses the same basic derivations as presented by Arya. A summary of the extension of the theory is presented in this section with a more detailed development in Appendix A.. The significant difference in the method development by Watanabe is that the equilibrium of the system is expressed in terms of the deformations and the limit of these expressions is taken as the element size shrinks to zero. This differential equation is then similar in many respects to the orthotropic plate equation except that the term representing the transverse stiffness is absent and the equation includes a term for the torsional warping stiffness. Therefore, the solution will satisfy the following differential equation:

$$D_x \frac{\partial^4 w}{\partial x^4} + H \frac{\partial^4 w}{\partial x^2 \partial y^2} - C_x \frac{\partial^6 w}{\partial x^4 \partial y^2} = P(x) \qquad (10)$$

where D_x, H, P(x) have the same definition as in the previous section and C_x = torsional warping stiffness per unit width. The basic dimensions as used for multi-beam bridges are similar to those used in beam and slab bridges as shown in Figure 16. Using the Levy series to determine the solution of the differential equation for the bridge with a concentrated load acting at a distance v from the centerline of the bridge at midspan, the deflection of the bridge can be expressed in the following form:

$$W = \sum_{m=1}^{\infty} \frac{H_m}{16} \frac{D_x}{(D_{xy} + D_{yx})^2} \left(\frac{W}{m\phi\pi}\right)^3 F(y, v, m, \phi, g_m) \qquad (11)$$

where

$\phi = \frac{W}{2L}\sqrt{\frac{D_x}{D_{xy} + D_{yx}}}$, a combined flexural-torsional stiffness parameter, and

$g_m = \sqrt{1 + \frac{C_x}{D_{xy} + D_{yx}} \left(\frac{m\pi}{L}\right)^2}$, a torsional warping parameter.

The longitudinal moments in the bridge are then found by differentiating this equation twice with respect to x and multiplying by the longitudinal stiffness (Equation (4)). The moment coefficient for a concentrated load at midspan may be found by taking the ratio of the moment as determined by Equation (4) and dividing by the moment caused by the same load distributed uniformly in the transverse direction. Thus,

$$K_m = \frac{\phi\pi \sum_{m=1}^{\infty} \frac{H_m}{mg_m} F(y, v, m, \phi, g_m) \sin \frac{m\pi x}{L}}{\sum_{m=1}^{\infty} \frac{H_m}{m^2} \sin \frac{m\pi x}{L}} . \qquad (12)$$

Parameters and Loading System

Moment coefficient curves were calculated using the integration of the above equation for various numbers of beams, values of ϕ, and values of C_x. From the results of these calculations, it was found that the number of elements involved in the bridge did not greatly affect (maximum difference of approximately 5 percent) the value of the moment coefficients per unit width. Therefore, sixteen beams were chosen for design reference. Furthermore, as in the case of beam and slab bridges, the

determination of K_m was made using the first nine terms of the Levy series solution. Since this series for multi-beam bridges converges at least as rapidly as the beam and slab series, the computed K_m value is within about 1 to 2 percent of the true value.

It was also found that if the torsional warping factor (C_x) was included, there was a small difference of 3 to 4 percent in the moment coefficient values when compared with similar values for a C_x value of zero. This makes the constant g_m equal to 1.0. The results are, therefore, conservative for open sections where the torsional stiffness is increased by resistance to torsional warping.

The values of ϕ used in determining the moment coefficients were:

$$\phi = 0.1,\ 0.3,\ 0.5,\ 0.7,\ 1.0,\ 2.0.$$

The widths of bridges chosen for the analysis were the same as those listed for beam and slab bridges, except that bridge widths over 53 ft were not included.

The values of D were calculated for the same truck loading combinations as listed in the previous section and shown in Figures 18 and 19.

Maximum Load Factors

Table 5 lists the results of the computations for the minimum D value for each bridge width and for ϕ, the flexural torsional stiffness parameter value. This minimum value gives the maximum load factor.

It can be seen in Table 5, that for multi-beam bridges, the following effects on the load factor or value of D were obtained.

TABLE 5

THEORETICAL RESULTS FOR MULTI-BEAM BRIDGES VALUE OF D IN EQUATION: LF = S/D

	W, WIDTH OF BRIDGE, FT (N_w, NO. OF WHEEL LOADS)								
ϕ	28 (4)	33 (4)	37 (4)	39 (6)	41 (6)	45 (6)	49 (6)	51 (8)	53 (8)
0.1	6.85	8.00	8.82[a]	6.44	6.76	7.35[a]	7.90[a]	6.32	6.55
0.3	6.32	7.18	7.81[a]	6.24	6.48	6.96	7.27[a]	6.10	6.29
0.5	5.85	6.47	6.98	6.03	6.22	6.57	6.82[a]	5.89	6.02
0.7	5.46	5.91	6.31	5.85	6.00	6.24	6.43	5.69	5.81
1.0	5.03	5.34	5.62	5.64	5.75	5.88	5.95	5.46	5.55
2.0	4.40	4.54	4.72	4.78[b]	4.93[b]	5.10[b]	5.25	5.08	5.14

Note: Unless indicated, central loading with all lanes loaded controlled.

[a]Eccentric loading, all lanes loaded, controlled.

[b]Central loading, two lanes loaded, controlled.

1. As the value of ϕ decreases, for a given bridge width, the value of D increases (lower load factor and better distribution). Thus, if the cross-sectional properties of the bridge are constant, as the length of the bridge increases the value of D increases since ϕ would be inversely proportional to that length.

2. For a given value of ϕ and number of lanes, the distribution improves (higher D value) as the bridge widens. This is obvious since there is more total longitudinal stiffness to support the same statical moment. The effect is more significant at lower values of ϕ.

The critical loading case is shown in Table 5 and in the majority of cases considered was the central loading case with all lanes loaded.

However, there were several instances where the full eccentric loading controlled with the exterior beam critical or where a partial central loading controlled. In this latter case, the difference between the critical partial and full loading cases was very small. As indicated for beam and slab bridges, it was felt that the use of the absolute critical case for design, rather than the consideration of the critical beam, and loading criteria, would lead to a satisfactory design without the complications of including these factors.

As stated previously, the information presented in Table 5 can be used to design multi-beam bridges, but does not readily lend itself to such use. A reduction of this raw data to a more usable form is given in the next chapter.

CONCRETE BOX GIRDER BRIDGES

Development of Theory

The analysis of the concrete box girder sections was carried out using a modification of the theory of prismatic folded plate structures. The use of this theory for analyzing concrete box girder bridges was developed by Scordelis of the University of California at Berkeley (222). The direct stiffness solution was developed using a folded plate harmonic analysis based on an elasticity method (41). Scordelis used elastic plate theory for loads normal to the plane of the plates and two-dimensional plane stress theory for loads in the plane of the plates.

Using these theories, a computer program, MUPDI, was developed by Scordelis. This computer program can be used to analyze box girder bridges, with and without intermediate diaphragms, under concentrated or

distributed loads anywhere on the bridge. The program was used as the basis for studying the parameters affecting the bridge behavior. The basic program, however, was altered slightly so that the format was compatible with the Iowa State computer system. In addition, some subroutines were eliminated or changed to compute only those quantities needed for this investigation. A subroutine was also written to compute the equivalent longitudinal beam moments and the corresponding bending moment coefficients.

The basic assumptions used in the analysis are as follows (222).

1. The elements of the box girder are rectangular plates of uniform thickness and are made of an elastic isotropic and homogeneous material.
2. The force deformation relationships are linearly elastic so that superposition is valid.
3. The bridge is simply supported at the ends.
4. Diaphragms are considered to be nondeformable in their own plane, but perfectly flexible normal to their own plane.
5. Stresses and displacements in a plate element due to normal loading shall be determined by classical thin plate bending theory as applied to plates supported on all sides.
6. Stress and displacements in a plate element due to in-plane loading shall be determined by classical thin plate theory assuming a condition of plane stress.

Parameters and Loading System

For beam and slab bridge and multi-beam bridge, the analysis was carried out using a simple variation of only one or two parameters. However, due to the nature of the method of analysis used for the solution of the box girder problem and the complexity of the cross section, each variable had to be specified independently. The major variables studied for the analysis of box girders were:

1. span length,
2. overall width,
3. overall depth of the cross section,
4. number of girders (vertical longitudinal plates),
5. number of transverse diaphragms,
6. thickness of webs and flanges, and
7. edge conditions.

To estimate the ranges which must be considered for each of these variables, the information on their ranges obtained by Scordelis (222) from two hundred California box girder bridges was used along with additional information secured from the California Department of Highways and the Iowa State Highway Commission. In summary, the variables ranged as follows:

1. Span length: The span lengths of the majority of simple span box girder bridges fall within the range of 50 to 110 ft. Spans of 50 ft, 80 ft, and 110 ft were considered in the analysis to incorporate the entire range.

2. Overall width: Overall widths considered herein correspond to the widths studied for the beam and slab and multi-beam bridges, except that the narrowest width (28 ft) was not considered.

3. Depth of cross section: According to the sources cited above, the depth of the bridge is related to the span. The depth/span ratio ranges from 0.05 to 0.07 for reinforced concrete bridges, although a prestressed box girder bridge may have a ratio as low as 0.045. In this study, depth/span ratios of 0.05 and 0.07 were considered.

4. Number of girders: The number of girders equals the number of cells plus one. The number of cells and the width of the cells were chosen such that the transverse spacing between the vertical webs of the girders was within the normal design range of from 7 to 9 ft. Therefore for the widths of bridges studied, bridges with 4, 6, and 8 cells were included.

5. Number of diaphragms: The geometries considered included bridges with no diaphragms and with one or two diaphragms. Since the most common design is one with no diaphragms, this case was studied in depth. Six combinations of length and depth were considered for each width of bridge. However, to determine the effect of the diaphragms on the load distribution characteristics, limited studies of bridges with diaphragms were conducted. For the case of only one interior diaphragm (at center span), two combinations of span and depth were considered for selected widths. For the case with two diaphragms (at the third-span points of the bridge), only the most critical situation of the shortest bridge with the deepest section was studied.

6. Thickness of webs and flanges: The thicknesses of the plates used in the general study were 6.5 in. for the top flange, 5.5 in. for the bottom flange, and 8.0 in. for the webs. These dimensions are felt to be typical of the designs used in practice for most box girder bridges.

However, it was found that these dimensions could be increased to 7.0, 6.0 and 12.0 in., respectively, in those cases where the depth of the bridge may be limited (e.g. prestressed bridges with d/L of 0.045). Additional information was obtained for these greater thicknesses in a few cases to determine the overall effect of the change in thickness.

7. Edge conditions: A cantilever overhang of 3.5 ft was assumed to exist in all cases studied for two reasons. First, this configuration is commonly used in many designs. And second, this condition puts the exterior wheels directly over the exterior web, tending to maximize the moment in this section for the eccentric loading case.

Table 6 illustrates the range and values of each variable considered.

The loading patterns used in the computation of the maximum load factors (i.e. minimum D value) included the same as those shown in Figures 18 and 19 for beam and slab bridges as well as two special box girder loading cases. These two special cases are shown in Figure 20 and were developed to maximize the moment coefficients due to the peaked condition of the influence lines in the region of the webs.

TABLE 6

VARIABLES IN BOX GIRDER BRIDGE STUDY

	NUMBER OF CELLS												
	4					6						8	
	NUMBER OF WHEELS												
	4		6					8					12
Width of bridge W, ft	33	37	39	41	45	45	49	51	53	57	61	61	75
Cell width, ft	6.5	7.5	8.0	8.5	9.5	6.3	7.0	7.3	7.7	8.3	9.0	6.8	8.5
Depth/span d/L	0.07 0.05	0.07 0.05	0.07 0.05	0.07 0.05	0.07 0.05	0.07 0.05	0.07 0.05	0.07 0.05	0.07 0.05	0.07 0.05	0.07 0.05	0.07 0.05	0.07 0.05
	Number of diaphragms considered, N_d												
Span, ft													
50	0, 1, 2 <u>0</u>[a]	0, 1, 2 <u>0</u>	0, 1, 2 <u>0</u>	0 0	0, 1, 2 <u>0</u>	0, 1, 2 0	0, 1, 2 0	0, 1, 2 0	0 0	0 <u>0</u>	0, 1, 2 0	0, 1, 2 <u>0</u>	0 0
80	0 0	0 0	0 0	0 0	0 0	0 0	0 0	0 0	0 0	0 0	0 0	0 0	0 0
110	0 <u>0</u>, 1	0 <u>0</u>, 1	0 <u>0</u>, 1	0 0	0 <u>0</u>, 1	0 0, 1	0 <u>0</u>, 1	0 0, 1	0 0	0 <u>0</u>	0 0, 1	0 <u>0</u>, 1	0 0

[a] Underlined values refer to combinations where variations in thickness were studied.

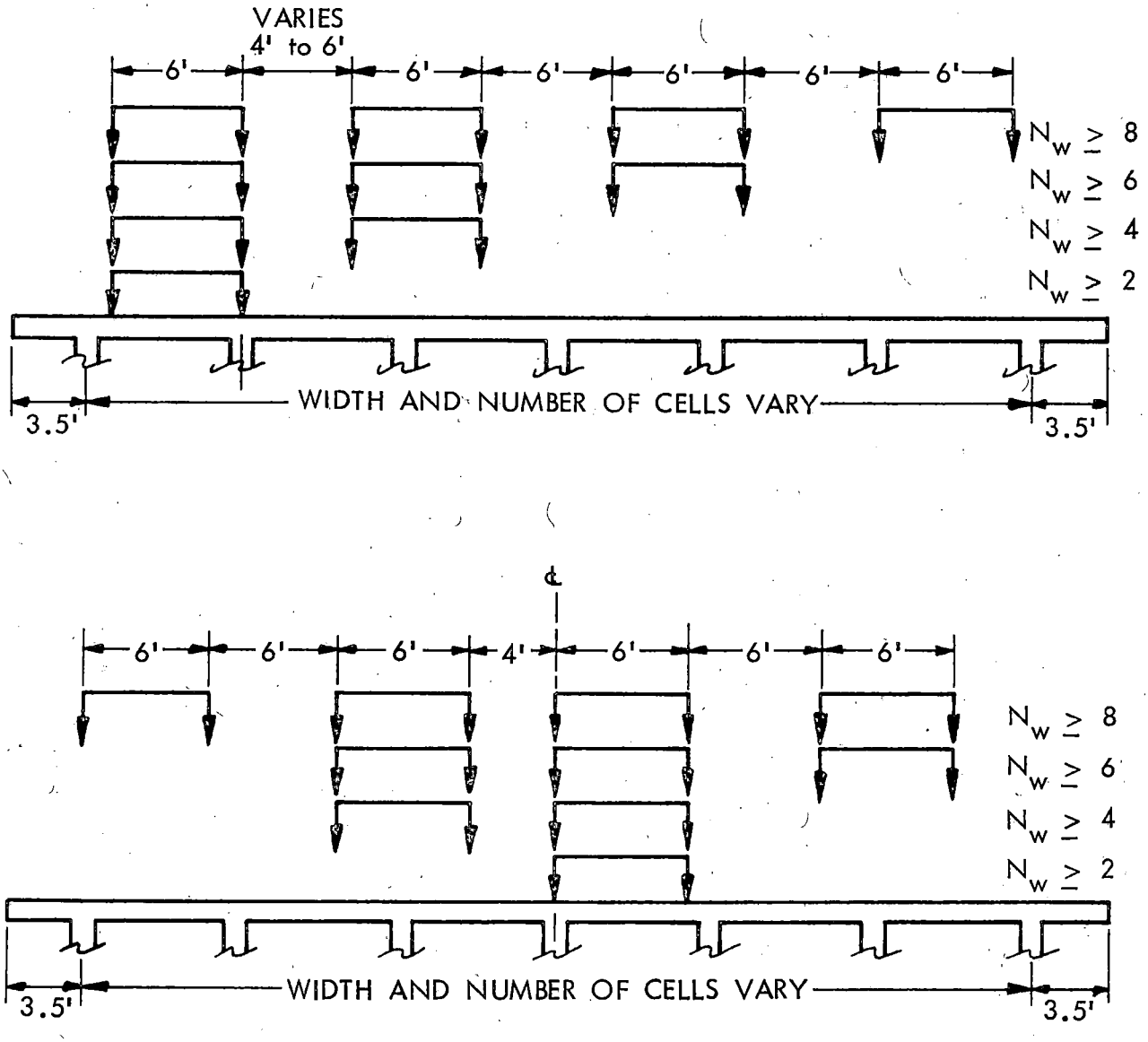

Figure 20. Additional loading cases considered for concrete box girder bridges.

Maximum Load Factors

Influence lines were generated for the girder moment coefficients for each of the combinations listed in Table 6. The final moment coefficients from the actual truck loads were found by superposition

using these influence lines. As in the study of beam and slab and multi-beam bridges, the final moment coefficient is reduced to D as used in the S/D load factor equation. The value of S used in this equation is modified as explained in Chapter 4. The results of these computations, along with the critical girder and loading cases, are tabulated in Table 7. The absolute minimum value of D for all loading cases considered is shown in the table. The reduction of these data to a proposed design equation is discussed in Chapter 4.

It should be pointed out, however, that because of the complexity of the analysis and because of the integral nature of the section, the most accurate design can only be obtained by an analysis of the complete section. However, for ordinary design purposes, it is felt that a satisfactory distribution procedure can be obtained from the preceding analysis and range of variables.

The results presented in Table 7 do, however, show several significant facts about the behavior of box girder bridges.

1. For a particular bridge cross section, as the span increases the distribution of loads improves since the value of D increases.

2. The inclusion of diaphragms improves the load distribution characteristics (D increases). A single diaphragm at midspan apparently is better in distributing the loads than a pair of diaphragms at the third points of the span. However, this is probably due to the fact that all wheel loads were placed at midspan and, thus, were directly over the single diaphragm. Actually, the benefits from diaphragms should be computed for the wheel loads in their true longitudinal position.

TABLE 7

THEORETICAL RESULTS FOR BOX GIRDER BRIDGES VALUE OF D IN EQUATION: LF = S/D

N_w	W	N_g	N_d	L	d/L	D	
4	33	5	0	50	0.07	6.35	
			0	50	0.05	6.47	(6.53)[a]
			0	80	0.07	6.67	
			0	80	0.05	6.76	
			0	110	0.07	6.86	
			0	110	0.05	6.92	(7.00)
			1	50	0.07	7.04	
			1	110	0.05	7.43	
			2	50	0.07	6.52	
4	37	5	0	50	0.07	6.39	
			0	50	0.05	6.61	(6.69)
			0	80	0.07	6.90	
			0	80	0.05	7.08	
			0	110	0.07	7.21	
			0	110	0.05	7.34	(7.44)
			1	50	0.07	7.60	
			1	110	0.05	8.28	
			2	50	0.07	6.76	
6	39	5	0	50	0.07	6.22	
			0	50	0.05	6.26	(6.29)
			0	80	0.07	6.39	
			0	80	0.05	6.39	
			0	110	0.07	6.50	
			0	110	0.05	6.48	(6.53)
			1	50	0.07	6.63	
			1	110	0.05	6.80	
			2	50	0.07	6.25	
6	41	5	0	50	0.07	6.03	
			0	50	0.05	6.08	
			0	80	0.07	6.23	
			0	80	0.05	6.25	
			0	110	0.07	6.35	
			0	110	0.05	6.36	
6	45	5	0	50	0.07	5.99	
			0	50	0.05	6.08	(6.13)
			0	80	0.07	6.25	
			0	80	0.05	6.33	
			0	110	0.07	6.43	
			0	110	0.05	6.48	(6.54)
			1	50	0.07	6.50	
			1	110	0.05	6.93	
			2	50	0.07	6.20	

TABLE 7

CONTINUED)

N_w	W	N_g	N_d	L	d/L	D	
6	45	7	0	50	0.07	5.94	
			0	50	0.05	6.03	
			0	80	0.07	6.23	
			0	80	0.05	6.32	
			0	110	0.07	6.40	
			0	110	0.05	6.48	
			1	50	0.07	6.36	
			1	110	0.05	6.90	
			2	50	0.07	6.09	
6	49	7	0	50	0.07	5.85	
			0	50	0.05	6.01	(6.06)
			0	80	0.07	6.24	
			0	80	0.05	6.41	
			0	110	0.07	6.50	
			0	110	0.05	6.66	(6.74)
			1	50	0.07	6.51	
			1	110	0.05	7.29	
			2	50	0.07	6.11	
8	51	7	0	50	0.07	6.15	
			0	50	0.05	6.17	(6.20)
			0	80	0.07	6.30	
			0	80	0.05	6.32	
			0	110	0.07	6.40	
			0	110	0.05	6.41	(6.44)
			1	50	0.07	6.49	
			1	110	0.05	6.69	
			2	50	0.07	6.18	
8	53	7	0	50	0.07	5.91	
			0	50	0.05	5.95	
			0	80	0.07	6.10	
			0	80	0.05	6.14	
			0	110	0.07	6.23	
			0	110	0.05	6.26	
8	57	7	0	50	0.07	5.65	
			0	50	0.05	5.73	(5.77)
			0	80	0.07	5.89	
			0	80	0.05	5.98	
			0	110	0.07	6.06	
			0	110	0.05	6.15	(6.20)

TABLE 7

CONTINUED

N_w	W	N_g	N_d	L	d/L	D	
8	61	7	0	50	0.07	5.79	
			0	50	0.05	5.89	
			0	80	0.07	6.06	
			0	80	0.05	6.19	
			0	110	0.07	6.27	
			0	110	0.05	6.40	
			1	50	0.07	6.18	
			1	110	0.05	6.90	
			2	50	0.07	5.96	
8	61	9	0	50	0.07	5.68	
			0	50	0.05	5.77	(5.81)
			0	80	0.07	5.97	
			0	80	0.05	6.11	
			0	110	0.07	6.19	
			0	110	0.05	6.33	(6.39)
			1	50	0.07	5.98	
			1	110	0.05	6.71	
			2	50	0.07	5.78	
12	75	9	0	50	0.07	5.89[b]	
			0	50	0.05	5.96[b]	
			0	80	0.07	6.00[b]	
			0	80	0.05	6.06[b]	
			0	110	0.07	6.08[b]	
			0	110	0.05	6.12[b]	

Note: Unless indicated, eccentric loading controlled with the first interior girder critical. All lanes were loaded.

[a]Values in parenthesis refer to special computations where thicknesses were varied.

[b]Central loading controlled with center girder critical.

3. If the depth of the section increases (d/L increases), the load distribution is slightly worse due to the reduction in torsional stiffness. This is, however, more than offset by the increase in the longitudinal moment of inertia. Thus, the resultant extreme fiber

stress decreases. Also, if the thicknesses of the section elements are held within the ranges selected for study, no significant change in distribution behavior is expected.

CHAPTER 4. DEVELOPMENT OF DESIGN PROCEDURES

GENERAL

In the development of any design procedure, the main consideration to be kept in mind is the realization that the final procedure must not be so complicated that it is totally unacceptable to the practicing engineer. In addition, the procedure must offer improvement in accuracy over previously accepted procedures. Therefore, the objective becomes one of finding the simplest procedure with the best accuracy with respect to the known theoretical and experimental behavior.

The present design criteria have remained essentially unchanged for the last 25 years except where new bridge types have been introduced. The criteria have proved to be conservative in predicting the maximum moments in most structures considered. In addition, only a very limited number of variables is considered in the current procedures. The procedures given herein were developed so that the design moments can be more realistic in keeping with the actual behavior of the bridge and can consider all of the significant variables affecting that behavior.

The main objection to the present design procedures has been that the design of the members is based only on the type of bridge and the spacing between longitudinal girders (as in the case of beam and slab bridges and box girder bridges). It is apparent from the results given in Chapter 3 that as the aspect ratio of the bridge (width to length ratio) decreases, the load distribution characteristics of the bridge should improve. Secondly, there are no provisions for the flexural and torsional stiffness characteristics of the individual bridge. For example, there has been no design benefit from adding diaphragms or

deepening the slab. It is necessary that the final procedure(s) eliminate these objections, to the extent that this is feasible, so that improvements in designs can be obtained.

Although the results of the studies outlined in Chapter 3 showed that the critical girder or beam could be either the exterior girder or an interior girder, it was felt that, since the critical condition varied with the combination of parameters, the design criteria should be uniform for all beams and should be based on the absolute critical case. In the normal range of parameters, the differences between the critical cases for both girder positions did not warrant this consideration. Thus, a common design criteria has been developed for all beams.

BEAM AND SLAB BRIDGES

In beam and slab bridges, it was found that the major variables describing the behavior of the bridge for a particular case could be combined into a flexural stiffness parameter, θ_x (the relative flexural stiffness ratio multipled by the aspect ratio of the bridge), and the torsional stiffness parameter, α (the relative ratio of the torsional stiffness to the flexural stiffness of the bridge). There are several analytical and graphical methods which can be applied to the theoretical data of Table 4 to show the relationship between D (in S/D) and the stiffness parameters.

The method used to determine a possible relationship was to sketch contour lines of constant D on a coordinate system using $\sqrt{\alpha}$ as one coordinate and θ as the other coordinate. A typical example of this type of representation is shown in Figure 21. These plots clearly show that for the practical

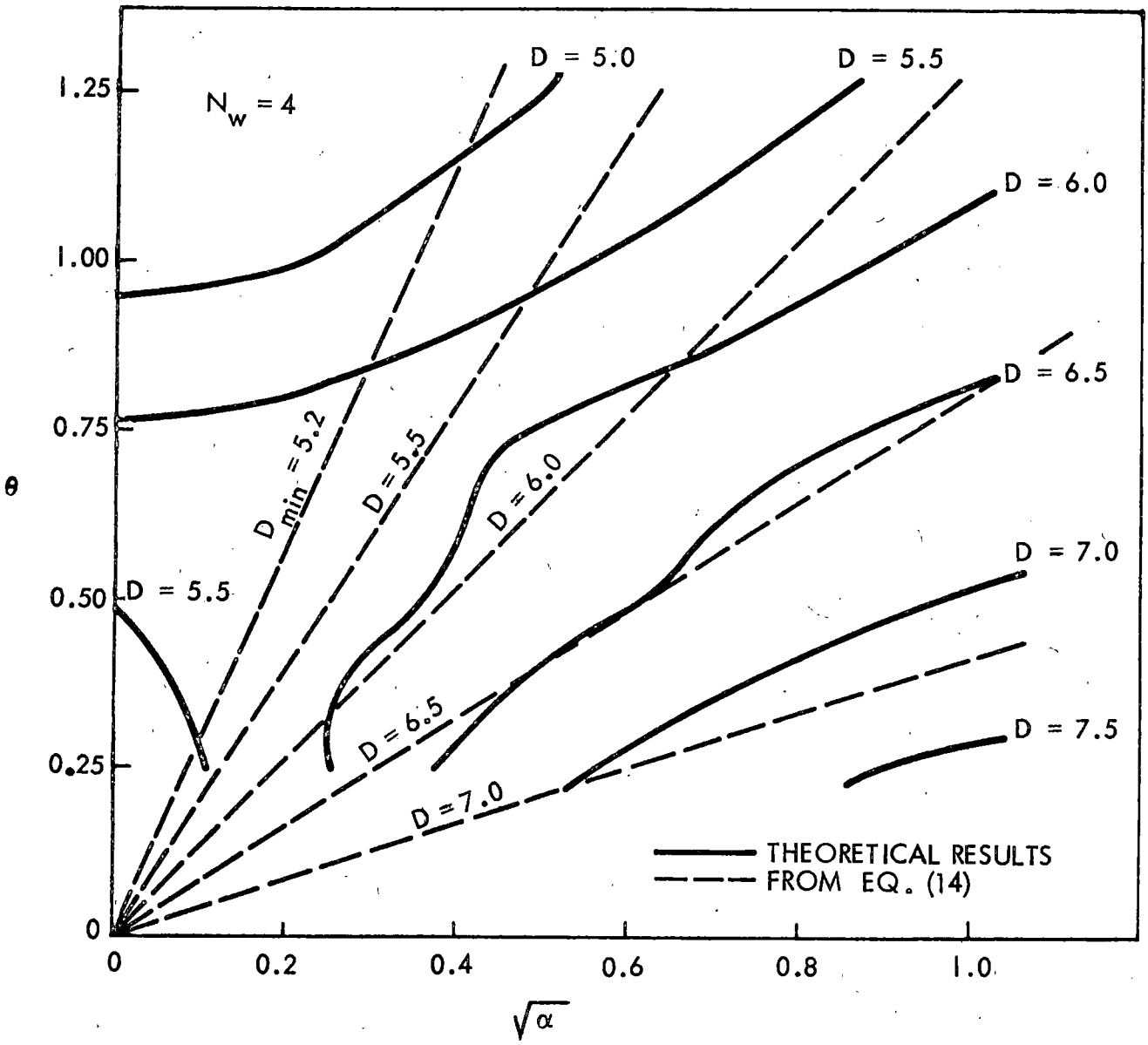

Figure 21a. Contours of D for beam and slab bridges, W = 33 ft.

ranges of θ and α the contour lines are nearly straight lines converging on the coordinate axes. This indicates that for a particular bridge width, a parameter which could be used in the design procedure is $\theta/\sqrt{\alpha}$. This ratio, which will be referred to as C, is used rather than considering θ and $\sqrt{\alpha}$ each as an independent parameter. Thus,

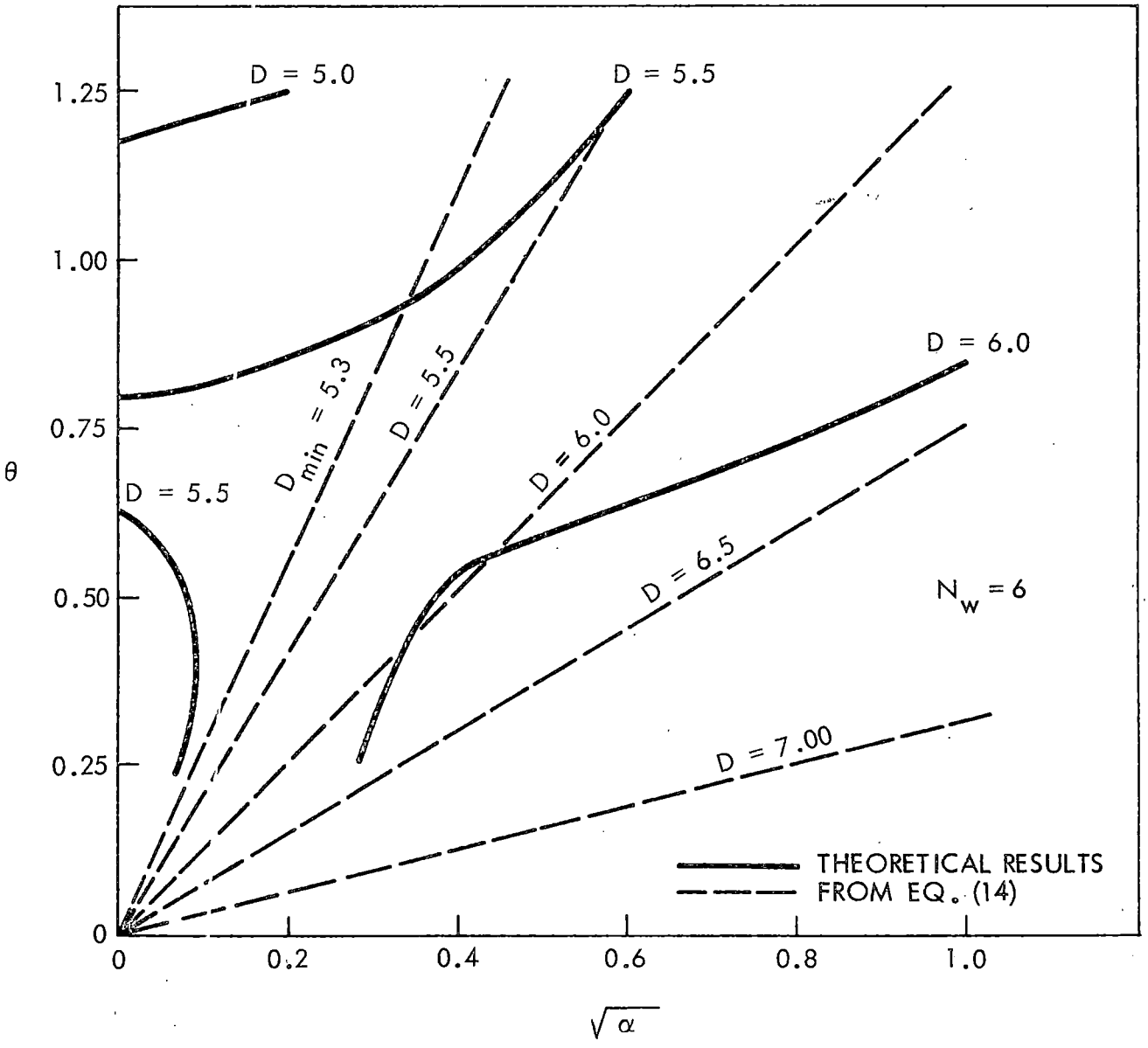

Figure 21b. Contours of D for beam and slab bridges, W = 39 ft.

$$C = \frac{W}{(\sqrt{2})L}\sqrt{\frac{D_x}{D_{xy} + D_{yx}}}\,. \qquad (13)$$

There remains then the question of the influence of the deviation of the actual contours from the straight lines (use of one parameter for

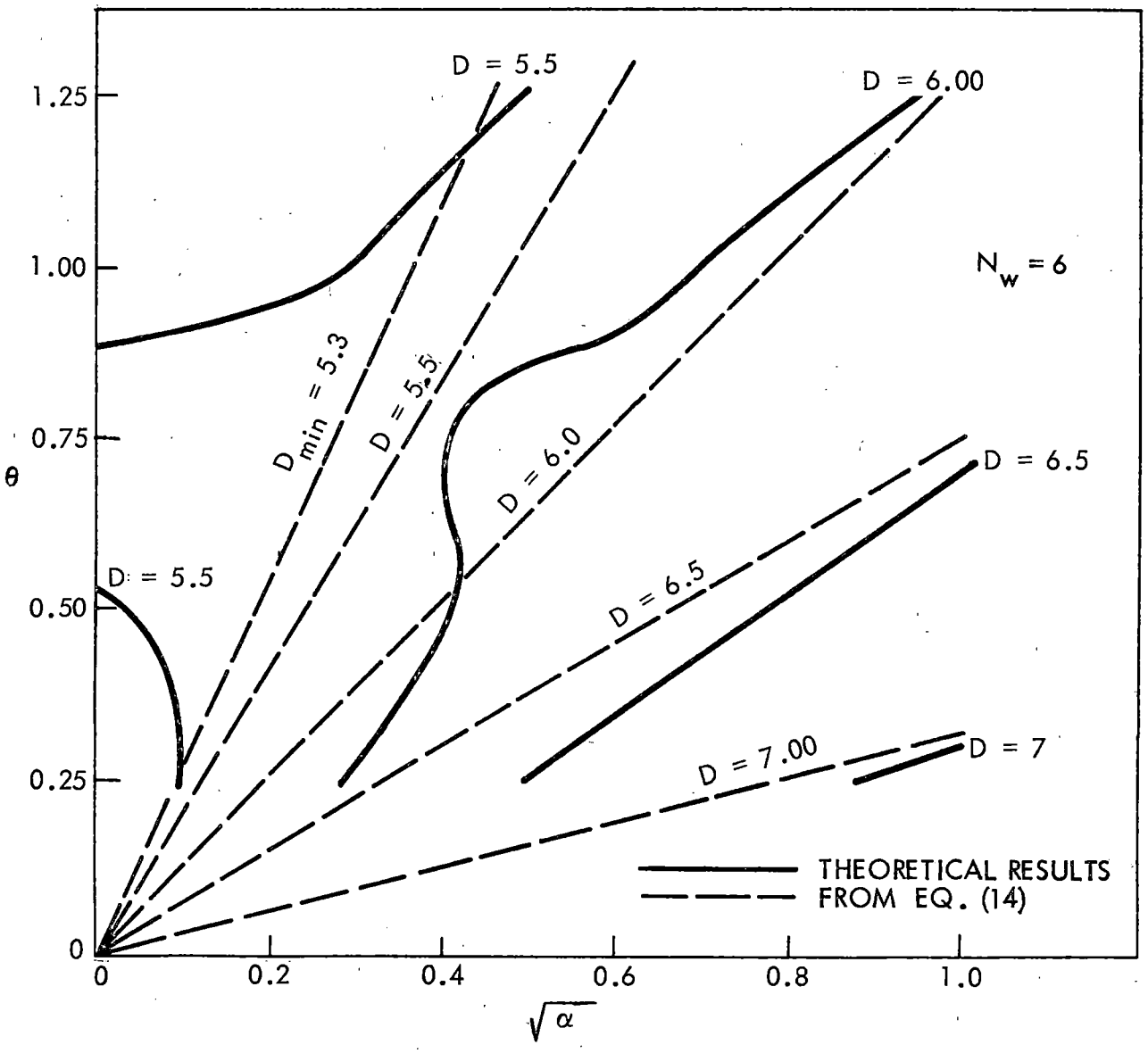

Figure 21c. Contours of D for beam and slab bridges, W = 45 ft.

the two), the effect of the bridge width, and the number of wheel loads acting on the bridge. This can be seen in the plot of D vs C for all values listed in Table 4. These plots, Figures 22 – 24, show that the D values are comparatively well banded with respect to the value of C for each particular set of wheel loads. One of the simplest equations

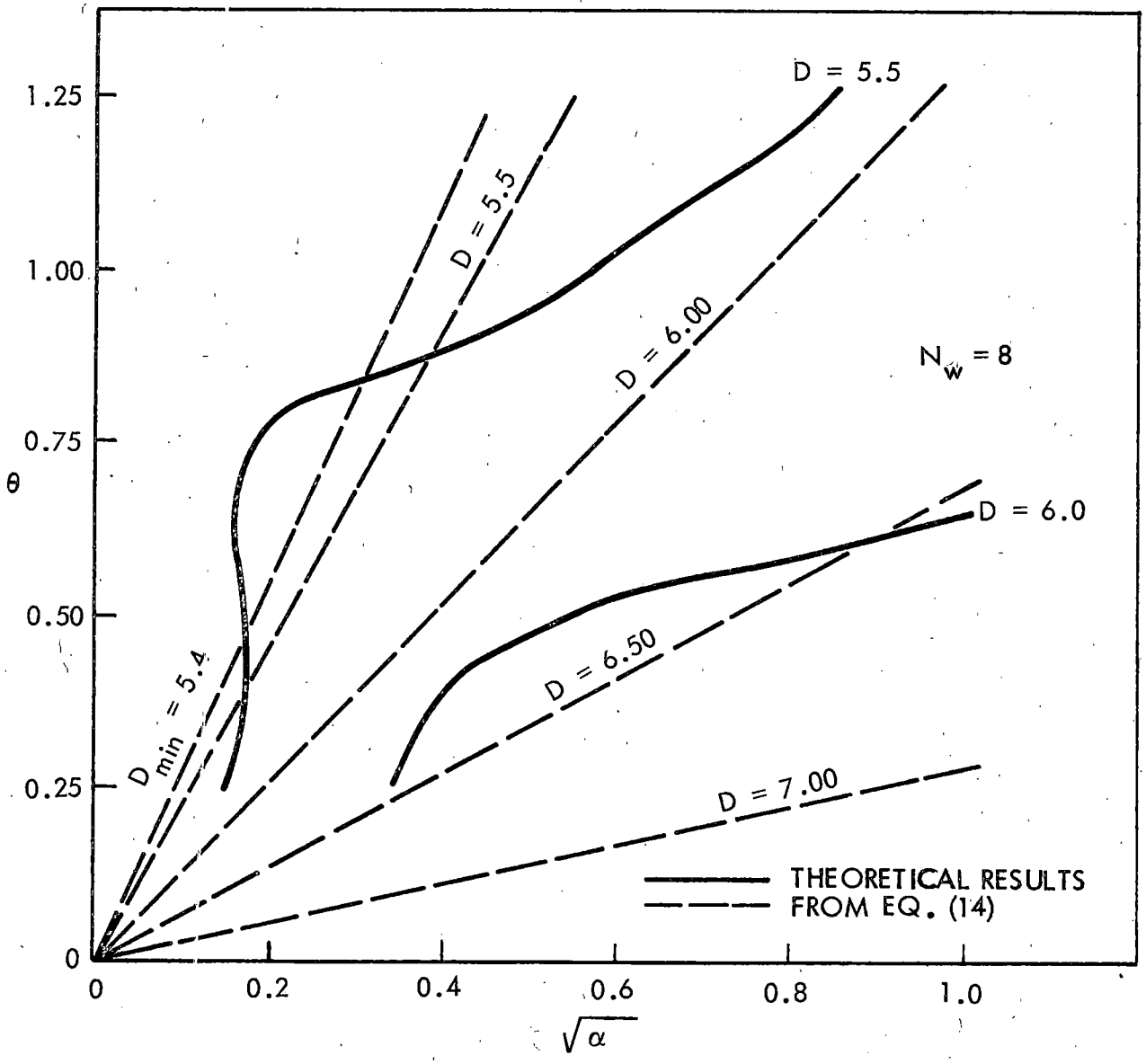

Figure 21d. Contours of D for beam and slab bridges, W = 51 ft.

which best suits these results and incorporates all variables, is in the following form:

$$D = 5.0 + \frac{N_w}{20} + (3.0 - \frac{N_w}{7})(1.0 - \frac{C}{3})^2 \qquad C \leq 3$$

$$D = 5.0 + \frac{N_w}{20} \qquad C \geq 3 \qquad (14)$$

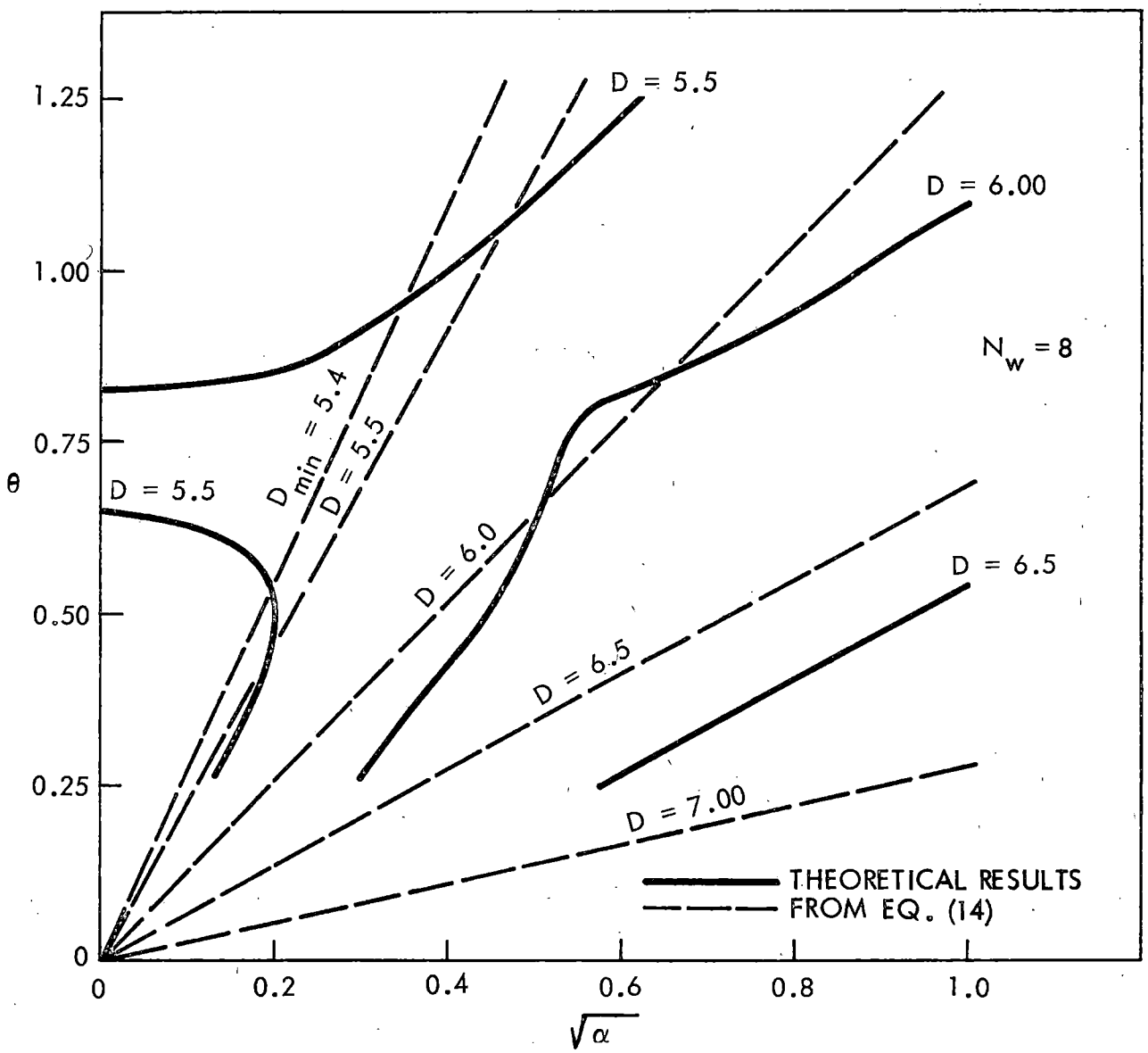

Figure 21e. Contours of D for beam and slab bridges, W = 57 ft.

also,

$$D \leqq \frac{W}{N_w}$$

where $C = \theta/\sqrt{\alpha}$, and N_w = number of design wheels from AASHO Article 1.2.6, modified to conform to the criteria used in this study. Equation (14)

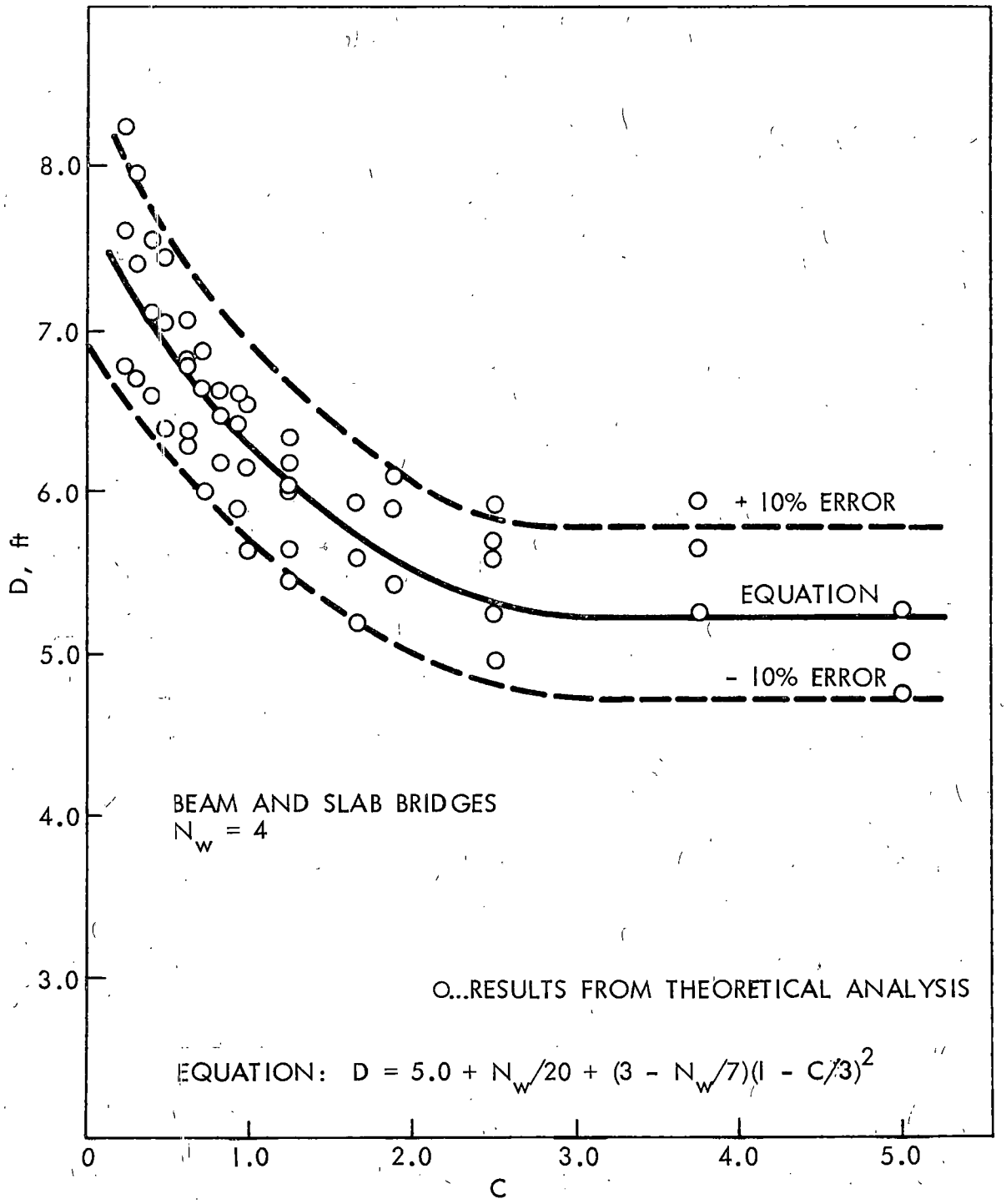

Figure 22. Variation of D with bridge stiffness parameter C for beam and slab bridges, $N_w = 4$.

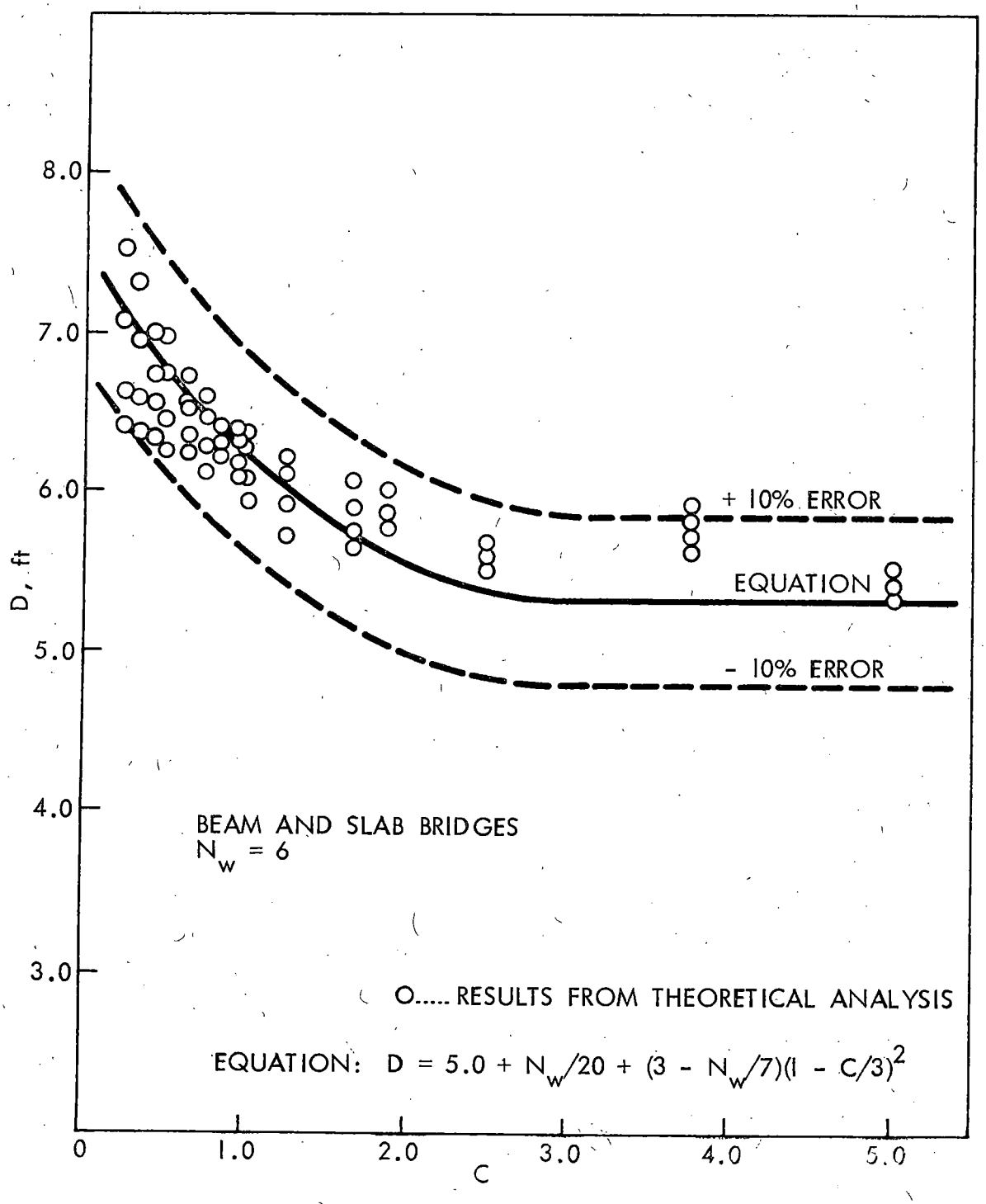

Figure 23. Variation of D with bridge stiffness parameter C for beam and slab bridges, $N_w = 6$.

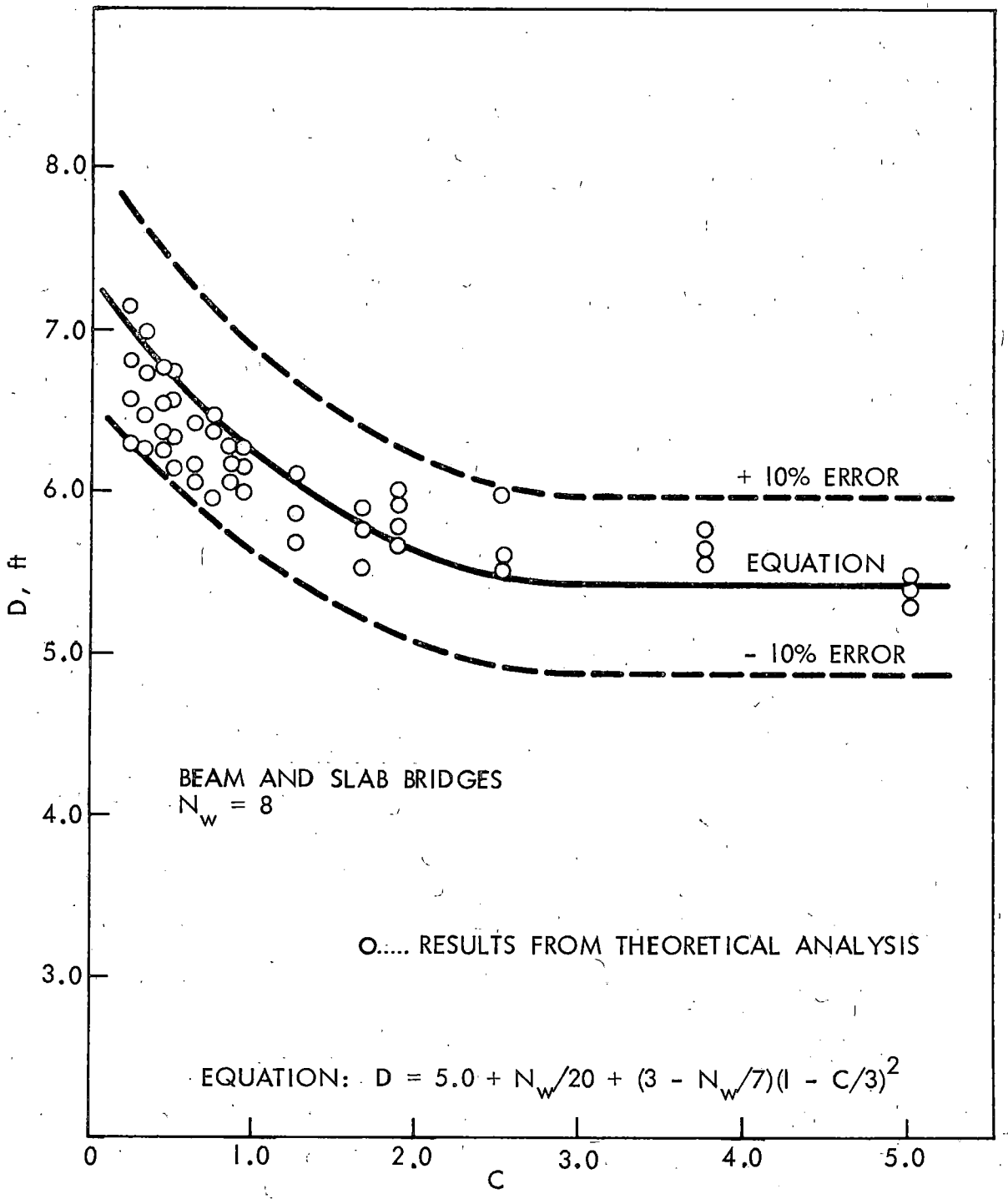

Figure 24. Variation of D with bridge stiffness parameter C for beam and slab bridges, $N_w = 8$.

can also be expressed directly in terms of the total number of design traffic lanes (N_L) by changing the N_w term to $2(N_L)$. Thus, the equation becomes

$$D = 5.0 + \frac{N_L}{10} + (3.0 - \frac{2N_L}{7})(1.0 - \frac{C}{3})^2 \qquad C \leq 3$$

$$D = 5.0 + \frac{N_L}{10} . \qquad C \geq 3 \qquad (14a)$$

N_L in this case would be obtained from a new Article 1.2.6 — Traffic Lanes, which would be based on the lane criteria used in this study. This criteria is, in effect, the width of the roadway (curb to curb) in feet, divided by 12, reduced to the nearest whole number. Then N_w in Equation (14) is just twice the number of lanes.

The details involved in the computation of C can be found in Appendix B. However, in the case of composite steel box girder bridges, because of the special nature of the cross section, the effective torsional rigidity is somewhat less than the torsional rigidity computed using standard procedures. Thus, the computed C would be less than the effective C to be used in Equation (14). By comparison of the above equation with the extensive results of Johnston, Mattock and others (97, 135), it was found that the effective rigidity was approximately 25 percent of the indicated torsional rigidity, and, thus, for composite steel box girders, the effective C is twice the computed C. Table 8 summarizes these results showing the relationship of D from Equation (14) to the theoretical results (97) and the D from the new load distribution equation (97, 135) and from Article 1.7.104 of the 1966-1967 AASHO Interim Specification (279). It can be seen that the use of Equation (14) with the modified C gives better correlation than the new specifications.

TABLE 8

COMPARISON OF PROCEDURES FOR LOAD DISTRIBUTION IN COMPOSITE BOX GIRDER BRIDGES

Bridge number (97)	50-4	50-6	75-2	75-3	75-5	100-4	100-6
Number of lanes	3	4	2	3	4	3	4
Span, feet	50	50	75	75	75	100	100
Number of girders	4	5	3	3	4	4	5
Girder spacing, feet	10.50	10.50	10.50	14.33	13.33	10.50	10.50
D, from theory (97)	5.58	5.52	6.44	6.10	5.70	6.12	5.71
D, from box girder equation (97, 135)	6.33	6.33	6.45	6.90	6.64	6.33	6.33
D, from Equation (14) using effective C	5.66	5.61	6.28	6.07	6.06	6.18	6.02

However, it is felt that the current interim specifications are more readily usable in design offices, especially considering the small differences in the D values.

Equation (14) seems to indicate that there is no influence of the transverse stiffness of the bridge, EI_y on the load distribution characteristics of the bridge. However, it must be remembered that the ranges of the parameters θ and $\sqrt{\alpha}$ have been previously established. This, therefore, automatically limits the minimum value of I_y. For example, assuming that the value of θ is limited to a maximum of 1.00

$$\theta = \frac{W}{2L}\sqrt[4]{\frac{D_x}{D_y}} = 1.00$$

then the value of I_y must be at least equal to or greater than one-sixteenth of I_x multiplied by the fourth power of the aspect ratio of the bridge or

$$I_y \geq \frac{W^4}{16L^4} I_x \qquad (\theta \leq 1.00)$$

of if $\theta \leq 1.25$,

$$I_y \geq \frac{W^4}{40L^4} I_x \; . \qquad (\theta \geq 1.25)$$

For the practical range of bridge design, it is obvious that this criterion will always be satisfied. In reality, the major effect of an increase in I_y is included in a change in the torsional stiffness parameter. This change may be significant if the I_y is increased due to thickening of the slab but will probably be minimal if due to including diaphragms. The reason that individual diaphragms are ineffective in this analysis is that an equivalent plate is used to represent the actual bridge system. Therefore, the true effects of a transverse diaphragm on the distribution characteristics are not represented because the stiffness of these members has been distributed longitudinally along the bridge. Thus, in the case of bridges with transverse diaphragms, Equation (13) yields conservative results. However, unless the diaphragms are rigid and closely spaced, their effects or distribution will usually be minor. For the general bridge system with various considerations of flexural and torsional stiffnesses, Equation (13) will produce D values that are within $\pm$ 10 percent of the correct value with respect to the equivalent plate.

In the design of a beam and slab bridge the determination of the Load Factor is as follows:

$$\text{Load Factor, Beam and Slab} = S/D \qquad (15)$$

where

S = the average distance between beams in beam and slab bridges (S will be taken as 1.0 ft for slab bridges to determine the moment per foot).

D = the width of bridge in feet necessary for the design of one line of wheels as determined by Equation (13).

The design load per beam is then the Load Factor times the magnitude of the wheel load.

MULTI-BEAM BRIDGES

In multi-beam bridges, it was found that only one physical parameter ϕ is required to predict the distribution. It can be seen from Equations (11) and (13) that the parameter ϕ in terms of physical properties is identical to the C used in beam and slab bridges except that it must be multiplied by the square root of 2. Thus, C, a stiffness parameter, for multi-beam bridges becomes

$$C_{\text{multi-beam}} = (\sqrt{2})\,\phi.$$

Using the same methods as outlined for beam and slab bridges, it was found that the D values have the same type of relationship to the C values. It was also found that the banding in the D vs C plot is not as strong as for the beam and slab bridges, but was scattered due to the sensitivity of the D value to the width of the bridge. However, it was found that if the S value used to compute the load factor, S/D, was changed to correspond to the average width of bridge for a given number of wheel loads, the same equations for D in beam and slab bridges could also be used for multi-beam bridges. The values of D modified for the change in

the definition of S are given in Table 9. The variation of the modified D with C for multi-beam bridges is shown in Figures 25 – 27. Thus, for multi-beam bridges, S in Equation (15) to determine the load factor should be taken as:

$$S_{\text{multi-beam}} = (6N_w + 9)/N_g \qquad (16)$$

where

N_w = the number of longitudinal lines of wheel loads

N_g = the number of beam elements

and D should be taken as given in Equation (13). The design load per beam is then obtained by multiplying the wheel load by the Load Factor.

TABLE 9

THEORETICAL RESULTS FOR MULTI-BEAM BRIDGES VALUE OF D IN EQUATION: LF = S/D; $S = (6N_w + 9)/N_g$

	W, WIDTH OF BRIDGE IN FT (N_w, NO. OF WHEEL LOADS)								
ϕ	28 (4)	33 (4)	37 (4)	39 (6)	41 (6)	45 (6)	49 (6)	51 (8)	53 (8)
0.1	8.08	8.00	7.87	7.43	7.42	7.35	7.25	7.07	7.04
0.3	7.45	7.18	6.97	7.20	7.12	6.96	6.67	6.82	6.76
0.5	6.90	6.47	6.23	6.96	6.83	6.57	6.26	6.59	6.48
0.7	6.44	5.91	5.63	6.75	6.59	6.24	5.90	6.36	6.25
1.0	5.93	5.34	5.01	6.51	6.31	5.88	5.46	6.10	5.97
2.0	5.19	4.54	4.21	5.55	5.41	5.10	4.82	5.68	5.53

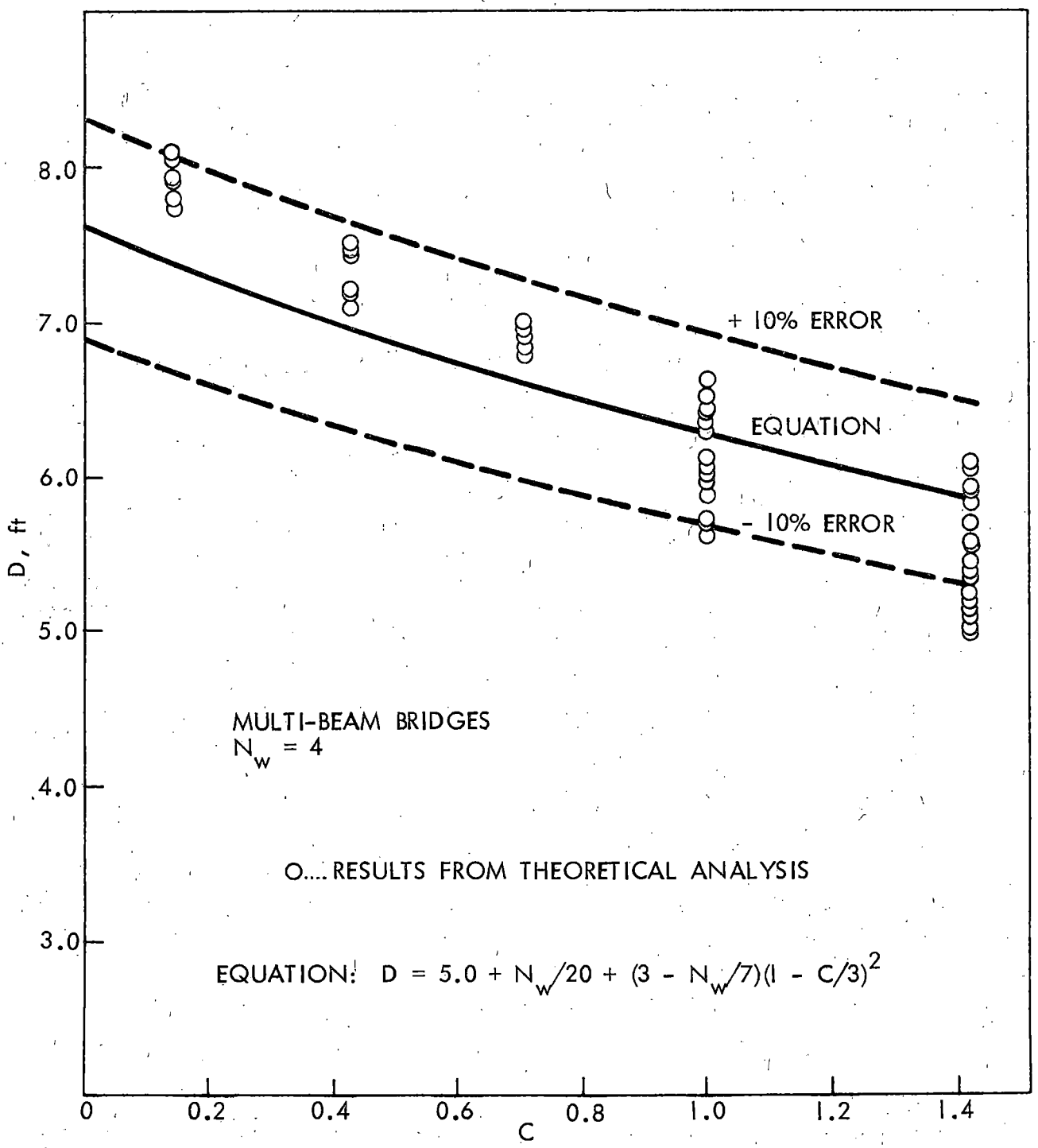

Figure 25. Variation of D with bridge stiffness parameter C for multi-beam bridges, $N_w = 4$.

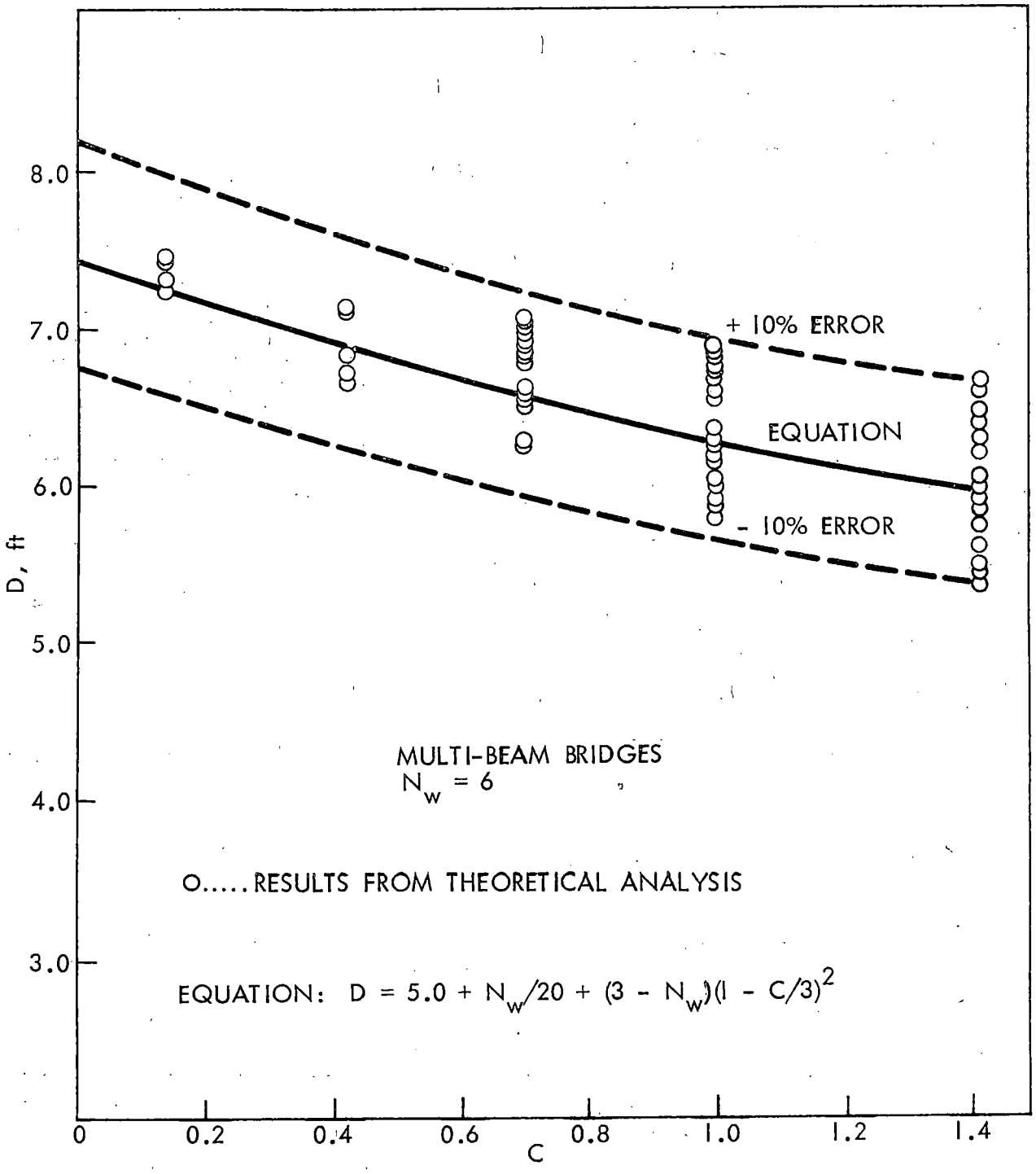

Figure 26. Variation of D with bridge stiffness parameter C for multi-beam bridges, $N_w = 6$.

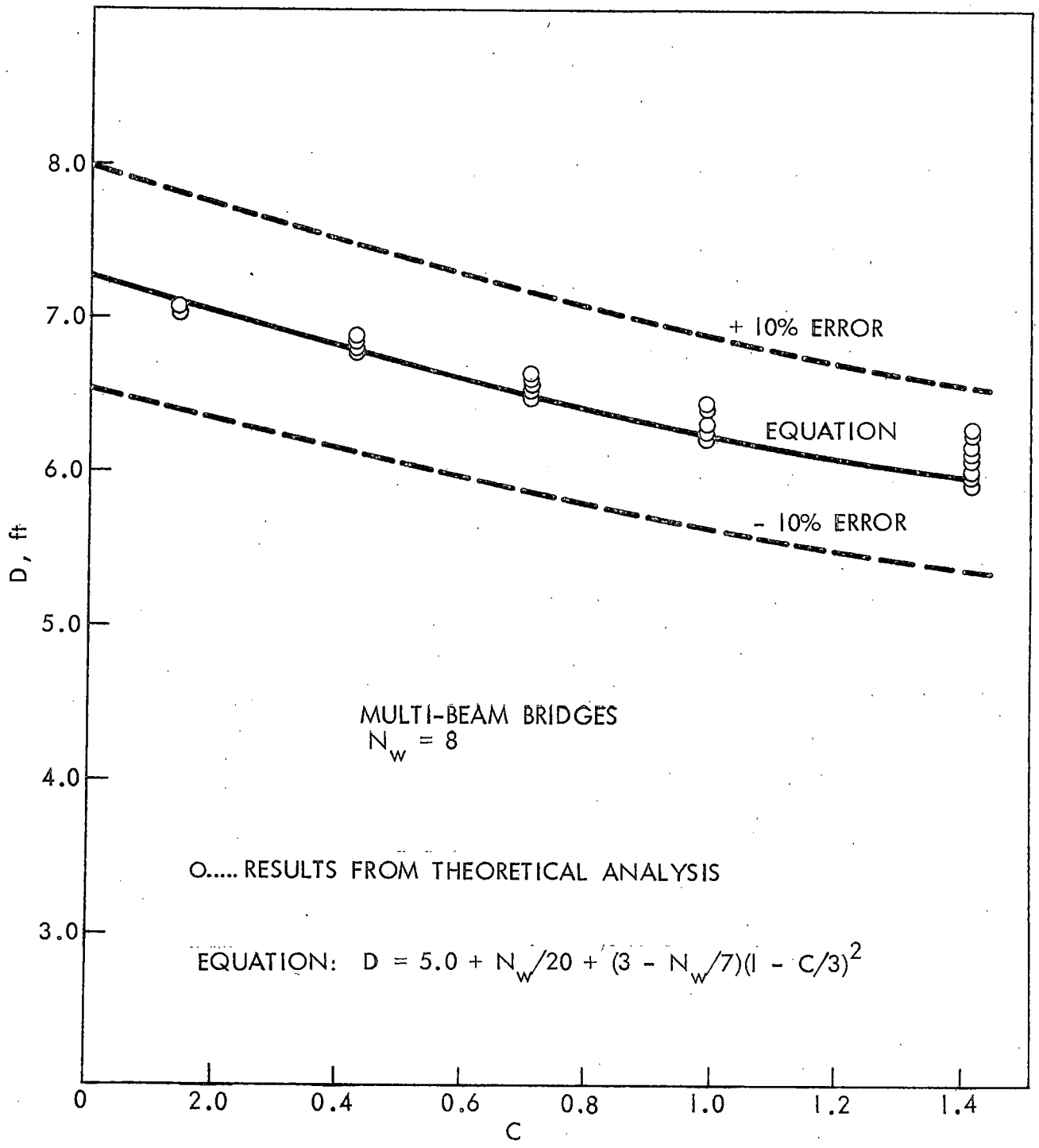

Figure 27. Variation of D with bridge stiffness parameter C for multi-beam bridges, $N_w = 8$.

CONCRETE BOX GIRDER BRIDGES

In concrete box girder bridges, no attempt was made to analyze these sections based on equivalent plate type of approach. Therefore, the parameters involved in the study were based on the basic dimensions of the bridge itself. However, the dimensionless parameters found to affect the load distribution characteristics to the greatest extent were the aspect ratio (W/L), the depth of box girder bridge width ratio (d/W), the number of vertical webs (or girders), N_g, and the number of diaphragms, N_d. It was found that by defining the stiffness parameter of the bridge (C) as,

$$C = 0.55 \frac{W}{L} \left(1 + N_g \sqrt{\frac{d}{W}}\right) \cdot \left(\frac{1}{\sqrt{1 + N_d}}\right) \qquad (17)$$

and S in Equation (15) as,

$$S = \text{Maximum } \left(S_a \text{ or } \frac{6N_w + 9}{N_g}\right)$$

where

S_a = the actual girder spacing,

N_w = the number of wheel loads, and

N_g = the number of girders.

Then D in Equation (15) can be defined by Equation (14) as used in the previous discussion for beam and slab and multi-beam bridges. The actual values of C and D as found from the analytical solutions as well as the values of D as computed using C and S from Equation (17) together with Equation (14) are listed in Table 9. This table also lists the error of the value of D from the equations with respect to the actual computed theoretical value. The results are also shown in Figures 28 – 30.

The results shown in Table 10 clearly indicate the validity of the proposed definitions of D and S. In nearly every case the difference between the values of D computed using the theory of prismatic folded plates (222) and those obtained using the procedure proposed in Equation (17) is less than five percent. Only in two cases is the error greater than 10 percent and these are conservative differences.

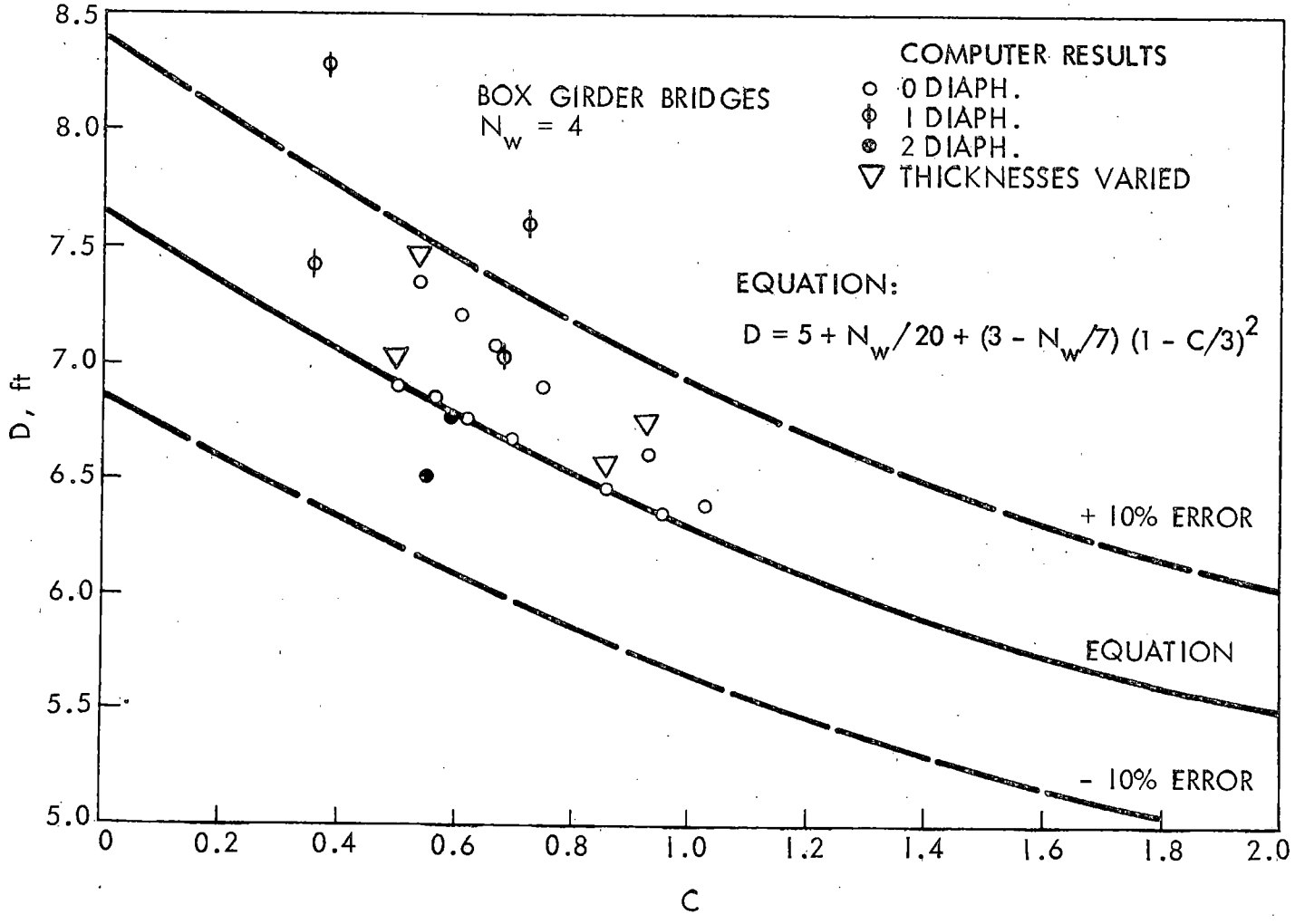

Figure 28. Variation of D with bridge stiffness parameter C for concrete box girder bridges, $N_w = 4$.

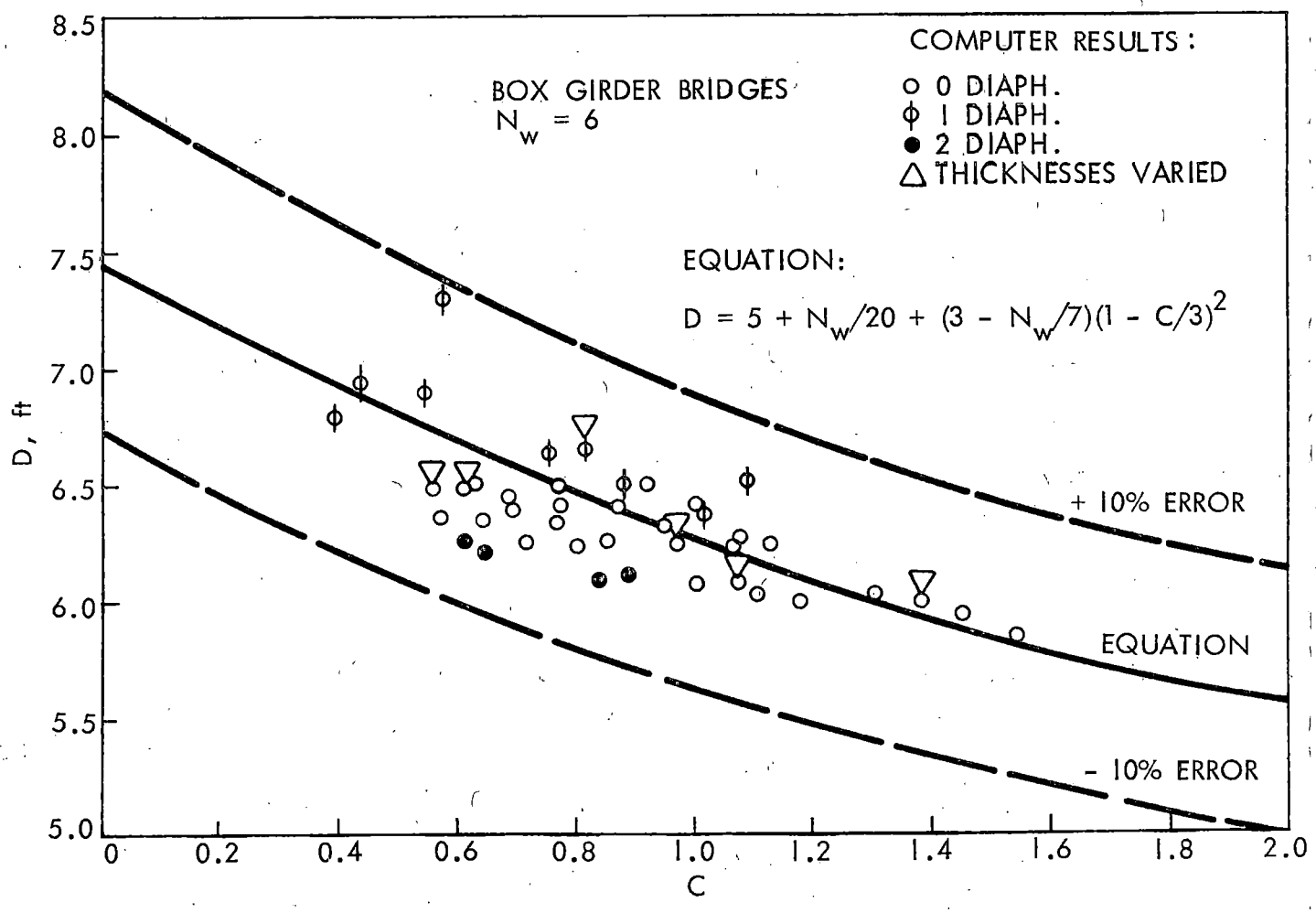

Fig. 29. Variation of D with bridge stiffness parameter C for concrete box girder bridges, $N_w = 6$.

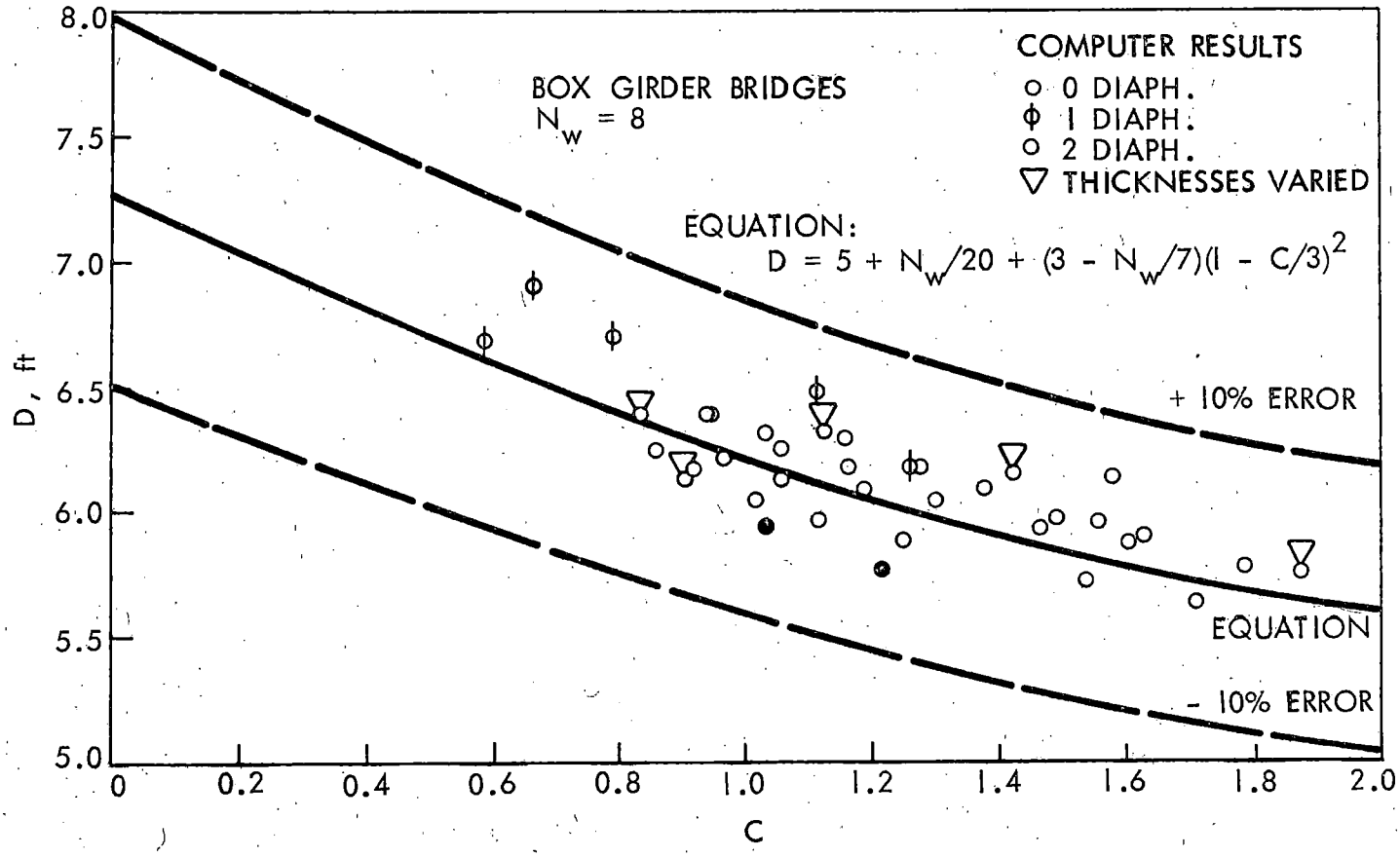

Figure 30. Variation of D with bridge stiffness parameter C for concrete box girder bridges, $N_w = 8$.

TABLE 10

CONCRETE BOX GIRDER BRIDGE PARAMETER STUDY RESULTS

N_w	W	N_g	N_d	L	d/L	C (EQUATION (17))	^1D (TABLE 7)	^2D (EQUATION (14))	PERCENT DIFFERENCE BETWEEN 1 AND 2
4	33	5	0	50	0.07	0.952	6.35	6.34	+ 0.2
			0	50	0.05	0.858	6.47 (6.53)	6.43	+ 0.6 (+ 1.6)[a]
			0	80	0.07	0.693	6.67	6.63	+ 0.6
			0	80	0.05	0.620	6.76	6.75	+ 0.1
			0	110	0.07	0.562	6.86	6.82	+ 0.6
			0	110	0.05	0.500	6.92 (7.00)	6.90	+ 0.3 (+ 1.4)
			1	50	0.07	0.674	7.04	6.65	+ 5.9
			1	110	0.05	0.354	7.43	7.11	+ 4.5
			2	50	0.07	0.550	6.52	6.82	- 4.4
4	37	5	0	50	0.07	1.029	6.39	6.24	+ 2.4
			0	50	0.05	0.931	6.61 (6.69)	6.34	+ 4.3 (+ 5.5)
			0	80	0.07	0.747	6.90	6.58	+ 4.9
			0	80	0.05	0.671	7.08	6.65	+ 6.5
			0	110	0.07	0.606	7.21	6.75	+ 6.8
			0	110	0.05	0.540	7.34 (7.44)	6.82	+ 7.6 (+ 8.2)
			1	50	0.07	0.728	7.60	6.58	+ 15.5
			1	110	0.05	0.382	8.28	7.07	+ 17.1
			2	50	0.07	0.594	6.76	6.77	- 0.1
6	39	5	0	50	0.07	1.068	6.22	6.20	+ 0.3
			0	50	0.05	0.969	6.26 (6.29)	6.28	- 0.3 (+ 0.1)
			0	80	0.07	0.774	6.39	6.50	- 1.7
			0	80	0.05	0.695	6.39	6.56	- 2.6
			0	110	0.07	0.626	6.50	6.67	- 2.5
			0	110	0.05	0.560	6.48 (6.53)	6.73	- 3.7 (- 3.0)
			1	50	0.07	0.755	6.63	6.50	+ 2.0
			1	110	0.05	0.396	6.80	6.90	- 1.4
			2	50	0.07	0.617	6.25	6.67	- 6.3
6	41	5	0	50	0.07	1.107	6.03	6.15	- 1.9
			0	50	0.05	1.001	6.08	6.24	- 2.6
			0	80	0.07	0.800	6.23	6.45	- 3.4
			0	80	0.05	0.719	6.25	6.56	- 4.7
			0	110	0.07	0.647	6.35	6.62	- 4.1
			0	110	0.05	0.579	6.36	6.69	- 4.9
6	45	5	0	50	0.07	1.180	5.99	6.09	- 1.6
			0	50	0.05	1.074	6.08 (6.13)	6.20	- 1.9 (- 1.1)
			0	80	0.07	0.853	6.25	6.39	- 2.2
			0	80	0.05	0.767	6.33	6.50	- 2.6
			0	110	0.07	0.689	6.43	6.58	- 2.3
			0	110	0.05	0.619	6.48 (6.54)	6.67	- 2.8 (- 2.1)
			1	50	0.07	0.885	6.50	6.37	+ 2.0
			1	110	0.05	0.436	6.93	6.86	+ 1.0
			2	50	0.07	0.646	6.20	6.62	- 6.3

TABLE 10

CONTINUED

N_w	W	N_g	N_d	L	d/L	C (EQUATION (17))	^1D (TABLE 7)	^2D (EQUATION (14))	PERCENT DIFFERENCE BETWEEN 1 AND 2
6	45	7	0	50	0.07	1.454	5.94	5.87	+ 1.2
			0	50	0.05	1.305	6.03	5.98	+ 0.8
			0	80	0.07	1.071	6.23	6.20	+ 0.5
			0	80	0.05	0.950	6.32	6.30	+ 0.3
			0	110	0.07	0.875	6.40	6.37	+ 0.5
			0	110	0.05	0.774	6.48	6.50	- 0.3
			1	50	0.07	1.019	6.36	6.24	+ 1.9
			1	110	0.05	0.547	6.90	6.73	+ 2.5
			2	50	0.07	0.840	6.09	6.39	- 4.7
6	49	7	0	50	0.07	1.542	5.85	5.81	+ 0.7
			0	50	0.05	1.387	6.01 (6.06)	5.92	+ 1.5 (+ 2.4)
			0	80	0.07	1.131	6.24	6.13	+ 1.6
			0	80	0.05	1.006	6.41	6.24	+ 2.7
			0	110	0.07	0.924	6.50	6.35	+ 2.4
			0	110	0.05	0.817	6.66 (6.74)	6.43	+ 3.6 (+ 4.8)
			1	50	0.07	1.091	6.51	6.15	+ 5.8
			1	110	0.05	0.578	7.29	6.69	+ 9.0
			2	50	0.07	0.891	6.11	6.37	- 4.1
8	51	7	0	50	0.07	1.581	6.15	5.82	+ 5.6
			0	50	0.05	1.428	6.17 (6.20)	5.92	+ 4.2 (+ 4.7)
			0	80	0.07	1.160	6.30	6.10	+ 3.3
			0	80	0.05	1.035	6.32	6.19	+ 2.1
			0	110	0.07	0.945	6.40	6.27	+ 2.1
			0	110	0.05	0.838	6.41 (6.44)	6.38	+ 0.5 (+ 0.9)
			1	50	0.07	1.119	6.49	6.12	+ 6.0
			1	110	0.05	0.592	6.69	6.60	+ 1.4
			2	50	0.07	0.915	6.18	6.31	- 2.1
8	53	7	0	50	0.07	1.627	5.91	5.79	+ 2.1
			0	50	0.05	1.464	5.95	5.90	+ 0.8
			0	80	0.07	1.190	6.10	6.08	+ 0.3
			0	80	0.05	1.060	6.14	6.18	- 0.6
			0	110	0.07	0.969	6.23	6.25	- 0.3
			0	110	0.05	0.858	6.26	6.34	- 1.3
8	57	7	0	50	0.07	1.706	5.65	5.75	- 1.7
			0	50	0.05	1.535	5.73 (5.77)	5.84	- 1.9 (- 1.2)
			0	80	0.07	1.250	5.89	6.03	- 2.3
			0	80	0.05	1.115	5.98	6.12	- 2.3
			0	110	0.07	1.016	6.06	6.21	- 2.4
			0	110	0.05	0.901	6.15 (6.20)	6.31	- 2.5 (- 1.7)

TABLE 10

CONTINUED

N_w	W	N_g	N_d	L	d/L	C (EQUATION (17))	^1D (TABLE 7)	^2D (EQUATION (14))	PERCENT DIFFERENCE BETWEEN 1 AND 2
8	61	7	0	50	0.07	1.788	5.79	5.69	+ 1.8
			0	50	0.05	1.610	5.89	5.80	+ 1.6
			0	80	0.07	1.302	6.06	5.99	+ 1.2
			0	80	0.05	1.164	6.19	6.10	+ 1.5
			0	110	0.07	1.060	6.27	6.18	+ 1.5
			0	110	0.05	0.945	6.40	6.27	+ 2.1
			1	50	0.07	1.263	6.18	6.01	+ 2.8
			1	110	0.05	0.668	6.90	6.51	+ 6.0
			2	50	0.07	1.032	5.96	6.19	- 3.7
8	61	9	0	50	0.07	2.108	5.68	5.56	+ 2.2
			0	50	0.05	1.878	5.77 (5.81)	5.66	+ 1.9 (+ 2.7)
			0	80	0.07	1.555	5.97	5.84	+ 2.2
			0	80	0.05	1.377	6.11	5.95	+ 2.7
			0	110	0.07	1.276	6.19	6.01	+ 3.0
			0	110	0.05	1.128	6.33 (6.39)	6.12	+ 3.4 (+ 4.4)
			1	50	0.07	1.491	5.98	5.88	+ 1.7
			1	110	0.05	0.798	6.71	6.40	+ 4.8
			2	50	0.07	1.219	5.78	6.06	- 4.6
12	75	9	0	50	0.07	2.413	5.89	5.65	+ 4.2
			0	50	0.05	2.168	5.96	5.69	+ 4.7
			0	80	0.07	1.777	6.00	5.80	+ 3.5
			0	80	0.05	1.582	6.06	5.89	+ 2.9
			0	110	0.07	1.451	6.08	5.95	+ 2.4
			0	110	0.05	1.285	6.12	6.02	+ 1.7

[a]Values in parenthesis refer to cases where the thicknesses were varied.

INITIAL DESIGN CONSIDERATIONS

The design of bridges as determined by the use of the equations in the previous sections presupposes an actual knowledge of the bridge geometries which is not actually the case. The only information usually available prior to design is the value of the aspect ratio of the bridge and possibly the beam spacing and slab thickness. Therefore, initial values of D must be found to expedite the design procedure. To provide

information in this regard, it is suggested that "C" be approximated for preliminary design purposes by:

$$C = (\frac{W}{L})K \tag{18}$$

where

W = width of the bridge,

L = length of the bridge, and

K = a coefficient dependent on the bridge type.

Table 11 lists values of K as determined from bridges already built which conform to the present AASHO Specifications. The K value suggested for composite steel box girder bridges does consider the effective torsional rigidity. However, the table gives an indication of the range of the stiffness parameter which can be expected for each bridge type.

It is recommended that if the current AASHO Specifications are changed to correspond to the recommendations in this report, that the values of K listed in Table 11 be studied in about five years and modified to conform to the practice at that time. The reason for this statement is that present design criteria tend to make the bridge conform to the design criteria. Therefore, bridges with a very small aspect ratio now tend to be conservative; thus, the C values tend to be unnaturally high compared with an optimum design.

Figure 31 illustrates for a four-lane bridge the design moment per foot of bridge width for various bridge lengths and various values of C under HS-20 loading. The current AASHO design equation for slabs (Section 1.3.2C) for HS-20 loading is also shown. This figure clearly shows the change in design moment due to the change in the value of C

TABLE 11

VALUES OF K TO BE USED IN THE RELATION: C = K(W/L)

BRIDGE TYPE	DECK MATERIAL AND BEAM TYPE	K
Beam and slab (includes concrete slab bridge)	Concrete deck:	
	Noncomposite steel I-beams	3.0
	Composite steel I-beams	4.8
	Nonvoided concrete beams (prestressed or reinforced)	3.5
	Separated concrete box-beams	1.8
	Separated steel box-beams (composite box girders)	2.6
	Concrete slab bridges	
Multi-beam	Nonvoided rectangular beams	0.7
	Rectangular beams with circular voids	0.8
	Box section beams	1.0
	Channel beams	2.2
Concrete box girder	Without interior diaphragms	1.8
	With interior diaphragms	1.3

for various lengths of bridges. Therefore, an alternate initial design for a four-lane bridge would be to determine the value of C from Equation (17) and to determine the design moment per foot from Figure 32. The design moment per girder would then be

$$M = [M_{(\text{Figure } 32)}]S. \tag{19}$$

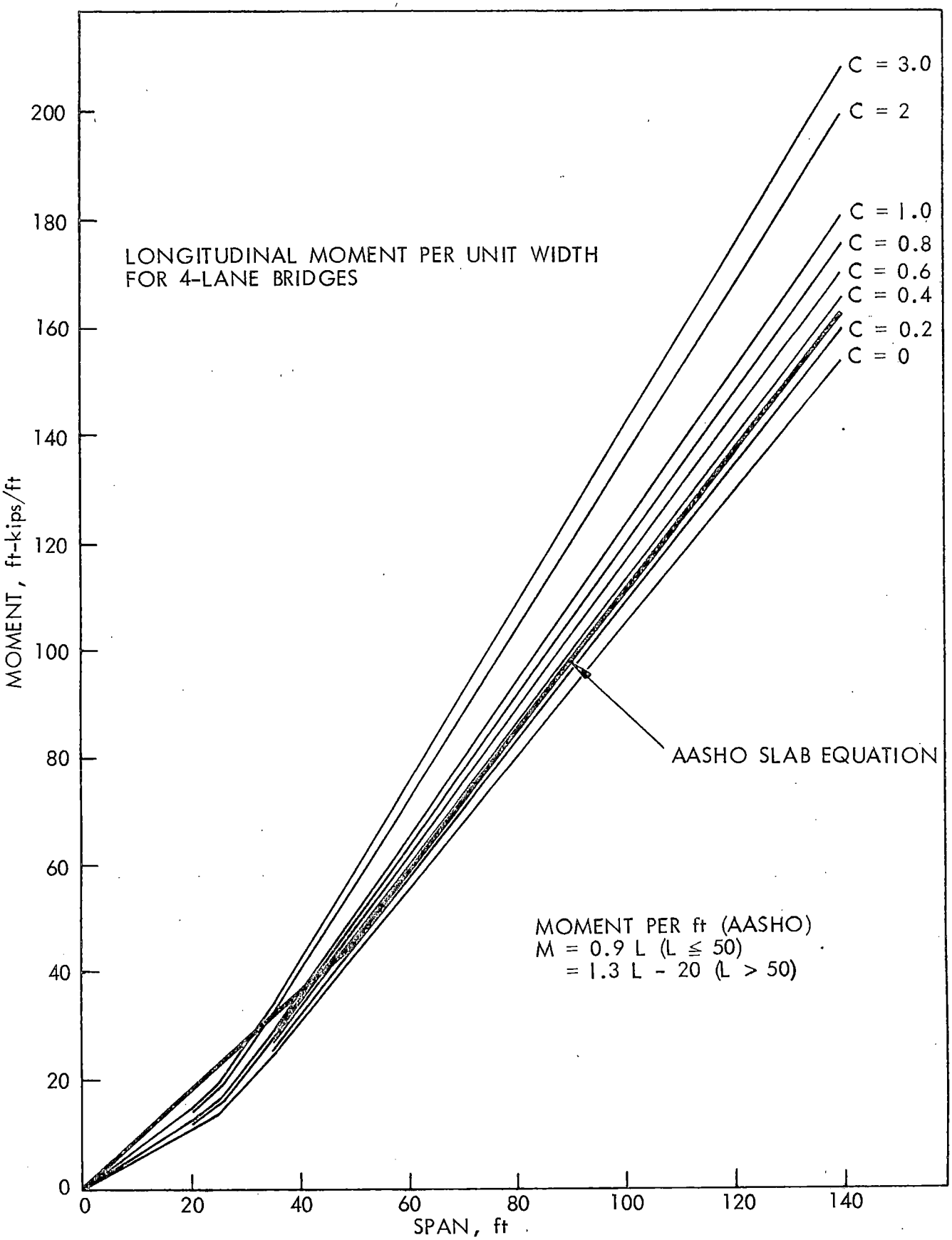

Figure 31. Comparison of design moments from Equation (14) with current AASHO slab equation.

A more accurate value of C would then be determined from this preliminary design. Similar figures could be constructed for this procedure for bridges with different numbers of lanes.

EFFECTS OF EDGE STIFFENING

In the case of beam and slab bridges having curbs and rails, the effect of additional members may be taken into account by defining the effective width of the bridge as

$$W_e = (N_g - 2)S + 2(\frac{I_e}{I_i})S \tag{20}$$

where

W_e = the effective width,

I_e = moment of inertia of exterior girder section,

I_i = moment of inertia of interior girder section,

S = beam spacing, and

N_g = number of longitudinal beams.

For bridges having nominal safety curbs (up to 2 ft wide and about 1 ft deep), the effect of these additional edge members (such as built up curbs and rails) can be neglected, a common practice. This conclusion is based on a study of actual bridges that showed the effective width obtained by Equation (20) to be about equal to a width computed from $(N_g)S$.

However, for bridges having stiffer curbs (acting integrally with the slab) and possibly an additional longitudinal member which supports the curb, the previous definition of effective width (Equation (20)) should be used to determine the design moment for the beams. However, C should

be found using the actual overall bridge width. Thus, the interior beams should be designed using Equation (15) where S is the actual beam spacing, and the exterior girders should be designed using Equation (15) where S is the effective spacing S_e, for the exterior girders as defined in Equation (20) or,

$$S_e = \frac{I_e}{I_i} S \tag{21}$$

and, thus, the

$$\text{load factor} = S_e/D.$$

For low values of I_e/I_i (i.e. less than 5) it is felt that this design procedure will be sufficiently accurate.

The edge stiffening members in slab bridges are usually designed in the form of safety or sidewalk curbs. Considerable work has been done on the slab bridges with curbs. Jensen (95) presented a design procedure in which empirical formulas are used in determining the moments in curbs and in the slabs. Test results have shown this to be correct. A review of this method is felt to be unwarranted due to length of subject matter required.

Rowe (199) presented a method in which the effect of edge-stiffening beam can be taken into account accurately. This method, however, would be difficult to adopt for use in a design office due to its complexity. Pama and Cusens (166) also studied edge beam stiffening of multi-beam bridges. They concluded that as the flexural rigidity of the edge-stiffening beam increases, the absolute maximum value of K_m no longer occurs at the edge but moves to the center of the bridge. Also the absolute value of K_m decreases at a diminishing rate. Although the study

is on multi-beam bridges, the same conclusions are applicable to slab bridges.

The edge member decreases the maximum longitudinal moments in two ways (199):

1. the decrease in the mean moment caused by the additional stiffness at the edges (due to increase in the effect width), and
2. the reduction in the maximum distribution coefficient due primarily to the edge shear forces.

The decrease in the longitudinal moment per unit width may be readily taken into account by using the effective width:

$$W_e = W_c + 2 \frac{I_e}{I_s} S_c \qquad (22)$$

where

W_c = curb to curb width,

I_e = moment of inertia of edge beam (curb) per unit width,

I_s = moment of inertia of slab per unit width, and

S_c = width of edge beam (curb).

Thus for slab bridges, the load factor per foot of width is 1/D. For the curb portion of the bridge, the effective width is

$$S_e = \frac{I_e}{I_s} S_c \qquad (23)$$

and

$$\text{Load Factor} = \frac{S_e}{D} . \qquad (24)$$

For low values of I_e/I_s it is felt that this design procedure is sufficiently accurate.

CONTINUITY EFFECTS

Bridges which have end conditions other than simple supports as assumed in this report require special attention. When the ends of a bridge are restrained against rotation the immediate effect is the reduction of the mean positive moment. The secondary moments in the bridge due to its flexibility and the eccentricity of the loading are not equally reduced. This problem has been given some attention by Rowe (199). The method of design in this case can be handled by assuming that the effective length of the bridge for load distribution effects (Equation (14)) is the distance between points of contraflexure of the bridge. Equation (15) can then be used as before to determine the load factor per beam. It is felt that this procedure will be conservative but should be clarified through future additional theoretical work. In the case of concrete box girder bridges, considerable work on the effects of continuity has been conducted (221) and is continuing at the University of California at Berkeley. However, no specific design recommendations have been published.

CHAPTER 5. PROPOSED REVISIONS TO AASHO SPECIFICATIONS

GENERAL

In the previous chapters, the bases for the proposed revisions to the specifications (279) have been presented. The development of the proposals were outlined specifically in Chapter 4.

The current procedures for distribution of loads have been shown generally to be conservative in predicting beam moments. Numerous investigators (2, 6, 135, 151, 182, 222, 228) have realized, however, that more realistic procedures are required and have proposed numerous revisions to the specifications for specific bridge types. It was the purpose of this investigation to make an overall study of the wheel load distribution in most of the types of short and medium span bridges and propose revisions where required.

Because of the extreme simplicity of the current requirements, it is obvious that any change to make them more realistic must entail some increase in complexity. The proposals presented herein are a balance between the need for an accurate distribution criteria and for a usable design office criteria. It should be noted that as the complexity of the bridge system increases, the simplification of the theoretical procedures requires more approximations. Thus, considerations of unusual conditions are required. The use of any theory outlined herein for a total computerized analysis of the basic behavior will lead to the most accurate design and would be the optimum considerations. It is felt, though, that the changes proposed will lead to sufficiently accurate designs.

PROPOSED SPECIFICATIONS

Based on the research summarized herein the following revisions are recommended in "Section 3, Distribution of Loads" of the 1965 edition of the AASHO Standard Specifications for Highway Bridges (279) as revised by the 1966-1967 Interim Specifications.

1.3.1 – DISTRIBUTION OF LOADS TO STRINGERS, LONGITUDINAL BEAMS AND FLOOR BEAMS.

(A) Position of Wheel Loads for Shear – unchanged.

(B) Live Load Bending Moment in Stringers and Longitudinal Beams for Bridges Having Concrete Decks*.

In calculating bending moments in longitudinal beams or stringers, no longitudinal distribution of the wheel load shall be assumed. The lateral distribution shall be determined as follows:

(1) Load Fraction (all beams)

The live load bending moment for each beam shall be determined by applying to the beam the fraction of a wheel load (both front and rear) determined by the following relations:

$$\text{Load Fraction} = \frac{S}{D}$$

---

*In view of the complexity of the theoretical analysis involved in the distribution of wheel loads to stringers, the empirical method herein described is authorized for the design of normal highway bridges. This section is applicable to beam and slab, concrete slab, multi-beam, and concrete box girder bridges. For composite steel box girder bridges, the criteria specified in Article 1.7.104 should be used.

where S is

S_a for beam and slab bridges*

$\frac{12N_L + 9}{N_g}$ for multi-beam bridges**, and the maximum of the two values for concrete box girder bridges

and the value of D determined by the following relationship:

$$D = 5 + \frac{N_L}{10} + (3 - \frac{2N_L}{7})(1 - \frac{C}{3})^2 , \qquad C \leq 3$$

$$= 5 + \frac{N_L}{10} , \qquad C > 3$$

where: S_a = average beam spacing, feet,

N_L = total number of design traffic lanes from Article 1.2.6,

N_g = number of longitudinal beams,

C = a stiffness parameter which depends upon the type of bridge, bridge and beam geometry and material properties.

The value of C is to be calculated using the relationships shown below. However, for preliminary designs, C can be approximated using the values given in Table 1.3.1. For beam and slab*** and multi-beam bridges:

---

*For slab bridges, S = 1 and the load fraction obtained is for a one foot width of slab.

**A multi-beam bridge is constructed with precast reinforced or prestressed concrete beams which are placed side by side on the supports. The interaction between the beams is developed by continuous longitudinal shear keys and lateral bolts which may or may not be prestressed.

***For noncomposite construction, the design moment may be determined in proportion to the relative flexural stiffnesses of the beam and slab section.

$$C = \frac{W}{L} \cdot \left[\frac{E}{2G} \cdot \frac{I_1}{(J_1 + J_t)} \right]^{1/2}$$

For concrete box girder bridges:

$$C = \frac{1}{2} \frac{W}{L} (1 + N_g \sqrt{\frac{d}{W}}) \cdot \left[\frac{E}{2G(1 + N_d)} \right]^{1/2}$$

where: W = the overall width of the bridge, feet,

L = span length, feet (distance between live load points of inflection for continuous spans),

E = modulus of elasticity of the transformed beam section,

G = modulus of rigidity of the transformed beam section,

I_1 = flexural moment of inertia of the transformed beam section per unit width*,

J_1 = torsional moment of inertia of the transformed beam section per unit width* ($J_1 = J_{beam} + \frac{1}{2} J_{slab}$),

J_t = 1/2 of the torsional moment of inertia of a unit width of bridge deck slab*

and for concrete box girder bridges:

d = depth of the bridge from center of top slab to center of bottom slab,

N_g = number of girder stems, and

N_d = number of interior diaphragms.

For concrete for girder bridges, the cantilever dimension of any slab extending beyond the exterior girder shall preferably not exceed S/2.

---

*For the deck slab and beams consisting of reinforced or prestressed concrete, the uncracked gross concrete section shall be used for rigidity calculations.

When the outside roadway beam or stringer supports the sidewalk live load and impact, the allowable stress in the beam or stringer may be increased 25 percent for the combination of dead load, sidewalk live load, traffic live load, and impact.

TABLE 1.3.1 VALUES OF K TO BE USED IN THE RELATION: $C = K \frac{W}{L}$.

BRIDGE TYPE	BEAM TYPE AND DECK MATERIAL	K
Beam and slab (includes concrete slab bridge)	Concrete deck:	
	Noncomposite steel I-beams	3.0
	Composite steel I-beams	4.8
	Nonvoided concrete beams (prestressed or reinforced)	3.5
	Separated concrete box-beams	1.8
	Concrete slab bridge	0.6
Multi-beam	Nonvoided rectangular beams	0.7
	Rectangular beams with circular voids	0.8
	Box section beams	1.0
	Channel beams	2.2
Concrete box girder	Without interior diaphragms	1.8
	With interior diaphragms	1.3

(2) Total Capacity of Stringers.

The combined design load capacity of all the beams in a span shall not be less than required to support the total live and dead load in the span.

(3) Edge Beams (Longitudinal).

Edge beams shall be provided for all concrete slab bridges having main reinforcement parallel to traffic. The beam may consist of a slab section additionally reinforced, a beam integral with and deeper than the slab, or an integral reinforced section of slab and curb.

It shall be designed to resist a live load moment of 0.10 PS, where

P = wheel load, in pounds (P_{15} or P_{20})

S = span length, in feet.

This formula gives the simple span moment. Values for continuous spans may be reduced 20 percent unless a greater reduction results from a more exact analysis.

(C) Live Load Bending Moment in Stringers and Longitudinal Beams Supporting Timber Floors and Steel Grids*.

(1) Interior Stringers and Beams

(This section should include those parts of current Article 1.3.1(B)(1) which are applicable to these floor systems.)

(2) Outside Roadway Stringers and Beams

The live load bending moment for outside roadway stringers or beams shall be determined by applying to the stringer or beam the reaction of the wheel load obtained by assuming the flooring to act as a simple span between stringers or beams.

(D) Bending Moment in Floor Beams (Transverse) — unchanged.

(E) Dead Load for Stringers and Beams.

---

*Article 1.3.1(B)(2) is also applicable to this article.

The dead load considered as supported by the roadway stringer or beam shall be that portion of the floor slab carried by the stringer or beam. However, curbs, failings and wearing surface, if placed after the slab has cured, may be considered equally distributed to all roadway stringers and beams.

1.3.2 – change titles and modify:

DISTRIBUTION OF LOADS AND DESIGN OF FLOOR SYSTEMS

(A) Concrete Slabs

(1) Span Lengths – same as Article 1.3.2(A)

(2) Edge Distance of Wheel Load – same as Article 1.3.2(B)

(3) Bending Moment – same as Article 1.3.2(C) except that Case B is applicable only to slabs supported by transverse floor beams and the approximate formula in this case should be changed to:

HS-20 Loading: •LLM = 900S foot-pounds

HS-15 Loading: unchanged

The last paragraph on lateral distribution for multi-beam bridges should be deleted.

(4) Distribution Reinforcement – same as Article 1.3.2(E)

(5) Shear and Bond Stress in Slabs – same as Article 1.3.2(F)

(6) Unsupported Edges, Transverse – same as Article 1.3.2(G)

(7) Cantilever Slabs – same as Article 1.3.2(H)

(8) Slabs Supported on Four Sides – same as Article 1.3.2(I)

(9) Median Slabs – same as Article 1.3.2(J).

(B) Timber Flooring

Same as Article 1.3.4 except that subsection headings changed to:

(1) Flooring Transverse

(2) Flooring Longitudinal

(3) Continuous Flooring

(C) Composite Wood-Concrete Members.

Same as Article 1.3.5 except that subsection headings changed to:

(1) Distribution of Concentrated Loads for Bending Moment and Shear

(2) Distribution of Bending Moments in Continuous Spans

(3) Design

(D) Steel Grid Floors.

Same as Article 1.3.6 except that subsection headings changed to:

(1) General

(2) Floors Filled with Concrete

(3) Open Floors

1.3.3 — MOMENTS, SHEARS AND REACTIONS — same as Article 1.3.7

1.3.4 — DISTRIBUTION OF WHEEL LOADS THROUGH EARTH FILLS — same as Article 1.3.3

COMMENTARY

The major change proposed is in Article 1.3.1(B) where a complete revision is recommended. The majority of the other changes suggested are only made in order to make the entire Section 3 consistent in design approach since many of the systems covered were not within the scope of this study. For example, it is suggested that current Article 1.3.2(D) on "Edge Beams Longitudinal" be moved to Article 1.3.1(B)(3) in order that the design of longitudinal beams be consolidated. The change suggested

in Article 1.3.2(A)(3) is due to the inclusion of slab bridge design in Article 1.3.1(B). Thus, the slabs designed under Article 1.3.2(A)(3) will be those spanning transverse floor beams and the longer spans are no longer applicable.

It should be noted that the proposal just presented is also based on a change in Article 1.2.6 — TRAFFIC LANES. Since the lanes used in the development were 12 ft wide, it is further recommended that Article 1.2.6 be changed to:

"The lane loading or standard trucks shall be assumed to occupy a width of 10 ft. These loads shall be placed in design traffic lanes having a width of 12 ft, which are placed in a position to produce maximum stress. The lanes may not overlap. The lane loadings or standard trucks shall be assumed to occupy any position within these individual design traffic lane which will produce the maximum stress. The number of design traffic lanes shall be equal to the roadway width between curbs (in feet) divided by 12, reduced to the nearest whole number." If this change is not considered in conjunction with the recommendations for changes in Section 3, then the following definition should be used in Article 1.3.1(B)(1):

$N_L = W_C/12$, reduced to the nearest whole number.

W_C = roadway width between curbs (ft).

In the development of the lateral load distribution criteria for composite steel-concrete box girders, the use of Article 1.2.9 — REDUCTION IN LOAD INTENSITY, was not recommended. This recommendation was included in Article 1.7.104 of the 1966-67 Interim Specifications (279). It is

#83
P.41

felt, however, that the purpose of Article 1.2.9 is to consider the probability of all lanes being fully loaded simultaneously. At those occasional periods when this loading may occur, the structure could sustain the overload temporarily. This overload could be considered as a factor being included in the factors of safety in the design stresses. In the few instances where less than all lanes are loaded to obtain the critical condition, the difference between the maximum beam moment for the fully loaded condition and the critical condition is very small. Thus, the continued use of the load intensity reduction is recommended.

GARBAGE

SIGNIFICANCE OF PROPOSED CHANGES

The proposed changes, in many cases, do not significantly affect current designs. However, they do make them more realistic and do consider the benefits derived from improving bridge properties. The design of a bridge using the detailed data outlined in Chapter 3 would lead to even more accurate analysis since conservative assumptions have been made in developing the empirical equations proposed.

In general, the proposal permits the considerations of the significant variables affecting load distribution. Since the present AASHO criteria were developed on the basis of the behavior of typical bridges of the types considered, it should be expected that the average values for distribution coefficients in the proposal would be near those in the current specifications.

The major benefit of the proposal is the consideration of the effect of individual and new bridge geometries on load distribution. For example, by increasing the slab thickness the load distribution characteristics

will generally improve. This improvement is reflected in the proposed specifications, whereas it is not in the current specifications. Although, to some extent the torsional rigidity of the beams is considered in the present specifications (by use of different D values for steel stringers, concrete T-beams and concrete box girders), it is an integral part of the proposal for all variations of beam geometry. In addition, the aspect ratio (W/L) has a significant effect on the distribution and it is not currently considered. Since the designer can obtain lower design live loads per beam with appropriate changes in the cross section, he is more likely to incorporate them. Thus, economies should result.

In the present specifications, separate design criteria are proposed for interior and exterior beams, yet the study showed that the critical beam can be either, and is a function of the bridge properties and loading. Thus, a single criterion for all beams is proposed.

The specific significance of the changes will be discussed for each of the bridge types considered.

Concrete Slab Bridges

The significance of the proposal can be readily seen in Figure 32. For spans less than about 50 ft, the new criteria will generally require less moment than currently specified. This span is about the upper economic limit and, thus the section required to carry the static live load in this bridge type can be expected to have a similar or smaller thickness.

Beam and Slab Bridges

The D value currently required varies from 5.5 for steel I-beam stringers and prestressed concrete girders to 7.0 for concrete box girders. The proposal will yield D values in about the same range, but, more important, will permit an increase in D if the specific cross section has the improved distribution properties. The specific benefits can be seen in Table 12. This effect of improved distribution can be noted, in particular, for prestressed concrete beams where the D values can vary significantly depending on the cross section. It should be noted that the use of the new criteria should lead to more economical designs as such changes as increased slab thickness and improved beam torsional rigidity will lower design beam moments, which is not generally the case presently.

TABLE 12

COMPARISON OF PROPOSED SPECIFICATIONS AND CURRENT SPECIFICATIONS FOR BEAM AND SLAB BRIDGES

BEAM TYPE	SPAN RANGE FT	BRIDGE WIDTH RANGE FT	C RANGE[a]	CURRENT D[b]	PROPOSED D RANGE[b]
Composite steel I-beam	41 – 90	29 – 37	1.96 – 2.40	5.5	5.3 – 5.7
Noncomposite steel I-beams	50 – 70	25 – 30	1.50 – 1.60	5.5	5.9
Concrete T-beams	40 – 70	29 – 36	1.33 – 1.46	6.0	5.9 – 6.1
Prestressed concrete I-beams	35 – 100	29 – 37	1.59 – 3.83	5.5	5.2 – 5.9[c]
Prestressed concrete box-beams	61 – 72	33 – 46	0.67 – 0.83	5.5	6.5 – 6.7

[a] Based on typical bridges included in field tests and provided by various state highway departments.

[b] In load fraction equation: LF = S/D.

[c] Typical value for longer spans, about 5.8.

Multi-Beam Bridges

The D value currently required for this bridge type is based on slab design for main reinforcement parallel to traffic. The distribution width per wheel is equal to 4.0 + 0.06L and varies from 5.2 for a span of 20 ft to a maximum of 7.0. This range is essentially the same as the proposed criteria will give, although the resultant distributions will not necessarily be the same. The relationship between the proposed and current specifications can be obtained by examining the distribution widths computed for the multi-beam bridges described in Chapter 2. These widths are shown in Table 13. The ratio of the resultant wheel load

TABLE 13

DISTRIBUTION WIDTHS FOR MULTI-BEAM BRIDGES

BRIDGE	SPAN FT	C	E[a] FT	D[b] FT
North Carolina	30	1.28	5.80	6.02
Centerport	32	0.53	5.92	6.86
Langstone	31	0.59	5.86	6.76

[a]Section 1.3.2(B) — Case B: Current specifications (279).

[b]Proposed specifications.

fractions may vary somewhat due to the different criteria for effective beam width. However, it can be seen that the new criteria considers the wheel to be distributed over a wider area (better distribution). These bridges are quite narrow in comparison to today's standards, where

the actual and effective beam widths are practically identical and the difference between E and D shown in the table would be a realistic comparison of design moment per beam. Thus, it is expected that economies will result.

Concrete Box Girder Bridges

The current specifications indicate that a wheel load shall be distributed over a width of 7 ft. It can be seen in Table 10 that this width (D) can actually vary from about 5.7 for short span bridges with four lanes to about 8.3 for longer span (110 ft) bridges with two lanes. However, the proposed specifications are somewhat conservative in the higher D values and the value is limited to about 7. Of more importance, it should be noted that for most designs the actual D value is about 10 percent less than currently specified, indicating that current designs may be slightly unconservative.

Summary

In summary, the proposed specification does provide a more realistic approach to load distribution. In some cases, significant economies may result. In other cases, such as the concrete box girder bridges, higher design moments are specified. However, in each case, the load fraction applied to the beam, and the resultant moment, will more truly represent the actual conditions.

CHAPTER 6. CONCLUSIONS

The purpose of the research summarized in this report was to study the distribution of wheel loads in highway bridges and to recommend, where warranted, changes in the AASHO "Standard Specifications for Highway Bridges." The study was generally limited to short and medium span bridges of the following types: slab, beam and slab, multi-beam, and concrete box girder.

After an extensive bibliography search and a study of available methods of analysis, it was found that the distribution of wheel loads in these bridge types could be accurately determined using the following theories:

1. beam and slab bridges: orthotropic plate theory,
2. multi-beam bridges: articulated plate theory, and
3. concrete box girder bridges: prismatic folded plate theory.

These procedures have been used to obtain extensive results relating the behavior of highway bridges with the variables affecting the behavior. From these studies it is was found that:

1. Although generally predicting conservative load distribution in bridges, the current AASHO load distribution criteria (279) do not realistically consider the significant variables affecting behavior. However, it should be noted that present criteria do give realistic values for many typical beam and slab bridges. Yet, substantial improvements in geometry can be made without a resulting change in the distribution of loads as currently specified.

2. Accurate empirical relationships between the variables which significantly affect the load distribution and the fraction of wheel

loads carried by each beam can be obtained. Relationships of this type are presented herein.

3. The major variables which affect the load distribution in each of the major bridge types are: relative flexural stiffness in longitudinal and transverse directions, relative torsional stiffness in the same directions, bridge width and effective bridge span. Each of these variables is considered in the relationships developed.

The results of the analytical studies and the development of empirical load distribution equations have been used to prepare specific recommendations for changes in the current load distribution criteria. It is felt that with these new criteria, prediction of wheel load distribution will be more accurate and will more truly indicate the behavior of the bridge types studied.

APPENDIX A

DEVELOPMENT OF THEORIES AND MOMENT COEFFICIENT EQUATIONS

BEAM AND SLAB BRIDGES

Orthotropic Plate Theory (5, 65)

Using the stress-strain relationships and the equations of equilibrium, the following governing differential equation for laterally loaded orthotropic plates has been obtained (245):

$$D_x \frac{\partial^4 w}{\partial x^4} + 2H \frac{\partial^4 w}{\partial x^2 \partial y^2} + Dy \frac{\partial^4 w}{\partial y^4} = P(x, y) \qquad (A.1)$$

where x and y are the axis of the coordinate system used in Figure 19.

The following definitions are based on an assumed Poisson's ratio of zero.

$D_x = EI_x$, flexural rigidity per unit width in x direction,

$D_y = EI_y$, flexural rigidity per unit width in y direction,

$H = D_{xy} + D_{yx}$, sum of orthogonal torsional rigidities,

$D_{xy} = GJ_x$, torsional rigidity per unit width in x direction,

$D_{yx} = GJ_y$, torsional rigidity per unit width in y direction,

E = modulus of elasticity in x direction,

G = modulus of rigidity,

I_x = moment of inertia per unit width in x direction,

I_y = moment of inertia per unit width in y direction,

J_x = torsional moment of inertia per unit width in x direction,

J_y = torsional moment of inertia per unit width in y direction,

P(x, y) = lateral loading, and

w(x, y) = deflection of bridge.

The orthotropic plate considered is simply supported along the two opposite sides of length 2b (or W) and freely supported along the other two sides of length L (Figure 16). The boundary conditions are:

1. $w = 0,\ M_x = 0$ at $x = 0$ and $x = L$ and
2. $M_y = 0,\ R_y = 0$ at $y = -b$ and $y = +b$

where M_x and M_y are the bending moments in the longitudinal and transverse directions respectively and R_y is the reactive force at the free edges. The solution to the governing differential equation may be obtained in two parts (245) as:

$$w(x, y) = w_h + w_p \tag{A.2}$$

where W_h is the general solution to the homogeneous differential equation and W_p is a particular solution. For W_h, the Levy series can be used:

$$w_n = \sum_{m=1}^{\infty} Y_m \sin \frac{m\pi x}{L} \tag{A.3}$$

where Y_m is a function of y only. This series automatically satisfies the first boundary equations. If this series is substituted into the homogeneous differential equation, the mth term is:

$$D_x Y_m \left(\frac{m\pi}{L}\right)^4 + 2H\left(\frac{m\pi}{L}\right)^2 \frac{d^2 Y_m}{dy^2} + D_y \frac{d^4 Y_m}{dy^4} = 0 \tag{A.4a}$$

or

$$\frac{D_x}{D_y}\left(\frac{m\pi}{L}\right)^4 Y_m + 2\frac{H}{\sqrt{D_x D_y}}\sqrt{\frac{D_x}{D_y}}\left(\frac{m\pi}{L}\right)^2 \frac{d^2 Y_m}{dy^2} + \frac{d^4 Y_m}{dy^4} = 0 \tag{A.4b}$$

if

$$\theta = \frac{b}{L}\sqrt[4]{\frac{D_x}{D_y}} = \frac{b}{L}\sqrt[4]{\frac{I_x}{I_y}}$$

$$\alpha = \frac{(D_{xy} + D_{yx})}{2\sqrt{D_x D_y}} = \frac{G}{E} \cdot \frac{(J_x + J_y)}{2\sqrt{I_x I_y}}$$

$$\frac{E}{G} = 2.$$

Then,

$$(m\pi)^4 \frac{\theta^4}{b^4} Y_m + 2(m\pi)^2 \frac{\theta^2}{b^2} \alpha \frac{d^2Y_m}{dy^2} + \frac{d^4Y_m}{dy^4} = 0 \qquad \text{(A.4c)}$$

the roots of the characteristic equations are (199),

$$\gamma 1,\ 2,\ 3,\ 4 = \pm \frac{m\pi\theta}{b} \left(\sqrt{\frac{1+\alpha}{2}} \pm i\sqrt{\frac{1-\alpha}{2}}\right)$$

or

$$\gamma 1,\ 2,\ 3,\ 4 = \pm \frac{m\pi\theta}{b} (c \pm if)$$

or the characteristic equation is

$$Y_m = e^{m\pi c\theta \frac{y}{b}} A_m \cos(m\pi f\theta \frac{y}{b}) + \frac{B_m}{f} \sin(m\pi f\theta \frac{y}{b})$$
$$+ e^{-m\pi c\theta \frac{y}{b}} C_m \cos(m\pi f\theta \frac{y}{b}) + \frac{F_m}{f} \sin(m\pi f\theta \frac{y}{b}) \qquad \text{(A.5)}$$

$$c = \sqrt{\frac{1-\alpha}{2}}$$

$$f = \sqrt{\frac{1+\alpha}{2}}\ .$$

For the particular solution, the case of an infinitely wide plate which is simply supported on the two opposite edges is considered. If the load is applied at y = 0, and the absolute value of y is used, then constants A_m and B_m in the characteristic equation must be zero.

Thus for this type of loading, Y_m becomes

$$Y_m = e^{-m\pi c\theta \left|\frac{y}{b}\right|} \left[C_m \cos(m\pi\theta f \left|\frac{y}{b}\right| + \frac{F_m}{f} \sin(m\pi\theta f \left|\frac{y}{b}\right|)\right]. \qquad \text{(A.6a)}$$

The slope in the y direction must be zero at y = 0 or,

$$Y_m = G_m e^{-m\pi\theta c\left|\frac{y}{b}\right|} \left[\cos(m\theta\pi f \left|\frac{y}{b}\right|) + \frac{c}{f} \sin(m\pi\theta f \left|\frac{y}{b}\right|)\right]. \qquad \text{(A.6b)}$$

Thus,

$$w_p = \sum_{m=1}^{\infty} G_m e^{-m\pi\theta c\left|\frac{y}{b}\right|}\left[\cos\left(m\theta\pi f\left|\frac{y}{b}\right|\right) + \frac{c}{f}\sin\left(m\pi\theta f\left|\frac{y}{b}\right|\right)\right]\sin\frac{m\pi x}{L} . \qquad (A.7)$$

If a Fourier sine series expansion for a concentrated load is used at y = 0 and x = u then,

$$P_m = \frac{2P_o}{L}\sin\frac{m\pi u}{L}\sin\frac{m\pi x}{L} = H_m \sin\frac{m\pi x}{L} . \qquad (A.8)$$

The solution for G_m is found from the boundary condition that the reactive force in the slab at y = 0 must be equal to $P_m/2$ or

$$G_m = \frac{b^3}{2\sqrt{2(1+\alpha)}\, D_y m^3 \pi^3 \theta^3} .$$

For a load at y = v Equation (A.7) becomes,

$$w_p = \sum_{m=1}^{\infty} G_m e^{-m\pi c\theta\left|\frac{y-v}{b}\right|}\left[\cos\left(m\pi f\theta\left|\frac{y-v}{b}\right|\right) + \frac{c}{f}\sin\left(m\pi f\theta\left|\frac{y-v}{b}\right|\right)\right]\sin\frac{m\pi x}{L}$$

The combined solution $(w_h + w_p)$ must satisfy the boundary equations at the two edges of the actual bridge: namely the moments and reactive forces are zero. Using these boundary conditions the general solution is,

$$w = \sum_{m=1}^{\infty} \frac{H_m}{2\sqrt{2(1+\alpha)}}\left(\frac{b}{m\pi\theta}\right)^3 \left[A_m \cosh\phi\cos\psi + B_m \sinh\phi\cos\psi\right.$$

$$+ C_m \cosh\phi\sin\psi + F_m \sinh\phi\sin\psi + (\cosh|\phi-\gamma| - \sinh|\phi-\gamma|)$$

$$\left.(\cos|\psi-\delta| + \frac{c}{f}\sin|\psi-\delta|)\right]\sin\frac{m\pi x}{L} \qquad (A.9)$$

where

$$A_m = \frac{Q}{M_m}\Big\{[\cosh\gamma\cos\delta\,(c\sin\ell - f\cos\ell) - \sinh\gamma\sin\delta\,(c\cos\ell + f\sin\ell)][-\sinh k\cos\ell + \frac{c}{f}\cosh k\sin\ell)] + \cosh\gamma\cos\delta\,(\alpha\sin\ell + h\cos\ell) - \sinh\gamma\sin\delta\,(\alpha\cos\ell - h\sin\ell)][2c\cosh k\cos\ell + \frac{\alpha}{h}\sinh k\sin\ell)]\Big\}$$

$$B_m = \frac{Q}{N_m}\Big\{[\sinh\gamma\cos\delta\,(c\sin\ell - f\cos\ell) - \cosh\gamma\sin\delta\,(c\cos\ell + f\sin\ell)][-\cosh k\cos\ell + \frac{c}{f}\sinh k\sin\ell)] + [\sinh\gamma\cos\delta\,(\alpha\sin\ell + h\cos\ell) - \cosh\gamma\sin\delta\,(\alpha\cos\ell - h\sin\ell)][2c\sinh k\cos\ell + \frac{\alpha}{f}\cosh k\sin\ell)]\Big\}$$

$$C_m = \frac{-Q}{N_m}\Big\{[\sinh\gamma\cos\delta\,(c\sin\ell - f\cos\ell) - \cosh\gamma\sin\delta\,(c\cos\ell + f\sin\ell)][\sinh k\sin\ell + \frac{c}{f}\sinh k\sin\ell)] + [\sinh\alpha\sin\ell + h\cos\ell) - \cosh\gamma\cos\delta\,(\alpha\cos\ell - h\sin\ell)][-2c\cosh k\sin\ell + \frac{\alpha}{f}\sinh k\cos\ell)]\Big\}$$

$$F_m = \frac{-Q}{M_m}\Big\{[\cosh\gamma\cos\delta\,(c\sin\ell - f\cos\ell) - \sinh\gamma\sin\delta\,(c\cos\ell + f\sin\ell)][\cosh k\sin\ell + \frac{c}{f}\cosh k\cos\ell)] + [\cosh\gamma\cos\delta\,(\alpha\sin\ell + h\cos\ell) - \sinh\gamma\sin\delta\,(\alpha\cos\ell - h\sin\ell)][-2c\sinh k\sin\ell + \frac{\alpha}{f}\cosh k\cos\ell)]\Big\}$$

$$Q = \cosh k - \sinh k$$

$$h = \sqrt{1 - \alpha^2}$$

$$\phi = m\pi\theta \sqrt{\frac{1 + \alpha}{2}} \frac{y}{b}$$

$$\psi = m\pi\theta \sqrt{\frac{1 - \alpha}{2}} \frac{y}{b}$$

$$\gamma = m\pi\theta \sqrt{\frac{1 + \alpha}{2}} \frac{v}{b}$$

$$\delta = m\pi\theta \sqrt{\frac{1 - \alpha}{2}} \frac{v}{b}$$

$$\ell = m\pi\theta \sqrt{\frac{1 - \alpha}{2}}$$

$$k = m\pi\theta \sqrt{\frac{1 + \alpha}{2}}$$

$$\theta = \frac{b}{L} \sqrt[4]{\frac{D_x}{D_y}}$$

$$M_m = (2\alpha + 1)f \sinh k \cosh k - (2\alpha - 1)c \sinh \ell \cosh \ell$$

$$N_m = (2\alpha + 1)f \sinh k \cosh k + (2\alpha - 1)c \sinh \ell \cosh \ell.$$

It will be noted that the function enclosed in brackets in Equation (A.9) is independent of x and will hereafter be referred to as

$$[\cdots\cdots] = F(y, v, m, \theta, \alpha).$$

The moment coefficient used in measuring the load distribution characteristics of the bridge is defined as the actual longitudinal moment at a transverse point on the bridge divided by the average moment across the bridge at this point.

If P_o/W equals the magnitude of the uniform concentrated line load acting transversely across the bridge then in terms of the Fourier sine series

$$\frac{P_o}{W} = \frac{2P_o}{WL} \sum_{m=1}^{\infty} \sin \frac{m\pi u}{L} \sin \frac{m\pi x}{L} = \sum_{m=1}^{\infty} \frac{H_m}{W} \sin \frac{m\pi x}{L} .$$

The average deflection becomes

$$w_a = \left(\frac{L}{\pi}\right)^4 \frac{1}{W} \sum_{m=1}^{\infty} \frac{H_m}{m^4} \sin \frac{m\pi x}{L} . \qquad (A.10)$$

The moment in the longitudinal direction with Poisson's ratio equal to zero is

$$M_x = - D_x \frac{\partial^2 w}{\partial x^2} . \qquad (A.11)$$

Thus, the ratio of the actual moment to the average moment becomes

$$K_m = \frac{\theta\pi}{\sqrt{2(1 + \alpha)}} \frac{\sum_{m=1}^{\infty} \frac{H_m}{m} F(y, v, m, \theta, \alpha) \sin \frac{m\pi x}{L}}{\sum_{m=1}^{\infty} \frac{H_m}{m^2} \sin \frac{m\pi x}{L}} . \qquad (A.12)$$

MULTI-BEAM BRIDGES

Articulated Plate Theory (261)

The following basic assumptions are made for the analysis:

1. Beams are made of a homogeneous, isotropic and elastic material.
2. All beam elements in a bridge are the same with regard to their geometric and mechanical properties. No edge-stiffening effect is considered.
3. Beams are prismatic.
4. Beams are all simply supported.
5. Deflections of beam elements are small compared with their depth.
6. The connection between beams is hinged along the middepth of the shear key so that no relative movement except the transverse rotation is possible. In the case of dry-packed mortar connections, cracks are assumed at the location of shear keys.

7. The effect of prestress in transverse direction is not taken into account.
8. In the design of multi-beam bridges, the longitudinal positions of the wheel loads are set to be at the midspan.
9. Poisson's ratio will be taken to be zero in the actual computation.
10. Skew bridges will not be considered.
11. The number of beam elements is large enough so that the differential calculus can be applied.
12. The calculations will be based on the cross-sectional area of the beam elements (transformed).

Figure A.1 shows a multi-beam bridge and its cross section. Single arrows indicate various forces while the double arrows indicate moments or torques obeying the right-hand screw law. The basic equations will be obtained by considering the equilibrium of a unit beam element under load (6):

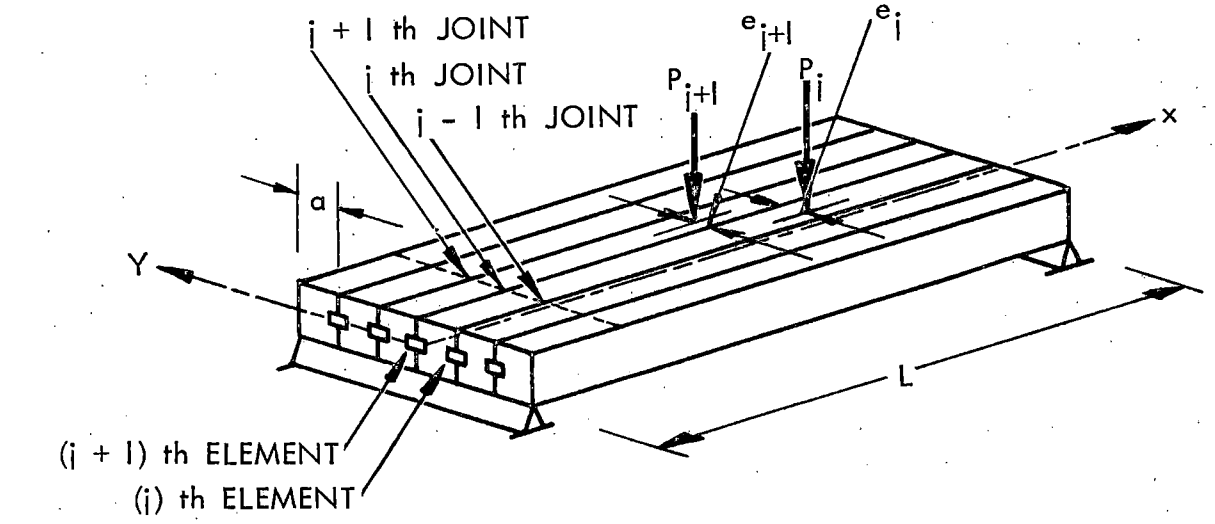

(a) MULTI-BEAM BRIDGE

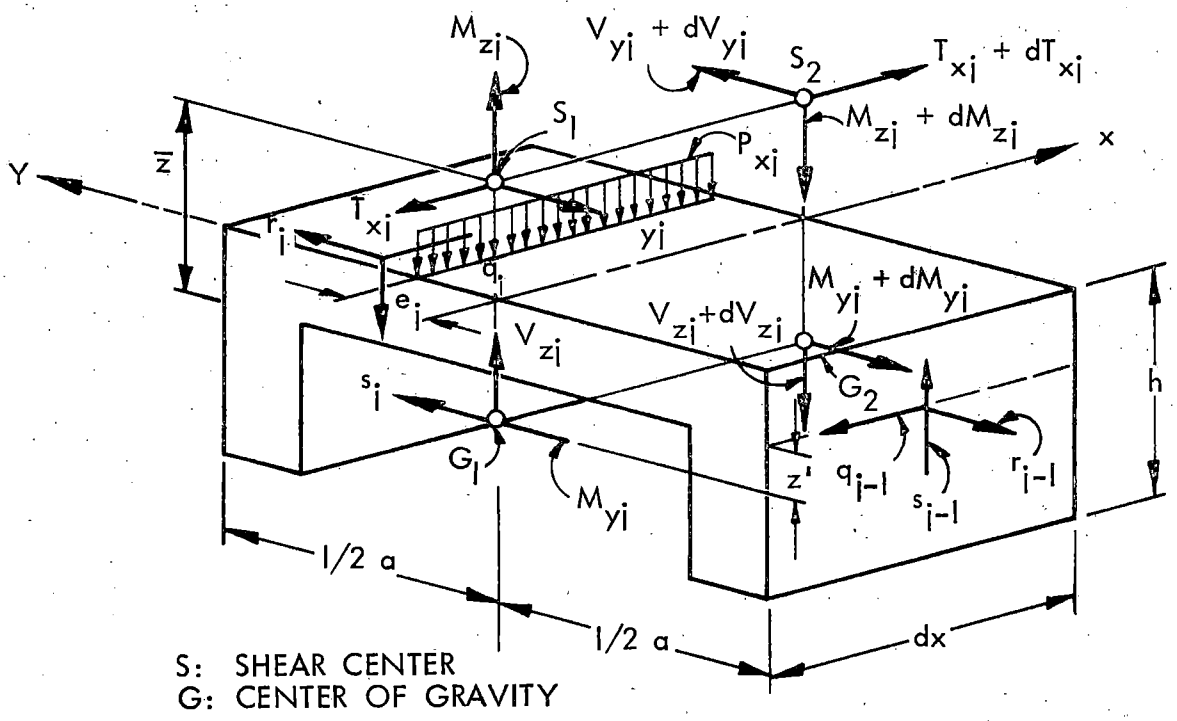

(b) CROSS SECTION OF A MULTI-BEAM BRIDGE AND FORCES APPLIED ON IT

Figure A.1. Cross section of a multi-beam bridge and forces applied on it.

Equilibrium of Vertical Forces

The equilibrium of vertical forces requires that the algebraic sum of these forces should vanish

$$- V_{zj} + (V_{zj} + dV_{zj}) + (s_j - s_{j-1})dx + p_{xj}dx = 0.$$

Therefore

$$\frac{dV_{zj}}{dx} = - (s_j - s_{j-1}) - p_{xj} . \qquad (A.13)$$

The algebraic sum of moments and torques which have the vectorial direction in y-direction should vanish, so

$$- M_{yj} + (M_{yj} + dM_{yj}) - V_{zj}dx - (q_j - q_{j-1})z'dx = 0.$$

Hence,

$$\frac{dM_{yj}}{dx} = V_{zj} + (q_j - q_{j-1})z'. \qquad (A.14)$$

The algebraic sum of moments and torques in x-direction should vanish:

$$- T_{xj} + (T_{xj} + dT_{xj}) - (r_j - r_{j-1})\bar{z}dx - (s_j + s_{j-1}) \cdot 1/2\ bdx$$

$$- p_{xj}e_j dx - \bar{\Omega}(dq_j + dq_{j-1}) = 0.$$

Hence,

$$\frac{dT_{xj}}{dx} = P_{xj}e_j + \bar{\Omega}\frac{d}{dx}(q_j + q_{j-1}) + (r_j - r_{j-1})\bar{z} + (s_j + s_{j-1}) \cdot 1/2\ a. \qquad (A.15)$$

From structural mechanics, the following relations between the moment M_{yj} and the deflection w and between the torque T_{xj} and the angle of rotation ϕ are known.

$$M_{yj} = - EI \frac{d^2 w}{dx^2}$$

$$T_{xj} = - GJ_L \frac{d\dot{\phi}}{dx} + EC \frac{d^3 \dot{\phi}}{dx^3} . \tag{A.16}$$

Combining all the relationships presented here, the following relationships are obtained:

$$EI \frac{d^4 w}{dx^4} = p_{xj} + (s_j - s_{j-1}) - \frac{d}{dx} (q_j - q_{j-1})z' \tag{A.17}$$

$$- EC \frac{d^4 \dot{\phi}}{dx^4} + GJ_L \frac{d^2 \dot{\phi}}{dx^2} = - p_{xj} e_j - \frac{d}{dx} (q_j + q_{j-1})\bar{\Omega}$$

$$- (r_j - r_{j-1})\bar{z} - (s_j + s_{j-1}) \cdot 1/2\ a. \tag{A.18}$$

The relationship between the deflection and rotation is found as

$$w_{j+1} - w_j = 1/2\ a(\dot{\phi}_j + \dot{\phi}_{j+1}). \tag{A.19}$$

Now, assuming the uniformity of shears, deflections and the transverse normal forces r_j, the horizontal shearing forces q_j will be negligible compared with the transverse shear forces s_j. Letting the distance between the stations designated by j and j + 1 tend to be infinitesimally small, then

$$e_j \to 0.$$

Also, Equations (A.17) – (A.19) will be rewritten as follows:

$$\frac{EI}{a} \frac{\partial^4 w}{\partial x^4} = \frac{p_x}{a} + \frac{\partial s}{\partial y} \tag{A.20}$$

$$- \frac{EC}{a} \frac{\partial^4 \dot{\phi}}{\partial x^4} + \frac{GJ_x}{a} \frac{\partial^2 \dot{\phi}}{\partial x^2} = - s \tag{A.21}$$

$$\frac{\partial w}{\partial y} = \dot{\phi} . \tag{A.22}$$

Set

$$D_x = \frac{EI_x}{a} \; ; \; C_x = \frac{EC}{a} \; ; \; D_{xy} = \frac{GJ_x}{a} \tag{A.23}$$

then, Equations (A.20) – (A.22) become

$$D_x \frac{\partial^4 w}{\partial x^4} - C_x \frac{\partial^6 w}{\partial x^4 \partial y^2} + D_{xy} \frac{\partial^4 w}{\partial x^2 \partial y^2} = \frac{p_x}{a} \; . \tag{A.24}$$

It should be noted that p_x represents an impulse type function; in other words, this is of finite value at the loading point and zero at the other points.

A modification is made to take into account the transverse torsional stiffness. If there is a transverse torsional stiffness existing, Equation (A.20) can be rewritten as follows:

$$D_x \frac{\partial^4 w}{\partial x^4} + D_{yx} \frac{\partial^4 w}{\partial x^2 \partial y^2} = \frac{p_x}{a} + \frac{\partial s}{\partial y} \; . \tag{A.25}$$

Then the basic equation corresponding to Equation (A.24) will be as follows:

$$D_x \frac{\partial^4 w}{\partial x^4} - C_x \frac{\partial^6 w}{\partial x^4 \partial y^2} + (D_{yx} + D_{xy}) \frac{\partial^4 w}{\partial x^2 \partial y^2} = \frac{p_x}{a} \tag{A.26}$$

where $D_{yx} = GJ_y/L$, the transverse torsional stiffness per unit width.

Important Parameters Involved

Stiffness and Rigidity

Before mentioning the various controlling parameters, the rigidities and stiffnesses must be defined. In the analysis, the rigidity is defined as a reduced force to deformation ratio. For example, EI and GJ are flexural rigidity and torsional rigidity, respectively. Also, the stiffness is defined as a quantity designating a reduced force to deformation ratio of the unit length or width of the structural system. For instance,

D_x, D_{xy} and C_x are flexural stiffness, torsional stiffness and torsional warping stiffness, respectively.

The controlling parameters will be divided into three categories. These are: first, the geometric dimensions; second, the mechanical properties; and third, the design criteria used by engineers. Each of these three parameters is explained subsequently.

Geometric dimensions: The following parameters can be classified into this group:

1. Number of beam elements: N.
2. Ratio of width of a beam element to the span length: therefore,

$$\beta = a/L. \tag{A.27}$$

Mechanical properties: The previous parameters depend on only the geometry of bridges, but the next two parameters depend also on the mechanical properties of the material.

1. Flexure-torsion parameter: ϕ, where ϕ is defined by the equation:

$$\phi = \frac{\text{half bridge width}}{\text{span length}} \sqrt{\frac{\text{flexural stiffness in long. direction}}{\text{total torsional stiffness}}}$$

$$= 1/2 \; N \; \beta\sqrt{D_x/(D_{xy} + D_{yx})} = 1/2 \; N \; \beta\sqrt{\kappa} \tag{A.28}$$

where

$$\kappa = D_x/(D_{xy} + D_{yx}). \tag{A.29}$$

2. Torsional warping parameter: λ, where λ is defined by the equation:

$$\lambda = \frac{\text{torsional warping stiffness}}{\text{flexural stiffness} \cdot (\text{beam width})^2} = \frac{C_x}{D_x a^2}. \tag{A.30}$$

Solution of the Fundamental Equation

Equation (A.26) may be solved by expanding the solution in terms of trigonometric series. Since only simply supported bridges are being considered, the deflection w may be expressed by the series

$$w = \sum_{m=1}^{\infty} w_m = \sum_{m=1}^{\infty} \bar{w}_m \sin \frac{m\pi x}{L} . \tag{A.31}$$

Similarly, the load p can be expressed as

$$p = \sum_{m=1}^{\infty} H_m = \sum_{m=1}^{\infty} \bar{H}_m \sin \frac{m\pi x}{L} \tag{A.32}$$

where $\bar{H}_m$ can be determined as

$$\bar{H}_m = \frac{2p}{L} \sin \frac{m\pi u}{L} \tag{A.33}$$

where u is the longitudinal position designating the wheel load. As the next step, $\bar{H}_m$ in the y-direction can be expanded to represent the load intensity $\bar{p}_m$

$$\bar{p}_m = \bar{H}_m \delta(y)$$

where $\delta(y) = 1$ at the loading point

$= 0$ at the other points. (A.34)

Finally, the load intensity q can be expressed as follows:

$$q = \sum_{m=1}^{\infty} \bar{p}_m \sin \frac{m\pi x}{L} . \tag{A.35}$$

Substitution of Equations (A.31), (A.33), (A.34) and (A.35) into Equation (A.26) yields:

$$\frac{d^2 \bar{w}_m}{dy^2} - \phi_m^2 \bar{w}_m = - \frac{\bar{p}_m}{C_x (\frac{m\pi}{L})^4 + (D_{xy} + D_{yx})(\frac{m\pi}{L})^2} \tag{A.36}$$

where

$$\phi_m = \sqrt{\frac{D_x}{D_{xy} + D_{yx}}} \frac{m\pi/L}{\sqrt{1 + \frac{C_x}{D_{xy} + D_{yx}} (\frac{m\pi}{L})^2}} = \frac{2L\phi}{Na} \frac{m\pi/L}{g(m)}$$

$$= \frac{2m\pi}{Na} \frac{\phi}{\sqrt{1 + m^2\pi^2\beta^2\kappa\lambda}} = \frac{2m}{Na} \bar{\phi}$$

where ϕ and λ have been defined by Equations (A.28) and (A.30). Also $g(m)$ and $\bar{\phi}$ are given by:

$$g(m) = \sqrt{1 + m^2\pi^2\beta^2\kappa\lambda} \tag{A.37}$$

$$\bar{\phi} = \frac{\pi\phi}{g(m)} \ . \tag{A.38}$$

Using a nondimensionalized coordinate system, where

$$\sigma = \frac{2y}{Na} \tag{A.39}$$

$$\psi = \frac{2e}{Na} \ . \tag{A.40}$$

Equation (A.36) becomes

$$\frac{d^2\bar{w}_m}{d\sigma^2} - m^2\bar{\phi}^2\bar{w}_m = - \frac{(\frac{1}{2} Na)^2 \bar{p}_m(\sigma)}{D_x(\frac{m\pi}{L})^4 + (D_{xy} + D_{yx})(\frac{m\pi}{L})^2} \ . \tag{A.41}$$

The complementary solution of Equation (A.41) is obtained as:

$$\bar{w}_{mc} = C_1 e^{m\bar{\phi}\sigma} + C_2 e^{-m\bar{\phi}\sigma} . \tag{A.42}$$

To obtain the particular solution of Equation (A.41) the width of a bridge is assumed infinitely large. Noting that $p_m(\sigma)$ represents an impulse load acting at $\sigma = \psi$, the solution is found in the following form:

$$\bar{w}_{mp} = C_m e^{-m\bar{\phi}|\sigma - \psi|} \tag{A.43}$$

where the absolute value of $|\sigma - \psi|$ is used for symmetry and C_m is determined from a condition that the reaction force along the line $\sigma = \psi$ is equal to half of the load. Therefore,

$$D_x \frac{\partial^5 w_{mp}}{\partial x^4 \partial y} - (D_{xy} + D_{yx}) \frac{\partial^3 w_{mp}}{\partial x^2 \partial y} = \frac{1}{2} \bar{H}_m \sin \frac{m\pi x}{L} \Bigg|_{\sigma=\psi-0} \tag{A.44}$$

The left term becomes

$$\left[\left(\frac{m\pi}{L}\right)^4 + (D_{xy} + D_{yx})\left(\frac{m\pi}{L}\right)^2\right] \frac{2}{Na} \frac{\partial \bar{w}_m}{\partial \sigma} \Bigg|_{\sigma=\psi-0} \sin \frac{m\pi x}{L} . \tag{A.45}$$

Since

$$\frac{\partial \bar{w}_m}{\partial \sigma} = m\bar{\phi} C_m$$

the constant C_m can be obtained in the form:

$$C_m = \frac{Na}{4} \frac{1}{m\bar{\phi}} \left(\frac{L}{m\pi}\right)^2 \frac{\bar{H}_m}{(D_{xy} + D_{yx})} \frac{1}{g(m)^2} . \tag{A.46}$$

Therefore, the complete solution $\bar{w}_m$ can be shown as follows

$$\bar{w}_m = \frac{L^2 Na \bar{H}_m}{4(D_{xy} + D_{yx}) m^3 \pi^2 \bar{\phi} g(m)^2} \left(A_1 e^{m\bar{\phi}\sigma} + A_2 e^{-m\bar{\phi}\sigma} + e^{-m\bar{\phi}|\sigma-\psi|}\right). \tag{A.47}$$

Let W_o be the deflection of an idealized beam with the flexural rigidity of $(EI)_{total}$, where

$$(EI)_{total} = NaD_x = \text{total flexural rigidity of a bridge section}$$

then, the beam equation is

$$(EI)_{total} \frac{d^4 W_o}{dx^4} = p. \tag{A.48}$$

Expanding W_o in terms of trigonometric series:

$$W_o = \sum_{m=1}^{\infty} W_{om} = \sum_{m=1}^{\infty} \bar{W}_{om} \sin \frac{m\pi x}{L} \tag{A.49}$$

and using Equation (A.32), the relation is

$$\bar{W}_{om} = \frac{\bar{H}_m}{NaD_x} \left(\frac{L}{m\pi}\right)^4 . \tag{A.50}$$

Constants A_1, A_2 in Equation (A.47) are determined from a boundary condition that the reaction force along the two edges must vanish; hence,

$$C_x \frac{\partial^5 w_m}{\partial x^4 \partial y} - (D_{xy} + D_{yx}) \frac{\partial^3 w_m}{\partial x^2 \partial y} \Bigg|_{\sigma=\pm 1} = 0. \tag{A.51}$$

This condition is identical with the condition:

$$\frac{\partial^3 w_m}{\partial x^2 \partial \sigma} \Bigg|_{\sigma=\pm 1} = 0 \tag{A.52}$$

or

$$\frac{\partial \bar{w}_m}{\partial \sigma} \Bigg|_{\sigma=\pm 1} = 0. \tag{A.53}$$

By substituting Equation (A.47) into Equation (A.53), the constants A_1 and A_2 are as follows:

$$A_1 = \frac{e^{m\bar{\phi}\psi} + e^{-m\bar{\phi}(2+\psi)}}{e^{2m\bar{\phi}} - e^{-2m\bar{\phi}}} \; ; \; A_2 = \frac{e^{-m\bar{\phi}\psi} + e^{-m\bar{\phi}(2-\psi)}}{e^{2m\bar{\phi}} - e^{-2m\bar{\phi}}} . \tag{A.54}$$

The mean moment M then is obtained in terms of the mean deflection w_o

$$M = \sum_{m=1}^{\infty} M_m = \sum_{m=1}^{\infty} \bar{M}_m \sin \frac{m\pi x}{L}$$

$$= - D_x \frac{d^2 W_o}{dx^2} = - D_x \sum_{m=1}^{\infty} \frac{d^2 W_{om}}{dx^2} = D_x \sum_{m=1}^{\infty} \left(\frac{m\pi}{L}\right)^2 \bar{W}_{om} \sin \frac{m\pi x}{L} . \tag{A.55}$$

Therefore

$$\bar{M}_m = D_x \left(\frac{m\pi}{L}\right)^2 \bar{W}_m = \frac{\bar{H}_m}{Na} \left(\frac{L}{m\pi}\right)^2 . \tag{A.56}$$

Statics requires that

$$\frac{1}{Na} \int_{-1/2Na}^{1/2Na} \bar{m}_m dy = \bar{M}_m$$

or

$$1/2 \int_{-1}^{1} \bar{m}_m d\sigma = \bar{M}_m \tag{A.57}$$

where m_m refers to the bending moment per unit width and is given as:

$$m_m = - D_x \frac{\partial^2 w_m}{\partial x^2} = D_x \left(\frac{m\pi}{L}\right)^2 \bar{w}_m \sin \frac{m\pi x}{L} = \bar{m}_m \sin \frac{m\pi x}{L} \tag{A.58}$$

where $\bar{m}_m = D_x \left(\frac{m\pi}{L}\right)^2 \bar{w}_m$.

The relation indicated by Equation (A.57) can be proved in the following manner. By simple calculations with the use of Equation (A.54),

$$\int_{-1}^{1} (A_1 e^{m\bar{\phi}\sigma} + A_2 e^{-m\bar{\phi}\sigma} + e^{-m\bar{\phi}|\sigma - \psi|}) d\sigma = \frac{2}{m\bar{\phi}} . \tag{A.59}$$

Subsequently, referring to Equations (A.47) and (A.56)

$$1/2 \int_{-1}^{1} \bar{m}_m d\sigma = \frac{D_x}{2} \left(\frac{m\pi}{L}\right)^2 \frac{L^2 Na \bar{H}_m}{4(D_{xy} + D_{yx}) m^3 \pi^2 \bar{\phi}} \frac{2}{m\bar{\phi}} \frac{1}{g(m)^2}$$

$$= 1/4 \frac{D_x}{(D_{xy} + D_{yx})} \frac{Na}{m^2} \frac{\bar{H}_m}{\bar{\phi}^2 g(m)^2} = \frac{\bar{\phi}^2 L^2}{N^2 a^2} \cdot \frac{Na}{m^2} \cdot \frac{\bar{H}_m}{\pi^2 \bar{\phi}^2}$$

$$= \frac{\bar{H}_m}{Na} \left(\frac{L}{m\pi}\right)^2 = \bar{M}_m .$$

From this equation, the condition represented by Equation (A.57) is satisfied by the condition indicated by Equation (A.45).

Definition of Deflection Coefficient

The deflection coefficient is defined by the equation:

$$K_d = \frac{\sum_{m=1}^{\infty} w_m}{\sum_{m=1}^{\infty} W_{om}} . \qquad (A.60)$$

From Equations (A.47), (A.49), (A.50) and (A.54)

$$K_d = \frac{\sum_{m=1}^{\infty} \bar{w}_m \sin \frac{m\pi x}{L}}{\sum_{m=1}^{\infty} \bar{W}_{om} \sin \frac{m\pi x}{L}} = \frac{D_x L^2 N^2 a^2}{4(D_{xy}+D_{yx})\pi^2} \frac{\pi^4}{L^4} \frac{\sum_{m=1}^{\infty} \frac{\bar{H}_m}{m^3 \bar{\phi} g(m)^2}}{\sum_{m=1}^{\infty} \frac{\bar{H}_m}{m^4} \sin \frac{m\pi x}{L}} \cdot \sin \frac{m\pi x}{L}$$

$$(A_1 e^{m\bar{\phi}\sigma} + A_2 e^{-m\bar{\phi}\sigma} + e^{-m\bar{\phi}|\sigma-\psi|}) = (\pi\phi)^2 \frac{1}{\pi\phi} \frac{1}{\sum_{m=1}^{\infty} \frac{\bar{H}_m}{m^4} \sin \frac{m\pi x}{L}}$$

$$\sum_{m=1}^{\infty} \frac{\bar{H}_m}{m^3 g(m)} (A_1 e^{m\bar{\phi}\sigma} + A_2 e^{-m\bar{\phi}\sigma} + e^{-m\bar{\phi}|\sigma-\psi|}) \sin \frac{m\pi x}{L} . \qquad (A.61)$$

Finally, the deflection coefficient K_d is as follows:

$$K_d = \pi\phi \frac{\sum_{m=1}^{\infty} \frac{\bar{H}_m}{m^3 g(m)} \left[\frac{e^{m\bar{\phi}\psi} + e^{-m\bar{\phi}(2+\psi)}}{e^{2m\bar{\phi}} - e^{-2m\bar{\phi}}} e^{m\bar{\phi}\sigma} + \frac{e^{-m\bar{\phi}\psi} + e^{-m\bar{\phi}(2-\psi)}}{e^{2m\bar{\phi}} - e^{-2m\bar{\phi}}} \cdot e^{-m\bar{\phi}\sigma} + e^{-m\bar{\phi}|\sigma-\psi|} \right] \sin \frac{m\pi x}{L}}{\sum_{m=1}^{\infty} \frac{\bar{H}_m}{m} \sin \frac{m\pi x}{L}} .$$

(A.62)

Definition of Moment Coefficient Per Unit Width

The moment coefficient per unit width is defined as:

$$K_m = \frac{\sum_{m=1}^{\infty} m_m}{\sum_{m=1}^{\infty} M_m} . \qquad (A.63)$$

From moment-deflection relations

$$K_m = \frac{-D_x \sum_{m=1}^{\infty} \frac{\partial^2 w_m}{\partial x^2}}{-D_x \sum_{m=1}^{\infty} \frac{d^2 W_{om}}{dx^2}} = \frac{\sum_{m=1}^{\infty} \bar{w}_m \left(\frac{m\pi}{L}\right)^2 \sin \frac{m\pi x}{L}}{\sum_{m=1}^{\infty} \bar{W}_{om} \left(\frac{m\pi}{L}\right)^2 \sin \frac{m\pi x}{L}} .$$

Upon substitutions, the moment coefficient per unit width K_m is obtained as

$$K_m = \pi\phi \frac{\sum_{m=1}^{\infty} \frac{\bar{H}_m}{mg(m)} \left[\frac{e^{m\bar{\phi}\psi} + e^{-m\bar{\phi}(2+\psi)}}{e^{2m\bar{\phi}} - e^{-2m\bar{\phi}}} e^{m\bar{\phi}\sigma} + \frac{e^{-m\phi\psi} + e^{-m\bar{\phi}(2-\psi)}}{e^{2m\bar{\phi}} - e^{-2m\bar{\phi}}} e^{-m\bar{\phi}\sigma} + e^{-m\bar{\phi}|\sigma-\psi|} \right] \sin \frac{m\pi x}{L}}{\sum_{m=1}^{\infty} \frac{\bar{H}_m}{m^2} \sin \frac{m\pi x}{L}} .$$

(A.64)

Definition of Moment Coefficient Per Beam

The moment coefficient per beam is defined as

$$K_{mb} = \frac{\sum_{m=1}^{\infty} \int_{\sigma-\frac{1}{N}}^{\sigma+\frac{1}{N}} m_m(\xi) d\xi}{\frac{1}{N} \sum_{m=1}^{\infty} \int_{-1}^{1} m_m(\xi) d\xi} \qquad (A.65)$$

where σ designates the position of the centroid of the beam element concerned. Since

$$\int_{-1}^{1} m_m d\sigma = 2M_m$$

the definition can be rewritten as

$$K_{mb} = \frac{1}{2} N \frac{\sum_{m=1}^{\infty} \int_{\sigma-\frac{1}{N}}^{\sigma+\frac{1}{N}} m_m(\xi)d\xi}{\sum_{m=1}^{\infty} M_m} . \qquad (A.66)$$

Due to the singularity of the function m_m at the loading point, two cases must be considered in integrating m_m

$$\int_{-1}^{1} m_m(\xi)d\xi .$$

These cases are, first, the coefficient for the loaded beam element; second, that for the unloaded beam element. They may be distinguished by knowing the sign of the function D_o defined by the equation (Figure A.2):

$$D_o = [(\sigma - \tfrac{1}{N}) - \psi][(\sigma + \tfrac{1}{N}) - \psi]. \qquad (A.67)$$

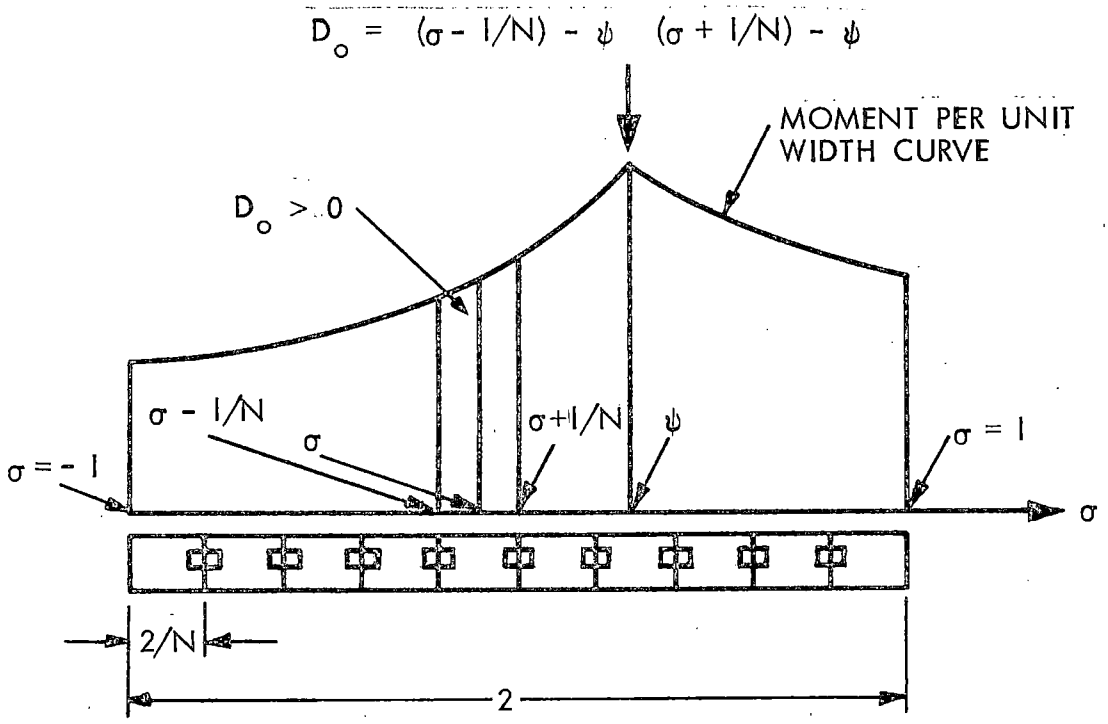

BEAM SEGMENT AWAY FROM CONCENTRATED LOAD

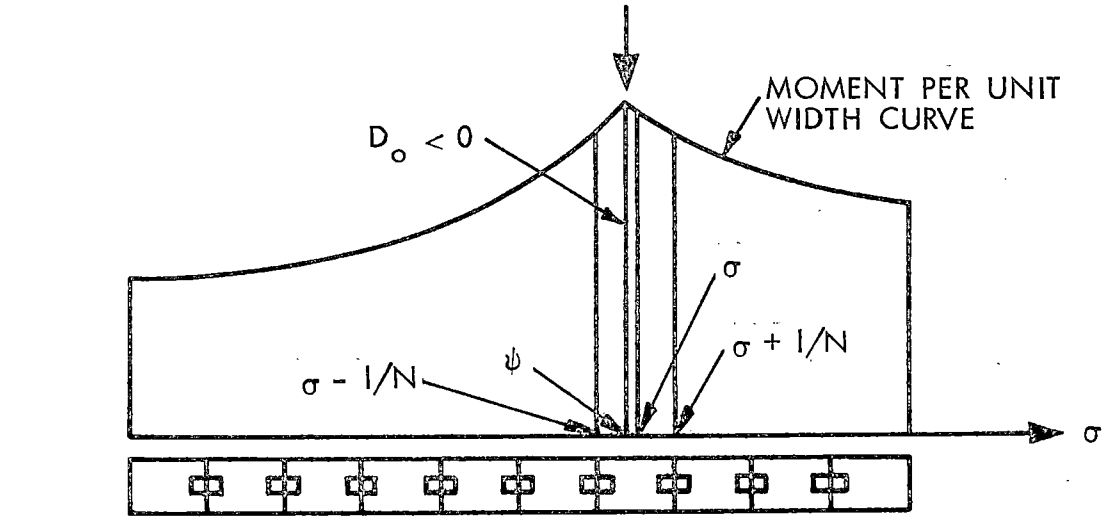

BEAM SEGMENT UNDER CONCENTRATED LOAD

Figure A.2. Moment coefficient curves for multi-beam bridges.

Coefficient for Unloaded Beam Element

By simple computations K_{mb} is found for $D_o \geqq 0$:

$$K_{mb} = \frac{1}{2} N \frac{1}{\sum_{m=1}^{\infty} \frac{\bar{H}_m}{m^2} \sin \frac{m\pi x}{L}} \sum_{m=1}^{\infty} \frac{\bar{H}_m}{m^2} \left\{ \frac{e^{m\bar{\phi}\psi} + e^{-m\bar{\phi}(2+\psi)}}{e^{2m\bar{\phi}} - e^{-2m\bar{\phi}}} \right.$$

$$\left[e^{m\bar{\phi}(\sigma+1/N)} - e^{m\bar{\phi}(\sigma-1/N)} \right] + \frac{e^{-m\bar{\phi}} + e^{-m\bar{\phi}(2-\psi)}}{e^{2m\bar{\phi}} - e^{-2m\bar{\phi}}} \left[e^{-m\bar{\phi}(\sigma-1/N)} - e^{-m\bar{\phi}(\sigma+1/N)} \right]$$

$$\left. + e^{-m\bar{\phi}(|\sigma-\psi|-1/N)} - e^{-m\bar{\phi}(|\sigma-\psi|+1/N)} \right\} \sin \frac{m\pi x}{L} . \qquad (A.68)$$

Coefficient for Loaded Beam Element

Similarly, for $D_o < 0$ the coefficient is

$$K_{mb} = \frac{1}{2} N \frac{1}{\sum_{m=1}^{\infty} \frac{\bar{H}_m}{m^2} \sin \frac{m\pi x}{L}} \sum_{m=1}^{\infty} \frac{\bar{H}_m}{m^2} \left\{ \frac{e^{m\bar{\phi}\psi} + e^{-m\bar{\phi}(2+\psi)}}{e^{2m\bar{\phi}} - e^{-2m\bar{\phi}}} \right.$$

$$\left[e^{m\bar{\phi}(\sigma+1/N)} - e^{m\bar{\phi}(\sigma-1/N)} \right] + \frac{e^{-m\bar{\phi}\psi} + e^{-m\bar{\phi}(2-\psi)}}{e^{2m\bar{\phi}} - e^{-2m\bar{\phi}}}$$

$$\left[e^{-m\bar{\phi}(\sigma-1/N)} - e^{-m\phi(\sigma+1/N)} \right] + 2 - e^{m\bar{\phi}\,1/N} \left[e^{m\phi(\sigma-\psi)} - e^{-m\bar{\phi}(\sigma-\psi)} \right] \Bigg\} \sin \frac{m\pi x}{L}$$

APPENDIX B

EVALUATION OF PARAMETERS FOR LOAD DISTRIBUTION IN HIGHWAY BRIDGES

In beam and slab bridges, the following two bridge parameters are considered the most significant regarding the lateral distribution of wheel loads.

1. Flexural parameter, θ:

$$\theta = \frac{W}{2L} \sqrt[4]{\frac{D_x}{D_y}}$$

2. Torsional parameter, α:

$$\alpha = \frac{1}{2} \frac{D_{xy} + D_{yx}}{\sqrt{D_x D_y}}$$

where

L = span length, ft,

W = bridge width, ft,

D_{xy} = torsional stiffness in the longitudinal direction, lb in.^{2}/ft,

D_{yx} = torsional stiffness in the transverse direction, lb in.^{2}/ft,

D_x = flexural stiffness in the longitudinal direction, lb in.^{2}/ft,

D_y = flexural stiffness in the transverse direction, lb in.^{2}/ft.

It was found that these two parameters can be combined into one parameter to predict the wheel load distribution. This new parameter C is defined by

$$C = \theta/\sqrt{\alpha} = \frac{\sqrt{2}}{2} \left(\frac{W}{L}\right) \sqrt{\frac{D_x}{D_{xy} + D_{yx}}} .$$

Also in multi-beam bridges, it was found that the most important cross-sectional parameter was ϕ as defined by

$$\phi = \frac{W}{2L}\sqrt{\frac{D_x}{D_{xy} + D_{yx}}} .$$

It can be easily seen that the parameters in beam and slab bridges and in multi-beam bridges are essentially identical, the only difference being the numerical constant. In other words, the relationship between parameters C and ϕ is

$$C = (\sqrt{2})\,\phi .$$

Therefore, the evaluation of the constant or parameter C can be carried out in the same manner both in beam and slab bridges and in multi-beam bridges.

The assumptions on which the parameter calculations are based may be summarized as:

1. A typical interior beam or diaphragm and its portion of the deck slab (the width of a beam or diaphragm spacing) are used for parameter calculations.
2. Full transverse flexural and torsional continuity of the diaphragms is assumed only when they are rigidly connected to the longitudinal beams.
3. The torsional rigidity of steel beams or diaphragms is ignored.
4. For flexural and torsional rigidity calculations of steel beam-concrete deck bridge types, the steel cross-sectional area should be expressed as an equivalent area of concrete.
5. The uncracked gross area of the concrete cross section may be used for ridigity calculations involving prestressed or reinforced concrete structural members.

6. Standard engineering procedures are used for computing the torsional and flexural rigidities of typical bridge systems.

Using these assumptions, the stiffness parameter C can be found by using bridge dimensions and the mechanical properties of materials for different cross sections as outlined in subsequent sections.

The effect of diaphragms is generally small or negligible and, thus, is normally not considered in determining the stiffness parameter C. Thus in subsequent sections, the stiffness of the diaphragms is not indicated in the calculations. However, if consideration of the diaphragms is desired, the torsional stiffness in the transverse direction, D_{yx}, should be increased by the torsional stiffness of the diaphragm divided by its spacing (stiffness/ft).

Steel Beams and Concrete Deck

Noncomposite Cross Section

The moment of inertia of the total cross section which has the width of S is expressed as follows: (see Figure B.1a)

$$I = nI_b + \frac{1}{12} St_s^3$$

where

I_b = moment of inertia of a beam element in $in.^4$,

n = modular ratio = E_s/E_c,

S = beam spacing, ft, and

t_s = thickness of slab, in.

Therefore, the longitudinal flexural stiffness is

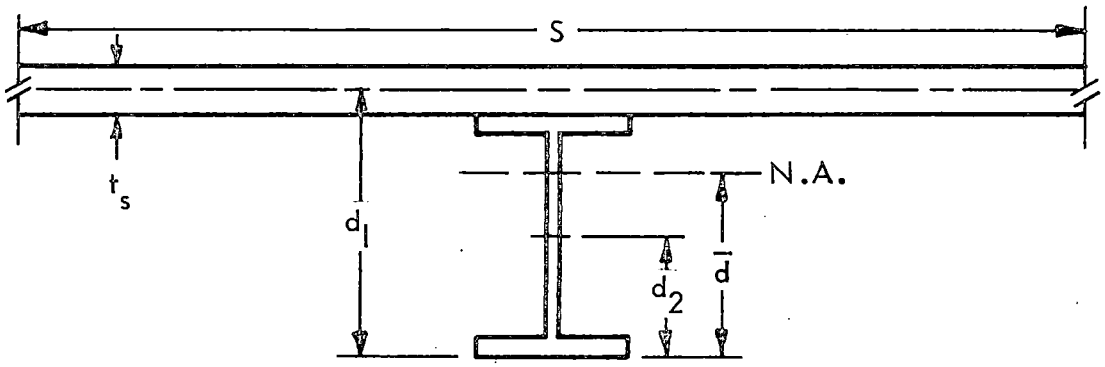

A. STEEL BEAM AND CONCRETE DECK

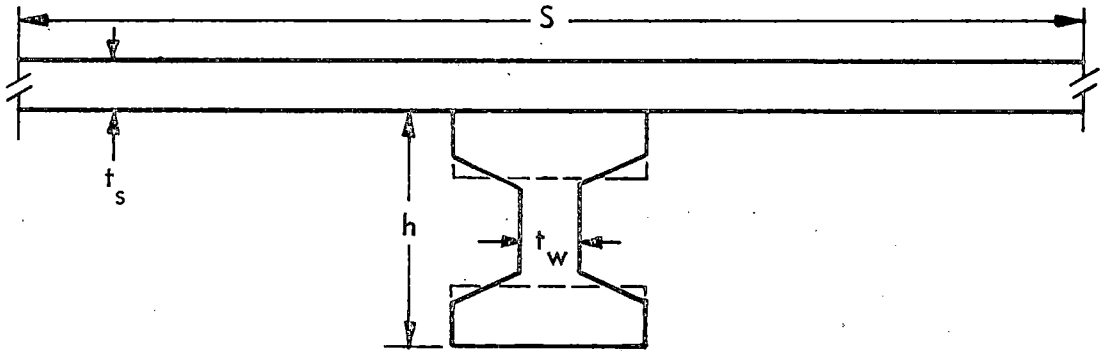

B. NONVOIDED CONCRETE BEAM SHOWING ASSUMED RECTILINEAR SHAPES

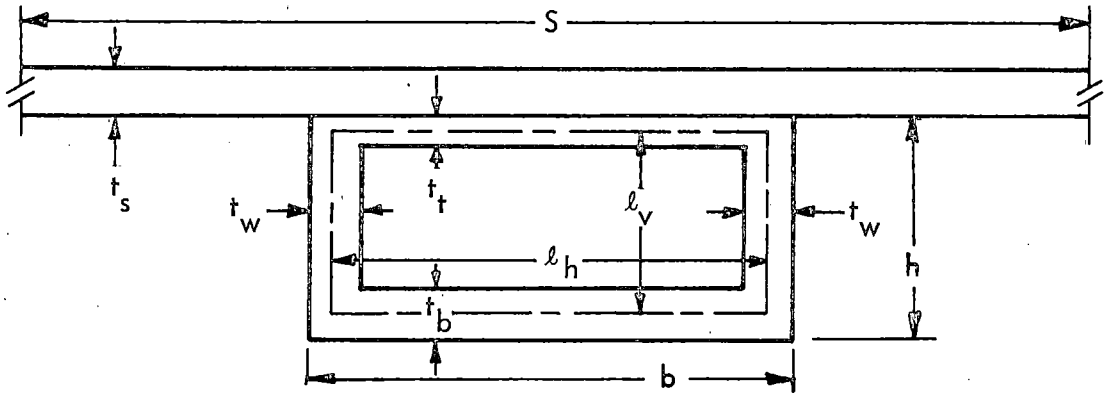

C. SEPARATED CONCRETE BOX-BEAM

Figure B.1. Nomenclature for calculation of bridge stiffness parameter C, beam and slab bridges.

$$D_x = \frac{E_c I}{S} = t_s^3 \left(\frac{nI_b}{St_s^3} + \frac{1}{12}\right).$$

Also, the torsional stiffnesses are given by

$$D_{xy} = \frac{G_c}{6} t_s^3 \; ; \; D_{yx} = \frac{G_c}{6} t_s^3 .$$

Finally,

$$C = \frac{\sqrt{6}}{2} \sqrt{\frac{E_c}{G_c}} \cdot \frac{W}{L} \cdot \sqrt{\frac{nI_b}{St_s^3} + \frac{1}{12}} .$$

For most cases, the second term in the square root term is negligible compared with the first term, or

$$\boxed{C = 1.9 \cdot \frac{W}{L} \cdot \sqrt{\frac{nI_b}{St_s^3}}} \qquad \nu = 0.2 \text{ (Poisson's ratio)}$$

$$\boxed{C = 1.7 \cdot \frac{W}{L} \cdot \sqrt{\frac{nI_b}{St_s^3}}} \qquad \nu = 0.$$

Moreover, the expression of C for slab bridges can be derived by neglecting the moment of cross section of steel beam element, I_b. Therefore,

$$C = 0.55 \cdot \frac{W}{L} \qquad \nu = 0.2$$

for slab bridges.

$$C = 0.5 \cdot \frac{W}{L} \qquad \nu = 0$$

Composite Cross Section

The position of the neutral axis is given by: (see Figure B.1a)

$$\bar{d} = \frac{St_s d_1 + nA_b d_2}{St_s + nA_b}$$

where

d_1 = distance indicating the position of the center of gravity of the slab portion,

d_2 = distance indicating the position of the center of gravity of the beam portion, and

A_b = cross-sectional area of the beam portion.

Therefore, the moment of inertia of the cross section, I, is given as follows:

$$I = nI_b + \frac{1}{12} St_s^3 + St_s(d_1 - \bar{d})^2 + nA_b(\bar{d} - d_2)^2 .$$

Thus, the following is the expression for the flexural stiffness

$$D_x = E_c t_s^3 \left[\frac{nI_b}{St_s^3} + \frac{1}{12} + \frac{nA_b}{St_s + nA_b} \left(\frac{d_1 - d_2}{t_s} \right)^2 \right] .$$

The torsional stiffnesses are similarly:

$$D_{xy} = \frac{G_c}{6} t_s^3 \; ; \; D_{yx} = \frac{G_c}{6} t_s^3 .$$

Finally:

$$C = \sqrt{6} \sqrt{\frac{E}{G}} \frac{1}{2} \frac{W}{L} \sqrt{\frac{nI_b}{St_s^3} + \frac{1}{12} + \frac{nA_b}{St_s + nA_b} \left(\frac{d_1 - d_2}{t_s} \right)^2} .$$

It was found that the following relation exists practically:

$$\sqrt{\frac{nI_b}{St_s^3} + \frac{1}{12} + \frac{nA_b}{St_s + nA_b} \left(\frac{d_1 - d_2}{t_s} \right)^2} \fallingdotseq 1.6 \sqrt{\frac{nI_b}{St_s^3}} .$$

Hence,

$$\boxed{C = 3.0 \frac{W}{L} \sqrt{\frac{nI_b}{St_s^3}}} \qquad \nu = 0.2$$

$$\boxed{C = 2.8 \frac{W}{L} \sqrt{\frac{nI_b}{St_s^3}}} \qquad \nu = 0$$

Nonvoided Concrete Beams and Concrete Deck

The expression for the flexural stiffness is exactly in the same form. The torsional stiffnesses are as follows: (see Figure B.1b)

$$D_{xy} = G_c \sum_{i=1} K_i \frac{b_i}{S} t_i^3 + G_c \frac{1}{6} t_s^3$$

$$D_{yx} = \frac{G_c}{6} t_s^3$$

where

b_i = length of the ith rectilinear portion of the concrete beam

K_i = St. Venant's torsion constant for the ith rectilinear portion of the concrete beam, and

t_i = thickness of the ith rectilinear portion of the concrete beam.

Therefore

$$C = \frac{\sqrt{6}}{2} \sqrt{\frac{E_c}{G_c}} \sqrt{\frac{\frac{I_b}{St_s^3} + \frac{1}{12} + \frac{nA_b}{St_s + nA_b} \left(\frac{d_1 - d_2}{t_s}\right)^2}{1 + 3 \sum_{i=1}^{R} K_i \frac{b_i}{S} \left(\frac{t_i}{t_s}\right)^3}} \cdot \frac{W}{L} .$$

Upon making use of the simplification:

$$\sqrt{\frac{I_b}{St_s^3} + \frac{1}{12} + \frac{nA_b}{St_s + nA_b} \left(\frac{d_1 - d_2}{t_s}\right)^2} = 1.6 \sqrt{\frac{nI_b}{St_s^3}} ,$$

gives

$$C = 1.6 \frac{\sqrt{6}}{2} \sqrt{\frac{E_c}{G_c}} \sqrt{\frac{I_b}{St_s^3} / \left[1 + \frac{h}{S} \left(\frac{t_w}{t_s}\right)^3\right]}$$

because practically

$$K_i \doteq \frac{1}{3} \text{ and } \sum_{i=1}^{R} K_i \frac{b_i}{S} \left(\frac{t_i}{t_s}\right)^3 \doteq \frac{1}{3} \frac{h}{S} \left(\frac{t_w}{t_s}\right)^3 .$$

Finally

$$\boxed{C = 3.0 \frac{W}{L} \sqrt{\frac{I_b}{St_s^3 + ht_w^3}}} \qquad \nu = 0.2$$

$$\boxed{C = 2.8 \frac{W}{L} \sqrt{\frac{I_b}{St_s^3 + ht_w^3}}} \qquad \nu = 0$$

Separated Concrete or Steel Box Beams and Concrete Deck

Again, the expression for the flexural stiffness is exactly in the same form as before (see Figure B.1c). The torsional stiffnesses at this time are as follows:

$$D_{xy} = \frac{G_c}{6} t_s^3 + \frac{4(l_h l_v)^2 G_c}{\left(2 \frac{l_v}{t_w} + \frac{l_h}{t_t} \cdot \frac{t_t + t_b}{t_b}\right) S}$$

$$D_{yx} = \frac{G_c}{6} t_s^3$$

where

$l_h = h - \frac{1}{2}(t_b + t_t) = h - \bar{t}$,

$l_v = b - t_w$,

$\bar{t} = \frac{1}{2}(t_b + t_t)$

t_b = thickness of the bottom flange of box beam, in.,

t_t = thickness of the top flange of box beam, in.,

t_w = web thickness, in.,

h = height of box beam element, in., and

b = width of box beam element, in.

Therefore

$$C = \frac{1.6}{2}\sqrt{\frac{E_c}{G_c}} \cdot \frac{W}{L} \cdot \sqrt{\frac{I_b}{b^2h^2}\left(\frac{h}{t_w} + \frac{b}{\bar{t}}\right)} \Bigg/ \left(1 - \frac{t_w}{b}\right)\left(1 - \frac{\bar{t}}{h}\right).$$

Here, the approximate relationship as follows was used:

$$\sqrt{\frac{nI_b}{St_s^3} + \frac{1}{12} + \frac{nA_b}{St_s + nA_b}\left(\frac{d_1 - d_2}{t_s}\right)^2} \doteq 1.6\sqrt{\frac{nI_b}{St_s^3}} .$$

Finally,

$$\boxed{C = 1.2\,\frac{W}{L}\sqrt{\frac{I_b}{b^2h^2}\left(\frac{h}{t_w} + \frac{b}{\bar{t}}\right)} \cdot \left(1 + \frac{t_w}{b}\right)\left(1 + \frac{\bar{t}}{h}\right)} \qquad \nu = 0.2$$

$$\boxed{C = 1.1\,\frac{W}{L}\sqrt{\frac{I_b}{b^2h^2}\left(\frac{h}{t_w} + \frac{b}{\bar{t}}\right)} \cdot \left(1 + \frac{t_w}{b}\right)\left(1 + \frac{\bar{t}}{h}\right)} \qquad \nu = 0$$

Note: It was assumed that the geometrical mean value is approximately equal to the algebraic mean value; i.e.,

$$\bar{t} = \frac{1}{2}(t_t + t_b) \doteq \sqrt{t_t \cdot t_b} .$$

Also, since t_w/b and $\bar{t}/h$ are much smaller than unity,

$$1/\left(1 - \frac{t_w}{b}\right) = 1 + \frac{t_w}{b} \; ; \; 1/\left(1 - \frac{\bar{t}}{h}\right) = 1 + \frac{\bar{t}}{h} .$$

Solid Concrete Cross Section without Voids for Slab and Multi-Beam Bridges

For slab bridges this can be considered to be a special case of steel beams and concrete deck. Therefore I_b and A_b can be set equal to zero in the expression of C for steel beams and concrete deck (refer to Figure B.1a, B.2c). However, in the derivation of the expression for C in beam and slab bridges it was assumed that

$$D_{xy} = \frac{G_c}{6} t_s^3 .$$

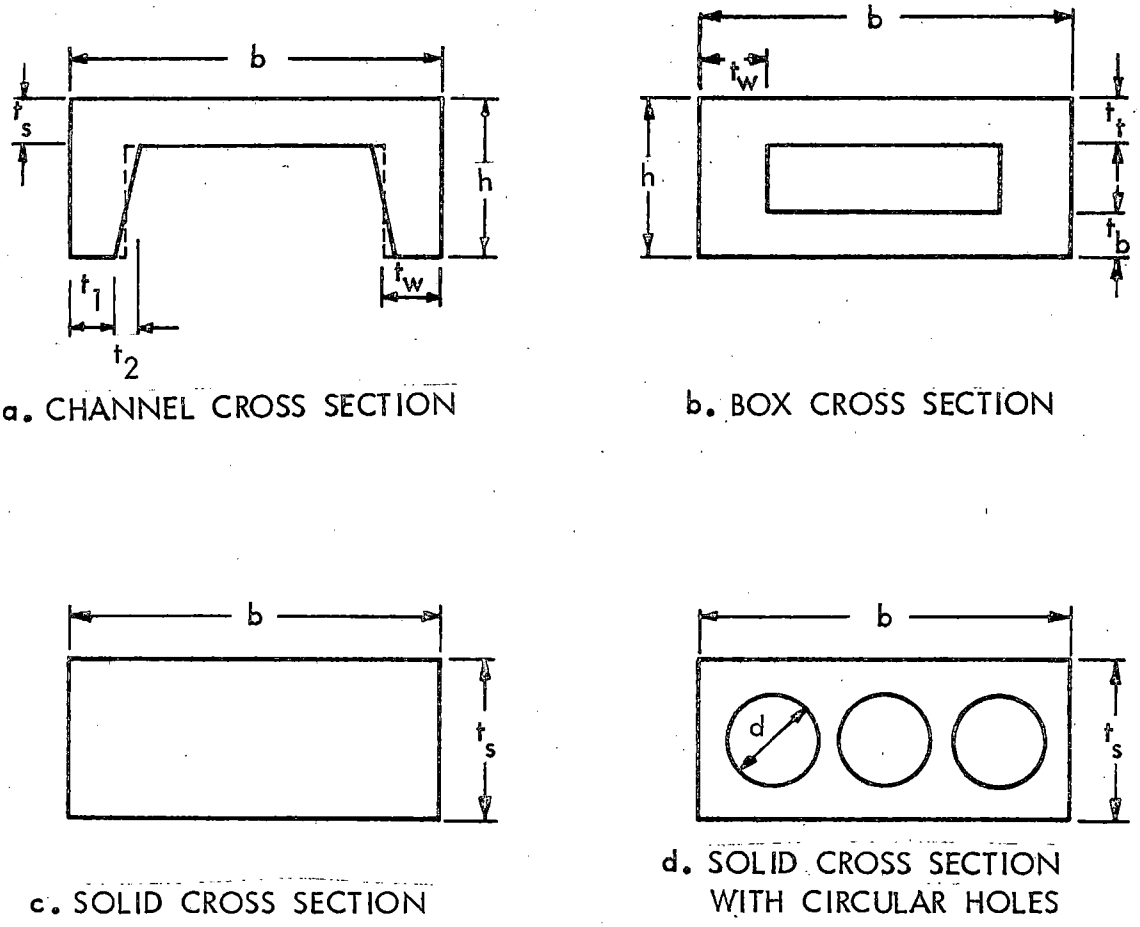

Figure B.2. Nomenclature for calculation of bridge stiffness parameter C, multi-beam bridges.

Therefore, St. Venant's torsion constant K_1 for the longitudinal torsion in slabs was assumed to 1/6 which corresponds to the torsional resistance of a small transverse section of the slab. Hence, it may be better to use the general coefficient K_1 in slab bridges for the torsional stiffness in the longitudinal direction for multi-beam bridges. Now, the flexural stiffness can be obtained as follows:

$$D_x = \frac{1}{12} E_c t_s^3 .$$

Also, for torsional stiffness in general

$$D_{xy} = G_c K_1 t_s^3 \; ; \; D_{yx} = \frac{G_c}{6} t_s^3 \; .$$

Therefore, the following general expression for C is obtained:

$$C = \frac{1}{12\ K_1 + 2} \cdot \frac{W}{L} \qquad \nu = 0.$$

Thus, for multi-beam bridges K_1 can be found from Table B.1 and for slab bridges K_1 can be assumed to 1/6.

TABLE B.1

COEFFICIENTS FOR SOLID SECTIONS

$S/t_s = b/t_s$	K_1	C	
1.0	0.14	0.521	W/L
1.5	0.20	0.480	W/L
2.0	0.23	0.459	W/L
3.0	0.26	0.442	W/L
10.0	0.31	0.418	W/L
∞	0.33	0.408	W/L

Ordinarily, b/t_s falls in between 1.0 and 1.5 for multi-beam bridges; hence,

$$\boxed{C = 0.5 \frac{W}{L}} \qquad \nu = 0.$$

It would be interesting to note that the expression for C is identical both for slab and multi-beam bridges. However, it was found necessary to revise the value of beam spacing when the same load distribution

formula LF = S/D is used in multi-beam bridges as was shown in Chapter 4. That is, instead of using the real beam spacing b, the following length should be considered for it:

$$S = (6N_w + 9)/N.$$

The comparison of the load fraction between slab bridge and multi-beam bridge is shown in Table B.2.

TABLE B.2

LOAD FRACTIONS FOR SLAB AND MULTI-BEAM BRIDGES

W, FT	N_w	SLAB BRIDGE		MULTI-BEAM BRIDGE	
		S, FT	LOAD FRACTION	S, FT	LOAD FRACTION
27	4	27/N	27/(N · D)	33/N	33/(N · D)
33	4	33/N	33/(N · D)	33/N	33/(N · D)
37	4	37/N	37/(N · D)	33/N	33/(N · D)
39	6	39/N	39/(N · D)	45/N	45/(N · D)
45	6	45/N	45/(N · D)	45/N	45/(N · D)
49	6	49/N	49/(N · D)	45/N	45/(N · D)
51	8	51/N	51/(N · D)	57/N	57/(N · D)
57	8	57/N	57/(N · D)	57/N	57/(N · D)
61	8	61/N	61/(N · D)	57/N	57/(N · D)
63	10	63/N	63/(N · D)	69/N	69/(N · D)
69	10	69/N	69/(N · D)	69/N	69/(N · D)
73	10	73/N	73/(N · D)	69/N	69/(N · D)

Here,

$$D = 5 + \frac{N_w}{20} + (3 - \frac{N_w}{7})(1 - \frac{C}{3})^2 \qquad C \leqq 3$$

$$= 5 + \frac{N_w}{20} \qquad C \geqq 3,$$

and N = number of girders.

Solid Concrete Cross Section with Circular Voids for Multi-Beam Bridges

Since the number of holes does not influence the value of C significantly the same formula as in Section 4 can be used (see Figure B.2d).

Box Concrete Cross Section for Multi-Beam Bridges

The expression of C for this cross section will be obtained as a special case of the cross sections dealt in 3 (see Figure B.2b). Here, the moment of inertia of a beam portion is given by:

$$I_b = \frac{1}{12}\left[bh^3 - (b - 2t_w)(h - 2\bar{t})^3\right]$$

$$\doteq \frac{bh^3}{6}\left(1 - 2\frac{\bar{t}}{h}\right)\left[3\frac{\bar{t}}{h} + \frac{t_w}{b}\left(1 - 2\frac{\bar{t}}{h}\right)^2\right]$$

$$\doteq \frac{bh^3}{6}\left(1 - 2\frac{\bar{t}}{h}\right)\left[3\frac{\bar{t}}{h} + \frac{t_w}{b}\left(1 - 4\frac{\bar{t}}{h}\right)\right].$$

where $\bar{t} = \frac{1}{2}(t_t + t_b)$.

However, ordinarily,

$$3\frac{\bar{t}}{h} \gg \frac{t_w}{b}\left(1 - 4\frac{\bar{t}}{h}\right).$$

Therefore,

$$I_b = \frac{bh^3}{2} \cdot \left(1 - 2\frac{\bar{t}}{h}\right)\frac{\bar{t}}{h}.$$

Assuming that the Poisson's ratio is zero:

$$\boxed{C = 0.5\frac{W}{L}\sqrt{1 + \frac{h}{b}\cdot\frac{\bar{t}}{t_w}\left(1 + \frac{t_w}{b}\right)}} \qquad \nu = 0.$$

Channel Concrete Cross Section for Multi-Beam Bridges

This section can be regarded as a special case of the nonvoided concrete beams and concrete deck section (see Figure B.2a). The moment of inertia of the beam portion (actually, of the leg portion of the channel cross section) can be obtained as follows:

$$I_b = \frac{t_w h^3}{6} \left(1 - \frac{t_s}{h}\right)^3 .$$

where

$$t_w \doteq \frac{1}{2} (t_1 + t_2).$$

As in previous cases (in nonvoided concrete beams and concrete cross section) it can be considered that

$$K_i = 1/3.$$

Compared with continuous slab in beam and slab bridge, the longitudinal torsional stiffness is somewhat different:

$$D_{xy} = \frac{G_c}{3} t_s^3 + \sum_{i=1}^{R=2} G_c K_i \frac{b_i}{b} t_i^3 = \frac{G_c}{3} t_s^3 + \frac{2}{3} G_c \frac{h - t_s}{b} t_w^3 .$$

Therefore,

$$D_{xy} + D_{yx} = G_c t_s^3 \left[\frac{1}{2} + \frac{2}{3} \frac{h - t_s}{b} \left(\frac{t_w}{t_s}\right)^3\right]$$

$$= \frac{1}{2} G_c t_s^3 \left[1 + \frac{4}{3} \frac{h - t_s}{b} \left(\frac{t_w}{t_s}\right)^3\right] .$$

Then, C can be obtained as follows

$$C = (1/\sqrt{3}) \cdot \frac{W}{L} \cdot (1.6) \cdot \sqrt{\frac{t_w (h - t_s)^3}{b t_s^3 + \frac{4}{3} (h - t_s) t_w^3}}$$

where it is assumed that

$$\sqrt{\frac{n I_b}{S t_s^3} + \frac{1}{12} + \frac{n A_b}{S t_s + n A_b} \left(\frac{d_1 - d_2}{t_s}\right)^2} = 1.6 \sqrt{\frac{n I_b}{S t_s^3}} .$$

Finally the expression of C is written as follows:

$$\boxed{C = 0.92 \frac{W}{L} \sqrt{\frac{t_w (h - t_s)^3}{b t_s^3 + \frac{4}{3} (h - t_s) t_w^3}}} \qquad \nu = 0.$$

Also, the following expression was found to approximate the rigorous expression within small error:

$$C = 1.1 \frac{W}{L} \sqrt{\frac{t_w (h - t_s)^3}{b t_s^3 + h t_w^3}} \qquad \nu = 0.$$

APPENDIX C

BIBLIOGRAPHY

1. ABDEL-SAMAD, S. R., "Analysis of Multicell Box Girders with Diaphragms." Unpublished Ph. D. thesis. University of Illinois Library, Urbana, Illinois (1967).

2. ABDEL-SAMAD, S. R., WRIGHT, R. N., and ROBINSON, A. R., "Analysis of Box Girders with Diaphragms." Proceedings of the American Society of Civil Engineers 94, No. ST10: pp. 2231-2256 (1968).

3. ALBERT, O., "Design of a Modern Highway Bridge." Polytechnic Institute of Brooklyn, Department of Civil Engineering, Brooklyn, New York (1955).

4. ALBRECHT, A., "Der Verbundträger als Kombination von Strahlträger mit Eisenbetonplatte." Ingenieur (Utrecht) 43: pp. 241-248 (1967).

5. ARENDTS, J. G., "Study of Experimental and Theoretical Load Distribution in Highway Bridges." Unpublished M. S. thesis, Iowa State University Library, Ames, Iowa (1968).

6. ARYA, A. S., KHACHATURIAN, N. and SIESS, C. P., "Lateral Distribution of Concentrated Loads on Multibeam Highway Bridges." Civil Engineering Studies Structural Research Series Report 213, University of Illinois, Urbana, Illinois (1960).

7. ARYA, A. S. and LOHTIA, R. P., "Distribution of Wheel Loads on Multibeam Highway Bridges. Indian Concrete Journal 38, No. 4: pp. 127-135 (1964).

8. ARYA, A. S. and LOHTIA, R. P., "Distribution of Wheel Loads on Multibeam Highway Bridges." Indian Concrete Journal 39, No. 4: pp. 146-151 (1965).

9. ARYA, A. S. and SURANA, C. S., "Distribution of IRC Standard Loads in Slab and Girder Bridges." Indian Concrete Journal 39, No. 12: pp. 466-473 (1965).

10. AU, T., "Moments in Composite Beam Bridges by Orthotropic Plate Theory." Journal of the American Concrete Institute 59, No. 12: pp. 1957-1964 (1962).

11. AU, T., "Use of Orthotropic Plate Theory in Bridge Design," Proceedings of the American Society of Civil Engineers 89, No. ST1: pp. 245-250 (1963).

12. AZIZ, E. M. and EDWARDS, A. D., "Some Aspects of the Economics of Continuous Prestressed Concrete Bridge Girders." Structural Engineer 44, No. 2: pp. 49-54 (1966).

13. BABARUDDIN, S., "Analysis of Slab and Girder Highway Bridges." Unpublished Ph. D. thesis, University of Illinois Library, Urbana, Illinois (1965).

14. BALDWIN, J. W., "Field Tests of a Three-Span Continuous Highway Bridge." Highway Research Record 76: p. 140 (1965).

15. BALDWIN, J. W., "Impact Study of a Steel I-Beam Highway Bridge." Engineering Experiment Station Bulletin 58, University of Missouri, Columbia, Missouri (1964).

16. BERGSTRASSER, M., "Versuche mit Freiaufliegenden Rechteckigen Platten unter Einzelkraftbelastung." Forschungsarbeiten auf dem Gebiete des Ingenieurwesens, No. 302 (1928).

17. BEST, B. C., "Tests of a Prestressed Concrete Bridge Incorporating Transverse Mild Steel Shear Connectors." Cement and Concrete Association Research Report 16 (1963).

18. BEST, B. C. and ROWE, R. E., "Abnormal Loading on Composite Slab Bridges." Cement and Concrete Association Research Report 7 (1959).

19. BEST, B. C. and ROWE, R. E., "Composite Slab Bridges." Civil Engineer 14, No. 6, 7: pp. 237, 347 (1960).

20. BOOMSLITER, G. P., CATHER, C. H. and WORRELL, D. T., "Distribution of Wheel Loads on a Timber Bridge Floor." Engineering Experiment Station Bulletin 24, West Virginia University, Morgantown, West Virginia (1951).

21. BORTSCH, R., "Die Einspannomente des Fahrbahnträger zweiwandiges Balkenbrücken." Beton und Eisen 36, No. 5, 6: pp. 89-96, 107-110 (1937).

22. BOUWKAMP, J. G., et al., "Behavior of a Single Span Composite Girder Bridge." Structures and Material Research Report SESM-65-6, University of California, Berkeley, California (1965).

23. BRAMER, C. R., UYANIK, M. E. and MOREADITH, F. L., "Prestressed Concrete Channel Bridges for Secondary Roads: An Investigation of the Elastic Load Distribution Under Live Loading." Engineering Research Department Report ERD-110-E, North Carolina State University, Raleigh, North Carolina (1962).

24. BRETTHAUER, G. and KAPPET, H., "Zur Querverteilung bei unsymmetrisch geraden und gekruemmenten zweistegigen Plattenbalkenbruecken." Beton und Stahlbetonbau 58, No. 12 (1963).

25. BROOKS, D. S., "The Design of Interconnected Bridge Girders." Civil Engineering and Public Works Review 53 (London) (1958).

26. CARPENTER, J. E. and MAGURA, D. D., "Structural Model Testing — Load Distribution in Concrete I-Beam Bridges." Portland Cement Association Bulletin D94 (1965).

27. CHU, K. H. and DUDNIK, E., "Concrete Box Girder Bridges Analyzed as Folded Plates." Unpublished paper. Proceedings of the 63rd American Concrete Institute Annual Convention (1967).

28. CHU, K. H. and KRISHNAMOORTHY, G., "Moments in Composite Beam Bridges by Orthotropic Plate Theory." Journal of the American Concrete Institute 59: p. 705 (1962).

29. CHU, K. H. and KRISHNAMOORTHY, G., "Use of Orthotropic Plate Theory in Bridge Design." Proceedings of the American Society of Civil Engineers 88, No. ST3: p. 35 (1962).

30. CHU, K. H. and PINJARKAR, S. G., "Multiple Folded Plate Structures." Proceedings of the American Society of Civil Engineers 92, No. ST2: p. 297 (1966).

31. CLOUGH, R. and SCHEFFY, C., "Stress Measurements, San Leandro Creek Bridge." Transactions of the American Society of Civil Engineers 120: p. 939 (1955).

32. CORNELIUS, W., FRÖHLICH, H. and HAULENA, E., "Brücken in Verbundbauweise." Zeitschrift VDI 91, No. 21: pp. 553-555 (1949).

33. CRAEMER, H., "Load-Bearing Capacity of Ideal Plastic Beam and Plates Supported on Four Sides on Ideal Plastic Support." (Translated title), Stahlbau 22, No. 9: pp. 200-205 (1953).

34. CRAEMER, H., "Load Distributing Effect of a Plate Upon Beams." Civil Engineering and Public Works Review 49 (London), No. 575: p. 510 (1954).

35. CROSS, H. and MORGAN, N. D., Continuous Frames of Reinforced Concrete. John Wiley and Sons, New York, New York (1932).

36. CUEN, C. P., "Composite Steel and Reinforced Concrete Construction for Highway Bridges." Roads and Streets 82, No. 12: pp. 48-49 (1939).

37. CUSENS, A. R. and ABBASI, A. F., "Influence of Transverse Prestress on Strength of Prestressed Concrete Bridge Slabs." Magazine of Concrete Research 15, No. 44 (1963).

38. CUSENS, A. R. and PAMA, R. P., "Design of Concrete Multi-Beam Bridge Decks." Proceedings of the American Society of Civil Engineers 91, No. ST5: pp. 255-278 (1965).

39. DAVIS, R. E., KOZAK, J. J. and SCHEFFEY, C. F., "Structural Behavior of a Concrete Box Girder Bridge." Highway Research Record 76: p. 32 (1965).

40. DEAN, D. L., "Analysis of Ribbed Plates." Final Report — Part I, Project ERD-110-67-4. North Carolina State University Highway Research Program, Raleigh, North Carolina (1968).

41. DEFRIES-SKENE, A. and SCORDELIS, A. C., "Direct Stiffness Solution for Folded Plates." Proceedings of the American Society of Civil Engineers 90, No. ST4: pp. 15-48 (1964).

42. DEWS, N. A., "Three Span Bridges." Roads and Road Construction 21, 22, No. 251, 258: pp. 311-315, 175-177 (1944).

43. DODGE, A., "Influence Functions for Beams on Elastic Foundations." Proceedings of the American Society of Civil Engineers 90, No. ST4: p. 63 (1964).

44. DOUGLAS, W. J. and VAN HORN, D. A., "Lateral Distribution of Static Loads in a Prestressed Concrete Box-Beam Bridge — Drehersville Bridge." Fritz Engineering Laboratory Report 315.1, Lehigh University Institute of Research, Lehigh, Pennsylvania (1966).

45. DUBERG, J. E., KHACHATURIAN, N. and FRADINGER, R. E., "A Method for the Analysis of Multi-Beam Bridges." Proceedings of the American Society of Civil Engineers 86, No. ST7: pp. 109-138 (1960).

46. ELLIS, J. S., "A Bridge Designed by the Plastic Theory." Engineering Institute of Canada Transactions 3, No. 1: pp. 18-22 (1959).

47. ERICKSON, E. C. O. and ROMSTAD, K. M., "The Distribution of Wheel Loads on Timber Bridges." U. S. Forest Products Laboratory Research Paper FPL44 (1965).

48. EVANS, R. H. and CHUNG, H. W., "Shrinkage and Deflection of Composite Prestressed Concrete Beams." Concrete and Constructional Engineering 61, No. 4: pp. 135-143 (1966).

49. EWELL, W. W., OKUBO, S. and ABRAMS, J. I., "Deflections in Grid-works and Slabs." Transactions of the American Society of Civil Engineers 117: p. 869 (1952).

50. FADER, I., "Grid Analysis by Reaction Distribution." Proceedings of the American Society of Civil Engineers 87, No. ST6: pp. 77-103 (1961).

51. FALK, S., "Die Berechnung geschlossener Rahmenträgwerke nach dem Reduktionsverfahren." Ingenieur Archieve 26: p. 96 (1958).

52. FENVES, S. J., VELETSOS, A. S. and SIESS, C. P., "Dynamic Studies of Bridges on the AASHO Test Road." Civil Engineering Studies Structural Research Series Report 227, University of Illinois, Urbana, Illinois (1962).

53. FOSTER, G. M., "Tests on a Rolled Beam Bridge Using H20-S16 Loading." Highway Research Board Research Report 14-B: pp. 10-38 (1952).

54. GERSCH, B. C., "Dynamic Testing Program of the T. and N. O. Railroad Overpass, El Paso Co., Texas." Texas Highway Department Research Report 64-5 (1964).

55. GIFFORD, F. W., "Test on a Prestressed Concrete Hollow-Box Bridge Deck." Magazine of Concrete Research 13, No. 39 (1961).

56. GOLDBERG, J. E., GLAUZ, W. D. and SETLUR, A. V., "Computer Analysis of Folded Plate Structures." Civil Engineering Report CE218, Purdue University, Lafayette, Indiana (1965).

57. GOLDBERG, J. E. and LEVE, H. L., "Theory of Prismatic Folded Plate Structures." International Association of Bridge and Structural Engineers Publications 17 (1957).

58. GOLDSTEIN, A., LIFHTFOOT, E. and SAWKO, F., "Analysis of a Three-Span Continuous Grillage Having Varying Section Properties." Structural Engineer 39, No. 8: pp. 245-254 (1961).

59. GOUDA, M. A., "Distribution of Torsion and Bending Moments in Connected Beams and Slabs." Journal of the American Concrete Institute 31, No. 8: p. 757 (1960).

60. GRAVES, J. R., "Diaphragm Design for Texas Bridges." Western Construction News 23, No. 8: pp. 93-95 (1948).

61. GRUBER, E., "Die Querverteilung der Lasten bei Brücken mit zwei Hauptträgern." Bauingenieur 23, No. 45/46: pp. 323-332 (1942).

62. GUILFORD, A. A. and VAN HORN, D. A., "Lateral Distribution of Vehicular Loads in a Prestressed Concrete Box-Beam Bridge-Berwick Bridge." Fritz Engineering Laboratory Report 315.4, Lehigh University Institute of Research, Lehigh, Pennsylvania (1967).

63. GUILFORD, A. A. and VAN HORN, D. A., "Lateral Distribution of Vehicular Loads in a Prestressed Concrete Box-Beam Bridge – White Haven Bridge." Fritz Engineering Laboratory Report 315.7, Lehigh University Institute of Research, Lehigh, Pennsylvania (1968).

64. GUPTA, L., "Design of Deck Slabs of Bridges for Concentrated Loads." Indian Concrete Journal 31: p. 122 (1957).

65. GÜRBÜZ, O., "Theories of Transverse Load Distribution on Simple Span, (Non-Skewed) Beam-and-Slab and Slab Bridges." Unpublished M. S. thesis. Iowa State University Library, Ames, Iowa (1968).

66. GUSTAFSON, W. C. and WRIGHT, R. N., "Analysis of Skewed Composite Girder Bridges." Proceedings of the American Society of Civil Engineers 94, No. ST4 (1968).

67. GUYON, Y., "Calcul des ponts dalles." Annales des Ponts et Chaussées 119, No. 29: pp. 555-589 (1949).

68. GUYON, Y., "Calcul des Ponts Larges à poutres multiples Solidarisées par les entretoises." Annales des Ponts et Chaussées 116: pp. 553-612 (1946).

69. HASS, B., "Eine Ungewöhnliche Belastung der Brüke über die Norderelbe." Bautechnik 41, No. 5: p. 145 (1964).

70. HAULENA, E., "Brüken in Verbundbauweise." Zeitschrift VDI 90, No. 5: pp. 145-150 (1948).

71. HAYES, J. M. and SBAROUNIS, J. A., "Vibration Study of a Three-Span Continuous I-Beam Bridge." Highway Research Board Bulletin 124 (1956).

72. HEINS, C. P., JR. and LOONEY, C. T. G., "An Analytical Study of Eight Different Types of Highway Bridge Structures." Civil Engineering Department, University of Maryland, College Park, Maryland (1966).

73. HEINS, C. P., JR. and LOONEY, C. T. G., "The Analysis of Curved Orthotropic Highway Bridges by the Finite Difference Technique." Civil Engineering Department, University of Maryland, College Park, Maryland (1967).

74. HEINS, C. P., JR. and LOONEY, C. T. G., "Bridge Analysis Using Orthotropic Plate Theory." Proceedings of the American Society of Civil Engineers 94, No. ST2 (1968).

75. HEINS, C. P., JR. and LOONEY, C. T. G., "The Solution of Continuous Orthotropic Plates on Flexible Supports as Applied to Bridge Structures." Civil Engineering Department, University of Maryland, College Park, Maryland (1966).

76. HENDRY, A. W. and JAEGER, L. G., "A General Method for the Analysis of Grid Frameworks." Proceedings of the Institution of Civil Engineers 4: pp. 939-971 (1955).

77. HENDRY, A. W. and JAEGER, L. G., The Analysis of Grid Frameworks and Related Structures. Prentice-Hall, Englewood Cliffs, New Jersey (1959).

78. HENDRY, A. W. and JAEGER, L. G., "The Analysis of Interconnected Bridge Girders by the Distribution of Harmonics." Structural Engineer 34, No. 7: pp. 241-266 (1956).

79. HENDRY, A. W. and JAEGER, L. G., "Load Distribution in Highway Bridge Decks." Proceedings of the American Society of Civil Engineers 82, No. ST4: pp. 1023-1 – 1023-43 (1956).

80. HETENYI, M., "A Method for Calculating Grillage Beams." Stephan Timoshenko Sixtieth Anniversary Volume, New York, New York (1938).

81. HINDMAN, W. S. and VANDEGRIFT, L. E., "Load Distribution over Continuous Deck Type Bridge Floor Systems." Engineering Experiment Station Bulletin XIV, No. 122, Ohio State University, Columbus, Ohio (1945).

82. HOLCOMB, R. M., "Distribution of Loads in Beam-and-Slab Bridges." Unpublished Ph. D. dissertation. Iowa State University Library, Ames, Iowa (1956).

83. HÖLLERER, O., "Beitrag zur Berechnung durchlaufender Trägerrostbrücken mit drei oder vier torsion weiche Hauptträgern." Stahlbau 34, No. 5: p. 150 (1965).

84. HOMBERG, H., "Kreuzwerke, Statik der Trägerroste und Platten." Forschungshefte aus dem Gebiete des Stahlbaues. Springer-Verlag, Berlin, Germany (1951).

85. HOMBERG, H., "Über die Lastberteilung durch Schubkäfte, Theorie des Plattenkreuzwerke." Stahlbau 21, No. 3, 4, 5, 10: pp. 42, 64, 77, 190 (1952).

86. HONDROS, G. and MARSH, J. G., "Load Distribution in Composite Girder-Slab Systems." Proceedings of the American Society of Civil Engineers 86, No. ST11: pp. 79-110 (1960).

87. HOUSTON, W. D. and SCHRIEUER, W. R., "Load Distribution Test, Sussex Street Bridge, Ottawa, Canada." Proceedings of the World Conference on Prestressed Concrete, Part II, Sec. V: pp. 20.1-20.11 (1957).

88. HUBER, M. T., "Die Theorie der Kreuzweise bewehrten Eisenbetonplatte nebst Anwendungen aufmehrere bautechnisch Aufgaben über Rechteckplatten." Der Bauingenieur 4: pp. 355-360, 392, 395 (1923).

89. HUBER, M. T., "Über die Biegung einer Rechteckplatte von ungleicher Biegungssteifigkeit in der Längs-und Querrichtung." Der Bauingenieur 5: pp. 259-263, 305-310 (1924).

90. HUFFINGTON, N., "Theoretical Determination of Rigidity Properties of Orthogonally Stiffened Plates." Transactions of the American Society of Mechanical Engineers, Journal of Applied Mechanics 78: p. 16 (1956).

91. HULSBOS, C. L., "Lateral Distribution of Loads in Multi-Beam Bridges." Highway Research Board Bulletin 339: p. 67 (1962).

92. HULSBOS, C. L. and LINGER, D. A., "Dynamic Tests of a Three-Span Continuous I-Beam Highway Bridge." Highway Research Board Bulletin 279 (1961).

93. IHLENBURG, W., "Plates Supported by Elastic Girders." (Translated title), Stahlbau 22, No. 8, 9: pp. 169-171, 209-214 (1953).

94. JENSEN, V. P., "Solutions for Certain Rectangular Slabs Continuous over Flexible Supports." Engineering Experiment Station Bulletin 303, University of Illinois, Urbana, Illinois (1938).

95. JENSEN, V. P., KLUGE, R. W. and WILLIAMS, C. B., "Highway Slab Bridges with Curbs: Laboratory Tests and Proposed Design Method." Engineering Experiment Station Bulletin 346, University of Illinois, Urbana, Illinois (1943).

96. JOHNSON, C., "Wheel Load Distribution for Shear in Timber Bridge Stringers." Public Works 74, No. 4: pp. 16-7 (1943).

97. JOHNSTON, S. B. and MATTOCK, A. H., "Lateral Distribution of Load in Composite Box Girder Bridges." Department of Civil Engineering, University of Washington, Seattle, Washington (1967).

98. KARRHOLM, G. and SAMUELSSON, A., "Bridge Slabs with Edge-Beams." Chalmers Tekniska — Handlingar 249: p. 73 (1963).

99. KELLEY, E. F., "Effective Width of Concrete Bridge Slabs Supporting Concentrated Loads." Public Roads 7, No. 1: p. 7 (1926).

100. KHACHATRUIAN, N., ROBINSON, A. R. and POOL, R. B., "Multi-Beam Bridges with Elements of Channel Section." Proceedings of the American Society of Civil Engineers 93, No. ST6: pp. 161-187 (1967).

101. KINNIER, H. L., "A Dynamic Stress Study of the Weyer's Cave Bridge." Vibration Survey of Composite Bridges, Progress Report, Virginia Council of Highway Investigation and Research Report 2 (1963).

102. KINNIER, H. L. and McKEEL, W. T., JR., "A Dynamic Stress Study of the Aluminum Bridge over the Appomattox River at Petersburg." Vibration Survey of Composite Bridges, Progress Report, Virginia Council of Highway Investigation and Research Report 4 (1965).

103. KINNIER, H. L. and McKEEL, W. T., JR., "A Dynamic Stress Study of the Hazel River Bridge." Vibration Survey of Composite Bridges, Progress Report, Virginia Council of Highway Investigation and Research Report 3 (1964).

104. KRUG, S. and STEIN, P., "Einflussfelder Orthogonal Anisotroper Platten." Springer-Verlag, Berlin, Germany (1961).

105. LASH, S. D., DAUPHIN, E. L. and MORAN, P., "Laboratory Tests of Full-Scale Pony Truss Bridge." Queen's University — Ontario Joint Highway Research Programme Report 22, Ontario, Canada (1964).

106. LASH, S. D. and JOYCE, T. C. R., "Laboratory Tests of Full-Scale Pony Truss Bridge: 1. Tests with Laminated Timber Deck." Queen's University — Ontario Joint Highway Research Programme Report 21, Ontario, Canada (1963).

107. LASSLEY, T. I., GAUGER, F. N. and TUMA, J. J., "Analysis of Continuous Beam Bridges: Volume III, Influence Lines by High Speed Computer, Volume IV, Dead Load Deflections by High Speed Computer." Oklahoma Research Bulletin 139, Engineering Research Institute, University of Oklahoma, Norman, Oklahoma (1964).

108. LAZARIDES, T. O., "The Design and Analysis of Openwork Prestressed Concrete Beam Grillages." Civil Engineering and Public Works Review 47, No. 552: p. 471 (1952).

109. LEONHARDT, F., "Die Vereinfachte Berechnung Zweiseitig gelagerter Trägerroste." Bautechnik 16: pp. 535-552 (1938).

110. LEONHARDT, F. and ANDRA, W., Die Vereinfachte Trägerrostberechnung. Julius Hoffuman Press, Stuttgart, Germany (1950).

111. LI, SHU-TIEN and BLACKWELL, R. V., "Design Yield Moment of Continuous Concrete Deck Slabs under Vehicular Loading." Unpublished paper, 63rd American Concrete Institute Annual Convention (1967).

112. LIGHTFOOT, E. and SAWKO, F., "The Analysis of Gridframeworks and Floor Systems by Electronic Computer." Structural Engineer 38, No. 3 (1960).

113. LIN, C. and VAN HORN, D. A., "The Effect of Midspan Diaphragms on Load Distribution in a Prestressed Concrete Box-Beam Bridge, Philadelphia Bridge." Fritz Engineering Laboratory Report 315.6, Lehigh University Institute of Research, Bethlehem, Pennsylvania (1968).

114. LIN, T. Y., HORONJEFF, R., CLOUGH, R. W. and SCHEFFEY, C. F., "Investigation of Stresses in the San Leandro Creek Bridge." University of California Institute of Transportation and Traffic Engineering Research Report 13, Berkeley, California (1953).

115. LINGER, D. A. and HULSBOS, C. L., "Dynamic Load Distribution in Continuous I-Beam Highway Bridges." Highway Research Record 34 (1963).

116. LINGER, D. A. and HULSBOS, C. L., "Forced Vibration of Continuous Highway Bridges." Highway Research Board Bulletin 339 (1962).

117. LITTLE, G., "The Distribution of a Load in a Box Section Bridge from Tests on a Xylonite Model." Magazine of Concrete Research 6, No. 18 (1954).

118. LITTLE, G., "Tests for Load Distribution in a Model Prestressed Concrete Bridge." Civil Engineering and Public Works Review 50, No. 535, 536: pp. 285-287, 421-2 (1955).

119. LITTLE, G. and ROWE, R. E., "The Effect of Edge Stiffening and Eccentric Transverse Prestress in Bridges." Cement and Concrete Association Technical Report TRA/279 (1957).

120. LITTLE, G. and ROWE, R. E., "The Effect of Edge Stiffening Beams on Bridges." Cement and Concrete Association Technical Report TRA/221 (1956).

121. LITTLE, G. and ROWE, R. E., "Load Distribution in Multi-Webbed Bridge Structures from Tests on Plastic Models." Magazine of Concrete Research 7, No. 21: pp. 133-142 (1955).

122. LOUNT, A. M., "Distribution of Loads on Bridge Decks." Proceedings of the American Society of Civil Engineers 83, No. ST4 (1957).

123. LOVE, J. S., JR., BARNOFF, R. M. and LARSON, T. D., "Composite Action from Corrugated Bridge Deck Forms." Department of Civil Engineering, Pennsylvania State University, University Park, Pennsylvania (1967).

124. LYSE, I. and MADSEN, I. E., "Structural Behavior of Battledeck Floor Systems." Transactions of the American Society of Civil Engineers 125: pp. 365-387 (1960).

125. MALTES, H., "Numerical Solutions for Interconnected Bridge Girders." Transactions of the American Society of Civil Engineers 125: pp. 365-387 (1960).

126. MANNING, R. C., "Combined Action of Concrete Slabs and Supporting Structural Steel Beams." Engineering Institute of Canada Engineering Journal 29, No. 3: 149-153 (1946).

127. MARGUERRE, K., "Über die Beanspruchung von Plattenträgern." Stahlbau 21, No. 8: p. 129 (1952).

128. MARTIN, I. and HERNANDEZ, J., "Orthogonal Gridworks Loaded Normally to their Planes." Proceedings of the American Society of Civil Engineers 86, No. ST1: pp. 1-12 (1960).

129. MASSONNET, C., "Complete Solutions Describing the Limit State of Reinforced Concrete Slabs." Magazine of Concrete Research 19, No. 58: pp. 13-32 (1967).

130. MASSONNET, C., "Complements to the Design Method of Multiple Beam Bridges." (Translated title), Annales des Travaux Publics de Belgique 107: pp. 680-748 (1954).

131. MASSONNET, C., "Contribution to the Calculation of Multiple Beam Bridges." (Translated title), Annales des Travaux Publics de Belgique 103, No. 3, 5, 6: pp. 377-422, 749-796, 927-964 (1950).

132. MASSONNET, C., "Methods of Calculation of Bridges with Several Longitudinal Beams Taking into Account their Torsional Resistance." International Association of Bridge and Structural Engineers Publications 10: pp. 147-182 (1950).

133. MASSONNET, C., DEHAN, E. and SEYVERT, J., "Experimental Research on Interconnected Beam Bridges." (Translated title), Annales des Travaux Publics de Belgique, No. 2 (1955).

134. MATTOCK, A. H. and JOHNSTON, S. B., "An Analytical and Model Study of Composite Box Girder Bridges." Unpublished paper, presented at the 63rd American Concrete Institute Annual Convention (1967).

135. MATTOCK, A. H., FOUNTAIN, R. S., et al., "Criteria for Design of Steel-Concrete Composite Box Girder Highway Bridges." Unpublished revision of the American Association of State Highway Officials Bridge Specifications. Department of Civil Engineering, University of Washington, Seattle, Washington (1967).

136. MATTOCK, A. H. and JOHNSTON, S. B., "Behavior under Load of Composite Box-Girder Bridges." Proceedings of the American Society of Civil Engineers 94, No. ST10: 2351-2370 (1968).

137. MATTOCK, A. H. and JOHNSTON, S. B., "Lateral Distribution of Load in Composite Box Girder Bridges." Highway Research Abstracts 36, No. 12: p. 50 (1966).

138. MATTOCK, A. H. and KAAR, P. H., "Precast-Prestressed Concrete Bridges 6: Test of Half-Scale Highway Bridge Continuous over Two Spans." Portland Cement Association Journal, Research and Development Laboratory Report 3, No. 3 (1961).

139. McCULLOUGH, C. B. and PAXSON, G. S., "Timber Highway Bridges in Oregon." Proceedings of the Highway Research Board 23: pp. 235-250 (1943).

140. MELAN, E. and SCHINDLER, R., Die genaue Berechnung von Trägerrosten. Springer-Verlag, Vienna, Austria (1942).

141. MIRANDA, C. and NAIR, K., "Finite Beams on Elastic Foundations." Proceedings of the American Society of Civil Engineers 92, No. ST2: p. 131 (1966).

142. MORICE, P. B., "Concentrated Load on Prestressed Concrete Bridge Decks." Institution of Engineers Journal (India) 35, No. 7, Part 1 (1955).

143. MORICE, P. B., "Local Effects of Concentrated Loads on Bridge Deck Slab Panels." Civil Engineering and Public Works Review 51, No. 597, 598: pp. 304-306, 436-438 (1956).

144. MORICE, P. B. and LITTLE, G., "The Analysis of Right Bridge Decks Subjected to Abnormal Loading." Cement and Concrete Association Report Db11 (1956).

145. MORICE, P. B. and LITTLE, G., "Load Distribution in Prestressed Concrete Bridge Systems." Structural Engineer 32, 33, No. 3, 1: pp. 83-111, 21-34 (1954, 1955).

146. MORICE, P. B. and LITTLE, G., "Load Tests on a Small Prestressed Concrete Highway Bridge." Institution of Civil Engineers Transactions 4 (1955).

147. MORICE, P. B., LITTLE, G. and ROWE, R. E., "Design Curves for the Effects of Concentrated Loads on Concrete Bridge Decks," Cement and Concrete Association Report Db11a (1956).

148. NARUOKA, M. and YONEZAWA, H., "The Application of Theory of the Orthotropic Plate to the Continuous Beam Bridge." Proceedings of the Japan National Congress of Applied Mechanics 5: pp. 107-110 (1955).

149. NARUOKA, M. and YONEZAWA, H., "A Research on the Application of the Theory of Orthotropic Plates to Steel Highway Bridges." International Association of Bridge and Structural Engineers Preliminary Publication, Lisbon, Portugal (1956).

150. NARUOKA, M. and YONEZAWA, H., "On the Design Bending Moment of Highway Beam Bridge." Proceedings of the Japan National Congress of Applied Mechanics 6: pp. 165-170 (1956).

151. NASSER, K. W., "Design Procedure for Lateral Load Distribution in Multi-Beam Bridges." Prestressed Concrete Institute Journal 10, No. 4: pp. 54-68 (1965).

152. NEWMARK, N. M., "A Distribution Procedure for the Analysis of Slabs Continuous over Flexible Beams." Engineering Experiment Station Bulletin 304, University of Illinois, Urbana, Illinois (1938).

153. NEWMARK, N. M., "Design of I-Beam Bridges." Transactions of the American Society of Civil Engineers 114: pp. 997-1022 (1948).

154. NEWMARK, N. M., "Numerical Procedure for Computing Deflections, Moments, and Buckling Loads." Transactions of the American Society of Civil Engineers 108: pp. 1161-1188 (1943).

155. NEWMARK, N. M. and SIESS, C. P., "Design of Slab and Stringer Bridges." Public Roads 23, No. 7: pp. 157-164 (1943).

156. NEWMARK, N. M. and SIESS, C. P., "Moments in I-Beam Bridges." Engineering Experiment Station Bulletin 334, University of Illinois, Urbana, Illinois (1942).

157. NEWMARK, N. M. and SIESS, C. P., "Research on Highway Bridge Floors at the University of Illinois." University of Illinois Bulletin, Reprint series, No. 52, Urbana, Illinois (1954).

158. NEWMARK, N. M., SIESS, C. P. and PENMAN, R. R., "Studies of Slab and Beam Highway Bridges Part I: Tests of Simple-Span Right I-Beam Bridges." Engineering Experiment Station Bulletin 363, University of Illinois, Urbana, Illinois (1946).

159. NICOLSKY, V. A., "Remarques sur le calcul des Ponts larges a poutres, multiples." Annales des Ponts et Chaussées 122, No. 5: p. 613 (1952).

160. NOVAK, M. E., HEINS, C. P., JR. and LOONEY, C. T. G., "Induced Dynamic Strains in Bridge Structures Due to Random Truck Loadings." Progress Report for Maryland State Roads Commission and U. S. Bureau of Public Roads. Department of Civil Engineering, University of Maryland, College Park, Maryland (1968).

161. OEHLER, L. T., "Vibration Susceptibilities of Various Highway Bridge Types." Proceedings of the American Society of Civil Engineers 83, No. ST4 (1957).

162. OLIVARES, A., et al., "Experimental Analysis of a Grillage Girder Bridge." Proceedings of the International Association of Bridge and Structural Engineers 21: pp. 237-242 (1961).

163. OLIVARES, A. E., et al., "Load Distribution in Beam-Grille Bridges." Indian Concrete Journal 37, No. 4: pp. 138-140 (1963).

164. ORAN, C. and VELETSOS, A. S., "Analysis of Static and Dynamic Response of Simple-Span Multi-Girder Highway Bridges." Civil Engineering Studies Structural Research Series Report 221, University of Illinois, Urbana, Illinois (1961).

165. PAMA, R. P. and CUSENS, A. R., "Design of Multi-Beam Bridge Decks." Proceedings of the American Society of Civil Engineers 91, No. ST5: pp. 255-278 (1965).

166. PAMA, R. P. and CUSENS, A. R., "Edge Beam Stiffening of Multi-Beam Bridges." Proceedings of the American Society of Civil Engineers 93, No. ST2: pp. 141-161 (1967).

167. PAUW, A. and BREEN, J. E., "Transfer of Load between Precast Bridge Slabs." Highway Research Board Bulletin 279 (1961).

168. PAXSON, G. S., "Load Distribution on Highway Bridges Having Adequate Transverse Diaphragms." Highway Research Board Research Report 14-B (1952).

169. PAXSON, G. S., "Loading Tests on a Steel Deck Plate Girder Bridge with Integral Concrete Floor." Oregon Highway Department Technical Bulletin 3 (1934).

170. PAYNE, H. L. and CALDWELL, H., "Ultimate Strength Design for Highway Bridges." Proceedings of the American Society of Civil Engineers 91, No. ST5: p. 43 (1965).

171. PIPPARD, A. J. S. and deWAELE, J. P. A., "The Loading of Interconnected Bridge Girders." Institution of Civil Engineers Journal 10, No. 1: pp. 97-114 (1938).

172. POOL, R. B., "An Investigation of Joint Forces in Multi-Beam Bridges." Unpublished Ph. D. thesis. University of Illinois Library, Urbana, Illinois (1963).

173. POOL, R. B., et al., "Analysis of Multi-Beam Bridges with Beam Elements of Slab and Box Section." Engineering Experiment Station Bulletin 483, University of Illinois, Urbana, Illinois (1965).

174. PRENTZAS, E. G., "Dynamic Behavior of Two Continuous I-Beam Bridges." Iowa Highway Research Board Bulletin 14 (1958).

175. RAHLWES, K., "Berechnung durchlaufender, in torsionssteife Längsträger eingespannter Fahrbahnplatten." Beton und Stahlbetonbau 59, No. 9: p. 202 (1964).

176. RAKSHIT, K. S., "Load Distribution in Bridge Decks: A Simplified Method." Indian Concrete Journal 38, No. 6: pp. 214-218 (1964).

177. RAMIREZ, J. A. N. and VELETSOS, A. S., "Response of Three-Span Continuous Highway Bridges to Moving Vehicles." University of Illinois Civil Engineering Studies Structural Research Series Report 276, University of Illinois, Urbana, Illinois (1964).

178. RAY, K. C., "Grid Floor as an Orthotropic Plate." Indian Concrete Journal 29, No. 11: pp. 271-275 (1955).

179. REDDY, D. V. and HENDRY, A. W., "A Moment Distribution Method for the Elasto-Plastic Analysis of Grid Frameworks." Civil Engineering and Public Works Review 56, No. 661: pp. 1051-1054 (London) (1961).

180. REDDY, D. V. and HENDRY, A. W., "A Rapid Moment and Torque Distribution Method for Grid Framework Analysis." Civil Engineering and Public Works Review (London) 54, No. 637: p. 867 (1959).

181. REDDY, D. V. and HENDRY, A. W., "Elasto-Plastic Analysis of an Interconnected Beam System." International Association of Bridge and Structural Engineers Publication 20 (1960).

182. REESE, R. T., "Load Distribution in Highway Bridge Floors — A Summary and Examination of Existing Methods of Analysis and Design and Corresponding Test Results." Unpublished M. S. thesis, Brigham Young University Library, Provo, Utah (1966).

183. REILLY, R. J. and LOONEY, C. T. G., "Dynamic Behavior of Highway Bridges: Final Report, Analysis of Results Tests on Three Bridges." Civil Engineering Department, University of Maryland, College Park, Maryland (1966).

184. REYNOLDS, G. C., "The Strength of Prestressed Concrete Bridge Grillages." Cement and Concrete Association Technical Report TRA/268 (1957).

185. REYNOLDS, G. C., "The Strength of Right Prestressed Concrete Slab Bridges with Edge Beams." Cement and Concrete Association Technical Report TRA/237 (1956).

186. RICHART, F. E. and LUGE, R. W., "Tests on Reinforced Concrete Slabs Subjected to Concentrated Loads." Engineering Experiment Bulletin 314, University of Illinois, Urbana, Illinois (1939).

187. RICHART, F. E., NEWMARK, N. M. and SIESS, C. P., "Highway Bridge Floors: A Symposium." Transactions of the American Society of Civil Engineers 114: p. 980 (1949).

188. RICHMOND, B., "Twisting of Thin-Walled Box Girders." Institution of Civil Engineers Proceedings 33: pp. 659-675 (1966).

189. ROESLI, A., "Lateral Load Distribution in Multi-Beam Bridges." Prestressed Concrete Bridge Members Progress Report. Fritz Engineering Laboratory Report 10, Lehigh University Institute of Research, Bethlehem, Pennsylvania (1955).

190. ROESLI, A., SMISLOVA, A., EKBERG, C. E. and ENEY, W. J., "Field Tests on a Prestressed Concrete Multi-Beam Bridge." Highway Research Board Proceedings 35: p. 152 (1956).

191. ROESLI, A. and WALTHER, R. E., "The Analysis of Prestressed Multi-Beam Bridges as Orthotropic Plates." World Conference on Prestressed Concrete Proceedings, San Francisco, California (1957).

192. ROSE, E. A., "Continuity Factors of Field Moments for Concentrated Vehicle Loads in Accordance with DIN 1072." (Translated title), Bauingenieur 37, No. 3: pp. 84-88 (1962).

193. ROWE, R. E., "The Analysis and Testing of a Type of Bridge Suitable for Medium Rightspans Subjected to Abnormal Loading." Cement and Concrete Association Technical Report TRA/292 (1958).

194. ROWE, R. E., "The Design of Right Concrete Slab Bridges for Abnormal Loading." Cement and Concrete Association Research Report Db. 12. (1958).

195. ROWE, R. E., "A Load Distribution Theory for Bridge Slabs Allowing for the Effect of Poisson's Ratio." Magazine of Concrete Research 7 (No. 20, 1955).

196. ROWE, R. E., "A Load Distribution Theory for No-Torsion Bridge Grillages with Various Support Conditions." Cement and Concrete Association Technical Report TRA/244 (1957).

197. ROWE, R. E., "A Note on the Transverse Moments in a Prestressed Concrete Bridge Slab." Magazine of Concrete Research 6, No. 18: pp. 149-150 (1954).

198. ROWE, R. E., "An Investigation of the Load Distribution Characteristics of Prestressed Concrete Bridge Slabs with Special Reference to Transverse Moments." Cement and Concrete Association Technical Report TRA/182 (1955).

199. ROWE, R. E., Concrete Bridge Design. John Wiley and Sons Inc., New York, New York (1962).

200. ROWE, R. E., "Load Distribution in Bridge Slabs with Special Reference to Transverse Bending Moments Determined from Tests on Three Prestressed Concrete Slabs." Magazine of Concrete Research 9, No. 27 (1957).

201. ROWE, R. E., "Load Distribution in No-Torsion Bridge Grillages with Various Support Conditions." Cement and Concrete Association Technical Report TRA/247 (1957).

202. ROWE, R. E., "Loading Tests on Langstone Bridge, Hayling Island, Hampshire." Cement and Concrete Association Technical Report TRA/289 (1958).

203. ROWE, R. E., "Loading Tests on St. Martin's Bridge, Stanford, Lincolnshire." Cement and Concrete Association Technical Report TRA/288 (1958).

204. ROWE, R. E., "Loading Tests on Two Prestressed Concrete Highway Bridges." Institution of Civil Engineers Proceedings 13 (1959).

205. ROWE, R. E., "The Analysis and Testing of a Type of Bridge Suitable for Medium Right Spans Subjected to Abnormal Loading." Cement and Concrete Association Technical Report TRA/292 (1958).

206. ROWE, R. E., "Transverse Moment in Right Concrete Slab Bridges Subjected to Abnormal Loading." Cement and Concrete Association Technical Report TRA/270 (1957).

207. RUNDELL, C. V., "Distribution of Concentrated Loads in Reinforced Concrete Slabs." Engineer 160, No. 4153: pp. 161-162 (1935).

208. SAKURAI, S., ITO, K. and NAROUKA, M., "Experimental Study of Multi-Cell Structures." Transactions of the Japan Society of Civil Engineers 87 (1962).

209. SAMI, S., "Continuous Girder Bridge with Variable Moment of Inertia." Proceedings of the American Society of Civil Engineers 86, No. ST1: pp. 19-39 (1960).

210. SANDERS, W. W., JR. and MUNSE, W. H., "The Lateral and Longitudinal Distribution of Loading in Steel Railway Bridges." University of Illinois Civil Engineering Studies Structural Research Series Report 208, University of Illinois, Urbana, Illinois (1960).

211. SARTWELL, A. D., HEINS, C. P., JR. and LOONEY, C. T. G., "The Analytical and Experimental Study of a Simple Girder Slab Bridges." Department of Civil Engineering, University of Maryland, College Park, Maryland (1968).

212. SATTLER, K., "Considerations on the Guyon-Massonnet Calculation Procedure for Simply Supported Beam Grillages and Extension of this Procedure on Arbitrary Systems." (Translated title), Der Bauingenieur 30: pp. 77-89 (1955).

213. SAWKO, F., "Bridge Deck Analysis: Electronic Computers Versus Distribution Methods." Civil Engineering (London) 60, No. 705: p. 534 (1965).

214. SAWKO, F. and BANERJEE, B., "Economics of Bridge Design." Concrete and Constructional Engineering 61, No. 3 (1966).

215. SCHAEFER, W., "Berechnung von Einflussfachen für die Statischen Grössen mehrteldriger orthotroper Fahrbahnplatten mit Hilfe von Eigen Funktionen." Stahlbau 33, No. 6: p. 177 (1964).

216. SCHAFFER, T. and VAN HORN, D. A., "Structural Response of a 45° Skew Prestressed Concrete Box-Girder Highway Bridge Subjected to Vehicle Loading." Fritz Engineering Laboratory Report 315.5, Lehigh University Institute of Research (1967).

217. SCHEFFEY, C. F., "Application of Digital Computers to Bridge Design." Proceedings of the American Society of Civil Engineers 83, No. ST4: p. 1308 (1957).

218. SCHEFFEY, C. F., "Dynamic Load Analysis and Design of Highway Bridges." Highway Research Board Bulletin 124 (1956).

219. SCHLEUSNER, A., "Näherungsweise Berechnung der lastverteilenden Wirkung von Brückenbeleagen." Bautechnik 31, No. 3: p. 79 (1954).

220. SCHORER, H., "Analysis and Design of an Elementary Prestressed Concrete Member." American Concrete Institute Journal 18: pp. 49-87 (1946).

221. SCORDELIS, A. C., "Analysis of Continuous Box Girder Bridges." Structures and Materials Research Report SESM-67-25, University of California, Berkeley, California (1967).

222. SCORDELIS, A. C., "Analysis of Simply Supported Box Girder Bridges." Structures and Materials Research Report SESM-66-17, University of California (1966).

223. SCORDELIS, A. C., "Discussion of 'Deflections in Gridworks and Slabs.'" Transactions of the American Society of Civil Engineers 117: pp. 892, 898 (1952).

224. SCORDELIS, A. C., DAVIS, R. E. and LO, K. S., "Load Distribution in Concrete Box Girder Bridges." Unpublished paper presented at 63rd American Concrete Institute Annual Convention (1967).

225. SCORDELIS, A. C., SAMARZICH, W. and PRITZ, D., "Load Distribution on a Prestressed Concrete Slab Bridge." Prestressed Concrete Institute Journal 5, No. 2: pp. 18-33 (1960).

226. SENNE, J. H., "Distribution of Loads in Beam and Slab Bridge Floors." Unpublished Ph. D. thesis, Iowa State University Library, Ames, Iowa (1961).

227. SHAW, F. S., "A Note on the Limit Analysis of Grid Frameworks." Civil Engineering Studies Structural Research Series Report 247, University of Illinois, Urbana, Illinois (1962).

228. SIESS, C. P. and KHACHATURIAN, N., "Proposed Revision to Standard Specifications for Highway Bridges to Provide for the Calculation of Moments in the Beams of Multi-Beam Bridges." Unpublished paper, University of Illinois, Urbana, Illinois (1962).

229. SIESS, C. P., NEWMARK, N. M., et al., "Studies of Slab and Beam Highway Bridges II." Engineering Experiment Station Bulletin 375, University of Illinois, Urbana, Illinois (1948).

230. SIESS, C. P., NEWMARK, N. M., et al., "Studies of Slab and Beam Highway Bridges III." Engineering Experiment Station Bulletin 396, University of Illinois, Urbana, Illinois (1952).

231. SIESS, C. P., NEWMARK, N. M., et al., "Studies of Slab and Beam Highway Bridges IV." Engineering Experiment Station Bulletin 405, University of Illinois, Urbana, Illinois (1952).

232. SIESS, C. P. and VELETSOS, A. S., "Distribution of Loads to Girders in Slab-and-Girder Bridges: Theoretical Analysis and Their Relation to Field Tests." Engineering Experiment Station Bulletin 513, University of Illinois, Urbana, Illinois (1954).

233. SIESS, C. P. and VIEST, I. M., "Studies of Slab and Beam Highway Bridges V." Engineering Experiment Station Bulletin 416, University of Illinois, Urbana, Illinois (1953).

234. SIESS, C. P. and VIEST, I. M., "Tests of Continuous Right I-Beam Bridges." Engineering Experiment Station Bulletin 512, University of Illinois, Urbana, Illinois (1952).

235. SMITH, T. K., "Impact Factor Studies on a Small Scale Laboratory Bridge." Unpublished M. S. thesis, Iowa State University Library, Ames, Iowa (1961).

236. STEIN, P., "Die Anwendung der Singularitätenmethode zur Berechnung orthogonal anisotroper Rechteckplatten einschliesslich Trägerrosten." Stahlbau-Verlags, BmbH, Köln, Germany (1959).

237. STEPHENSON, H. K., "Highway Bridge Live Loads Based on Laws of Chance." Proceedings of the American Society of Civil Engineers 83, No. ST4: p. 1314 (1957).

238. SVOTELIS, R. A., HEINS, C. P., JR. and LOONEY, C. T. G., "Analytical and Experimental Study of a Through Truss Bridge." Civil Engineering Department, University of Maryland, College Park, Maryland (1967).

239. SZABÖ, I., "Die Berechnung von Brücken-Trägerrosten." Stahlbau 27: pp. 141-147 (1958).

240. TAMBERG, K. G., "The Analysis of Right, Multi-Girder, Single-Span Bridge Decks as Equivalent Torsionally-Weak Grid Systems." Ontario, Canada Department of Highways Report 102 (1965).

241. TAMBERG, K. G. and CSAGOLY, P. F., "Application of Transformed Highway Loads to Influence Lines of Any Shape." Ontario, Canada Department of Highways Report RR131 (1967).

242. TAMBERG, K. G. and JUNG, F. W., "Functional Relationships between Actual Truck and Associated AASHO Design Loadings for Simple-Span Bridges." Ontario, Canada Department of Highways Report RR129 (1967).

243. THOMAS, F. G. and SHORT, A., "A Laboratory Investigation of Some Bridge Deck Systems." Institution of Civil Engineers Proceedings 1, No. 2 (1952).

244. THURLIMANN, B., "Influence Surface for Support Moments of Continuous Slabs." International Association of Bridge and Structural Engineers Proceedings 16: p. 485 (1956).

245. TIMOSHENKO, S. and WOINOWSKY-KRIEGER, S., Theory of Plates and Shells. Second Edition, McGraw-Hill, New York, New York (1959).

246. TRENKS, K., "Beitrag zur Berechnung orthogonal anisotroper Rechteckplatten." Der Bauingenieur 29, No. 10: pp. 372-377 (1954).

247. TUNG, D. H. H., "Analysis of Curved Twin Box-Girder Bridges." Unpublished paper presented at American Society of Civil Engineers Conference, Seattle, Washington (1967).

248. TUNG, D. H. H., "Torsional Analysis of Single Thin-Walled Trapezoidal Concrete Box-Girder Bridges." Unpublished paper presented at 63rd American Concrete Institute Annual Convention (1967).

249. TUNG, T. P., et al., "Highway Bridge Impact Problem." Highway Research Board Bulletin 124 (1956).

250. VALLETTE, R., "Calcul des systemes de poutres solidaires dans les ponts biais." Genie Civil 132, No. 1, 2 (1955).

251. VAN EENAM, N., "Live-Load Stress Measurements on Fort London Bridge: Final Report." Highway Research Board Proceedings 31 (1952).

252. VARNEY, R. F. and GALAMBOS, C. F., "Field Dynamic Loading Studies of Highway Bridges in the U. S. 1948-1965." Highway Research Record No. 76: pp. 285-308 (1965).

253. VIEST, I. M., "Summary Report on Bridge Research." Highway Research Board Special Report 73 (1962).

254. VIEST, I. M. and SIESS, C. P., "Composite Construction for I-Beam Bridges." Highway Research Board Proceedings 32: pp. 188 208

255. VINSON, J. and BRULL, M., "New Techniques of Solution for Problems in the Theory of Orthotropic Plates." American Society of Mechanical Engineers, 4th U. S. Congress of Applied Mechanics, Vol. 2: pp. 817-825 (1962).

256. VITOLS, V., CLIFTON, R. J. and AU, T., "Analysis of Composite Beam Bridges by Orthotropic Plate Theory." Proceedings of the American Society of Civil Engineers 89, No. ST4: pp. 71-94 (1963).

257. WAH, T., "The Longitudinal and Lateral Distribution of Loads in Open-Deck Railway Bridges." Unpublished Ph. D. thesis, University of Illinois Library, Urbana, Illinois (1953).

258. WALKER, W. H. and VELETSOS, A. S., "Response of Single-Span Highway Bridges to Moving Vehicles." Civil Engineering Studies Structural Research Series Report 272, University of Illinois, Urbana, Illinois (1963).

259. WALTHER, R. E., "Investigation of Multi-Beam Bridges: Prestressed Concrete Bridge Members Progress Report." Fritz Engineering Laboratory Report 14, Lehigh University Institute of Research, Bethlehem, Pennsylvania (1956).

260. WANSLEBEN, F., "Zur Berechnung von Brückfahrbahnen als Trägerroste." Bauingenieur 25, No. 2: p. 43 (1950).

261. WATANABE, E., "Study of Load Distribution in Multi-Beam Highway Bridges." Unpublished M. S. thesis, Iowa State University Library, Ames, Iowa (1968).

262. WEI, B. C. F., "Effects of Diaphragms in I-Beam Bridges." Unpublished Ph. D. thesis, University of Illinois Library, Urbana, Illinois (1951).

263. WEI, B. C. F., "Load Distribution of Diaphragms in I-Beam Bridges." Proceedings of the American Society of Civil Engineers 85, No. ST5: p. 17 (1959).

264. WESTERGAARD, H. M., "Computation of Stresses in Bridge Slabs Due to Wheel Loads." Public Roads (March 1930).

265. WESTERGAARD, H. M., "Formulas for the Design of Rectangular Floor Slabs and the Supporting Girders." Proceedings of the American Concrete Institute 22: pp. 26-43 (1926).

266. WHITE, A. and PURNELL, W. B., "Lateral Load Distribution Test on an I-Beam Bridge." Proceedings of the American Society of Civil Engineers 83, No. ST3: pp. 1255-1, 1255-20 (1957).

267. Wiesner, E., "Die Berechnung von Fahrbahnplatten bei Eisenbeton brücken." Beton and Eisen 33, No. 21: p. 333 (1934).

268. WILLIAMS, A., "The Determination of Influence Lines for Bridge Decks Monolithic with their Piers." Structural Engineer 42, No. 5: pp. 161-166 (1964).

269. WISE, J. A., "Dynamics of Highway Bridges." Highway Research Board Proceedings 32 (1953).

270. WOINOWSKI-KRIEGER, S., "Sur le calcul au eisaillement des planchers des ponts-routes." Ingenieur 46, No. 183: pp. 21-25 (1960).

271. WOLTER, F., "Prestressing and Loading Tests on a Bridge Element Built of Clamped-Together Segments." Bautechnik 17, No. 5: pp. 240-243 (1963).

272. WRIGHT, R. N., ABDEL-SAMAD, S. R. and ROBINSON, A. R., "Analysis and Design of Closed-Section Girder Bridges with Diaphragms: Final Report" — AISI Project 110, University of Illinois, Urbana, Illinois (1967).

273. WRIGHT, R. N., ABDEL-SAMAD, S. R. and ROBINSON, A. R., "BEF Analogy for Analysis of Box Girders." Proceedings of the American Society of Civil Engineers 94, No. ST7: pp. 1719-1793 (1968).

274. YAN, H., "Numerical Solution for Interconnected Bridge Girders." Civil Engineering (London) 49 (1954).

275. YONEZAWA, H., "A Study on the Stiffness of Beam Bridge." Transactions of the Japan Society of Civil Engineers 54 (1958).

276. ZIA, P., WILSON, W. T. and ROWAN, W. H., "A Study of Load Distribution Characteristics of Single and Double Layered Timber Bridge Decks Supported by Multiple Stringers." School of Engineering, North Carolina State University, Raleigh, North Carolina (1964).

277. ZIENKIEWICZ, O. and CHEUNG, Y., "Finite Element Method for Analysis of Elastic Isotropic and Orthotropic Slabs." Proceedings of the Institution of Civil Engineers 28, No. 6727: pp. 471-488 (1964).

278. "American Association of State Highway Officials Road Test Report 4: Bridge Research." Highway Research Board Special Report 61D (1962).

279. American Association of State Highway Officials, "Standard Specifications for Highway Bridges." Ninth Edition, (including 1966-1967 Interim Specifications), American Association of State Highway Officials, Washington, D. C. (1965).

280. An International Report of the AASHO-ARBE Joint Committee, "Report of Subcommittee on Standard Short Span Bridges." American Association of State Highway Officials, Washington, D. C. (1964).

281. "Catalog of Highway Bridge Plans." U. S. Department of Commerce, Bureau of Public Roads, Washington, D. C. (1957).

282. "Deflection Limitation of Bridges." Progress Report of the Committee on Deflection Limitations of Bridges of the Structural Division. Proceedings of the American Society of Civil Engineers 84, No. ST3: pp. 1633-1 – 1633-20 (1958).

283. "Design Manual for Orthotropic Steel Plate Deck Bridges." American Institute of Steel Construction, New York, New York (1962).

284. "Design of Highway Bridges in Prestressed Concrete." Portland Cement Association Structural and Railways Bureau Report ST84 (1959).

285. "Distribution of Live Load in Transverse Floors and Longitudinal Stringers." Proceedings of the American Railway Engineers Association 51: pp. 279-284 (1950).

286. "Distribution of Load Stresses in Highway Bridges." Highway Research Board Research Report 14-B (1952).

287. "Dynamic Studies of Bridges on the AASHO Road Test." Highway Research Board Special Report 71 (1962).

288. "Dynamic Tests on a Rolled-Beam Composite Continuous Span Bridge." South Dakota Department of Highways, Pierre, South Dakota (1955).

289. "Dynamic Tests of Two Cantilever Type Steel Girder Bridges." Nebraska Department of Roads Bridge Design Section, Lincoln, Nebraska (1961).

290. "Live Load Distribution on Three Bridge Types." Iowa State Highway Commission, Ames, Iowa (1966).

291. "Load Distribution Tests of Reinforced Concrete Slab Floors under Concentrated Loads." State of Ohio Highway Department Bulletin 28 (1915).

292. "Loading for Highway Bridges." Transactions of the American Society of Civil Engineers 119: p. 993 (1954).

293. Papers on Composite Construction. Der Bauingenieur 25, No. 3, 8 (1950).

294. Stahlbau Handbuch; 2. Huflage. Stahlbau-Verlags, BmgH, Köln, Germany (1961).

295. "Standard Plans for Highway Bridges." U. S. Department of Commerce, Bureau of Public Roads, Washington, D. C. (1962).

296. "Tests of Bridge Ties of Open Floor Bridges and of the Floor Timbers of Ballasted Floor Bridges." Proceedings of the American Railway Engineers Association 50 (1949).

297. "Two Books on Bridges Reviewed." Civil Engineering 35: p. 88 (1965).

APPENDIX D

PROJECT STATEMENT AND RESEARCH PLAN

In this appendix are presented the Research Problem Statement and the Objectives as given in the Project Statement for this investigation, as originally issued by the National Cooperative Highway Research Program. In addition, the Proposed Research Plan included in the Research Proposal submitted by Iowa State University (dated 30 July 1965) as modified on 19 November 1965 is given.

Research Problem Statement:

The factors currently in use for load distribution are inadequate for the various types of floor systems used in bridges. A large amount of research has been conducted on this problem, but the results of this work have not been correlated and evaluated in a manner such that suitable recommendations for changes in the specifications can be made. There is a need for a review of the past work, both analytical and experimental, and analyses to determine load distribution factors for each type.

Objectives:

The primary objective of this project is to recommend changes in specifications for distribution of wheel loads for use in design of floor systems for bridges.

The accomplishment of this research should include the following:

1. Review available analytical solutions and evaluate their adequacy by comparison with laboratory and field test data obtained from other research studies;

2. Identify those areas where experimental data are not yet adequate to determine whether analytical procedures are correct;

3. As necessary, extend existing, or develop new, analytical solutions such that all major types of floor systems are included. Laboratory and field tests are to be used to verify the analytical solutions;

4. Determine the variables that have an important influence on load distribution;

5. Recommend specification changes such that resulting designs will be more economical[1] and yet have adequate factors of safety.

It is intended that the major emphasis of the work will be limited to short and medium span bridges with no skew. Floor slabs supported by steel, reinforced concrete, or prestressed concrete beams are to be included as well as floor systems produced by adjacent box beams and similar types[2].

PROPOSED RESEARCH PLAN:

The research program will be divided into the following phases and studies. The details outlined in each phase will be developed by the Project Investigator and reviewed periodically, probably on a semi-annual basis, by consultation with the Research Engineer and his staff. The phases are intended to indicate the general order of proposed research; however, it is anticipated that there will be considerable overlap of endeavor.

Phase 1: Evaluation of current status of research on load distribution in highway bridges.

This study will include:

(a) A survey of all available analytical and experimental studies on load distribution, including:
1. published reports and papers
2. current research investigations.

Summarizations of this information will be made and an outline of the proposed analytical procedures developed.

(b) The collection of results of field tests of actual highway bridges.

The basis of this phase will be the work by Varney and Galambos on field dynamic loading studies as published in "Highway Research Board Record No. 76." Collaboration with these authors will constitute the major emphasis in this effort.

---

[1] In the Iowa State University proposal, the word "economical" was changed to the word "realistic."

[2] In the Iowa State University proposal, a sentence has been added here. "Only the load distribution to bridge floor systems of movable loads under static conditions will be considered."

(c) An evaluation of current specifications and of the proposed analytical solutions by comparison with available experimental data.

Phase 2: Extension and revision of past research.

(a) Determination of all variables that affect load distribution behavior in the types of bridges included in this study. In addition, this phase will also include the study of the range to be expected in these variables. Not only will current bridge design practice be included, but estimates of possible future changes in design practice will be made and their effects on the ranges of each variable considered. Among the variables which are already known to affect this behavior are: aspect ratio (beam spacing/beam span), relative stiffness of beams and floor slab, relative diaphragm stiffness, amount of horizontal prestress, extent of bridge continuity, and location of wheel loads. Any additional variables which affect the distribution will also be included.

(b) Identification of those ranges of each variable where currently available studies (experimental and analytical) are inadequate.

(c) Extension and revision of presently available, or development of new, analytical procedures to include areas determined in (2b).

A number of methods of analyses have been used in the development of these analytical solutions. It is anticipated that any required modifications in the proposed procedures will be made by considering the basic analytical techniques used in their development. However, since most of these methods include the consideration of the floor system as a grid work, it is hoped that the modifications of the procedures and extensions will be simplified. The methods of analyses of grids which have been used in the development of the distribution procedures may fall into four general categories.

1. Elementary methods of equating deflections at beam intersections.
2. Moment distribution and relaxation methods.
3. Plate theory.
4. Methods based on some simplifying assumption as to the construction of the grid and/or its mode of deflection.

Each of these methods considers the behavior of the floor system in a different manner, and the use of several of the methods of analysis may be suitable in arriving at a more realistic evaluation of floor system behavior.

(d) Development of a test program, with possibly laboratory and field studies, to obtain the required additional data to compare with presently available or new analytical procedures. The initiation of this development and any subsequent test program (Phase 3) will be made only if necessary because of the unavailability of sufficient test data to verify the analytical procedures and then only with the approval of the Research Engineer. The test program will, if required, be within the objectives of the project and within budgeted funds."

Phase 3: Laboratory and field test as developed in previous phase (see 2d).

Because of the varied types of bridges considered in this study, it is anticipated that, where possible, state highway departments will be approached to assist in field tests of actual bridges. When actual bridges that include the range of variables to be studied are not available, scale model laboratory bridges or bridge sections will be fabricated and tested.

The data from these tests will be compared with that obtained from previously developed or revised analytical procedures. These comparisons will indicate any required changes.

Phase 4: Development of design procedures.

(a) Revision of analytical procedures in line with information obtained in this research program to more accurately predict the actual load distribution.

(b) Simplification of analytical procedures so that they will be suitable for use in design offices.

(c) Development of specific recommendations for changes in the appropriate specifications controlling design wheel load distribution. These recommendations will attempt to more accurately indicate the actual load distribution and will consider all of the variables which affect this distribution.

KK/ljo

IOWA STATE UNIVERSITY
OF SCIENCE AND TECHNOLOGY
Ames, Iowa 50010

ENGINEERING RESEARCH INSTITUTE

April 10, 1969

Mr. Charles Pestotnik
Bridge Engineer
Iowa State Highway Commission
Ames, Iowa 50010

Dear Chuck:

Recently you were sent a copy of the Final Report - Distribution of Wheel Loads on Highway Bridges by W. W. Sanders, Jr. and H. A. Elleby. An errata sheet for that report has been prepared and a copy is enclosed. We would appreciate your incorporating these corrections in your copy.

Very truly yours,

Wallace

W. W. Sanders, Jr.
Associate Professor
Civil Engineering

jj
Encl.

FINAL REPORT

DISTRIBUTION OF WHEEL LOADS ON HIGHWAY BRIDGES[1]

W. W. Sanders, Jr. and H. A. Elleby

ERRATA SHEET

p. 49 – Eq. (1) should read:

$$D_x \frac{\partial^4 w}{\partial x^4} + 2H \frac{\partial^4 w}{\partial x^2 \partial y^2} + D_y \frac{\partial^4 w}{\partial y^4} = p(x, y)$$

p. 49 – Para. 2, lines 9 and 10: E should be E_x and E_y, respectively.

p. 49 – Para. 2, line 11: H should be 2H. Thus, $2H = D_{xy} + D_{yx}$.

p. 50 – line 4: $p_{(x)}$ should be $p(x, y)$.

p. 51 – Eq. (2) term $(\frac{w}{m\theta\pi})^3$ should be $(\frac{W}{m\theta\pi})^3$.

p. 52 – Eq. (4) should read:

$$M_x = - D_x \frac{\partial^2 w}{\partial x^2} .$$

p. 54 – Eq. (6) Σ should have limits $\sum_{j=1}^{N}$

p. 60 – Para. 2, line 9: 2 ft should be 1 ft.

p. 60 – Para. 2, last line: Fig. 18 should be Fig. 19.

p. 61 – lines 4 and 7: 2 ft should be 1 ft.

p. 61 – last line: Fig. 19 should be Fig. 18.

p. 61 – Fig. 18 and p. 62 – Fig. 19: bridge width should be W.

p. 68 – Eq. (10): the middle term on left side should be $2H \frac{\partial^4 w}{\partial x^2 \partial y^2}$.

p. 69 – Eq. (11): initial W should be w.

p. 85 – Para. 2, line 3: θ_x should be θ.

p. 85 – Para. 2, line 8: Table 4 should be Table 4A.

p. 88 – line 3: Table 4 should be Table 4A.

p. 97 – line 5: Eq. (13) should be Eq. (14).

---

[1]Engineering Research Institute, Iowa State University, Ames, Iowa (December 1968).

p. 98 — line 9: Eq. (13) should be Eq. (14).

p. 100 — Fig. 26: Equation should read:

$$D = 5.0 + N_w/20 + (3 - N_w/7)(1 - C/3)^2.$$

p. 102 — 3rd line from bottom: Table 9 should be Table 10.

p. 110 — line 3 and Eq. (19): Fig. 32 should be Fig. 31.

p. 118 — Note *** — 3rd line from bottom, "determined" should be "distributed.

p. 132 — Eq. (A.1) Dy should be D_y.

p. 132 — Para. 2, line 5: H should be 2H. Thus, $2H = D_{xy} + D_{yx}$.

p. 133 — lines 11 and 12: change W_h to w_h and W_p to w_p.

p. 134 — Eq. (A.5) should have brackets added as noted:

$$Y_m = e^{m\pi c\theta \frac{y}{b}} \left[A_m \cos\left(m\pi f\theta \frac{y}{b}\right) + \frac{B_m}{f} \sin\left(m\pi f\theta \frac{y}{b}\right)\right] + e^{-m\pi c\theta \frac{y}{b}} \left[C_m \cos\left(m\pi f\theta \frac{y}{b}\right) + \frac{F_m}{f} \sin\left(m\pi f\theta \frac{y}{b}\right)\right].$$

p. 138 — Eq. (A.10): $\frac{1}{W}$ term should be $\frac{1}{WD_x}$.

p. 162 — In equations for Separated Concrete or Steel Box Beams and Concrete Deck, equivalent transformed concrete areas shall be used for steel sections.

Additions to Commentary

p. 125 — add after line 9:

"The use should be restricted though to those cases where the specific critical lane loading pattern is known, such as reaction shear distribution (Article 1.3.1A). However, in the case of wheel load fractions used for determination of bending moment, where the critical loading pattern is not known and may be for less than the total number of lanes, the reduction should not be used. This restriction is currently practiced and is consistent with Article 1.107.4.

The equations for C, the stiffness parameter, given in the proposed Article 1.3.1(B)(1) includes the factor E/2G. It should be noted that further simplification of these equations can be obtained, if desired, by noting the relationship between E, the modulus of elasticity and G, the modulus of rigidity. If Poisson's ratio is assumed to be zero, the factor becomes one. If, in the case of concrete box girder bridges, Poisson's ratio is assumed to be 0.15, the equation for C shown becomes identical with Eq. (17)."

Int Girder of A.P.C. Box Bm Bridge:

(1) Van Horn

$$D.F. = \frac{2N_L}{N_B} + K\frac{S}{L}$$

$N_L = 3$ Lanes

$N_B = 5$ bms

$S = 9.5'$ @s

$L = 71.75'$

$W = 40'$ Rdwy

$K = .07 * 40 - 3(.1*3 - .26) - .2*5 - .12$

$= 1.56$

$$D.F. = \frac{2*3}{5} + 1.56\,\frac{9.5}{71.75}$$

$$= 1.2 + .206 = \boxed{1.406}$$

(2) Sanders & Elleby

$$D.F. = \frac{S}{D}$$

$$D = 5 + \frac{N_L}{10} + \left(3 - \frac{2N_L}{7}\right)\left(1 - \frac{c}{3}\right)^2$$

$$= 5 + \frac{3}{10} - \left(3 - \frac{2*3}{7}\right)\left(1 - \frac{1.8}{3}\right)^2 = 5.643$$

$$D.F. = \frac{9.5}{5.643} = \boxed{1.684}$$

(3) Present AASHO

$$D.F. = \frac{9.5}{5.5} = \boxed{1.727}$$

Ext Girder

(1) VanHorn

$$D.F. = \frac{8.5}{9.5} = .895 \text{ (Simple Bm R)}$$

$$D.F. = \frac{2NL}{S} = \frac{6}{5} = \boxed{1.2} \quad \text{GOVERNS}$$

(2) Sanders & Elleby

$$D.F. = \boxed{1.684} \quad \text{Same as Int. Bm}$$

(3) Present AASHO

$$\frac{9.5}{2 + .25 \times 9.5} = \boxed{1.49}$$

County _____ Design No. _____ Made by _____ Date _____
Project _____ File No. _____ Checked by _____ Date _____

Summary

	INT		EXT	
AASHO	1.727	1	1.49	1
VanHorn	1.406	.814	1.20	.805
Sanders	1.684	.975	1.684	1.13